LIÈGE université
Gembloux
Agro-Bio Tech

Tracking and controlling phenotypic switching of *Pseudomonas* sp. associated with biofilm formation

Fatemeh Ghazal Bajoul Kakahi

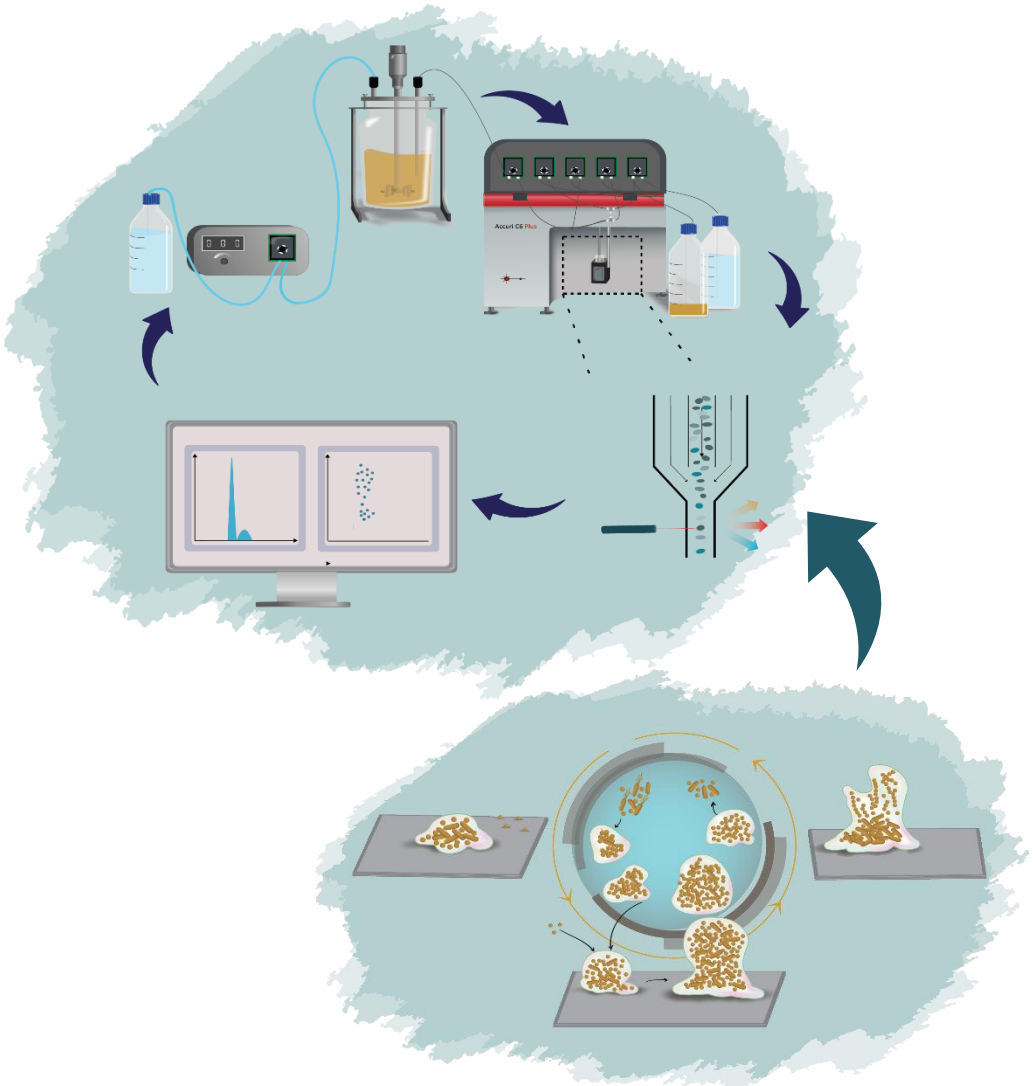

COMMUNAUTÉ FRANÇAISE DE BELGIQUE

UNIVERSITÉ DE LIÈGE – GEMBLOUX AGRO-BIO TECH

Tracking and controlling phenotypic switching of *Pseudomonas* sp. associated with biofilm formation

Bajoul Kakahi Fatemeh Ghazal

Dissertation originale présentée en vue de l'obtention du grade de docteur de l'Université de Liège – Gembloux Agro-Bio Tech en sciences agronomiques et ingénierie biologique

Promoteur(s) : Prof. Dr. Frank Delvigne

Année académique: April 2023-2024

Abstract

Phenotypic switching to a biofilm lifestyle is a significant survival strategy employed by bacteria under stressful conditions, necessitating a transition to a biofilm-specific phenotype. *Pseudomonas* sp. is renowned for its remarkable ability to thrive in extreme conditions, both in natural environments and within the human body, owing to its capacity to form biofilms. An example of this is *Pseudomonas putida* KT2440, a model plant-beneficial bacterium commonly found in soil, which can form biofilms depending on the surrounding environmental conditions. *P. putida* is widespread in the natural environment, colonizing the rhizosphere of various crop plants and persisting in the ecosystem.

The newly proposed biofilm developmental cycle in *Pseudomonas* sp. progresses through distinct stages, including aggregation and attachment, growth and accumulation, and finally disaggregation and detachment. Our research focuses on investigating the early initiation of biofilm formation, specifically the transition of individual cells from free-floating bacteria to the initial stages of biofilm formation, where aggregates float in the liquid phase. However, characterizing this process is challenging due to the lack of suitable fluorescent reporters and the formation of cell aggregates during the transition, which hinders single-cell analysis. To address this, we identified PI staining as a rapid, convenient, and reliable single-cell proxy that effectively monitors the phenotypic switching occurring in the early stages of biofilm development. By utilizing PI staining, we validated the significance of extracellular DNA (eDNA) in the cell-decision-making process, particularly in the initial stage of biofilm formation, shedding light on its impact on phenotypic diversification.

To further advance our research, we leveraged the association between PI-eDNA-associated cells and implemented reactive flow cytometry, coupled with a well-designed control strategy and an appropriate single-cell biomarker, in an advanced system known as Segrogostat. This approach allowed us to effectively assess and control the initial biofilm-phenotype state of bacteria with high temporal resolution.

Furthermore, our findings demonstrated that the early stages of biofilm development can be detected in planktonic cultures by evaluating the level of auto-aggregation and co-aggregation using flow cytometry as a high-throughput method, along with the identification of PI-eDNA-associated/PI-positive cells. We established a strong relationship between PI staining and cell auto-aggregation, reinforcing the link between these factors and biofilm formation.

This study opens novel avenues to possible applications of PI as a single-cell proxy, allowing us to capture the "key" subpopulations of cells involved in biofilm formation.

In this sense, this work paves the way to further understanding the early phenotypic switching involved in biofilm formation.

Keywords: Phenotypic heterogeneity, population control, auto-aggregation, stochastic switching, propidium iodide (PI), flow cytometry, extracellular DNA (eDNA), biofilm, co-aggregation, fitness, multi-species biofilm

Résumé

Le switch phénotypique à un mode de vie de type biofilm est une stratégie de survie importante employée par les bactéries dans des conditions stressantes, nécessitant une transition vers un phénotype spécifique au biofilm. *Pseudomonas* sp. est connu pour sa remarquable capacité à prospérer dans des conditions extrêmes, tant dans les environnements naturels que dans le corps humain, grâce à sa capacité à former des biofilms. Un exemple en est *Pseudomonas putida* KT2440, une bactérie bénéfique pour les plantes couramment présente dans le sol, qui peut former des biofilms en fonction des conditions environnementales environnantes. *P. putida* est répandu dans l'environnement, colonisant plus précisément la rhizosphère de différentes cultures et persistant dans l'écosystème.

Le nouveau modèle représentant le cycle de développement du biofilm proposé chez *Pseudomonas* sp. progresse par des étapes distinctes, comprenant l'agrégation et l'attachement, la croissance et l'accumulation, et enfin la désagrégation et le détachement. Notre recherche se concentre sur l'étude de l'initiation précoce de la formation du biofilm, en particulier la transition des cellules individuelles de bactéries libres à des stades initiaux de formation de biofilm, où les agrégats flottent dans la phase liquide. Cependant, la caractérisation de ce processus est difficile en raison du manque de marqueurs fluorescents appropriés et de la formation d'agrégats cellulaires pendant la transition, ce qui entrave l'analyse des cellules individuelles. Pour remédier à cela, nous avons identifié la coloration à l'iodure de propidium (PI) comme un indicateur rapide, pratique et fiable d'une seule cellule qui surveille efficacement le passage phénotypique se produisant aux premiers stades du développement du biofilm. En utilisant la coloration PI, nous avons validé l'importance de l'ADN extracellulaire (eDNA) dans le processus de prise de décision cellulaire, en particulier dans la phase initiale de formation du biofilm, éclairant son impact sur la diversification phénotypique.

Pour faire progresser davantage nos recherches, nous avons exploité la liaison entre les cellules liées à l'eDNA et la coloration PI au niveau d'une approche de cytométrie de flux réactive (système Ségrégostat). Cette approche nous a permis d'évaluer et de contrôler efficacement l'état phénotypique initial du biofilm des bactéries avec une haute résolution temporelle.

De plus, nos résultats ont démontré que les premiers stades du développement du biofilm peuvent être détectés dans les cultures planctoniques en évaluant le niveau d'auto-agrégation et de co-agrégation à l'aide de la cytométrie de flux en tant que méthode, ainsi qu'en identifiant les cellules liées à l'eDNA et positives à la PI. Nous

avons établi une relation entre la coloration PI et l'auto-agrégation cellulaire, renforçant le lien entre ces facteurs et la formation du biofilm.

Cette étude ouvre de nouvelles perspectives d'applications potentielles de la PI en tant qu'indicateur d'une seule cellule, nous permettant de capturer les "sous-populations clés" de cellules impliquées dans la formation du biofilm. Dans ce sens, ce travail ouvre la voie à une meilleure compréhension de la transition phénotypique précoce impliquée dans la formation du biofilm.

Mots-clés : Hétérogénéité phénotypique, contrôle de la population, auto-agrégation, commutation stochastique, iodure de propidium (PI), cytométrie de flux, ADN extracellulaire (eDNA), biofilm, co-agrégation, aptitude, biofilm multi-espèces.

Acknowledgments

Completing a PhD is a monumental achievement, and I still find it hard to believe that I have reached this milestone. This thesis is the result of four years of intensive research, brainstorming sessions, and professional and personal development. I want to raise a toast to everyone who has been a part of this incredible journey with me.

First and foremost, I want to express my immense gratitude to my Ph.D. supervisor, **Prof. Frank Delvigne**. Their unwavering support, guidance, and encouragement have been invaluable to me throughout the entire process. From the early stages of refining my research proposal to the final submission of my thesis, his constant presence and wealth of wisdom have played a crucial role in shaping my academic growth. The weekly meetings we held were of great value, serving as important checkpoints to keep me on track academically, while also providing me with generous encouragement. I am deeply thankful for the enormous contributions he has made to my development. I am particularly fortunate to have had a supervisor like **Frank**, who not only shared his extensive academic knowledge generously but also played a pivotal role in helping me establish myself within the academic community. His expertise and guidance have been instrumental in my journey. **Frank**, I consider myself incredibly lucky to have had a supervisor like you during my years of pursuing a Ph.D. Your remarkable academic prowess aside, your exceptional management skills fostered a sense of belonging and teamwork, making me feel like a valued member of a family. The experience was truly extraordinary and amazing.

I would also like to extend my heartfelt appreciation to the members of the reading committee for their dedication to reviewing my thesis and providing valuable feedback. **Prof. Pablo Ivan Nikel**, I am truly grateful for the opportunity to work with *Pseudomonas* strains from your laboratory. Your exceptional support and invaluable contributions have greatly enriched the articles that emerged from our collaboration. **Dr. Susann Mueller**, **Dr. Marc Ongena**, **Prof. Christophe Blecker**, and **Prof. Mazzucchelli Gabriel**, I owe a tremendous debt of gratitude to each of you for the unwavering support you have offered me throughout these four years. Thank you for your guidance and encouragement.

In addition to my supervisors, I am immensely grateful to my extraordinary lab mates, whose unwavering support has been a constant source of motivation for me. First and foremost, I want to extend my heartfelt thanks to **Dr. Martinez Alvarez Juan Andrés**, your assistance during my experiments, data analysis, and scientific writing has been invaluable. Not only you are an amazing person both inside and out, but your dedication and support have truly made a difference. **Vincent (Vini)**

Vandenbroucke, our "Google boy," I can't thank you enough for your golden heart and unwavering support. Your wonderful advice has always been beneficial to me. **Matheo**, you are an incredibly kind individual, and I will never forget your special singing after lunchtime (coffee♪, coffee ♪... coffee) always brought a smile to my face. **Dr. Fabian Moreno**, your enthusiasm and upbeat character made spending long hours in the lab an enjoyable experience. **Max and Hannah**, your positive vibes in our team brought much-needed sweetness to our intense work sessions. Additionally, I want to thank **Lucas** (fries lover), **Romain**, and **Fabian** for their kind support and valuable advice. **Tiphaine** and **Melanie**, it was always a pleasure to know you both and share even short experiences as colleagues. To all of you, my lab mates and friends, you have been my lifeline during the most challenging times. I am proud to say that we have become more than just lab partners; we have become good friends. Thank you all for your unwavering support, and for making our time in the lab a memorable and enjoyable journey.

Besides my lab mates, I am outstandingly thankful to **Sam** and **Andrew** for their incredible lab support and lots of encouragement during difficult periods. I also would like to thank **Farah**, **Adri**, **Ikram**, **Sofija, Barbara**, and **Imen** and our administrative and technical team **Marina, Cathy, Olivia, Margue, Romain, and Danielle**.

Last but not least, I would like to acknowledge my family for their enduring support of me during my doctoral work and my dissertation. I have been blessed with a very loving and supportive family. As for my husband **REZA**, I cannot begin to express my gratitude to him for all the love, support, the encouragement he has sent my way along this journey. He is my most enthusiastic cheerleader; he is my best friend, and he is an amazing husband and father. My Love, Reza, never asked me to stop working or even how long I planned to work; he simply did the dishes or took care of the kids without question. He is my rock. Without his willingness to be the primary caregiver, this dissertation would have taken even longer to complete; without his sunny optimism, I would be a much grumpier person; without his love and support, I would be lost. I am grateful to my husband not just because he has given up so much to make my career a priority in our lives, but because he has seen me through the ups and downs of the entire Ph.D. process. My beautiful and lovely kids (**Aurelie** and **Liam**) you are my inspiration to achieve greatness. Without you, I would not be where I am today.

Above all, I would like to special thank my parents, **Dina** and **Behzad**, who never failed to say that they were proud of me for doing this work, no matter how worried they were about me. Thank you for being my champions throughout my life. Your

unconditional love and support have meant the world to me, I hope that I have made you proud.

My sisters (**Leyla** and **Niluofar**) and my brother **Reza** gave quiet encouragement and positive belief in my success that kept me going regardless of the challenges that I faced. Special thanks to **Leyla** for all the help she did for me during my thesis writing.

Table of contents

Abstract i

Résumé iii

Acknowledgments iv

Table of contents vii

List of figures xix

List of tables xxiii

List of acronyms xxiv

Chapter 1 1

1. Characterization of phenotypic switching involved in early biofilm formation in *Pseudomonads* sp. 3

2. Objectives and research methodology 4

3. Chapter-by-chapter overview 6

Chapter 2 9

1. Revisiting the biofilm formation model: Starting the story from the liquid phase 11

2. eDNA is a key compound for biofilm formation, but also involved in biofilm switching 14

2.1. eDNA release in *Pseudomonas* sp. 15

2.2. eDNA release in other strains 16

3. Tracking biofilm switchers in the liquid phase 18

4. Tracking biofilm switchers: imaging and flow cytometry 23

5. Perspectives: Controlling biofilm switching in real time cytometry 26

Chapter 3 31

1. Abstract 33

2. Introduction 33

3. Material and methods 35

3.1. Strains and medium composition 35

3.2. Plasmid construction and genetic manipulations 37

3.3. Sample preparation 37

3.4. Bacteria staining protocols 38

3.5. Flow cytometry 38

3.6. Chemostat cultivation combined with online flow cytometry 39

3.7. DNase enzyme treatment 40

3.8. Confocal laser scanning microscopy (CLSM) 40

3.9. Quantification of biofilm and eDNA in 96-well plates 41

4. Results 42

4.1. Propidium iodide (PI) is a relevant single cell proxy for the detection of subpopulation of cells involved in the switching to biofilm.....42

4.2. Cell autoaggregation plays a crucial role in the continuum of phenotypic changes involved in the transition to a biofilm lifestyle.....47

4.3. P_{lapA}:YFP reporter exhibits low sensitivity and is not compatible with real-time monitoring based on automated flow cytometry.....50

4.4. Flow cytometry-based analysis identifies small changes in c-di-GMP signal in response to environmental nutrients 52

5. Discussion 53

6. Supplementary files.....57

Chapter 4 61

1. Abstract 63

2. Introduction 64

3. Material and methods 65

3.1. Strains and medium composition 65

3.2. Plasmid construction and genetic manipulations.....65

3.3. Plasmid transformation.....66

3.4. Quantification of biofilm growth in 96-well plates 69

3.5. eDNA production in planktonic cultures.....70

3.6. Biomass Quantification 71

3.7. Flow cytometry analyses (Off-line) 71

3.8. Microscopy images 72

3.9. Continuous cultivation with automated flow cytometry 72

4. Results 73

4.1. Biofilm switching is initiated early in the planktonic phase by a subpopulation of cells associated with eDNA 73

4.2. eDNA binding is correlated with cell auto-aggregation 75

4.3. Biofilm switching induces a fitness cost 77

4.4. Biofilm formation is associated with a bursty diversification processe 78

4.5. Control of bursts leads to reduced population diversification and biofilm formation 81

5. Discussion 83

6. Supplementary files 85

Chapter 5 91

1. Abstract 93

2. Introduction 93

3. Material and methods 96

3.1. Bacterial strains and growth conditions.....96

3.2. Labeling of strains with fluorescent proteins 97

3.3. Crystal violet assay for biofilm quantification 98

3.4. eDNA quantification in the planktonic phase.....99

3.5. Dry biomass quantification.....100

3.6. Microscopy and imaging of co-aggregate formed in liquid culture 100

3.7. Flow cytometry and PI staining.....101

3.8. Flow cytometry analysis of bacterial auto-aggregation auto and co-aggregation 101

4. Results 102

4.1. Using flow cytometry for detecting eDNA release, cellular aggregation, and co-culture composition 102

4.2. Cell auto-aggregation is exacerbated at the expense of final biofilm formation for a natural isolate 104

4.3. Fast biofilm switcher is able to capture slow biofilm switchers based on co-aggregation, leading to the formation of mixed biofilms 106

4.4. Unveiling co-aggregation capabilities: Enhanced co-aggregation of *P. putida* Δ*lap*A::YFP by natural isolate *P. composti*.....109

5. Discussion 113

6. Conclusion 118

7. Supplementary files 119

Chapter 6 123

1. Conclusion 125

1.1. Could we rely on PI-eDNA binding as a single-cell proxy that allows us to decipher the "key" subpopulation of cells involved in early biofilm formation? 127

1.2. Can the release of extracellular DNA (eDNA) by *Pseudomonas* sp. be considered as an early signal for controlling cell population involving biofilm switching? 128

1.3. What is the role of extracellular DNA (eDNA) in mediating co-aggregation in natural and synthetic co-cultures? 130

2. Perspective 131

Chapter 7 135

1. References 137

List of figures

Chapter 1 – General Introduction

Figure 1-1. Illustration of the main research methodology used in this research work.

Chapter 2 - State of the art

Figure 2-1. A. The original five-step model of biofilm development. B. Expanded model of biofilm formation with cell aggregates (adapted from (Sauer et al., 2022))

Figure 1-2. The life cycle of biofilm depicts functions of eDNA in the attachment, cell-cell adhesion, biofilm proliferation, detachment/dispersion, and HGT.

Figure 1-3. Scheme of the Segregostat set-up.

Chapter 3 - The quest for single-cell proxies related to biofilm switching

Figure 3-1. Flow cytometry and confocal laser scanning microscopy (CSLM) analyses illustrating the comparison of PI-positive cluster among planktonic and biofilm samples and effects of DNase treatment on PI- positive fraction of biofilm sample.

Figure 3-2. A. Biofilm formation ability of *P. putida* DGC, *P. composti (*natural isolate*), P. putida* KT2440*, P. putida Δlap*A**,** after 48h of batch cultivation. B. Comparison of PI-positive subpopulation fraction (%) during batch phase.

Figure 3-3. Flow cytometry and Confocal laser scanning microscopy (CSLM) images of *P. Putida* DGC (aggregation and biofilm) samples.

Figure 3-4. Effect of iron concentration on biofilm formation, extracellular DNA, and PI-positive subpopulation.

Figure 3-5. Analysis of the autoaggregation ability and Microscopy images of *P. putida* DGC, *P. putida* Δ*lapA*, and *P. Putida* KT2440, by flow cytometry.

Figure 3-6. Flow cytometry analysis of *Pseudomonas putida* KT2440- P_{lapA}::YFP in an automated bioreactor.

Figure 3-7. Flow cytometry analysis of *Pseudomonas putida* KT2440 Δ*lap*A Tn7::[*Ppel*A->gfp] under different carbon sources. The dynamic nature of GFP expression levels on a modified M9 medium containing different carbon sources.

Chapter 3 - Supplementary files

Figure 3-S1. Flow cytometry analysis of *Pseudomonas putida* KT2440 and evaluate the effect of deletion porins group B on PI positive fraction in *P. putida* KT2440 mutant.

Figure 3-S2. Plasmid maps. of A. pSEVA237Y plasmid map B. pSEVA237Y_pLapA sytem map

Figure 3-S4. Flow cytometry (Attune™ NxT -offline) analysis of *Pseudomonas putida* KT2440- p*lap*A::YFP during chemostat at different time points.

Figure 3-S5. Flow cytometry analysis of *Pseudomonas putida* KT2440 Δ*lap*A Tn7::[P*pel*A->gfp] on a modified M9 medium containing different carbon sources.

Chapter 4 - Release of extracellular DNA by *Pseudomonas* species as a major determinant for biofilm switching and an early indicator of cell population control

Figure 4-1. Cristal violet assay for the biofilm forming capability of different derivatives of *P. putida* KT2440 and *P. composti*. Time evolution of eDNA and PI positive cells (determined based on FC) during flask. Microscopy images (40x) of cells samples coming from flask experiments.

Figure 4-2. The scheme of the automated FC set up connected to a continuous cultivation device. Microscopy images (40X) taken during continuous cultivation. Binning of the time scatter profiles for the PI fluorescence, the FSC and SSC signals respectively. computation of the gradient of cells from the binned data for the PI fluorescence, the FSC and SSC signals respectively. Cumulated flux of cells extracted from the gradients of the three signals. Correlation matrix with the Pearson coefficients.

Figure 4-3. Planktonic dry weight and biofilm dry weight comparison in mono- and co-cultures after 24h. Dynamics of a co-culture *P. putida* DGC::GFP and *P. putida* Δ*lap*A::YFP cultivated in shake flask. Flow cytometry analysis of percentage of each strain in biofilm sample of co-culture after 24h.

Figure 4-4. Scheme of the Segregostat. Pulses of nutrients are added in the function of the ratio between PI negative and PI positive cells recorded by automated FC. Example of bursty diversification process involved in the sporulation of *Bacillus subtilis.* Applying environmental forcing based on Segregostat cultivation, the number of bursts is reduced. A more complex bursty diversification model proposed for *P. putida* KT2440. Time evolution of fluorescence bins associated with PI staining.

Figure 4-5. Evolution of entropy H recorded in function of the fitness cost associated to phenotypic switching in continuous cultivation (Chemostat cultivation, Segregostat cultivation). Comparative analysis of the mean level of information entropy H for the three modes of cultivation considered.

Chapter 4 -Supplementary files

Figure 4-S1. Flow cytometry analysis and confocal laser scanning microscopy (CSLM) images illustrating the comparison of PI positive cluster among planktonic and biofilm sample and effects of DNase treatment on PI positive fraction of biofilm sample.

Figure 4-S2. Biomass and glucose consumption (HPLC analysis) of A. *P. putida* Δ*lap*A::YFP , B. *P. putida* DGC::GFP , C. *P. putida* KT2440.

Figure 4-S3. Data processing steps related to automated FC. Processing the data from automated FC and computing of the flux of cells (F) and the entropy (H) of the cell population

Chapter 5 – Biofilm switching influences co-aggregation and the assembly of multi-species biofilm

Figure 5-1. Schematic illustration of the methodology used to explore microbial interactions and co-aggregation dynamics resulting from phenotypic switching in synthetic and natural co-cultures using flow cytometry and PI staining.

Figure 5-2. Comparing the biofilm formation, eDNA release, PI-positive subpopulation, and auto-aggregation percentage among synthetic and semi-synthetic strains.

Figure 5-3. Dynamics of a co-culture *P. putida* DGC::GFP and *P. putida* KT2440*::*YFP cultivated in a shake flask. Flow cytometry analysis of percentage of each strain in the co-culture. Planktonic and biofilm dry weight comparison in single species *P. putida* KT2440*::*YFP and dual-species *P. putida* DGC::GFP-*P. putida* KT2440*::*YFP . Percentage of PI cluster, eDNA release, auto-aggregation, and co-aggregation in mono-and dual-species after 30h. Flow cytometry analysis of percentage of each strain in biofilm sample of co-culture.

Figure 5-4. Dynamics diversity of composition of synthetic and natural co-cultures cultivated in a shake flask. Flow cytometry analysis of the percentage of each strain in the co-culture of **A.** *P. putida* DGC::GFP - *P. putida* Δ*lap*A::YFP **B.** *P. putida* DGC::GFP- *Providencia* sp. **C.** *P. Composti* - *P. putida* Δ*lap*A::YFP. Comparison of PI-positive cluster (%), co-aggregation, and eDNA content. Time evolution of eDNA and PI-positive cells and co-aggregation during the planktonic phase in dual-species during 30h planktonic growth.

Figure 5-5. Correlation between the presence of PI-positive subpopulations, eDNA content, and the degree of co-aggregation within a dual-species.

Figure 5-6. Illustration of strong co-aggregators of Case 1 (*P. putida* DGC::GFP - *P. putida* KT2440::YFP) and case 4 (*P. composti* - *P. putida* Δ*lap*A::YFP).

Chapter 5 -Supplementary files

Figure 5-S1. Time evolution of eDNA and PI-positive cells and co-aggregation during the planktonic phase in dual-species *P. putida* DGC::GFP and *P. putida* KT2440::YFP.

Figure 5-S2. Comparison of growth curves of mono-species and dual-species during 30h of batch cultivation.

Figure 5-S3: Planktonic and biofilm dry weight comparison in mono and co-culture of *P. putida* DGC::GFP - *P. putida* Δ*lap*A::YFP after 24h.

Figure 5-S4. Percentage of PI cluster, eDNA release auto-aggregation, and co-aggregation in mono-and dual-species of A. *P. putida* DGC::GFP - *P. putida* Δ*lap*A::YFP B. *P. putida* DGC::GFP- *Providencia* sp. after 30h.

Figure 5-S5: Macroscopic view of shake flasks experiments of semi-synthetic co-culture of *P. putida* DGC::GFP- *Providencia* sp. The microscopic picture of the bottom of the flasks of *P. putida* DGC::GFP- *Providencia* sp, **B.** *P. composti* - *P. putida* Δ*lap*A::YFP co-culture in shake flask. The microscopic picture the formation of large co-aggregates at the bottom of flask that were visible to the naked eye. Microscopy imaging of the big aggregates shows the presence of both stains in co-aggregates.

List of tables

Chapter 3 – The quest for single-cell proxies related to biofilm switching

Table 3-1. Bacterial strains and plasmids were used in this study.

Table 3-2. The primers are used to amplify the pSEVA237Y and pLapA.

Chapter 4 – Release of extracellular DNA by *Pseudomonas* species as a major determinant for biofilm switching and an early indicator of cell population control

Table 4-1. Bacterial strains and plasmids were used in this study.

Table 4-2. Oligonucleotides were used in this study.

Chapter 5 – Biofilm switching influences co-aggregation and the assembly of multi-species biofilm

Table 5-1. Bacterial strains and plasmids were used in this study.

Table 5-S1. Summary of the characterization of synthetic and natural strains.

Chapter 6 –Main conclusion and perspective

Table 6-1. Summary of main conclusion and perspective.

List of abbreviations

AFM: Atomic force microscopy

c-di-GMP: Cyclic diguanosine-5′-monophosphate

CLSM: Confocal laser scanning microscopy

CV: Crystal violet

DGC: Diguanylate cyclase

eDNA: Extracellular DNA

EIS: Electrochemical impedance spectroscopy

EPS: Extracellular polymeric substances

FC: Flow cytometry

FSC: Forward scatter

GFP: Green fluorescent protein

GRN: Gene regulatory network

HAQs: 4-hydroxy-2-alkylquinolines

HGT: Horizontal gene transfer

HQNO: (2-n-heptyl-4-hydroxyquinoline-Noxide)

LB: Lysogeny broth

MCS: Multiple cloning sites

MVs: Membrane vesicles ()

NM: Not measurable

Ns: Not significant

OM: Outer membrane

PBS: Phosphate-buffered saline

PI: Propidium iodide

PQS: Pseudomonas quinolone signal

QCM: Quartz crystal micro

QS: Quorum sensing

RID: Refractive Index Detector

ROS: Reactive oxygen species

RT: Room temperature

SD: Standard deviation

SEM: Scanning electron microscopy

SPR: Surface plasmon resonance

SSC: Side scatter

TEM: Transmission electron microscopy

YFP: Yellow fluorescent protein

Chapter 1

General introduction

1. Characterization of phenotypic switching involved in early biofilm formation in *Pseudomonads* sp.

Our understanding of bacterial life has traditionally classified bacteria in their natural environment into two distinct forms. The first form involves bacteria existing as independent cells, capable of self-regulation, and freely floating in their surroundings, known as planktonic bacteria. The second form entails bacteria coming together and organizing into microbial aggregates known as biofilms. Initially, the term "biofilm" was used to describe bacterial cells attached to a surface. However, recent advancements in research have illuminated that bacteria can aggregate and form biofilms even without being attached to surfaces (Costerton et al., 1978 ; Flemming & Wingender, 2010). A growing body of evidence suggests that biofilms can form in fluid environments as well. These aggregates can arise through various mechanisms such as clonal growth, co-aggregation, or induced by bacterial extracellular polymeric substances (EPS) or host fluids. What's fascinating is that these fluid-based aggregates exhibit many characteristics previously attributed exclusively to surface-associated biofilms. It's important to note that these biofilm-like aggregates are not limited to controlled laboratory conditions; they have been discovered as part of the human microbiota in numerous chronic infection sites and are even present in the environment (Bay et al., 2018; Bjarnsholt et al., 2013). This discovery challenges previous understanding of the biofilm life cycle and suggests a more general model for biofilm formation by highlighting the diverse and adaptable nature of bacterial life (Sauer et al., 2022).

Biofilms consist of cells surrounded by a matrix composed of extracellular polymeric substances (Hall-Stoodley et al., 2004; Irie et al., 2012). EPS, which has been found to contain a significant amount of protein and extracellular DNA (eDNA), plays a crucial role in the architecture of bacterial biofilms (Okshevsky et al., 2015). eDNA, in particular, has gained increasing attention as a key component of EPS. It is a versatile and multifunctional molecule that provides numerous advantages to microbial cells, facilitating their survival in highly challenging environmental conditions. During the growth of a biofilm, bacteria undergo a distinctive phenotypic shift, which sets them apart from their planktonic counterparts. These distinct phenotypic states play vital roles in various fields, including ecosystem dynamics, agriculture, industry, and medicine. Therefore, it is extremely important to understand the type of phenotype and environmental change under which bacteria transition from one state to the other.

Pseudomonas putida is an environmental, Gram-negative bacterium that is able to form biofilms on a variety of biotic and abiotic surfaces and can ubiquitously colonize the surface of plant roots (Martins Dos Santos et al., 2004; Nelson et al., 2002; Nikel et al., 2014; Timmis, 2002). *P. putida* has been a laboratory model for examining the lifestyle and activities of environmental bacteria (Weimer et al., 2020) . The process of biofilm development in *P. putida* is intricate and regulated by a complex gene regulatory network (GRN). Although substantial advancements have been achieved in comprehending the various stages of biofilm development, the current knowledge primarily concentrates on studying mature biofilms or examining differential gene expression during the transition from planktonic to biofilm states. However, there is still a need for quantitative approaches that can effectively anticipate the specific conditions governing this critical transition.

2. Objectives and research methodology

Our research work focuses on investigating the transition from free-floating bacteria to the initial stages of biofilm formation, including the development of primary biofilm phenotypes and aggregates. Our objective is to pinpoint the precise point at which a biofilm phenotype starts to emerge. In particular, we aim to introduce a reliable single-cell proxy that can effectively monitor the phenotypic switching that occurs during the early stages of biofilm development. To achieve this goal, we have employed automated flow cytometry (FC) as a high-throughput method with an appropriate single-cell proxy to track and control phenotypic switching during the transition between planktonic, aggregate, and biofilm states. The introduction of a cell-machine interface provides the ability to continuously monitor the switching behavior of individual cells in a population, enabling real-time responsiveness (Henrion et al., 2023) (Delvigne & Noorman, 2017). This innovative concept has gained significant traction in the creation of the Segregostat system (Nguyen et al., 2021; Sassi et al., 2019). The Segregostat utilizes online flow cytometry to accurately measure the rate of cell switching and subsequently initiate corresponding environmental switching **(Figure 1-1).**

Throughout our research, we achieved a significant breakthrough by introducing Propidium iodide (PI) as a highly effective biomarker for tracking phenotypic switching. We specifically targeted the unique characteristics of extracellular DNA to monitor the dynamics of biofilm switching at the single-cell level. The utilization of PI staining allowed us to validate the significance of eDNA across various population states, including the planktonic phase, aggregation, and biofilm, shedding light on its impact on phenotypic diversification. Our findings demonstrate that the early stages

of biofilm development can be detected in planktonic cultures by assessing the extent of auto-aggregation. Leveraging the benefits of reactive flow cytometry, coupled with a well-designed control strategy and an appropriate single-cell biomarker, we were able to accurately assess the initial biofilm-phenotype state of bacteria with high real-time resolution **(Figure 1-1).**

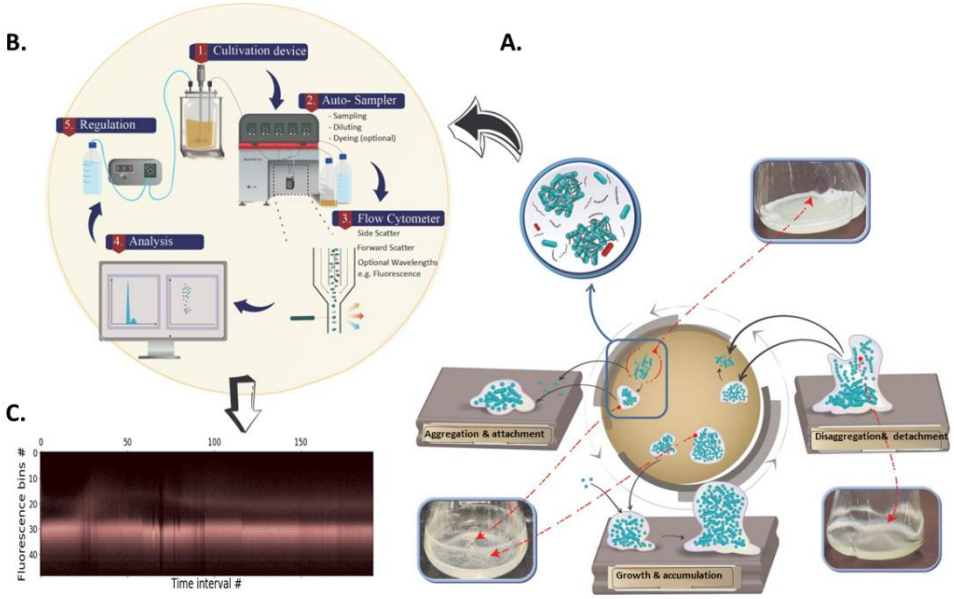

Figure 1-1. Illustration of the main research methodology used in this research work. **A.** Expanded model of biofilm formation incorporating cell aggregate: The focus of the research is on early biofilm formation including the transition of planktonic cells to aggregate phenotype in liquid phase. **B.** Graphic of bioreactor coupled with reactive automated flow cytometry and regulation pump to control microbial diversification. **C.** Example of time scatter plot obtained based on PI-staining.

Our study represents a pioneering investigation in the field, as it is the first to focus on real-time analysis of biofilm switching at the single-cell level. Through the combination of PI staining-based eDNA and advanced flow cytometry techniques, our research provides invaluable insights into the early dynamics of biofilm formation. This multifaceted approach enhances our understanding of biofilm behavior and facilitates the development of innovative methods for biofilm control and manipulation.

3. Chapter-by-chapter overview

State of art

This chapter provides a comprehensive literature review on early biofilm formation in a liquid phase. It begins with an overview of the life cycle of biofilms, emphasizing current models that incorporate the role of aggregates in biofilm formation. Afterward, the importance of extracellular eDNA as the main component of biofilm's EPS in a different stage of biofilm development is highlighted. In the following, the chapter delves into recent research and advanced methodologies for tracking biofilm switchers in the liquid phase. Finally, the chapter provides an overview of a novel methodology aimed at controlling and mitigating biofilms.

The quest for single-cell proxies related to biofilm switching

This chapter primarily focuses on the initial stages of biofilm formation, specifically the cell decision-making process involved in the transition of individual cells from a planktonic state to a sessile state. Characterizing this process is challenging due to the absence of appropriate fluorescent reporters and the formation of cell aggregates during the transition, which complicates single-cell analyses. Despite the limited sensitivity and detectability of various fluorescent biosensors evaluated in this study, we made an intriguing discovery that a simple propidium iodide (PI) staining method could aid in characterizing biofilm switching. Our research demonstrates that the presence of PI-positive subpopulations, indicative of extracellular DNA (eDNA) binding, correlates with the formation of aggregates and the biofilm-forming capabilities of *Pseudomonas putida* KT2440 and engineered derivatives with modified biofilm-forming abilities. By analyzing the dynamic changes in PI-positive cells using flow cytometry (FC) analysis, we identified multiple phenotypes. These results highlight that PI staining is a rapid, convenient, and versatile technique for monitoring the phenotypic switching of *Pseudomonas* sp. during early biofilm formation.

Control of biofilm switching in *Pseudomonas putida* KT2440 based on reactive flow cytometry

Building upon the findings of the previous chapter, which established a strong correlation between PI staining and both extracellular DNA release and cell auto-aggregation, two crucial steps in biofilm formation, we sought to recreate the dynamics of cell switching to the biofilm state for *Pseudomonas putida* KT2440 using automated flow cytometry. Our observations revealed a bursty diversification process, where a small subpopulation of cells made a sudden decision to transition to the sessile state, followed by a significant decrease in fitness for those cells that underwent the

switch. However, the bursty diversification processes associated with biofilm switching exhibited irregular patterns. This irregularity stemmed from the complex cell auto-aggregation that occurs during biofilm switching. To address this irregularity and promote the fitness of the non-differentiated fraction of cells, we devised a cell-machine interface that could automatically detect these bursts and deliver nutrient pulses based on a feedback control loop. This strategy yielded remarkable results, leading to a significant reduction in biofilm formation. These findings offer fresh insights into the early decision-making process underlying biofilm switching in *P. putida*. Furthermore, it suggests that the dynamics of phenotypic diversification could be strategically controlled to mitigate biofilm formation.

Biofilm switching influences co-aggregation and the assembly of multi-species biofilm

This chapter explores the remarkable potential of co-aggregation and extracellular DNA release in co-cultures comprising synthetic and natural strains with diverse capabilities in auto-aggregation and biofilm formation. To investigate the dynamics of these co-cultures, we employed flow cytometry and PI staining as powerful monitoring tools. Our findings unveil intriguing insights into the cooperative relationships within co-cultures. Specifically, we observed that the combination of *P. composti* with *P. putida* Δ*lap*A exhibited the strongest cooperative interaction, leading to the formation of visibly large macroscopic co-aggregates, as evidenced by the presence of *P. putida* Δ*lap*A. Similarly, when *P. putida* DGC::GFP was paired with *P. putida* KT2440::YFP, an increased degree of co-aggregation was observed, resulting in a higher population of PI-positive cells. These results underscore a robust correlation between the abilities of biofilm formation, co-aggregation, eDNA release, and the presence of PI-positive cells. By shedding light on these strong correlations, our data introduce novel methodologies for studying the dynamics of auto- and co-aggregation development at the single-cell level and highlights the importance of cooperative interactions among bacterial strains in shaping biofilm communities.

General conclusion and perspective

To the best of our knowledge, our study represents a pioneering investigation that explores an innovative methodology utilizing propidium iodide (PI) as a novel single-cell proxy for targeting extracellular DNA (eDNA). By leveraging the distinctive characteristics of eDNA and integrating control strategies with advancements in computational and control theory, specifically Segrogostat (Henrion et al., 2023; Sassi et al., 2019) we effectively evaluate the initial biofilm-phenotype state of bacteria.

However, it is crucial to expand our understanding of single-cell proxies to discover more precise alternatives that specifically focus on early phenotypic switching, unraveling the exact mechanism behind eDNA release, and exploring diverse control strategies within Segrogostat. These endeavors unlock new possibilities for regulating biofilm-related processes and other applications where biofilms play a critical role.

Chapter 2

State of the art

2.1. Revisiting the biofilm formation model: Starting the story from the liquid phase

Over the past 40 years, it has been shown bacteria typically exist in one of two phenotypic states: either a unicellular lifestyle, in which the cells are swimming freely, also called planktonic, or as immobilized, surface attached in which the cells are sessile and form biofilms (Berlanga & Guerrero, 2016; Costerton et al., 1978 ; H. C. Jones et al., 1969). In the canonical picture of biofilm development, it has traditionally been thought that individual bacterial cells seed a surface, these cells then proliferate to form first micro-colonies and later three-dimensional biofilm (Davey & O'toole, 2000; Monds et al., 2007; William Costeton et al., 1995). This model proposed that the formation of biofilms is a cyclic process that occurs in a five-stages process (**Figure 2-1A**) (Sauer et al., 2002; Stoodley et al., 2002).

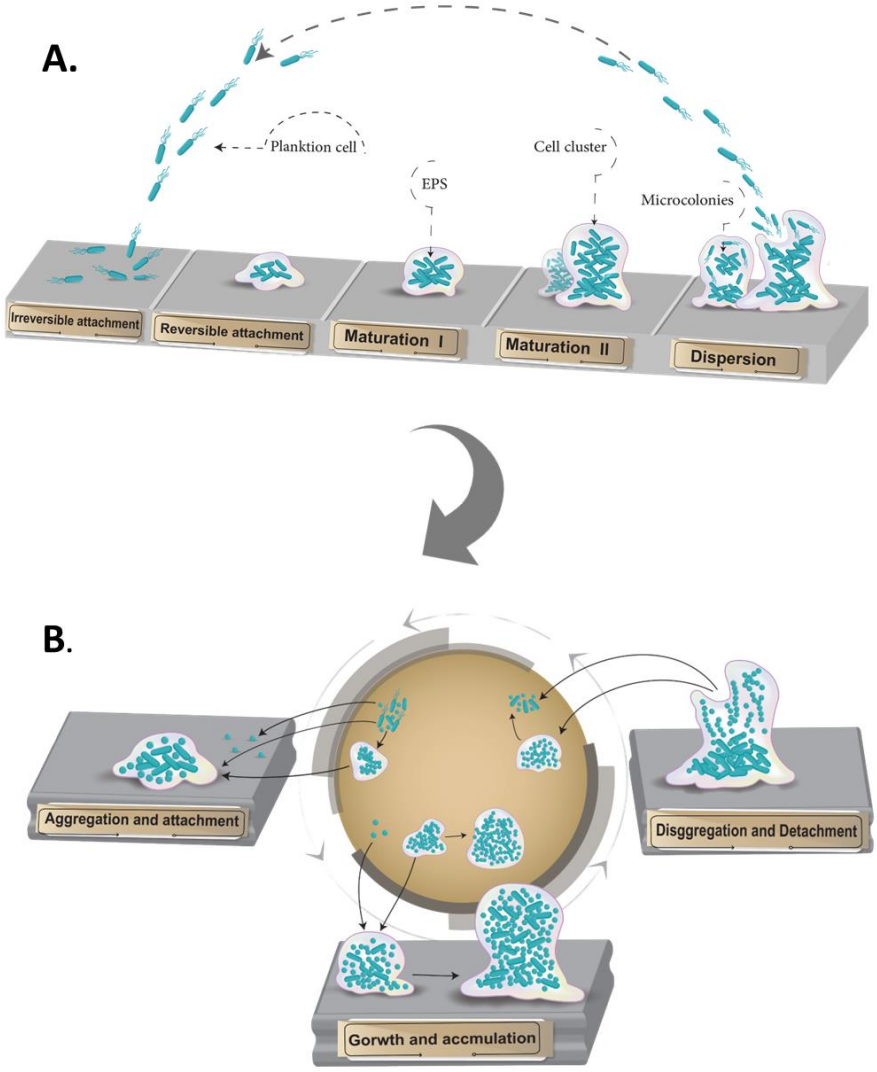

Figure 2-1. A. The original five-step model of biofilm development. These steps were referred to as reversible and irreversible attachment, maturation I and II (involving clump and microcolony formation, respectively), and dispersion (adapted from (Stoodley et al., 2002)). During the initial stage of reversible attachment, bacteria can attach to the substratum either through their cell pole or flagellum. This is followed by longitudinal attachment. The transition to irreversible attachment occurs simultaneously with a decrease in the reversal rates of flagella, a decrease in the expression of flagella genes, and the production of components that form the biofilm matrix. As the biofilm matures, cell clusters appear within

the matrix, forming layers several cells thick (referred to as maturation I stage). These clusters eventually develop into fully mature microcolonies (referred to as maturation II stage). Dispersion is observed when there is a decline in the matrix components and their degradation. The dispersed cells regain their motility and exhibit increased susceptibility to drugs compared to the cells within the biofilm. One limitation of the current biofilm model is its inability to account for non-surface-attached aggregates, which are commonly observed in clinical or environmental settings. **B.** Expanded model of biofilm formation with cell aggregates (adapted from (Sauer et al., 2022)). The updated model proposed for biofilm formation incorporates three main events that occur regardless of surfaces and the initiation from single-cell planktonic bacteria. These events are as follows: Aggregation and attachment: In this event, bacteria come together in aggregates or attach themselves to both biotic and abiotic surfaces. Growth and accumulation: During this event, the aggregated bacterial colonies expand by growing and recruiting surrounding cells, leading to the accumulation of biomass. Disaggregation and detachment: In this event, bacteria have the capability to leave the biofilm either as aggregates or as individual cells, depending on the specific mechanisms involved.

Each biofilm developmental stage exhibits unique patterns of gene expression (Stoodley et al., 2002). Adaptations of this model have also been made for other species, such as the soil bacterium *Bacillus subtilis* (Vlamakis et al., 2013), *Staphylococcus aureus* (Moormeier & Bayles, 2017), as well as for algal biofilms (Hu et al., 2021).

Nevertheless, many biofilm-producers bacteria tend to form dense aggregated clusters in liquid (planktonic phase) (Bossier & Verstraete, 1996; Haaber et al., 2012). Auto-aggregation i.e., the aggregation of cells belonging to the same species, is a process that is particularly important for *P. putida*, the bacterium that will be considered in this work (Farrell & Quilty, 2002; Nwoko & Okeke, 2021). In this context, it is becoming increasingly evident that biofilms do not necessarily require surface attachment to form. The aggregates floating in the liquid phase exhibit many of the features previously attributed only to surface-associated biofilms (Bay et al., 2018; Bjarnsholt et al., 2013; Kragh et al., 2023; Melaugh et al., 2023). The presence of cell aggregates in the liquid phase makes difficult the distinction between phenotypes related to planktonic and biofilm states. As an example, it has been shown that both *S. aureus* and *P. aeruginosa* can grow as a mixture of planktonic and aggregate cells in liquid cultures (Nørskov Kragh et al., 2018; Schleheck et al., 2009).

Many natural and infectious biofilms originate wholly or partially from pre-formed cell aggregates, where bacterial cells tend to clump as multicellular aggregates. Thus, it is very likely that when a biofilm is assembled, some cells may attach to the surface already in an aggregated state. In support of this view, evidence exists for the seeding

of infections by pathogenic bacteria already in an aggregated state (Faruque et al., 2006; Hall-Stoodley et al., 2004), and bacterial aggregates are abundant in cystic fibrosis(Bjarnsholt et al., 2009; Burmølle et al., 2010) and tuberculosis (Anton et al., 1996) infections.

Given the tendency of many bacteria to either auto- (same species) or co-aggregate (between different species) and the frequent observation of aggregates in various ecosystems (Burmølle et al., 2010; Monier & Lindow, 2003; Stoodley et al., 2002), it seems likely that natural biofilms are often initiated from pre-formed aggregates. Additionally, one of ecological benefit of seeding by aggregates is accelerated switching to a biofilm-like phenotype and increased tolerance to antibiotic and host defense, but at the expense of a fitness cost i.e., due to the production of matrix components or the reduced accessibility of aggregates to nutrient by comparison with individual cells (Alhede et al., 2011; Dastgheyb et al., 2015; Worlitzsch et al., 2002).

According to the importance of cellular aggregation, current models for biofilm formation should be reconsidered by incorporating the role of aggregates. Recently, Karin Sauer and colleagues developed a more general model for biofilm formation, including the three major steps i.e., aggregation, growth, and disaggregation for biofilm growth, irrespective of the presence of a surface **(Figure 2-1B).** This model accurately illustrates biofilm formation of all microorganisms, habitats, and microenvironments (Sauer et al., 2022).

2.2 eDNA is a key compound for biofilm formation, but also biofilm switching

Bacterial biofilms are composed of a community of cells either aggregated or attached to a surface and embedded in a self-produced extracellular polymeric substance (EPS) matrix. In most cases, EPS represents around 90% of the total biofilm biomass and is mainly composed of polysaccharides, lipids, proteins, and eDNA (Fulaz et al., 2019). Over the past few years, a great deal of attention has been given to extracellular DNA (eDNA) as an omnipresent component of *Pseudomonas* sp.'s biofilm. eDNA was first visualized on biofilms formed at a solid-liquid interface and was produced by *Pseudomonas aeruginosa* PA01 (Whitchurch et al., 2002). In this context, eDNA promoted the initial adhesion of cells to surfaces and cell aggregation and interacted with EPS to form fiber-like networks stabilizing the biofilms (Mann & Wozniak, 2012; Moshynets & Spiers, 2016). Physicochemical mechanistic explanations for eDNA-mediated adhesion and aggregation come also from the extended Derjaguin, Landau, Verwey, Overbeek (DLVO) theory. In this perspective, eDNA-mediated bacterial adhesion and aggregation would occur through attractive Lifshitz–Van der Waals and acid–base interactions despite existing electrostatic

repulsion. In the extended DLVO theory, acid–base attraction results from interactions between electron-accepting and electron-donating moieties on cells surfaces and eDNA (Das et al., 2010, 2011). Attractive short-range acid-base interactions would contribute to eDNA binding with other EPS biopolymers and other intercalating metabolites such as pyocyanin, facilitating EPS anchoring on bacterial cell surfaces. eDNA has clearly emerged to play a pivotal role in cell adhesion during the early stages of biofilm development and plays a key structural role in mature biofilms (Okshevsky et al., 2015; Vandana & Das, 2022). eDNA plays a crucial role in various aspects of the biofilm matrix, including providing structural integrity, facilitating bacterial adhesion, chelating metals, supporting metabolic vitality, enhancing antibiotic resistance, and enabling horizontal gene transfer (Das et al., 2010; Okshevsky et al., 2015)**(Figure 2-2).**

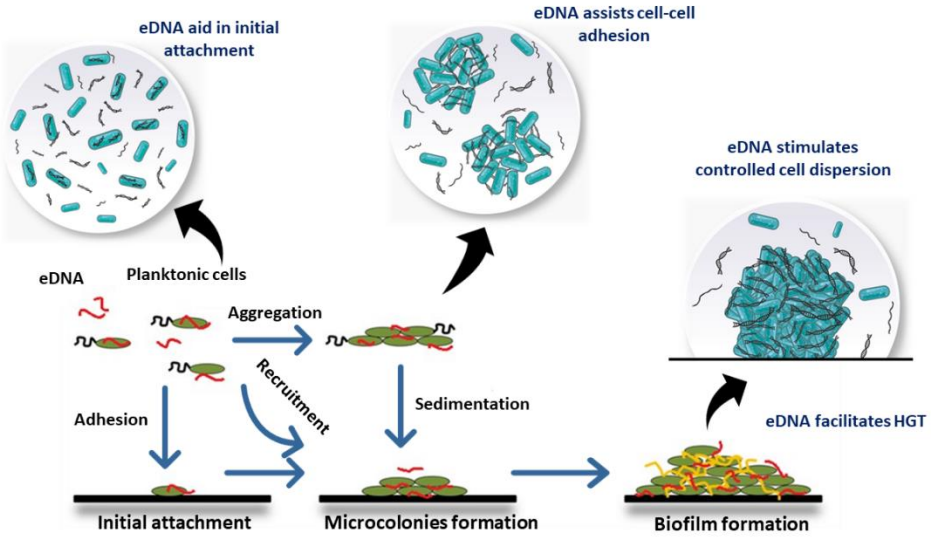

Figure 2-2. The life cycle of biofilms depicts functions of eDNA in the attachment, cell-cell adhesion, biofilm proliferation, detachment/dispersion, and HGT.

Despite all the intense research work conducted over several decades regarding the roles of eDNA in biofilms, the physiological mechanisms that are involved in eDNA release and regulation still remain unknown or only partly unveiled for a limited number of bacterial species (Sarkar et al., 2020). Biofilm eDNA is secreted in different ways, and microorganisms use different mechanisms for releasing eDNA. Based on

our current understanding, the lysis of bacterial cells is the main mechanism of eDNA release.

2.2.1. eDNA release in *Pseudomonas* sp.

Among Gram-negative bacteria, *P. aeruginosa* is one of the most investigated species for eDNA release. Large amounts of eDNA release in the case of *P. aeruginosa* were reported to be mediated by quorum sensing (QS) involving the signaling molecule N-acyl-L homoserine lactones and the *Pseudomonas* quinolone signal (PQS) in planktonic cell cultures (Allesen-Holm et al., 2006; Tahrioui et al., 2019; Webb et al., 2003). PQS and pyocyanin are best-known mechanisms to promote eDNA release through H_2O_2-mediated cell lysis in *P. aeruginosa* (Das & Manefield, 2012; Fuxman Bass et al., 2010; Nakamura et al., 2008). R- and F-pyocin gene clusters can promote eDNA release through explosive cell lysis in *P. aeruginosa* (Turnbull et al., 2016). Explosive cell lysis of *P. aeruginosa* has been demonstrated to play an important role in releasing membrane vesicles (MVs) and eDNA. Currently, it is considered that MVs are responsible for eDNA presence in the medium whether by its own lysis with the subsequent eDNA release or by triggering the lysis of a subpopulation of cells (Allesen-Holm et al., 2006). MVs production is not a random process but is dependent on QS signals. However, a little is known about the role of *P. aeruginosa* OMVs in releasing eDNA (Cirz et al., 2006; Ibáñez de Aldecoa et al., 2017). In addition, it has been reported eDNA release may be activated by lambda prophage induction In *P. aeruginosa* (Sarkar, et al., 2020)

In a recent study, Tahrioui and co-workers showed that 4-hydroxy-2-alkylquinolines (HAQs) molecules and PrrF small noncoding RNAs both play crucial roles in signaling eDNA release within *P. aeruginosa* biofilms (Tahrioui et al., 2019). They reported that HQNO(2-n-heptyl-4-hydroxyquinoline-Noxide) induces the production of reactive oxygen species (ROS), which results in cell membrane damage and consequent eDNA release (Tahrioui et al., 2019). Several other *pseudomonad* species are known to produce eDNA, such as *P. chlororaphis* (D. Wang et al., 2016), *P. putida* KT2440 (D'Alvise et al., 2010), *Pseudomonas fluorescens* (W Catlin & Cunningham, 1958) and *Pseudomonas stuzeri* (Stewart et al., 1983).

2.2.2. eDNA release in other strains

Gram-positive strains of *Neisseria gonorrhoeae*, which contain a specific genetic island, can release large amounts of DNA for natural transformation into the medium, during exponential phase, unrelated to cell lysis (Dillard & Seifert, 2001; Hamilton et al., 2005). Thus, eDNA must be released by an active mechanism, maybe such as the

type IV secretion system, or through association with vesicles. For *S. epidermidis*, QS-dependent eDNA secretion is mediated by autolysins (Qin et al., 2007).

eDNA is a very versatile and multifunctional molecule, contributing to bacterial aggregation and promoting intercellular adhesion (Lister & Horswill, 2014; Mlynek et al., 2020). The presence of extracellular DNA (eDNA) on bacterial cell surfaces promotes adhesion and surface aggregation through attractive Lifshitz-Van der Waals and acid-base interactions. eDNA creates favourable conditions for bacterial adhesion to hydrophobic surfaces and facilitates surface aggregation of adhering bacteria on hydrophilic surfaces, enhancing the overall adhesion process (Das et al., 2010, 2011). *P. aeruginosa*, upon growth in liquid culture, forms large aggregates containing massively packed viable cells and eDNA (Schleheck et al., 2009). *P. aeruginosa* PA01 eDNA-based planktonic cell clusters may represent a surface-colonizing adaptation if survival and attachment rates are better than for single cells (Schleheck et al., 2009). In *Staphylococcus epidermidis*, the eDNA improves initial cell adhesion and surface aggregation(Das et al., 2010). Furthermore, in *Neisseria gonorrhoeae*, the single-stranded eDNA is of considerable importance in initial biofilm formation (Zweig et al., 2014). In *Acidovorax temperans*, the eDNA can meditate the attachment to glass wool (Heijstra et al., 2009). eDNA arbitrates the attachment to abiotic material surfaces allowing bacterial anchorage (Blakeman et al., 2019) and stabilizes the biofilm architecture (Jurcisek & Bakaletz, 2007; Kiedrowski et al., 2011) by interlinking different polymeric components. eDNA can interact with other components of EPS, and it plays multiple roles in *Pseudomonas* biofilm formation. For example, the exopolysaccharide Psl/Pel–eDNA complex can form the biofilm skeleton to structurally support *P. aeruginosa* (Jennings et al., 2015; S. Wang et al., 2015). eDNA is found to be required for the early stage of the biofilm formation of *P. aeruginosa* after DNaseI treatments (Whitchurch et al., 2002). Na Peng and colleagues reported the interaction between eDNA and EPS plays a vital role in initial aggregation and the construction of 3D biofilm architecture *B. subtilis* SBE1 (Peng et al., 2020) Moreover, it has been reported aggregation can occur in the liquid phase mediated by host polymers such as mucin and eDNA (Secor et al., 2018). Additionally, eDNA play an essential role in multiple biological processes such as horizontal gene transfer (Hall & Mah, 2017; Molin & Tolker-Nielsen, 2003), actively contributes to biofilm tolerance by controlling the diffusion of antimicrobials (Doroshenko et al., 2014), acidify the local environment and stimulate antibiotic resistance phenotypes and virulence traits (Wilton et al., 2016), and serves as a nutrient source during starvation (Finkel & Kolter, 2001), promotes efficient extracellular electron transfer by phenazines (i.e., PYO) (Saunders et al., 2020).

Considering all the information, it becomes evident that eDNA is an exceptionally versatile and multifunctional molecule. It actively contributes to various stages of biofilm formation and facilitates bacterial aggregation by promoting intercellular adhesion. In our study, we specifically targeted the distinctive characteristics of eDNA to investigate the dynamics of biofilm switching at the single-cell level. Notably, we observed subpopulations of eDNA-bind bacteria (specifically *Pseudomonas putida*) in the liquid phase, which correlated with their biofilm-switching capabilities. Our findings demonstrate that early biofilm development can be detected in planktonic cultures by assessing the degree of aggregation and the ability of bacteria to release eDNA.

2.3. Tracking biofilm switchers in the liquid phase

It is critical to understand how phenotypic switching leads to the formation of biofilms, the understanding of which has important consequences from both a fundamental (i.e., microbial physiology) and applied (i.e., bioprocesses) point of view. Very little is known about phenotypic switching upon shifting between sessile and planktonic states. The shift between sessile and planktonic states is key for the fitness of the whole population since fast switching can impair the growth of cells in the liquid phase, whereas slow switching can affect cell survival upon stress exposure. These transitions depend on a complex array of factors that control this switch which is determined by the intrinsic properties of the individual cells as well as those of their surrounding environments. This transition is generally associated with the downregulation of motility genes and the upregulation of matrix production genes (Kampf et al., 2018; Römling et al., 2013). Many environmental cues induce each of the two opposing phenotypes and the gene regulatory network that orchestrates the shift is complex.

Current research indicates the second messenger, cyclic diguanosine-5′-monophosphate (c-di-GMP), seems to be globally involved in regulation of the switch between motile and sessile lifestyles (Hengge et al., 2009). In general, the low levels of c-di-GMP associated with downregulate the production of adhesins and extracellular matrix components and leads to free-swimming planktonic and motile states and high levels of c-di-GMP associated with production of adhesins and extracellular matrix components which enable bacteria to form biofilms (Römling et al., 2013). The first phenotypes clearly related to c-di-GMP signaling were cell differentiation in *Candida crescentus* (R. Paul et al., 2004) Later role of c-di-GMP for coordinating the “lifestyle transition” from motility to sessility and vice versa has been reported in many bacteria, such as *G. xylinus*, *V. cholerae*, *S. enterica*, *E. coli*,

Pseudomonas putida, *Pseudomonas fluorescens*, *Pseudomonas aeruginosa and Burkholderia cenocepacia* (Römling et al., 2005; Simm et al., 2004; Tischler & Camilli, 2004).

c-di-GMP is a ubiquitous second messenger that regulates a wide range of biological processes in bacteria, including motility, surface attachment, virulence and persistence. The regulatory networks controlling c-di-GMP are generally complex and understudied. c-di-GMP influences the decision-making in bacteria in response to the environmental signals they perceive as its concentration determines the cellular fate of bacteria. Over the years, various fluorescence-based sensors have been developed to detect c-di-GMP levels.

In *P. aeruginosa*, the initial surface-sensing and microcolony-forming stage of biofilm formation is associated with an increase in the levels of c-di-GMP (Laventie et al., 2019; Luo et al., 2015). Recently, transcriptional fusions of fluorescent proteins to c-di-GMP regulated promoters were used as indirect reporters of the intracellular dinucleotide to understand the mechanism of c-di-GMP regulation of *P. aeruginosa* after surface attachment (Rodesney et al., 2017; Rybtke et al., 2012). For example, a transcriptional fusion of the promoter of the *cdr*A gene, encoding a large adhesin in *Pseudomonas aeruginosa*, to the gene encoding for green fluorescent protein (GFP) has been previously used to analyse the c-di-GMP dynamics during surface attachment by time-lapse fluorescence confocal microscopy (Rodesney et al., 2017). This revealed that *P. aeruginosa* responds to surface attachment by a high concentration of c-di-GMP which is required for transition from planktonic to biofilm phase (Rodesney et al., 2017; Rybtke et al., 2012). Nair and co-workers have used similar constructs to visualize the spatial and temporal distribution of c-di-GMP in real-time in a biofilm (Nair et al., 2017). Using CFP as a constitutive marker and GFP as a c-di-GMP reporter, it was elucidated that there is a non-uniform distribution of c-di-GMP in the biofilm and that its concentration varies at different stages of biofilm development.

Moreover, Armbruster et al. monitored individual cells of *P. aeruginosa* producing c-di-GMP as they began to form biofilms. Unexpectedly, not all cells increased their c-di-GMP levels when they were first attached to a surface. A fluorescent reporter for c-di-GMP revealed the presence of two functionally distinct subpopulations: cells with high c-di-GMP represent ‘biofilm founders’ that rapidly initiate matrix production, while those with low levels represent ‘surface explorers’ which survey the surface (Armbruster et al., 2019)

Interestingly, c-di-GMP levels can also differ between individual cells of an isogenic population leading to phenotypic diversity, as demonstrated by *Salmonella Typhimurium* during infection (Petersen et al., 2019). Moreover, in *Caulobacter crescentus* asymmetrical distribution of c-di-GMP within the cell through local action of c-di-GMP-metabolizing enzymes was reported to be critical for positioning of the polar flagellum (Christen et al., 2010). Planktonic *P. aeruginosa* has been shown to achieve heterogeneity among very low levels of c-di-GMP through asymmetrical partitioning of a diguanylate cyclase during cell division, leading to diverse swimming motility behaviors (Kulasekara et al., 2013). More recently, this same asymmetrical cell division mechanism was shown to generate two subpopulations of *P. aeruginosa*, one piliated and one flagellated, that are each required for efficient tissue colonization (Laventie et al., 2019). Together, these studies support a role for c-di-GMP heterogeneity in generating diverse bacterial behaviors during both biofilm and planktonic growth.

Serra and Hengge 2019 showed the usage of a c-di-GMP pCsgD::*gfp* reporter in *E. coli* and further highlighted the role of c-di-GMP and its heterogeneity in the three-dimensional structure of a biofilm (Serra & Hengge, 2019). Furthermore, it has reported the application of a biosensor based on bimolecular fluorescence complementation of a YPet fusion to the c-di-GMP effector BldD (CensYBL) which can detect fluctuations in intracellular c-di-GMP levels in the Gram-negative species *E. coli* and *S. Typhimurium* (Halte et al., 2022)

c-di-GMP levels control the *Pseudomonas putida* lifestyle switch by means of a complex network involving multiple regulatory and signal transduction element (Fernández & Romero, 2014). *Pseudomonas putida* KT2440 is a non-pathogenic soil bacterium endowed with the ability to adapt to a large variety of physicochemical and nutritional niches (Benedetti et al., 2016; Nikel et al., 2014), and able to form biofilms depending on the environmental conditions (Volke & Nikel, 2018). In *P. putida* KT2440, biofilm formation is effectively dependent on the surface adhesion proteins LapA and LapF, which are known to play an important role in biofilm formation (Hinsa et al., 2003; Martínez-Gil et al., 2010). Additionally, the GacS/GacA two components system and the flagellar master regulator FleQ have been proposed to be involved in biofilm formation, but the mechanistic details are largely unknown (Martínez-Gil et al., 2014). FleQ interacted with its partner protein FleN to inversely modulate biofilm formation and motility in response to c-di-GMP. When the intracellular c-di-GMP levels were high, the FleQ-FleN complex enabled transcriptional activation of biofilm-related genes but caused transcriptional

repression of flagellar operons (Baraquet et al., 2012; Claudine & Harwood, 2013; Nie et al., 2017).

In *P. putida*, nutrient availability, and intracellular levels of c-di-GMP control the presence of LapA in the outer membrane (Fazli et al., 2014). The activity of the LapA-specific periplasmic protease LapG is inhibited by the transmembrane protein LapD in the presence of high c-di-GMP levels. Nutrient starvation induces c-di-GMP hydrolysis, resulting in the release of LapG inhibition by LapD, and the subsequent proteolytic cleavage of LapA causes biofilm dispersal (Gjermansen et al., 2005; Klausen et al., 2006; O'toole et al., 2000)

LapA is one of the largest proteins in *P. putida* and provides cell-surface interactions (El-Kirat-Chatel et al., 2014; Martínez-Gil et al., 2010). and participation in the initial, irreversible attachment of bacteria to the surface and suggests a later role as part of the matrix of mature biofilms. Such a role had been previously proposed (Gjermansen et al., 2010) along with the idea that LapA may interact directly with EPS. The second large extracellular protein, LapF, is the cell surface hydrophobicity factor (Lahesaare et al., 2016) and probably provides cell-cell interactions by regulating cell hydrophobicity (Martínez-Gil et al., 2010) and contributing to microcolony formation and mature biofilm formation.

It is worth noting that as previously reported, specific intracellular levels of c-di-GMP are under the detection limit in *P. putida* KT2440 (Matilla et al., 2011). The initial method to detect and quantify the c-di-GMP relied on cellulose synthesis as an indirect measure of the c-di-GMP level inside the cell (Amikam & Galperin, 2006). Other bacterial phenotypes like biofilm formation and swarming motility are correlated with c-di-GMP levels and are considered as proxies for c-di-GMP concentration within the cell (C. J. Jones & Wozniaka, 2017; O'Toole et al., 1999; Wolfe & Berg, 1989). Therefore, many researchers have focused on either indirect methods for c-di-GMP measurement or developing fluorescence-based biosensors mainly focusing on adhesion proteins LapA and LapF.

For instance, González et al 2016 generated two independent mutant libraries to identify genes involved in the signaling pathway leading to the pleiotropic phenotype associated with overexpression of Rup4959 (a multidomain response regulator) which in consequence increases diguanylate cyclase (DGC) activity. In this study, the researchers utilized a c-di-GMP biosensor and employed HPLC-MS quantification of the second messenger(Ramos-González et al., 2016). However, as quantifying the second messenger in the wild type was not possible by analytic methods because of the low levels, they took advantage of the reporter plasmid pCdrA::*gfp*^{C} (Ramos-

González et al., 2016). Similarly, Moreno and colleagues have used a reporter plasmid pCdrA::*gfp*^{C} and showed that arginine played a connecting role between cellular metabolism and c-di-GMP signaling in *P. putida* (Barrientos-Moreno et al., 2020). In another work, it has been reported the increased *lapA* expression is caused by global transcription regulator Fis overexpression. In this work, the impact of elevated Fis levels on the abundance of the LapA protein was detected by monitoring the fluorescence of a *lapF::gfp* fusion protein (Moor et al., 2014).

Additionally, Martínez-Gil et al examined the role of LapF in the colonization of abiotic and biotic surfaces by observing *lapF::gfp* transcriptional fusion which was only detectable within cells that are entangled in microcolonies and in mature biofilm (Martínez-Gil et al., 2010). Moreover, *P. putida* KT2440 harboring plasmids pMMG1 (*lapF*::*gfp*) and pMMG6 (containing a *lapA::mCherry* transcriptional fusion) was used to elucidate the role of both adhesins LapA and LapF during biofilm formation. They have shown expression from the *lapA* promoter increases with high levels of c-di-GMP, the opposite is true for *lapF*. The transcriptional regulator FleQ is essential for the modulation of *lapA* expression by c-di-GMP but has a minor effect on *lapF* (Martínez-Gil et al., 2014).

Over the years, transcriptional fusions of fluorescent proteins to c-di-GMP regulated promoters were used to obtain insights into the mechanism of c-di-GMP (Rodesney et al., 2017; Rybtke et al., 2012). However, these transcriptional fusions are species-specific and strictly c-di-GMP dependent promoters might not be known for a given model organism. Finally, riboswitches that specifically bind c-di-GMP were utilized to detect c-di-GMP levels by fusing RNA aptamers to those structures. The binding of c-di-GMP to the riboswitch results in a conformational change and fluorescence emission after addition of small fluorophores ligands(Kellenberger et al., 2013; Nakayama et al., 2012). In 2008, Sudarsan et al. reported the first c-di-GMP riboswitch termed c-di-GMP-I in eubacteria. Later, Lee et al. found another c-di-GMP riboswitch termed c-di-GMP-II in *Clostridium difficile*. c-di-GMP-I and c-di-GMP-II are two classes of riboswitches that bind c-di-GMP and control the expression of different genes in response to variations of the c-di-GMP (Lee et al., 2010; Sudarsan et al., 2008). Moreover, FRET-based biosensors have been extensively used to observe the intracellular concentration of c-di-GMP (Christen et al., 2010; Paul et al., 2010).

Although, fluorescence-based reporters have helped unveil the heterogeneity in the c-di-GMP distribution in cultures and provide insights into how the c-di-GMP pools are modulated by bacteria. Most techniques used for estimating the c-di-GMP

concentration lack single-cell resolution and many such sensors reflect only the free c-di-GMP concentration inside the cell and not the effector-bound c-di-GMP. Moreover, many of them are not optimized for monitoring long-term dynamics and most methods of c-di-GMP detection have limited sensitivity or difficulty in probe preparation.

However, despite the growing understanding of the biofilm cycle's structural and mechanistic details, little is known about the phenotypic switch during biofilm development in *P. putida*. As a result of the complexity of the gene regulatory network (GRN) governing biofilm formation in *P. putida*, it is relatively challenging to depend on a robust single-cell proxy to describe the phenotypic switching taking place in this process.

2.4. Tracking biofilm switchers: imaging and flow cytometry

Traditionally, Bacterial biofilms are usually assumed to originate from individual cells deposited on the surface. However, many biofilm-forming bacteria tend to aggregate in the planktonic phase, so it is possible that many natural and infectious biofilms originate wholly or partially from pre-formed cell aggregates (Burmølle et al., 2010; Monier & Lindow, 2003; Schleheck et al., 2009). The aggregates are typically motile, more adherent, display different metabolic signatures, and altered antimicrobial susceptibilities, which has resulted in aggregates being considered phenotypically between that of biofilm cells and planktonic cells, but distinct from both (Rumbaugh & Sauer, 2020; Sauer et al., 2022).

Biofilms comprise specialized subpopulations of cells, with different physiological characteristics compared to those living in the planktonic phase (Garcia-Betancur et al., 2012; Pamp et al., 2009; Vlamakis et al., 2008).In several contexts, including clinical, industrial, and environmental ones, there is a great interest in understanding how a biofilm is formed and how the cells composing it behave (Pamp et al., 2009).

The transition from planktonic cells to sessile cells to initiate biofilm formation and from sessile cells to detached cells and aggregates represents a tightly regulated developmental shift that has a substantial impact on cell fate. Therefore, switching between a planktonic and biofilm mode of growth is a critical step in bacterial development, which must be tightly regulated and tuned to environmental cues (Beloin et al., 2008; Claessen et al., 2014; Elias & Banin, 2012; Fazli et al., 2014; Fuqua et al., 2001; Karatan & Michael, 2013; Karatan & Watnick, 2009; Kolter & Greenberg, 2006; Monds & O'Toole, 2009; Parsek & Greenberg, 2005; Vlamakis et al., 2013). Unfortunately, these transitions depend on a dizzyingly complex array of

factors that are determined by the intrinsic properties of the individual cells as well as those of their surrounding environments and are thus challenging to describe.

The majority of biofilm studies focused on the mechanisms of bacterial adhesion and differential gene expression occurring during the switch from the planktonic state to the biofilm state (O'toole et al., 2000). Over the last decades, a broad range of model systems have been described for the in vitro study of biofilm formation and development (R. J. C. McLean et al., 2006).

Different methods exist for investigating biofilms; for instance, The flow chamber-based model system for studying biofilm formation and dynamics has the advantage of allowing online microscopic investigations of adaptive processes involving the evolution of species interactions in a biofilm community (Hansen et al., 2007). Given the nature of the biofilm, microscopy has been used as the choice method to analyze the structure, localization, or distribution of the biofilm components.

One of the frequently used methods is flow cell technology combined with confocal laser scanning microscopy (Pamp et al., 2009). By employing fluorescent reporter proteins or staining, organisms can be visualized and in situ detection of gene expression in a heterogeneous population at single-cell resolution and spatial organization can be investigated at single-cell resolution by means of fluorescence or confocal microscopy (Hare et al., 2021; Lelek et al., 2021; Mattiazzi Usaj et al., 2021) This tool is potentially useful for multiple lines of research in the field of bacterial gene regulation, especially for biofilm development. For example, Martin Nilsson and colleagues investigated the role of putative exopolysaccharide gene clusters in the formation and stability of *Pseudomonas putida* KT2440 biofilm in flow chambers, and after 48 h of biofilm formation. CLSM imaging was performed for the calculation of the amount of biofilm formed by each strain (Nilsson et al., 2011). Determining the bacterial growth phase and distinguishing between the planktonic and biofilm states of a cell can be achieved by utilizing sample staining in conjunction with microscopy or spectroscopy. However, these methods have limitations in providing comprehensive population-level data, and the staining protocols employed often compromise the sample's viability.

Nowadays, the analysis of microbial cells at a single-cell level is gaining increasing attention, as it becomes obvious that neither in the natural environment nor under industrial conditions do microorganisms occur as homogenous populations. Up to now, few studies have described the application of flow cytometry (FC) for the analysis of mature biofilms, although recently, the technique has gained more attention. Kim et al. used green fluorescent protein in strains of *Pseudomonas*

aeruginosa to identify and sort active or dormant biofilm cells (Kim et al., 2009). Kersten used FCM as an alternative technique to counting cellular subpopulations in a biofilm (Kerstens et al., 2015). This technique enables detailed investigation of the heterogeneous biofilm population due to its ability to perform multiparametric single-cell analysis. Flow cytometry-based approaches represent promising experimental protocols that provide an accurate insight into the diversity of such complex microbial populations (Díaz et al., 2010).

Moreover, it has been shown that flow cytometric bacterial phenotyping serves as an expandable platform that may be useful for single-cell quantitative detection of bacterial biofilm and planktonic cells with a combination of membrane permeable (SYTO 60) and impermeable (TOTO-1) dyes (Khomtchouk et al., 2019), The crucial advantage of using flow cytometric analysis is the ability to characterize and distinguish the different physiological states of microorganisms at the single-cell level (Joux & Lebaron, 2000; Nebe-Von-Caron et al., 2000). A combination of microscopic observations and flow cytometric measurements were applied to provide a reliable evaluation of the population dynamics within a *P. aeruginosa* biofilm (Wojciech et al., 2018) This powerful technique is also capable of observing ten thousand cells in a matter of minutes, providing statistically relevant data for the analysis of biofilm populations (Müller & Nebe-Von-Caron, 2010). Garcia-Betancur et al. reported the use of fluorescence microscopy combined with FCM to visualize and quantify the subpopulations of matrix producers and surfactin secretors (signaling molecule that triggers differentiation of matrix producers) within biofilms of *B. Subtilis* (Garcia et al., 2009).

Despite the increasing application of FC for analysing the physiological conditions of the cells in a biofilm, Michał Konieczny and colleagues reported the application of imaging flow cytometry which enables the detailed characterization of aggregates and discriminating small and large aggregates of microbial cells (Konieczny et al., 2021). This developed tool provided more detailed characteristics of bacterial aggregates within a biofilm structure combined with high-throughput screening potential.

While significant progress has been made in understanding individual phases of biofilm development, quantitatively predicting the conditions under which planktonic bacteria transition to the biofilm state remains challenging. Current methods mainly focus on mature biofilms or differential gene expression during the transition from planktonic to biofilm states. In this context, we propose a combination of flow cytometry and appropriate single proxies to track the initial stages of biofilm formation at the single-cell level. By focusing on the transition from free-floating to

primary biofilm phenotypes or aggregates, we aim to determine when a biofilm phenotype begins to emerge. This approach will provide valuable insights into the early stages of biofilm formation, complementing the existing knowledge on mature biofilms and gene expression dynamics.

2.5. Perspectives: Controlling biofilm switching in real time

Over the past decade, numerous efforts have been dedicated to characterizing and investigating the factors that influence and regulate each stage of biofilm formation. Several approaches have been developed to suppress biofilm formation, focusing on the application of substances that disrupt the activity of regulatory molecules or hinder the appropriate regulatory mechanisms employed by cells during biofilm development.

Extensive research has consistently demonstrated that bacteria in a sessile growth phase pose greater challenges in terms of control compared to bacteria in a free-floating state. This observation has spurred numerous studies aimed at comprehending and characterizing the initial stages of biofilm formation. In natural ecosystems, cells possess inherent programming that enables them to respond to external stimuli and adapt accordingly by switching to different phenotypic states (Acar et al., 2008; Schreiber & Ackermann, 2020). These phenotypic states are intricately linked to specific environmental conditions and are influenced by selection pressure, leading to fitness advantages. When we discuss the fitness benefits associated with biofilm formation, it may initially appear contradictory that the biofilm mode of growth could provide an advantage in reproductive fitness. This is because bacteria in biofilms generally exhibit a slower rate of growth compared to bacteria growing independently in liquid cultures. However, it is important to note that outside of controlled laboratory conditions, bacteria rarely encounter environments as nutrient-rich as culture media, in such less-than-ideal conditions, the biofilm mode of growth offers several fitness advantages. Firstly, biofilms provide protection against harmful conditions. The dense and structured nature of biofilms shields bacteria from various stressors such as toxins, antibiotics, and physical disturbances. By forming a collective community, biofilm bacteria can better withstand adverse circumstances and enhance their chances of survival (Vatansever & Turetgen, 2021; Vestby et al., 2020; Yin et al., 2019). Secondly, biofilms enable sequestration to nutrient-rich areas. Bacteria within biofilms can establish themselves in environments where resources are plentiful, such as on surfaces or within organic matter. This proximity to nutrients ensures a continuous supply of essential resources, promoting bacterial growth and survival (Herrera et al., 2007). Additionally, the biofilm mode of growth facilitates the utilization of cooperative benefits. Bacteria within biofilms can engage in cooperative

behaviors, such as sharing resources, communicating through signaling molecules, and coordinating actions. This cooperative nature allows biofilm bacteria to optimize resource utilization and exploit niche opportunities more effectively than planktonic bacteria, ultimately increasing their overall fitness. Therefore, despite the reduced growth rate compared to planktonic bacteria in nutrient-rich environments, the biofilm mode of growth provides numerous fitness advantages in less favorable conditions. Given the constant evolution of environmental conditions (Thattai & Van Oudenaarden, 2004), cells must continually adjust and optimize their phenotypic states to thrive in their surroundings. To switch from planktonic to biofilm mode of growth, bacteria undergo a number of physiological, metabolic, and phenotypic changes (Drenkard, 2003). This shift towards a biofilm-specific phenotype can activate mechanisms that contribute to antimicrobial resistance, enhanced virulence, and increased persistence (Mah & O'Toole, 2001) During the process of biofilm growth, bacteria assume a distinct phenotype specifically adapted for biofilm formation, which starkly differs from the characteristics exhibited by the corresponding planktonic cells.

Numerous strategies have been devised to effectively control microbial populations in various fields, spanning from biomedicine to bioprocess engineering. However, a more realistic alternative lies in controlling the cell switching phenomenon itself, which has become technically achievable through the implementation of cell-machine interfaces (Delvigne & Noorman, 2017; Nguyen et al., 2021; Sassi et al., 2019). In this context, automated real-time flow cytometry solutions have been developed to monitor bioreactor processes continuously, eliminating the need for operator intervention over extended durations and accommodating variable sampling frequencies. These advancements enable continuous and uninterrupted monitoring of bioreactor systems.

The implementation of a cell-machine interface offers the capability to monitor the switching process of individual cells within a population in real-time, allowing it to react accordingly. This innovative concept has been particularly embraced in the development of the Segregostat system (Nguyen et al., 2021; Sassi et al., 2019). The Segregostat relies on the utilization of on-line flow cytometry to record the rate of cell switching and to trigger environmental switching accordingly **(Figure 2-3).** This approach ensures that environmental perturbations are adjusted in accordance with the frequency of phenotypic switching, as previously determined through numerical simulations (Thattai & Van Oudenaarden, et al., 2004). In order to ensure the success of this control strategy, two crucial factors need to be considered: the efficiency of information transmission within biological systems and the timing of cells committing

to phenotypic switching. Assessing the efficiency with which a cell perceives and responds to extracellular perturbations involves quantifying the information transmission through biochemical networks. This can be accomplished by applying Shannon theory or information theory (Cheong et al., 2011). Information theory proves to be particularly valuable in this context as it provides a metric for quantifying the amount of information transferred from the external environment (input) to the cellular systems (output) under specific environmental conditions.

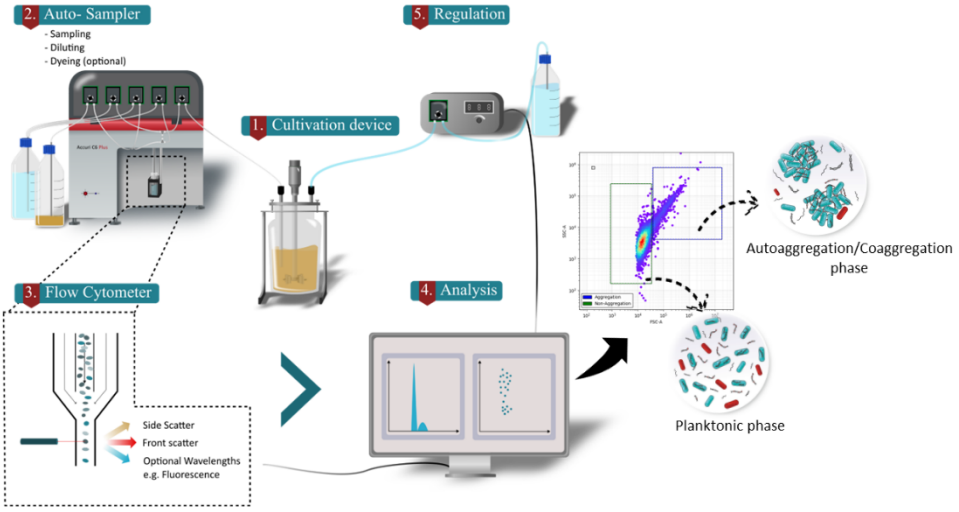

Figure 2-3. Scheme of the Segregostat set-up. Utilizing online flow cytometry to control cell population heterogeneity in continuous cultivations. A tailor-made MATLAB script based on FC data controlled the activation of the feedback control loop (Regulation). Nutrient pulses are added based on the function of the ratio between PI negative and PI positive cells, as recorded by automated FC.

The advancements in information theory have paved the way for a computational framework and experimental tools that can be applied to a wide range of biological systems. These developments hold huge potential for significant breakthroughs in various research areas. Notably, they offer the possibility of controlling complex cellular regulatory programs, such as the cell cycle program, as demonstrated by (Perrino et al., 2021).

Furthermore, these advancements also enable the control of microbial community composition, opening ways for applications in diverse fields ranging from bioproduction (Briat & Khammash, 2018a; Jiang et al., 2021) to biomedicine (Davidson et al., 2013; Din et al., 2020a). The ability to manipulate and regulate microbial communities holds great promise for enhancing bioproduction processes and advancing medical treatments.

Our work capitalizes on the practical benefits derived from combining control strategies with the advancements in computational and control theory. Specifically, we leverage the power of flow cytometry (FC) as a high-throughput method to rapidly measure the fluorescence characteristics of individual cells while simultaneously gathering information about the parent population from which these cells are randomly sampled. Interestingly, the device has the capability to automate environmental transitions by leveraging the phenotypic switching ability of the bacterial population. In this scenario, we take advantage of the exceptional characterization of a novel system to effectively assess the initial biofilm-phenotype state of the bacteria. By accumulating pertinent data with high real-time resolution and implementing control feedback strategies, we are able to regulate and manipulate biofilm formation in our study. This integration of online measurement not only aligns with the trend of digitalization but also offers numerous advantages (Delvigne & Goffin, 2014) By implementing online measurement through FC, we can achieve continuous monitoring of a process without incurring significant costs in terms of labor and time. This approach bridges the gaps between manual sampling intervals and provides detailed insights into the changes occurring in cell population distributions with high temporal resolution (Arnoldini et al., 2013; Kuystermans et al., 2016a).

To the best of our knowledge, our study represents the first investigation focused on real-time analysis of biofilm switching at the single-cell level. This novel research provides a valuable foundation for the control of phenotypic switching during the transition between planktonic, aggregate, and biofilm states. Moreover, it offers significant potential for regulating biofilm formation, particularly in bioprocesses that rely on the presence of "catalytic" biofilms.

By comprehensively understanding the dynamics of biofilm switching and its underlying mechanisms, we can develop targeted strategies to manipulate and control these transitions. This knowledge opens up new possibilities for controlling biofilm-related processes or other applications where biofilms play a crucial role.

Chapter 3

The quest for single-cell proxies related to biofilm switching

1. Abstract

The early initiation of biofilm development has so far been poorly investigated. This step comprises the early cell-decision making process linked with the switching of single cells from the planktonic state to the sessile one. This process is not easy to characterize because of the lack of related fluorescent reporters and the formation of cell aggregates during the transition from the planktonic to the sessile state, making difficult single cell analyses. Accordingly, we developed a reporter system consisting of a yellow fluorescent protein (YFP) under the control of the *lapA* promoter, related to the initial steps for biofilm production, as well as a GFP reporter to measure c-di-GMP concentration inside cells. However, both reporter systems exhibited low sensitivity and detectability. Surprisingly, we find out that a simple propidium iodide (PI) staining could help us to characterize biofilm switching. The occurrence of PI-positive subpopulations correlates with biofilm formation in the model bacterium *Pseudomonas putida* KT2440. Engineered *P. putida* derivatives with altered biofilm-forming capabilities exposed a whole available continuum of phenotypic states, including planktonic cells and cellular aggregates. These multiple phenotypes were identified by analyzing the dynamic change of PI-positive cells by flow cytometry (FC) analysis. Results demonstrate that PI is a fast, convenient, and versatile staining for extracellular DNA (eDNA) to rapidly monitor the phenotypic switching of *Pseudomonas* sp. during transitions in the bacterial lifestyle.

Keywords: Propidium iodide (PI), Flow cytometry, Extracellular DNA (eDNA), Biofilm, Aggregation, Sub-population, Phenotypic switching

2. Introduction

Biofilm formation initiates when planktonic cells interact with a surface, leading to a transition from planktonic to sessile growth and triggering a phenotypic change in bacteria. Microorganisms possess sensor-effector regulatory circuits that enable them to sense and respond to environmental changes, thereby modulating gene expression in response to external stimuli. They have also evolved various strategies, such as phenotypic switching, to adapt and thrive in fluctuating environments, generating population diversity, and enhancing bacterial fitness (Martínez-Granero et al., 2006; Van Den Broek et al., 2003). It is well-established that certain bacteria can generate population heterogeneity within an otherwise genetically homogeneous population, enabling the survival of a subset of the bacterial population in response to environmental fluctuations (Van Den Broek et al., 2005) (Achouak et al., 2004).This

phenomenon has been observed in *Pseudomonas* strains, such as *Pseudomonas putida*, where biofilm development undergoes various structural and metabolic changes that are tightly regulated by a complex gene regulatory network (GRN), including the phenotypic switch. Particularly, the precise detection of the early decision-making process linked with the switching of single cells from the planktonic state to the sessile one is still a technical challenge.

Current research indicates the second messenger, cyclic diguanosine-5′-monophosphate (c-di-GMP), plays a global role in regulating the transition between motile and sessile lifestyles in *P. putida* (Fernández & Romero, 2014). However, the regulatory networks controlling c-di-GMP are complex and not thoroughly studied. c-di-GMP influences the decision-making in bacteria in response to the environmental signals they perceive, as its concentration determines the cellular fate of bacteria (Petchiappan et al.,2020). Biofilm formation phenotypes are correlated with c-di-GMP levels and are considered proxies for c-di-GMP concentration within thecell (C. J. Jones & Wozniaka, 2017; O'Toole et al., 1999; Wolfe & Berg, 1989). Therefore, many researchers have focused on either an indirect method for c-di-GMP measurement or developing a fluorescence-based biosensor, mainly focusing on LapA as the one of main proteins in *P. putida* that participates in the initial attachment of bacteria to the surface (Fernández & Romero, 2014). Nevertheless, due to the complexity of the GRN governing biofilm formation in *P. putida*, relying on a robust single-cell proxy to describe the initial steps for biofilm production is challenging.

Recent studies have shown that propidium iodide (PI), a bacterial viability stain, may produce false signals of cell death by binding to extracellular DNA (eDNA), a component of bacterial extracellular polymeric substances (EPS) (Rosenberg et al., 2019). eDNA is considered an essential component of *Pseudomonas* sp. biofilms and has been found to significantly impact the structural integrity of the biofilm matrix, as well as protect bacterial cells from physical stress, antibiotics, and detergents (Chiang et al., 2013; Mulcahy et al., 2008; Whitchurch et al., 2002). eDNA has clearly emerged to play a pivotal role in cell adhesion during the early stages of biofilm development and plays a key structural role in mature biofilms (Okshevsky et al., 2015; Vandana & Das, 2022).

In this study, we explore different genetically-encoded fluorescent reporters for monitoring the dynamics of subpopulations involved in the early decision-making process leading to biofilm formation. While a fluorescence-based reporter was constructed to estimate *lap*A expression or monitor c-di-GMP, its low sensitivity and detectability limited its usefulness. Instead, we focus on the unique characteristics of

eDNA to monitor the early dynamics of biofilm switching at the single-cell level. Specifically, by using PI staining, we validate the importance of eDNA in different population states, particularly in the planktonic phase, aggregation, and its effect on phenotypic diversification. Our findings demonstrate that early biofilm development can be detected in planktonic cultures based on the degree of aggregation. Furthermore, we show that PI staining is not associated with modifications in the composition of the outer membrane but rather depends on the release of eDNA. This study provides insights into biofilm formation in *P. putida* KT2440, utilizing a biofilm-defective mutant (Δ*lap*A), a biofilm-overproducing derivative (DGC) (overexpressing a mutated, hyperactive diguanylate cyclase), and a natural isolate, *Pseudomonas composti*. Through a simple staining procedure using PI, we successfully track early biofilm formation during the transition from a free-floating to a sessile lifestyle.

3. Material and methods

3.1. Strains and medium composition

The bacterial strains were used in this study listed in **Table 3-1** (The strains kindly provided by Prof. Pablo I. Nikel, Denmark Technical University, Lyngby, except *P. putida* KT2440 P_{lapA}*::YFP,* which were constructed in our laboratory and *Pseudomonas. composti* natural isolated from mixed biofilm from cooling tower). All strains were preserved in 25% (v/v) glycerol at –80°C in working seed vials (2 mL). Before conducting the experiments, a single colony of each bacterium was used to inoculate 10 mL of lysogeny broth (LB) medium (10 g L^{-1} NaCl, 5 g L^{-1} yeast extract, and 12 g L^{-1} tryptone The cultures were grown with shaking at 30°C for 6 hours Both precultures and subsequent cultures of all bacteria were done in M9 minimal medium (33.7 mM Na2HPO4, 22.0 mM KH2PO4, 8.55 mM NaCl, 9.35 mM NH4Cl, 1 mM MgSO4, and 0.3 mM CaCl2), complemented with a trace elements (13.4 mM EDTA, 3.1 mM FeCl3·6H2O, 0.62 mM ZnCl2, 76 μM CuCl2·2H2O, 42 μM CoCl2·2H2O, 162 μM H3BO3, and 8.1 μM MnCl2·4H2O), 1 μg L^{-1} biotin and 1 μg L^{-1} thiamin) and supplemented with glucose (5 g L^{-1}) as the main carbon source (pH = 7.2). In the case of *P. putida* KT2440 Δ*lap*A Tn7::[*Ppel*A->gfp] strains M9 minimal medium supplemented either of Glucose, fructose or mannose (3.5 g L^{-1}), propionic acid (1.5g L^{-1}), succinate(2,25 g L^{-1}), or glycerol (2.77 mL/L).

For iron-dependent experiments, a concentrated FeCl3 solution was added to the media to give the final ferric iron concentrations described in the text. For *P. putida* DGC and *P. putida* KT2440 Δ*lap*A Tn7::[P*pel*A->gfp] strains, the media was

supplemented with gentamicin at a final concentration of 10 μg ml^{-1}. In the case of *P.putida* KT2440 P_{lapA}::YFP, kanamycin was added to the media at a final concentration of 50 μg ml^{-1}.

Table 3-1. Bacterial strains and plasmids used in this study

Strain	Relevant characteristics	Reference or source
***P. putida* KT2440**	Wild-type strain, derived from *P. putida* mt-2 (Worsey & Williams, 1975) cured of the TOL plasmid pWW0	(Bagdasarian et al., 1981)
***P. putida* Δ*lap*A**	Derivate of *P. putida* KT2440 with a clean deletion of *lapA* (*PP_0168*)	This study
***P. putida* DGC**	Derivate of *P. putida* KT2440 harboring the plasmid pS638::DGC-244	This study
P. putida* Δ*oprB-I	Derived from pGNW2 with homologous flanking region to oprB-I (PP_1019)	This study
P. putida* Δ*oprB-II	Derived from pGNW2 with homologous flanking region to oprB-II (PP_01445)	This study
P. putida* Δ*oprB-III	Derived from pGNW2 with homologous flanking region to oprB-III (PP_3570)	This study
***P. putida* KT2440 Δ*lap*A Tn7::[P*pel*A->gfp]**	Derivate of *P. putida* KT2440 with a clean deletion of lapA (PP_0168) - (mini-Tn*7*/ Gm^r /gfp)	This study
***P. putida* KT2440 P_{lapA}::YFP**	*lapA*::*yfp* transcriptional fusion, Km^r	This study
Pseudomonas. composti	Strains isolated from the cooling tower	(Kang et al., 2022)

3.2. Plasmid and strain construction

LapA inducible promoter

In order to synchronize the expression of *lapA* gene with a reporter suitable for FC, we decided to construct a transcription unit under the control of this gene promoter. This approach has been used before by (Martínez-Gil et al., 2014), where they reported two primer sequences to amplify *lapA* promoter ($P_{lap}A$). We used the same design for our transcription unit, but we used YFP as a reporter in this case. For this construction, we decided to use the pSEVA platform (SEVAHub), specifically the plasmid pSEVA237Y (Silva-Rocha et al., 2013). This is a promoterless plasmid with EYFP as cargo and an upstream multiple cloning sites (MCS) designed to test promoters **(Figure 3-S1-A).** For this cloning, we used Gibson Assembly reagent master mix (NEBuilder® HiFi DNA Assembly Master Mix,BioLabs, UK) according to the manufacturer's protocol. The primers used to amplify the pSEVA237Y and pLapA are shown in **Table 3-2**.

Table 3-2. The primers are used to amplify the pSEVA237Y and pLapA.

pLapA forward primer	**pLapA reverse primer**
ACCTGCAGGCATGCAAGCTTTACGGCT GCAGAGGTGTATG	ATGTTCATGACTCCCCTAGGAGGCGGG TACCTTCGATAAG
pSEVA237Y forward primer	**pSEVA237Y reverse primer**
TCCTAGGGGAGTCATGAACATATGGTGA GCAAGGGCGAGG	TACACCTCTGCAGCCGTAAAGCTTGCA TGCCTGCAGGTCG

The pLapA to primers are designed to amplify a 403 region upstream *lapA* because this promoter sequence was not precisely defined. The pSEVA237Y primers amplify the complete plasmid open in the MCS. Both PCR products generate slightly longer sequences due to the needed complementarity. The cloning protocol was followed as described by the provider. The final construction map is shown in **(Figure 3-S1-B).**

3.3. Sample preparation

Adherent cells were harvested by scraping from the wall of the bioreactor vessel with a cell scraper and resuspended in PBS. In the case of aggregation, 5 mL culture was aliquoted into a 15-mL Falcon tube, and aggregates were allowed to sediment for 10 min. Then, aggregates were carefully picked up from the bottom of the tube by using sterile cut pipette tips and transferred into 1.5-mL Eppendorf tubes. A quick spin at 1,400 rpm was applied for 15s, and the supernatant was removed. Both aggregates and biofilm samples were resuspended in sterile PBS and vortexed for 30

seconds. Before FC analysis, samples were gently sonicated (2X for 12s, with 25% amplitude) to disperse clumps into single cells without causing cell lysis. A planktonic sample has been filtered through a sterile syringe filter (5 μm) to eliminate aggregates before FC analysis.

3.4. Bacteria staining protocols

The four fluorescent stains used in this study were: (i) PI (P4170, Sigma-Aldrich); a stock solution was prepared at 1 mg mL^{-1} in sterile Milli-Q water and used at a final concentration of 1.5 μM in sterilized PBS; (ii) TOTO™-1 iodide (T3600, Invitrogen™ Thermo Fisher Scientific); a stock solution was prepared in DMSO (at 1 mM) and used at a final concentration of 2 μM in sterilized PBS; (iii) SYTOTM9 (S34854, InvitrogenTM Thermo Fisher Scientific); a stock solution was prepared in DMSO at 5 mM and used at a final concentration of 5 μM in sterilized PBS; and (iv) SYTO™60 (S11342, Invitrogen™ Thermo Fisher Scientific); a stock solution was prepared in DMSO at 5 mM and used at a final concentration of 10 μM in sterilized PBS. All bacterial samples were stained right before FC analysis by adding 1 μL of the PI stock solution to 1 mL of a cell suspension in PBS ($1X10^7$ cells mL^{-1}). The stained samples were incubated for 10 min in the dark at room temperature and analyzed by FC (live-dead gating was done based on heat-killed bacteria at 80°C for 1 h).

3.5. Flow cytometry

FC analysis of PI-stained bacteria was carried out using BD Accuri™ C6 device (BD Biosciences). Cell counts, red fluorescence (FL3), and Forward scatter (FSC) values were determined with FC. The software settings were as follows: Fluidics, medium; Threshold, 20,000 on FSC-H; Run with limits, 10,000 events. Gating of dead and alive signal populations was executed on Propidium iodide (FL3-A; 670 nm LP) scatter plot. FC analysis of PI staining bacteria was carried out on planktonic, aggregation, and biofilm samples. Cells were diluted to an appropriate density with filtered 1x phosphate-buffered saline (1× PBS; 8 g L^{-1} NaCl, 0.2 g L^{-1} KCl, 1.4 g L^{-1} Na2HPO4, and 0.2 g L^{-1} KH2PO4, pH 7.2) stained with PI and analyzed by FC.

Flow cytometry of auto-aggregation:

FC analysis (offline) for *P. putida* KT2440 P_{lapA}:YFP was carried out with an Attune NxT Acoustic Focusing Cytometer (Thermo Fisher Scientific, United States) containing a violet laser 405 nm (50 mW), a blue laser 488 nm (50 mW), and a red laser 638 nm (100 mW). Instrument calibration was performed with Attune performance tracking beads (2.4 and 3.2 μm) (Thermo Fisher, United States). Side scatter (SSC), Forward scatter (FSC), and BL2 (540/30) YFP were determined with FC. The software settings were as follows: Fluidics, medium; Threshold, 2000 on SSC-H; Run with limits, 20,000 events at a flow rate of 25 μl/min. Cells were diluted to an appropriate density OD600 (0.001-0.003 ≈700-1500 event/ μl) with filtered 1x PBS. FSC and SSC voltage and threshold were set based on wild-type bacteria. For the determination and quantification of possible aggregates and analysis similar to the one used in (Velastegui et al., 2023), in this case, a grand mean and standard deviation were calculated to propose a normal probability density function describing the cells that stay in the single non aggregated state (the vast majority) with this we constructed thresholds of increasing probability for the events to be increasing in size not conforming to a single state population but being part of another population state with different media and standard deviation. Therefore, the events that fall above two standard deviations only have 5/100 probability of being part of a single-cell floating population. Consequently, calculating and comparing the over-representation of this percentile across time gives us a quantitative measurement of cells that are more in not a single-cell floating state. The agglomeration state was then confirmed by observations in a microscope and the final biofilm production.

3.6. Chemostat cultivation combined with online flow cytometry

Bioreactor experiments were performed from overnight precultures in 500mL baffled flasks containing 50mL of culture medium and stirred with 170 rpm at 30°C. Cultures in the chemostat were performed in a lab-scale stirred bioreactor ((Biostat B-Twin, Sartorius) total volume: 2 L; working volume: 1 L). For the batch phase, the overnight cultures were diluted into 1 L of modified M9 medium at an initial OD600 of 0.3. The pH was maintained at 7.2 by the automatic addition of ammonia or phosphoric acid. The temperature was maintained at 30°C under the continuous stirring rate of 800 rpm and aeration rate of 1 VVM. Upon glucose depletion, the chemostat is started. For chemostat cultivations, the medium was continuously fed with the complete minimal medium at a dilution rate of 0.1 h^{-1} and subsequently

increased to 0.25 h^{-1} and 0.44 h^{-1}. The online FC platform (Accuri C6 BD Biosciences San Jose CA USA) has been used in combination with a chemostat cultivation system. The platform has been described in detail in a previous study (Sassi et al., 2019). Briefly, sample processing follows multiple steps, including sample acquisition and online staining, dilution threshold, and online FC analysis. Flow cytometry data were exported as an FCS file and processed by a custom Python script version (0.5.0).

3.7. DNase enzyme Treatment

Biofilm cells were prepared according to the protocol mentioned above. Then, the number of cells in the sample was adjusted to (1×10^7 cells mL^{-1}), and samples were resuspended in 500 µL of 1× DNase I buffer (10 mM Tris·HCl, pH = 7.5, 2.5 mM MgCl2, and 0.1 mM CaCl2) with or without DNase I (final concentration 160 U mL^{-1}, Roche, cat. # 04716728001) and were incubated at 37°C for 3h. After incubation, samples were pelleted by centrifugation at 8500 rpm for 10 min, resuspended in PBS, stained by PI, and analyzed by FC.

3.8. Confocal laser scanning microscopy (CLSM)

All samples were analyzed by confocal laser-scanning microscope (LSM) LSM880 Airyscan super-resolution system (Carl Zeiss, Oberkochen, Germany). The images were taken with the Plan- Apochromat 63×/1.4 Oil objective. We used an excitation wavelength of 488 nm and emission at 500-550 nm for green fluorescence and an excitation wavelength of 561 nm and emission at 580-18 615 nm for red fluorescence. Images were acquired continuously at a pixel resolution of 0.04 µm (regular Airyscan mode) in XY and 1-µm interval in Z step-size using the piezo drive. Before CLSM analysis, staining was performed with one or more fluorescent dyes in the following combinations: PI, SYTO9+PI, and TOTO1+SYTO60. An aliquot of 10-15 µL of 1:1 stain mixture solution has been added to a sample of planktonic, aggregate, and biofilm and incubated under the exclusion of light (10 min for PI, SYTO9+PI, and 20 min for TOTO1+SYTO60).

Microscopy images

Samples from *P. putida* KT2440, *P. putida* Δ*lap*A, and *P. putida* DGC culture were taken at 6h, during the batch phase and subjected to microscopy analysis. Microscopy images were acquired using a Nikon Eclipse Ti2-E inverted automated epifluorescence microscope (Nikon Eclipse Ti2-E, Nikon France, France) equipped with a DS-Qi2 camera (Nikon camera DSQi2, Nikon France, France), a 100× oil objective (CFI P-Apo DM Lambda 100× Oil (Ph3), Nikon France, France).

3.9. Quantification of biofilm growth and eDNA in biofilms in 96-well plates

The formation of biofilms by *Pseudomonas* strains over a two-day period was assessed using crystal violet staining in a 96-well plate lid with pegs extending into each well (Nunc-TSP lid, Invitrogen™ Thermo Fisher Scientific). To begin, precultures were grown overnight at 30°C until reaching an optical density of 1.0 at 600 nm (OD600 nm). The cell suspensions were then adjusted to an OD600 nm of 0.1 in M9 medium. Subsequently, 160 µL of the cell suspension was added to each well, while fresh medium served as a negative control. The plates were sealed with parafilm and incubated with shaking at 180 rpm and 30°C. The quantification of biofilm biomass was performed using a modified crystal violet staining assay, based on previous methods (Ren et al., 2014). For this assay, the peg lids of the Nunc-TSP lid culture system were taken out after 48 hours of cultivation and washed three times with PBS. The peg lids were then placed in plates containing 180 µL of a 1% (w/v) aqueous solution of crystal violet and stained for 20 minutes. Subsequently, the peg lids with crystal violet stain were placed into a new microtiter plate with 200 µL of 33% (w/v) glacial acetic acid in each well for 15 min. The optical density at 590 nm of each sample was measured using a microplate reader (Tecan SPARK, Männedorf, Switzerland).

In addition to biofilm quantification, the quantity of extracellular DNA (eDNA) associated with *Pseudomonas* biofilms was examined in triplicate using 96-well black plates (Cell culture microplate, µCLEAR®). The two-day biofilm cultures were rinsed three times with sterile distilled water. The eDNA was quantified using the QuantiFluor dsDNA dye (QuantiFluor dsDNA System, Promega, Madison, WI, USA) according to the manufacturer's protocol. In brief, each sample's eDNA was mixed with 200 µL of freshly prepared QuantiFluor dsDNA dye in TE buffer. The wells containing the dye were incubated for 5 minutes before measuring the fluorescence intensity (excitation wavelength = 504 nm and emission wavelength = 531 nm) using a Tecan microplate reader. A calibration curve was generated for each run using Lambda DNA (Invitrogen™ Molecular Probes).

4. Result

4.1. Propidium iodide (PI) is a relevant single cell proxy for the detection of subpopulation of cells involved in the switching to biofilm

Previous studies have demonstrated that PI can bind to eDNA and produce a false dead-red signal. In order to explore the potential use of PI as a single-cell proxy for

identifying subpopulations involved in the transition to biofilm, we conducted a systematic analysis using FC and confocal laser scanning microscopy (CLSM). To begin, we conducted a 24-hour batch phase cultivation of *P. putida* and collected biofilm samples at the end of the fermentation. To remove eDNA, we treated the samples with DNase I, using an untreated sample as a control. We then stained the samples with PI and analyzed them using FC. During the FC analysis, we divided the microbial population into two subpopulations based on PI uptake: PI-positive and PI-negative. The PI-negative subpopulation had fluorescence values of around 10^3 arbitrary units, indicating that these cells were unstained and had an intact, impermeable outer membrane. The partially stained bacterial subpopulation, with fluorescence values around 10^5 arbitrary units, was classified as PI-positive. FC analysis revealed a small subpopulation of PI-positive cells in the planktonic sample (**Figure 3-1A**). In order to investigate the influence of eDNA on the PI-positive subpopulation, the sample was subjected to confocal laser microscopy imaging. Planktonic cells were double-stained with PI and SYTO9, and it was observed that the two stains generally co-localized. Interestingly, within individual sections, green fluorescing cores were observed beneath the red-stained shells, indicating that PI staining was not indicative of membrane integrity, but rather the presence of eDNA outside the intact membrane (**Figure 3-1D**). However, the most strongly red cells lacked green signals and were considered as true dead signals. In the biofilm sample, prior to treatment with DNase, a majority of cells (62%) were found to be PI-positive **(Figure 3-1B).** However, after treatment with DNase enzyme, this subpopulation significantly decreased (32%) **(Figure 3-1C)**. To further confirm the role of eDNA in PI staining, DNase-treated biofilm samples were visualized using CLSM. The results clearly demonstrated that PI signals were much more intense in the non-treated sample compared to the sample treated with DNase (**Figure 3-1E and 3-1F**).

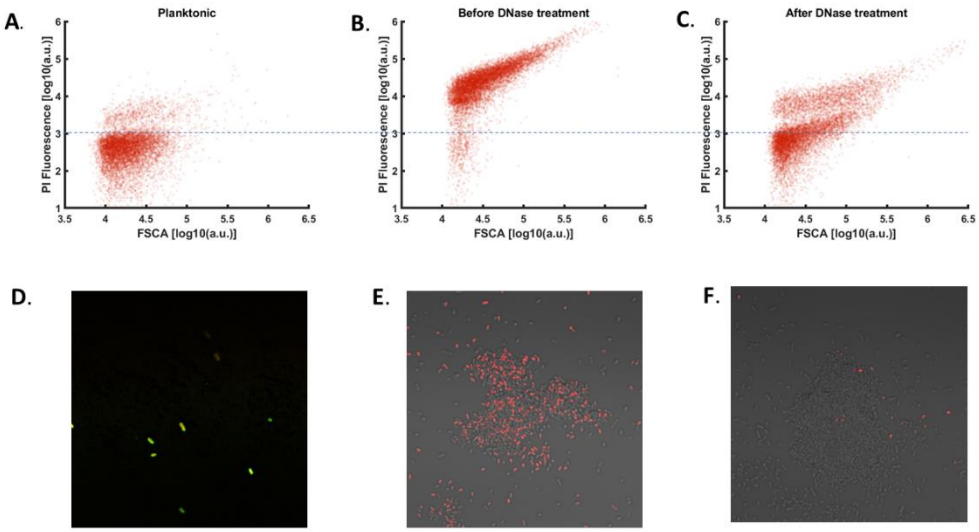

Figure 3-1. Flow cytometry analyses illustrating the comparison of PI-positive percentage among planktonic and biofilm samples and effects of DNase treatment on PI- positive fraction of biofilm sample **A.** Planktonic sample stained with propidium iodide **B.** Biofilm sample showing high PI uptake, before being treated by the DNase enzyme **C.** Biofilm sample after treatment with DNase enzyme, the PI-positive fraction decreases significantly. Confocal laser scanning microscopy (CSLM) images of planktonic and biofilm samples illustrating **D.** Planktonic sample co-stained with PI and SYTO 9. **E.** Biofilm cells stained with PI before being treated with DNase enzyme. **F.** Biofilm cells stained with PI after being treated with DNase enzyme.

To validate that the PI staining results directly correlate with biofilm formation, we conducted genetic modifications on *P. putida* KT2440. Our approach involved either decreasing or increasing biofilm formation by manipulating specific genetic factors. Firstly, we performed a knockout of *lap*A, which encodes the initial attachment protein. This genetic alteration resulted in a strain referred to as Δ*lap*A, which exhibited a notable inability to attach to abiotic surfaces. Consequently, biofilm formation was significantly reduced (Boyd et al., 2014). Conversely, to enhance biofilm formation, we introduced the plasmid pS638::DGC-244 into *P. putida*, generating the strain DGC. This plasmid carried a hyperactive di-guanylate cyclase, which led to an elevation in the concentration of cyclic-di-GMP, a critical second messenger molecule (B. Christen et al., 2006). The concentration of cyclic-di-GMP serves as a major regulator of biofilm formation, where higher concentrations promote adhesive behavior, while lower concentrations favor a planktonic lifestyle (Gjermansen et al., 2006). As the basal expression of the di-guanylate cyclase resulted

in a substantial increase in biofilm development, we refrained from supplementing the inducer to minimize perturbation to the cells. Simultaneously, we assessed the biofilm-forming capabilities of all four strains using a crystal violet microtiter plate assay. Our findings demonstrated that DGC and *P. composti* (natural isolate) exhibited robust biofilm formation and consequently produced a higher quantity of eDNA compared to the other strains tested (**Figure 3-2A**). Building upon these results, we further investigated the association between biofilm formation and the presence of the PI-positive subpopulation. We monitored the dynamic changes in the PI-positive subpopulation during biofilm development and observed significant variations among all tested strains. Notably, *P. putida* DGC and *P. composti* exhibited a notably higher PI-positive percentage compared to *P. putida* wild-type and the *P. putida* Δ*lap*A derivative (**Figure 3-2B**). Additionally, the proportion of PI-positive subpopulation increased during the mid-exponential growth phase and decreased toward the end of the batch phase. This observation could be attributed to the release of eDNA, which subsequently contributes to increased aggregation during the initial stages of the batch phase, while the biofilm formation decreases the number of small aggregates in the planktonic phase toward the end of the phase.

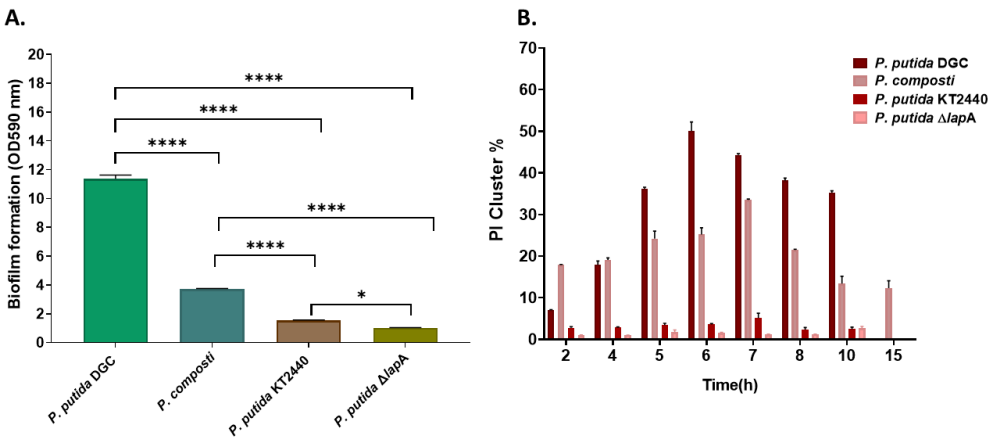

Figure 3-2. A. Biofilm formation ability of *P. putida* DGC, *P. composti (*natural isolate*), P. putida* KT2440 *, P. putida ⊿lap*A**,** after 48h of batch cultivation, n ≥ 5. **B.** Comparison of PI-positive subpopulation fraction (%) during batch phase n ≥ 3. The significance of the biofilm formation data was evaluated (*p*-values: **** $p < 0.0001$, * $p < 0.03$). The error bars represent the standard deviation (SD) within three technical replicates.

Hereafter, due to the strong biofilm formation capability of *P. putida* DGC strain aggregates and biofilm samples of this strain have been collected during the batch phase. We aimed to compare the corresponding PI-positive fractions of these samples

using both FC analysis and CLSM. The FC analysis revealed a significantly high percentage of PI-positive cells in aggregation samples (30.8%) and biofilm samples (41.8%) **(Figure 3-3A, 3-3C**). In addition to FC analysis, we employed CLSM to visualize the distribution of eDNA in the aggregation and biofilm samples. To achieve this, we combined the SYTO60 stain, which specifically stains bacterial cells in red, with the TOTO-1 stain, which stains eDNA in green **(Figure 3-3B, 3-3D).** The images obtained clearly demonstrated a substantial amount of eDNA in both types of samples. Notably, the DGC strain, being a strong biofilm former, exhibited a significantly higher production of eDNA compared to the other strains tested.

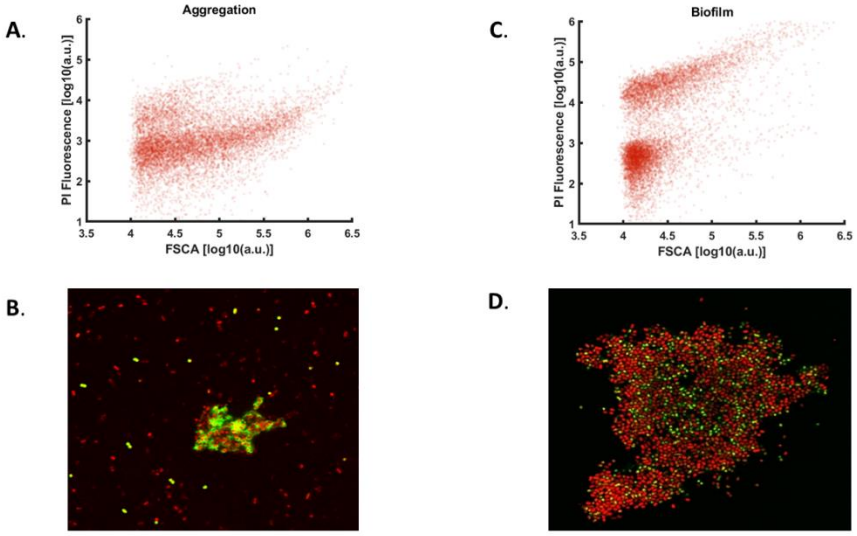

Figure 3-3. Flow cytometry and Confocal laser scanning microscopy (CSLM) images of *P. Putida* DGC (aggregation and biofilm) samples. **A.** FC analysis of aggregate cells stained with PI. **B.** CLSM of aggregate cells co-stained with TOTO-1 and SYTO60. **C.** FC analysis of biofilm cells stained with PI. **D.** CLSM of biofilm cells co-stained with TOTO-1 and SYTO60. TOTO-1 (Green signal for excellent visualization of eDNA in samples).

Iron has been shown to have a crucial role in modulating eDNA production and biofilm formation in various types of bacteria (Yang et al., 2007)(Allesen-Holm et al., 2006)(Banin et al., 2006)(Binnenkade et al., 2014)(Oh et al., 2018). In our study, we aimed to investigate the potential correlation between eDNA and iron concentration, as well as the population of PI-positive subpopulation in *Pseudomonas* sp. To achieve this, we designed a matrix consisting of a gradient of iron concentrations in a 96-well

plate format. We evaluated the extent of biofilm formation using crystal violet (CV) staining and quantified the amount of eDNA using a fluorescent dye-based method. Our findings revealed a decrease in the biofilm formation of *Pseudomonas* with increasing iron concentrations **(Figure 3-4A)**, which is consistent with the findings of a previous study by Yang (Yang et al., 2007). Additionally, the quantity of eDNA was assessed using PicoGreen, and the fluorescence intensity was measured immediately after adding the stain. The results demonstrated that the quantity of eDNA increased as the iron concentration decreased (**Figure 3-4B**). Furthermore, we examined the percentage of PI-positive subpopulation in the presence of high (100 µM) and low (5 µM) iron (Fe^{3+}) concentrations using FC in all four *Pseudomonas* strains. In all tested strains, except for *P. putida* Δ*lap*A, we observed an increase in the PI-positive subpopulation and biofilm formation as the iron concentration decreased (**Figure 3-4C**). Considering the association of eDNA with the biofilm matrix, we hypothesized that the significant difference in the percentage of PI-positive subpopulation between high and low iron concentrations could be attributed to a change in the quantity of eDNA present in the samples. However, for *P. putida* Δ*lap*A, a non-biofilm forming strain, we did not observe any changes in the PI-positive subpopulation or the ability to form biofilms.

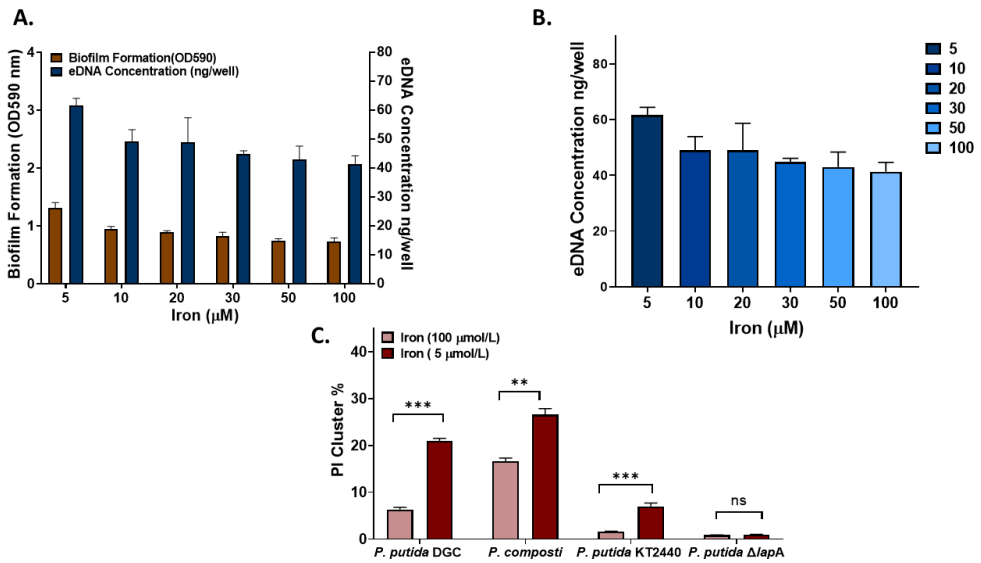

Figure 3-4. Effect of iron concentration on biofilm formation, extracellular DNA, and PI-positive subpopulation. **A.** Comparison of biofilm formation ability of *P. putida* KT2440 in the presence of different iron concentrations. **B.** eDNA quantity in the presence of different

iron concentrations. **C.** Comparison of PI-positive percentage among *P. putida* DGC, *P. composti* , *P. putida* KT2440, and *P.putida* Δ*lap*A in the presence of high (100µmol/L) and low iron concentration (5 µmol/L). The significance of PI cluster percentage data was evaluated (*p*-values: *** $p < 0.003$, ** $p < 0.03$, ns (not significant)). The error bars represent the standard deviation (SD) within three technical replicates.

Although, by considering the interference of eDNA with viability staining, we presumed that strains producing more biofilm exhibit higher fractions of PI-positive cells. However, previous experiments have suggested a potential connection between PI binding and changes in the outer membrane (OM) composition (Sassi et al., 2019). Deletion of specific porins in *E. coli* has been demonstrated to increase OM permeability, as indicated by PI staining (Brognaux et al., 2014); (Delvigne et al., 2011); (Brognaux et al., 2013).In our study, we systematically analyzed the impact of group B porins on the outer membrane permeability of *P. putida*. Our aim was to explore whether alterations in the porin composition of *Pseudomonas* OM are associated with PI staining. To investigate this, we generated single and multiple deletion mutants for genes encoding OprB porins (OprB-I, OprB-II, and OprB-III) and assessed the fraction of PI-positive cells at different time points. Throughout all time points, the observed PI staining and red fluorescence in FC were only present in 1-5% of the cell subpopulation across all tested mutants (**Figure 3-S1**). These findings indicate that the deletion of single, double, or even triple oprB genes did not significantly impact the fraction of PI-positive cells, suggesting that PI staining is not linked to increased OM permeability in *P. putida.*

4.2. Cell autoaggregation plays a crucial role in the continuum of phenotypic changes involved in the transition to a biofilm lifestyle

Autoaggregation and microcolony formation are among the first steps in building a biofilm. To investigate the impact of pre-formed aggregates in the planktonic phase on early biofilm formation, we have monitored aggregation development during the batch phase cultivation for strains under study. To assess the dynamic of autoaggregation properties of strains including *P. putida* KT2440, *P. putida* Δ*lap*A, and *P. putida* DGC during the batch phase, samples were collected at hourly intervals over a period of 30 hours and subjected to FC analysis (**Figure 3-5**). In case of *P. composti* we observed the formation of exceptionally large aggregates during the planktonic phase. However, in order to prevent technical complications during flow cytometry analysis, we intentionally excluded these large aggregates. Consequently, the measurement of auto-aggregation by FC did not accurately reflect the actual formation of auto-aggregates by this particular strain **(Figure3-S3).** We have gated

aggregation from the planktonic phase based on FSC and SSC signals. FC analysis indicated the presence of aggregates of phenotypic particles with a wide forward scatter distribution, indicative of variable particle sizes. These were distinguishable from single cells by their significantly bigger side- and forward-scatter values. Interestingly, we observed an increase in aggregation during the initial exponential growth phase, followed by a subsequent decrease upon entering the stationary phase, coinciding with the formation of the biofilm in the case of *P. putida* DGC **(Figure 3-5A)**. However, this phenomenon was scarcely observed in the case of *P. putida* Δ*lap*A, which exhibited very low levels of cell aggregation **(Figure 3-5B)**. In comparison, *P. putida* KT2440 displayed a more pronounced formation of aggregates compared to *P. putida* Δ*lap*A **(Figure 3-5C)**. Furthermore, we conducted microscopy imaging on samples that were taken at the 6-hour batch phase **(Figure 3-5D, 3-5E, 3-5F).** The obtained images provide compelling evidence of pronounced aggregation occurring specifically in the case of *P. putida* DGC **(Figure 3-5D).** The result indicates that the biofilm-forming capability of strains under this study is highly related to autoaggregation ability. The strong autoaggregation was observed in both *P. putida* DGC and of *P. composti* which produce significantly higher biofilm compared to other tested strains.

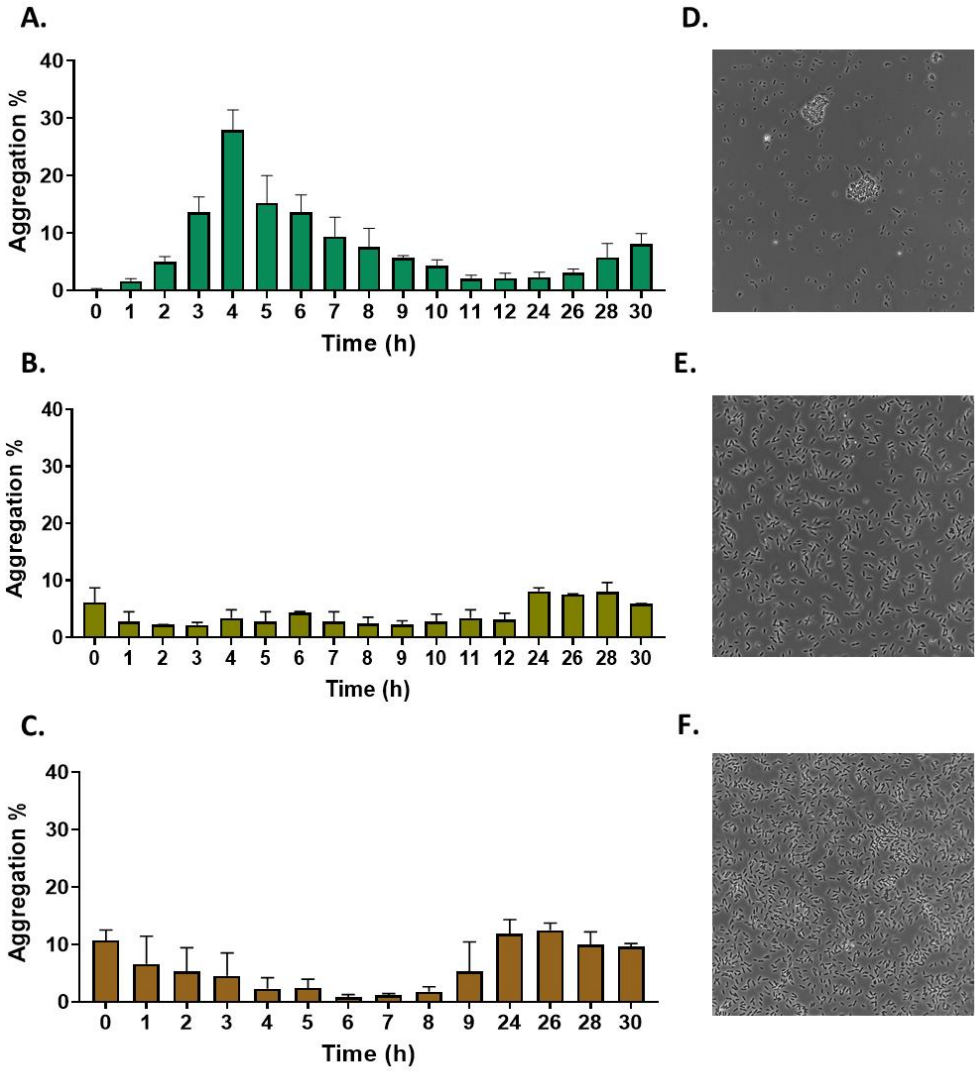

Figure 3-5. Analysis of the autoaggregation ability of **A.** *P. putida* DGC, **B.** *P. putida* Δ*lapA*, and **C.** *P. Putida* KT2440, by flow cytometry n ≥ 3. The error bars represent the standard deviation (SD) within three technical replicates. Microscopy images (40x) of cells samples from flask experiments for **D.** *P. putida* DGC, **E.** *P. putida* Δ *lap*A, **F.** *P. putida* KT2440 after 6h of batch cultivation n ≥ 3.

4.3. P_{lapA}:YFP reporter exhibits low sensitivity and is not compatible with real-time monitoring based on automated flow cytometry

Although we have demonstrated the potential of using PI for detecting subpopulations involved in the transition to biofilm, we attempted to examine the more accurate single-cell proxies at the gene level that could be monitored by automated online FC.

To achieve this, we constructed a *lap*A::yfp transcriptional fusion and introduced it into *P. putida* KT2440 and used advanced automated FC to investigate the dynamics of population diversification during batch cultivation (**Figure 3-6A**). During the batch phase, we did not observe any YFP expression through automated FC analysis. However, we took samples from the same batch phase at regular intervals and subjected them to off-line FC (Attune NTX). The results obtained from the offline analysis (**Figure 3-6D**) showed an increase in YFP signal related to the *lap*A promoter, which occurred 2 hours after inoculation and continued to increase after 10 hours. To further challenge the strain and promote the expression of the *lap*A promoter, we conducted a chemostat with different dilution rates, including 0.1 h^{-1} (**Figure 3-6C**) and 0.25 to 0.44h^{-1} (**Figure 3-6D**). Surprisingly, we did not observe any YFP expression during the chemostat at any of the dilution rates in FC BD Accuri™ C6. However, we took different samples during the chemostat and analyzed them using offline FC Attune NTX. The results obtained from the offline analysis during the countnius cultivation (**Figure 3-S4**) showed a small change in YFP signal related to the changing dilution rates. Although, the change was very low. It is worth noting that the difference in measurements between the automated and off-line FC analysis could be attributed to the low sensitivity and detectability of the signal, as well as the difference in FC resolution.

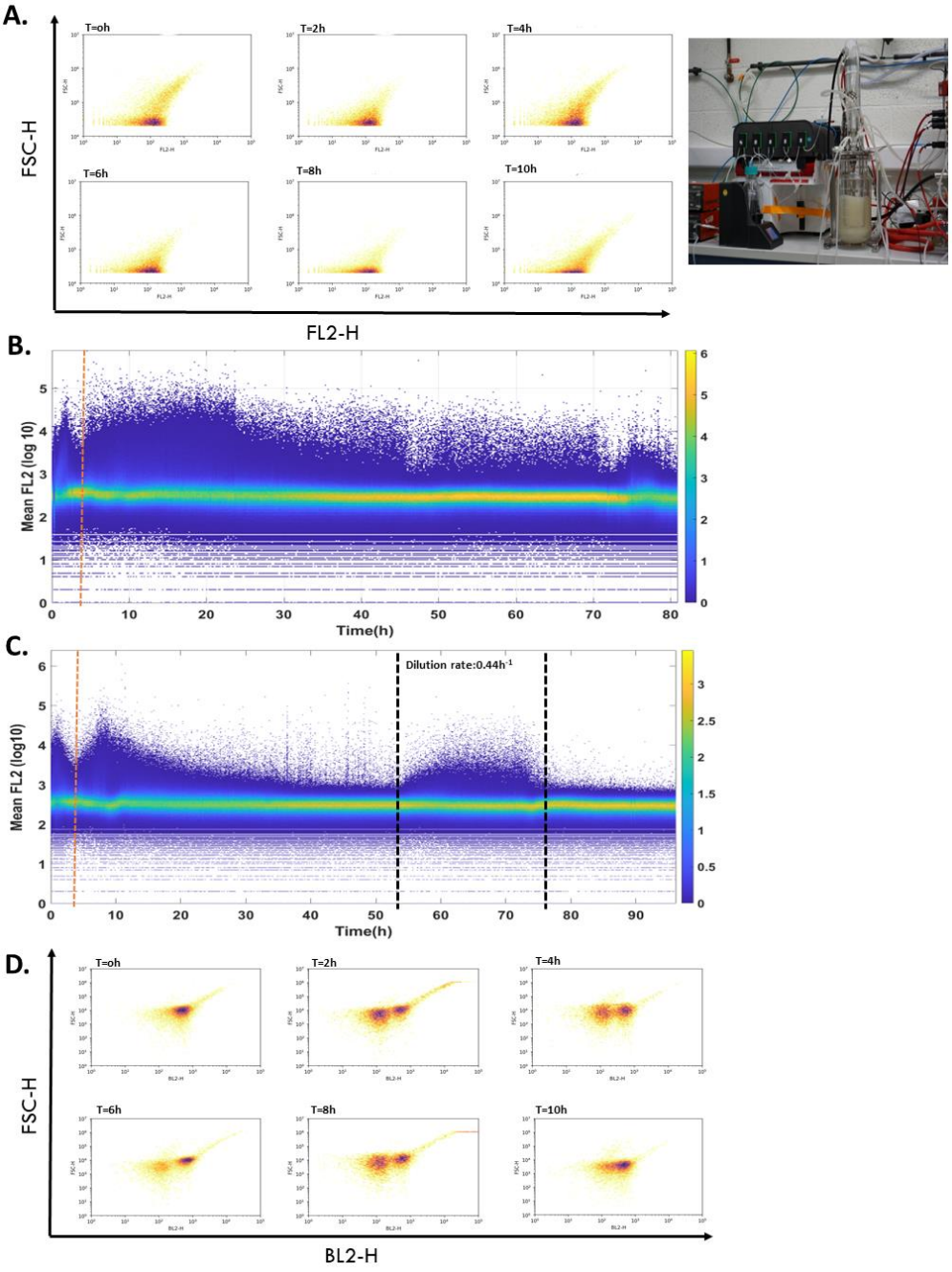

Figure 3-6. Automated flow cytometry analysis of *Pseudomonas putida* KT2440-P*lapA*::YFP in a bioreactor. **A.** FC analysis of (0,2,4,6,8 and 10h) of batch cultivation in bioreactor combined with automated FC (BD Accuri™ C6, FL2 is represented for YFP signal). Samples were systematically collected and subjected to automated analysis using

online FC. **B.** Time scatter plot of a mean of YFP fluorescence during chemostat cultivation for a dilution rate of $0.1h^{-1}$ **C.** Time scatter plot of a mean of YFP fluorescence during chemostat cultivation for a dilution rate of 0.25 $h^{-1,}$ and $0.44h^{-1}$ .The orange dash represents the end of the batch and the start of continuous cultivation -Black dash shows the duration of the higher dilution rate $0.44h^{-1}$ from 55h to 75h. **D.** Comparison of YFP-positive subpopulation of the same sample taken from a batch phase in bioreactor and analyzed in offline FC (Attune Ntx, BL2 is represented for YFP signal).

4.4. Flow cytometry-based analysis identifies small changes in c-di-GMP signal in response to environmental nutrients

Due to a low level of fluorescence of *P. putida* KT2440- P_{lapA}::YFP which was not able to be detected on automated FC, we attempted to focus on another biosensor system related to c-di-GMP. We have used *P. putida* KT2440 Δ*lap*A Tn7::[P*pel*A->gfp] and in the following tracking the c-di-GMP expression level in different conditions. In the first attempt to evaluate the efficiency of constructed strains, we cultivated the strain in a modified minimal medium M9 containing different carbon sources including glucose, glycerol, succinate, fructose, mannose, and propionic acid **(Figure 3-S5)**. Among all tested conditions, only glycerol and succinate have shown slight changes in the level of fluorescence expression during batch phase cultivation (**Figure 3-7).** Specifically, in the case of glycerol, we observed a more pronounced effect at the initial stages of cultivation, particularly at 4 hours and 6 hours of the batch phase **(Figure 3-7A).** Conversely, for succinate, a significant change in GFP levels was observed at 10 hours **(Figure 3-7B).** However, it is important to note that the change in the fluorescent signal was not substantial, resulting in only a slight shift in the GFP signal at specific time points. This limited change in the fluorescent signal can be attributed to the low detectability of c-di-GMP, suggesting that the biosensor used is not optimized for monitoring long-term dynamics. As a result, it is not suitable to combine this biosensor with our automated FC for monitoring the long-term dynamics of a phenotypic switch. Nevertheless, we proceeded to compare the corresponding PI-positive fractions and the dynamics of autoaggregation in these samples during the batch phase using FC **(Figure 3-7C-D)**. Interestingly, we observed that the formation of aggregates correlated with the changes in the GFP signal. Additionally, a higher fraction of PI-positive cells was observed when succinate was used as the sole carbon source **(Figure 3-7D).**

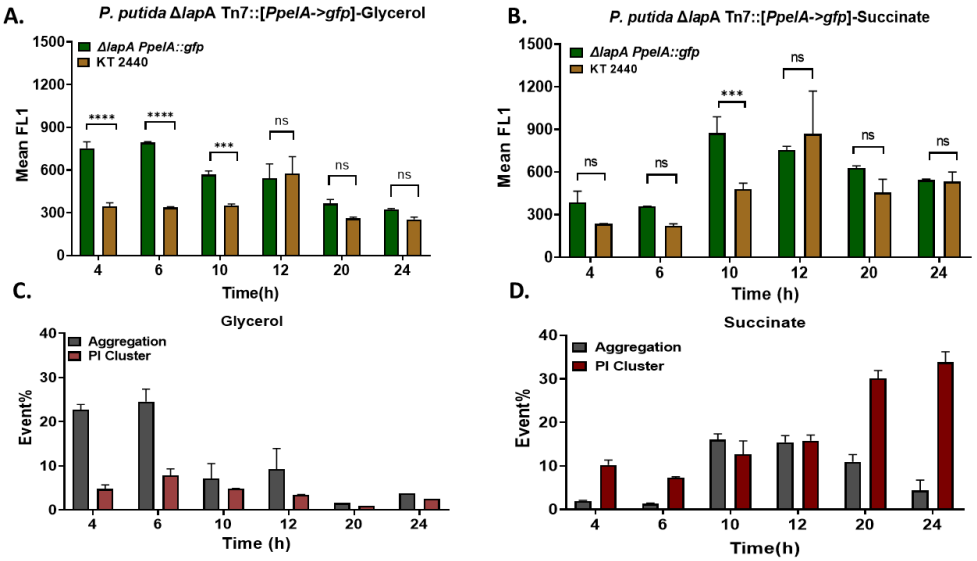

Figure 3-7. Flow cytometry analysis of *Pseudomonas putida* KT2440 Δ*lap*A Tn7::[*Ppel*A->gfp] under different carbon sources. The dynamic nature of GFP expression levels on a modified M9 medium containing either **A.** Glycerol or **B.** Succinate as the sole carbon source during the batch phase $n \geq 3$. The dynamic of PI and aggregation percentage on **C.** Glycerol or **D.** Succinate during batch phase $n \geq 3$. The significance of PI cluster and aggregation percentage data was evaluated (*p*-values: **** $p < 0.0001$, *** $p < 0.002$, ns (not significant)).

5. Discussion

Studies about the phenotypic diversification of microbial populations attract a lot of attention because of the possible new functionalities exhibiting diversified populations. The phenotypic diversification of *P. putida* encompasses its metabolic versatility, antibiotic resistance, biofilm formation, stress response, and quorum-sensing capabilities. In this work, we are focusing on phenotypic switching related to biofilm formation. According to our knowledge, all the current state of knowledge in biofilm development in *P. putida* has been limited to the systematic use of confocal microscopy on *P. putida* biofilms grown in flow cells or various strategies to classify and characterize genes involved in each stage of biofilm development (Fazli et al., 2014; Klausen et al., 2006). Despite the growing understanding of the biofilm cycle's structural and mechanistic details, little is known about the phenotypic switch during biofilm development in *P. Putida*. In this study, we explore the advantages of employing PI as a proxy for single-cell analysis to investigate the early decision-making processes involved in the transition to a biofilm lifestyle. PI is a staining compound renowned for its selective targeting of eDNA due to its molecular size,

which prevents it from entering intact cell membranes (Allesen-Holm et al., 2006). In our current investigation, we have identified PI as a valuable biomarker for tracking the transition of *P. putida* cells from the planktonic phase to the sessile phase. Our findings from FC and CLSM confirm that PI specifically binds to eDNA during a specific growth phase. The release of eDNA by specialized cells has attracted considerable attention (Okshevsky et al., 2015). However, recent studies have raised concerns about PI potentially overestimating dead cell counts in the presence of eDNA (Rosenberg et al., 2019). Gião and Keevil observed a misleading red signal when co-staining *Listeria monocytogenes* biofilms in tap water with PI and SYTO9, which did not indicate dead cells but was caused by the presence of eDNA (Gião & Keevil, 2014). Similarly, Gallo observed a similar phenomenon when staining biofilm cells of *Salmonella typhimurium* strain carrying the reporter P_{csgBA}*::gfp* with PI. They noticed a red corona surrounding green cells, indicating the localization of eDNA around live cells(Gallo et al., 2015). The CLSM results align with previous research conducted by Vilain and colleagues, who demonstrated the association of nucleic acid with the external surface of *Bacillus cereus* biofilms on glass wool, where PI had unrestricted access (Vilain et al., 2009).Recently, PI has been widely used by researchers to visualize eDNA in biofilms or cell aggregates through microscopy imaging (Deng et al., 2020; Moshynets et al., 2022; Secchi et al., 2022).

We have demonstrated that PI-positive sub-populations increase by manipulating the biofilm formation ability of *Pseudomonas* sp. In light of eDNA interfering with viability staining, we assume that the higher presence of eDNA leads to higher PI-positive fractions in strains producing more biofilm. We have also shown that the percentage of PI-positive fraction is more elevated in biofilm and aggregation samples. Since the quantity of eDNA is higher in the aggregation and biofilm sample, the observed difference could arise due to the binding between eDNA and PI.

We have shown that modifying the amount of eDNA by considering different iron concentrations directly affects PI-positive sub-population. Iron has been demonstrated to be essential in the modulation of eDNA production, for instance, by triggering prophage induction in *Shewanella oneidensis* (Binnenkade et al., 2014), mediating cell lysis during biofilm formation in Streptococcus pneumoniae (Trappetti et al., 2011), or, in the case of *P. aeruginosa*, regulating eDNA production in response to both the pqs quorum-sensing system and changes in the external iron concentration (Allesen-Holm et al., 2006)(Yang et al., 2007). Our findings are in line with studies that showed how high concentrations of iron suppress *P. aeruginosa* biofilm formation in both microtiter plate cultivations and flow-chamber systems (Musk et al., 2005). Simultaneously, low iron concentrations were reported to be necessary for

P. aeruginosa biofilm (microcolony) formation in an artificial sputum medium (Sriramulu et al., 2005). In *Campylobacter jejuni*, iron supplementation increased the accumulation of total reactive oxygen species (ROS) and the production of eDNA and extracellular polysaccharides, which leads to stimulating biofilm formation (Oh et al., 2018). Finally, biofilm formation was stronger in *A. baumannii* strains when iron concentrations were low and weaker when iron concentrations were high.

Previous studies in *E. coli* have confirmed that suppressing porins increases the occurrence of a partially PI-stained phenotype, suggesting increased outer membrane permeability (Sassi et al., 2019). While the mechanisms behind this are not fully understood, it has been hypothesized that modifications in outer membrane porin composition may play a role. However, in the case of *P. putida*, our results have shown that PI staining is not associated with changes in outer membrane composition but is likely dependent on the release of eDNA.

Bacterial aggregates are ubiquitous, but they have been considered as an alternative format of surface-attached biofilms and thus underestimated for years. However, it is now recognized that numerous bacteria capable of forming biofilms tend to aggregate during the planktonic phase (Kragh et al., 2023; Melaugh et al., 2023). Within this context, it is becoming more and more apparent that biofilms can form without necessarily needing to be attached to a surface. The presence of cell aggregates in the liquid phase makes difficult the distinction between phenotypes related to planktonic and biofilm states. As an example, it has been shown that both *S. aureus* and *P. aeruginosa* can grow as a mixture of planktonic and aggregate cells in liquid batch cultures (Nørskov Kragh et al., 2018), (Schleheck et al., 2009). It seems likely that natural biofilms are often initiated from pre-formed aggregates *P. aeruginosa*, upon growth in liquid culture, forms large aggregates containing massively packed viable cells and eDNA (Schleheck et al., 2009). For marine biofilms, the increased adhesiveness and surface conditioning of planktonic multicellular aggregates have been shown to accelerate bacterial attachment to a surface in early biofilm initiation (Bar-Zeev et al., 2012). Similarly, for *P. aeruginosa*, an increased affinity toward aggregation, probably an alternative for greater stickiness, has also been associated with increased biofilm formation (Häußler et al., 2003) (Déziel et al., 2001) We have shown that it is possible to detect early biofilm formation in the planktonic phase by determining the degree of aggregation by FC. Our result shows the autoaggregation ability of *Pseudomonas* sp. was highly correlated to their biofilm formation ability. Our research has shown that bacterial autoaggregation, which is a key characteristic of biofilm structure, can occur in the planktonic phase. By measuring the degree of aggregation using FC, we were able to detect early biofilm formation in the planktonic

state. Our findings indicate a strong correlation between the autoaggregation ability of *Pseudomonas* sp. and their capacity to form biofilms, as well as their eDNA content.

Despite our findings that support the potential effectiveness of PI as a reliable single-cell proxy for tracking early cell decisions in biofilm formation, extensive efforts have been dedicated to developing fluorescence-based reporters. These efforts primarily focused on indirect methods for measuring c-di-GMP or targeted specific proteins such as LapA and LapF, which play significant roles in biofilm initiation and maturation, respectively. In our study, we attempted to construct two fluorescence-based reporters, one related to LapA and the other to c-di-GMP. However, these biosensors did not demonstrate sufficient sensitivity and detectability in both cases. As a result, our research shifted its focus towards PI staining as a single-cell proxy to track early biofilm formation. In the subsequent chapter, we will delve into the details of applying PI staining in continuous cultivation to gain a more comprehensive understanding of the early stages of biofilm formation.

6. Supplementary files

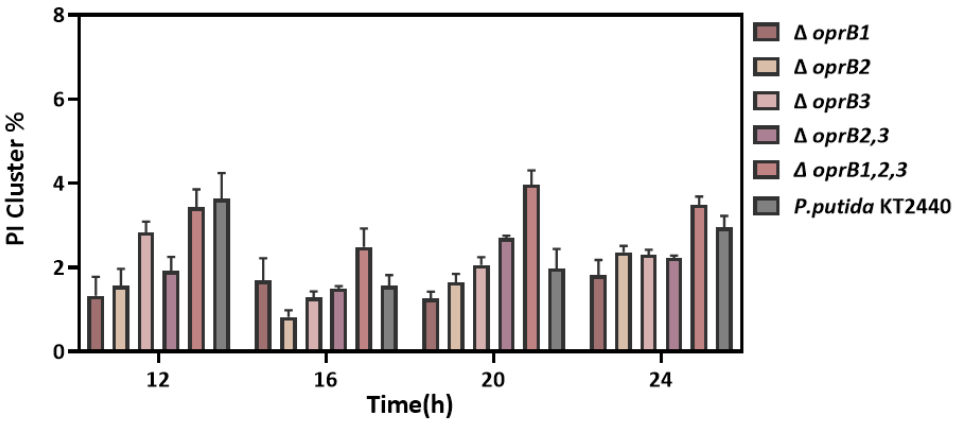

Figure 3-S1. Flow cytometry analysis of *Pseudomonas putida* KT2440 and evaluate the effect of deletion porins group B on PI positive fraction in *P. putida* KT2440 mutant, $n \geq 3$. The error bars represent the standard deviation (SD) within three technical replicates.

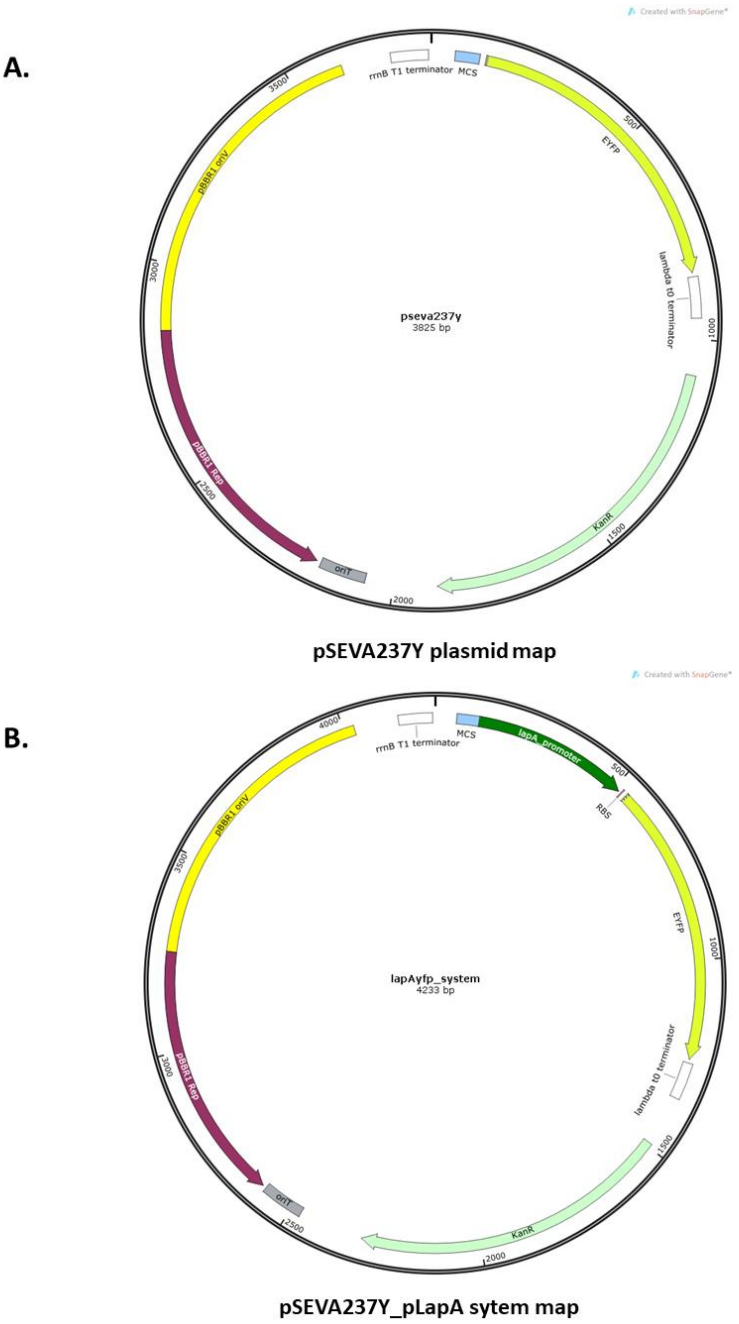

pSEVA237Y plasmid map

pSEVA237Y_pLapA sytem map

Figure 3-S2: Plasmid maps. Promoters, genes, terminators, and some relevant restriction sites are shown. Maps were designed with SnapGene Version 4.0.3. **A.** pSEVA237Y plasmid map **B.** pSEVA237Y_pLapA sytem map.

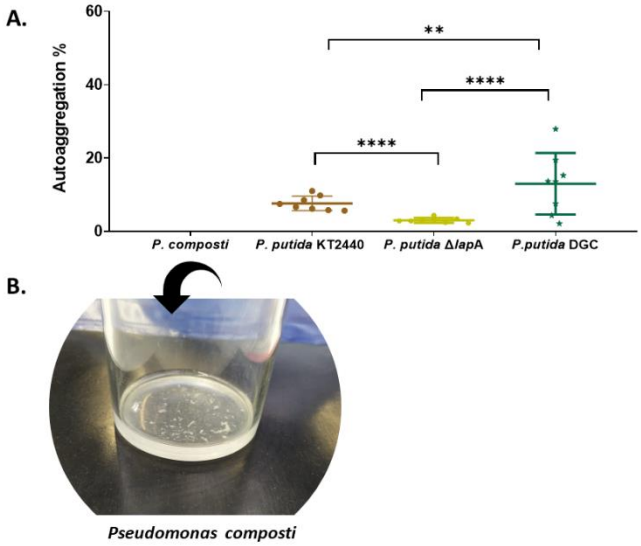

Figure 3-S3. A. Comparison of the degree of autoaggregation among *P. putida* KT2440, and Δ*lap*A by FC, n ≥ 2. For *P. composti* FC was not possible due to the formation of large aggregates.B. The significance of aggregation percentage data was evaluated (*p*-values: **** $p < 0.0001$, ** $p < 0.005$). **B.** Macroscopic view of aggregated cells of *P. composti* during the batch phase.

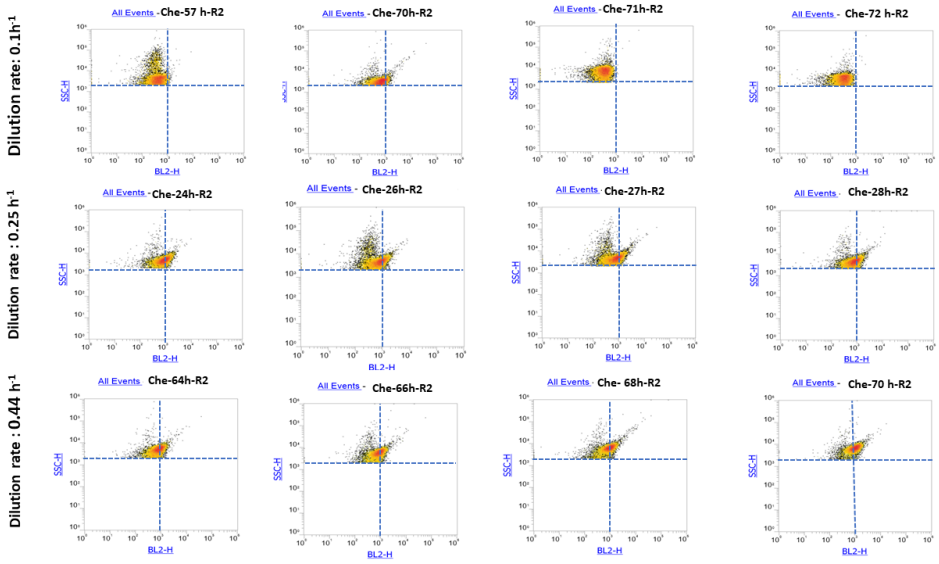

Figure 3-S3. Flow cytometry (Attune™ NxT -offline) analysis of *Pseudomonas putida* KT2440- P_{lapA}::*yfp* during chemostat at different time points n ≥ 2. The blue dash line

is a defined threshold based on a comparison to the control (*P. putida* KT2440) which shows a slight change in the YFP signal by increasing the dilution rate.

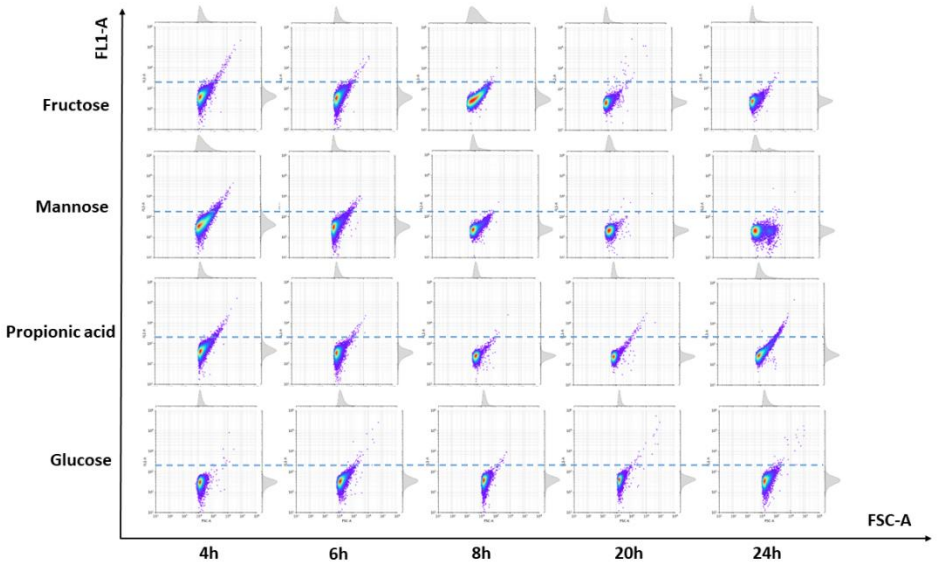

Figure 3-S4. Flow cytometry analysis of *Pseudomonas putida* KT2440 Δ*lap*A Tn7::[*Ppel*A->gfp] on a modified M9 medium containing fructose, mannose, propionic acid, and glucose as the sole carbon source during the batch phase $n \geq 3$. In all instances, not any GFP expression has been observed. The blue dash line is a defined threshold based on a comparison to the control (*P. putida* KT2440).

Chapter 4

Release of extracellular DNA by *Pseudomonas* species as a major determinant for biofilm switching and an early indicator of cell population control

1. Abstract

The different steps involved in biofilm formation have been the subjects of intensive researches. However, the very early cell decision-making process related to the switch from planktonic to sessile state still remains uncharacterized. Based on the use of *Pseudomonas putida* KT2440 and derivatives with varying biofilm-forming capabilities, we observed a subpopulation of cells bind to extracellular DNA (eDNA) in the planktonic phase, as indicated by propidium iodide (PI) staining. Strikingly, the size of this eDNA-bind/PI-positive subpopulation correlated with the overall biofilm forming capability of the bacterial population. This finding challenges the conventional view of phenotypic switching and suggests that, in *Pseudomonas*, biofilm switching is determined collectively based on the quantity of eDNA released in the supernatant. The whole process can be followed based on automated flow cytometry, and the appearance of PI-positive cells was considered as an early-warning indicator for biofilm formation. For this purpose, automated glucose pulsing was used successfully to interfere with the proliferation of PI-positive cells, resulting in a reduction of biofilm formation. This study provides insights into the collective determinants of biofilm switching in *Pseudomonas* species and introduces a potential strategy for controlling biofilm formation.

Keywords: phenotypic heterogeneity, population control, auto-aggregation, stochastic switching

2. Introduction

The transition from a planktonic to a biofilm state in a bacterial population can be influenced by a variety of factors and is a complex process that can vary depending on the microbial species considered and the environmental conditions (Penesyan et al., 2021; Philipp et al., 2023; Sauer et al., 2022). It has been suggested that a subpopulation of cells within a planktonic culture may play a role in initiating biofilm formation by binding to extracellular DNA (eDNA) (Secchi et al., 2022). These cells can further serve as pioneers that start the biofilm formation process by adhering to surfaces and facilitating the recruitment of other cells to form either a mono- or a multi-species biofilm. In this context, it has been recently suggested that the process of cell aggregation in the liquid phase is a critical step in the biofilm lifecycle (Cai, 2020; Kragh et al., 2023). These aggregates offer several fitness advantages over individual planktonic cells, including increased antibiotic resistance and improved surface colonization (Kragh et al., 2023; Nørskov Kragh et al., 2018; Schleheck et al., 2009). Bacterial aggregation is influenced by various factors, such as QS-state, eDNA, ions, and cationic polymers (Chandler et al., 2009; Das et al., 2014; Laganenka et al., 2016; Perez-Soto et al., 2018). Altogether, these findings indicate that bacteria display multicellular behaviors in the liquid phase that are distinct from those observed in surface-bound bacterial communities. Accordingly, cell auto- (i.e., aggregation between cells belonging to the same species) and co-aggregation (i.e., aggregation between cells belonging to different species) have then been added to the biofilm cycle model (Sauer et al., 2022).

The involvement of extracellular DNA (eDNA) in the formation of bacterial aggregates has been observed in various bacterial species (Allesen-Holm et al., 2006; Moscoso et al., 2006; Qin et al., 2007; Whitchurch et al., 2002). eDNA plays multiple roles within the aggregate, serving as a structural component, an energy and nutrition source, and a gene pool for horizontal gene transfer in naturally competent bacteria (Nagler et al., 2018). Additionally, eDNA has the ability to bind to bacterial flagella, leading to increased hydrophobicity of the cell surface. This, in turn, promotes bacterial aggregation and enhances the stability of the biofilm structure (Aqeel et al., 2019; Gloag et al., 2013; Mlynek et al., 2020; Pakkulnan et al., 2019). *Pseudomonas putida* KT2440 is a non-pathogenic soil bacterium endowed with the ability to adapt to a large variety of physicochemical and nutritional niches (Benedetti et al., 2016; Nikel et al., 2014), and able to form biofilms depending on the environmental conditions (Volke & Nikel, 2018). In our work, by using *P. putida* KT2440 and derivatives exhibiting either enhanced or reduced biofilm formation capabilities, we

observed a fraction of cells associated with eDNA in the planktonic phase. This observation was based on propidium iodide (PI) staining. More importantly, it was determined that the size of the fraction of eDNA-associated/PI-positive cells is correlated to the global biofilm formation capability of the cell population. This result is important since it suggests that biofilm switching does not follow the classical phenotypic switching mechanism where individual cells within the population decide to activate or repress gene circuits according to environmental cues (Acar et al., 2008; Kussell & Leibler, 2005; Thattai & Van Oudenaarden, 2004). Instead, biofilm switching in *Pseudomonas* species seems to be determined collectively based on the number of eDNA molecules released in the supernatant. Massive release of eDNA increases the probability of binding to cells and the number of eDNA-associated cells, in turn, increases the probability of cell aggregation and biofilm formation. In this work, we will use these characteristics to characterize the dynamics of *P. putida* population upon continuous cultivation based on automated flow cytometry (FC) (Henrion et al., 2023). In a second, reactive FC strategies will be implemented for acting on the cell phenotypic switching mechanisms associated with biofilm formation in an attempt to either reduce or enhance biofilm formation (Bertaux et al., 2022; Delvigne & Martinez, 2023).

3. Material and methods

3.1. Strains and medium composition

The bacterial strains used in this study are listed in **Table 4-1**. All strains were maintained in 25% (v/v) glycerol at –80°C in working seed vials (2 mL). Prior to experiments, one colony of each bacterium was used to inoculate 10 mL of lysogeny broth (LB) medium (10 g L^{-1} NaCl, 5 g L^{-1} yeast extract, and 12 g L^{-1} tryptone) and grown for 6 h with shaking at 30°C. Precultures and cultures of all bacteria were done in modified M9 minimal medium (33.7 mM Na2HPO4, 22.0 mM KH2PO4, 8.55 mM 6 NaCl, 9.35 mM NH4Cl, 1 mM MgSO4, and 0.3 mM CaCl2), complemented with a trace element (13.4 mM EDTA, 3.1 mM FeCl3·6H2O, 0.62 mM ZnCl2, 76 µM CuCl2·2H2O, 42 µM CoCl2·2H2O, 162 µM H3BO3, and 8.1 µM MnCl2·4H2O), 1 µg L^{-1} biotin and 1 µg L^{-1} thiamin) and supplemented with glucose (5 g L^{-1}) as the main carbon source (pH = 7.2). For strain DGC, the media was supplemented with gentamycin at a final concentration of 10 µg ml^{-1}.

3.2. Plasmid construction and genetic manipulations

Plasmid pS638::DGC was constructed by amplifying the hyperactive diguanylate cyclase mutant A0244 from *Caulobacter crescentus* (B. Christen et al., 2006), with the primer pair P1 and P2. The resulting amplicon and vector pSEVA638 were digested with *Bam*HI and *Sac*I (FD0054 and FD1133, Thermo Fisher Scientific). The fragments were purified (NucleoSpin Gel and PCR Clean-up Columns, Macherey Nagel) and ligated with T4 DNA ligase (EL0014, Thermo Fisher Scientific). *E. coli* DH5α was transformed with the ligation mixture and the cell suspension was plated on a gentamycin–selective plate. All the plasmids are listed in **Table 4-1**. Subsequently, the constructed pS638::DGC (where *DGC*A0244 was placed under transcriptional control of the inducible XylS/*Pm* expression system) plasmid was isolated from a single colony and its correctness was confirmed by sequencing. The plasmids for the deletion of *lap*A were constructed according to (Wirth et al., 2020). In short, ~500 bp homology arms (HA) flanking the gene coding sequences were amplified from the chromosomal DNA of *P. putida* KT2440 using the primer pair P5/P6 (*lap*A_HA1) and assembled into the suicide vector pSNW2 employing the USER cloning method (Cavaleiro et al., 2015).The purified plasmids were introduced into stationary *P. putida* KT2440 cells by electroporation and selected on LB agar medium supplemented with kanamycin (50 μg mL^{-1}). The corresponding pSNW2 derivative, now fully integrated into the bacterial chromosome, was resolved by transforming the cells with the auxiliary plasmid pQURE6 and selection on gentamicin (10 μg mL^{-1}) and 3-methyl benzoate (1 mM) (Volke et al., 2020). Resolved strains (GFP-negative and kanamycin-sensitive) were tested for the desired genotype by colony PCR (OneTaq® 2X Master Mix with Standard Buffer, New England Biolabs). Oligonucleotides were used in this study listed in **Table 4-2.**

3.3. Plasmid transformation

Plasmids pSEVA227M and pSEVA227Y (Table 4-1), propagated in *E.coli* and *P.putida* KT2440 (kindly provided by Prof. Victor de Lorenzo, CNB-CSIC, Spain) , were isolated with a plasmid extraction kit (NucleoSpin Plasmid EasyPure, Germany) according to the manufacturer's protocol and stored at -20°C. Electrocompetent cells of *P. putida* Δ*lap*A were prepared according to a slightly modified procedure originally described by (Choi et al., 2006). Briefly, 1 ml of cells in the early stationary phase (OD600 = 1–1.5) from cultures grown in LB medium were harvested by centrifugation at 8000×g and washed twice with 1 ml of 300 mM sucrose at room temperature (RT). Cells were resuspended in 100 μl of 300 mM sucrose. In the case

of *P. putida* DGC, electrocompetent cells were prepared by washing the biomass with 10% (v/v) glycerol. Briefly, 50 ml of a cell culture in the exponential phase (OD600 = 0.8) in LB medium were harvested by centrifugation at 8000×g and washed twice with 50 ice-cold glycerol, centrifuge and resuspend cells in 0.8 ml ice-cold glycerol, keep on ice. Then 50 µl of electrocompetent cells were mixed with 1µl plasmid DNA (50 ng/ µl) in a 1 mm electroporation cuvette. High voltage electroporation was performed using a Gene Pulser Xcell (Bio-Rad Gene Pulser, US) at 25 µF, 200 Ω, and 1600 kV. After applying the pulse, 1 ml of SOC medium was added immediately, and the cells were transferred to a culture tube and incubated at 30 °C for 1 h. Cells were plated on LB agar plates supplemented with 50 µg/mL of kanamycin and incubated at 30 °C for 48–72 h.

Table 4-1. Bacterial strains and plasmids were used in this study.

Strain	Relevant characteristics[a]	Reference or source
E. coli* DH5α λ*pir	Cloning host; F^- λ^- *endA1 glnX44*(AS) *thiE1 recA1 relA1 spoT1 gyrA96*(Nal^R) *rfbC1 deoR nupG* Φ80(*lacZΔM15*) Δ(*argF-lac*)*U169 hsdR17*(r_K^- m_K^+), λ*pir* lysogen	(Platt et al., 2000)
***P. putida* KT2440**	Wild-type strain, derived from *P. putida* mt-2 (Worsey & Williams, 1975) cured of the TOL plasmid pWW0	(Bagdasarian et al., 1981)
LapA	Derivate of *P. putida* KT2440 with a clean deletion of *lap*A (*PP_0168*)	This study
DGC	Derivate of *P. putida* KT2440 harboring the plasmid pS638::DGC-244	This study
pSEVA638	*oriV*(pBBR1); XylS/*Pm*→multiple cloning site (MCS); Gm^R	(Martínez-Garćía et al., 2015)
pS638::DGC-244	Derived from pSEVA638 with insertion of DGC-244 into the MCS	This study
pGNW2	*oriV*(R6K); P_{EM14g}*BCD→msfGFP*; Km^R	(Wirth et al., 2020)
pGNW2·Δ*lapA*	Derived from pGNW2 with homologous flanking region to *lap*A (*PP_0168)*	This study
pSEVA227M	Km^R; ori (RK2), Pem_7 – msf.GFP	(Silva-Rocha et al., 2013)
pSEVA227Y	KmR; ori (RK2), pBG 17– YFP	(Silva-Rocha et al., 2013)

Table 4-2. Oligonucleotides were used in this study. Oligonucleotides designed for USER cloning are indicated with a † symbol. Restriction sites are shown in italics, ribosomal binding site is underlined and start codon is shown in bold.

Oligonucleotide	Sequence (5'→3')	Use
P1	AAA *GAG CTC* TTA GGA GGA AAA ACA T**AT G**AA AAT CTC AGG CGC CCG GAC	Amplification of *dgc*A0240
P2	AAA *GGA TCC* TCA AGC GCT CCT GCG CTT G	
P3†	AGA TCC UAT TCA TCT ATA GAG TGC GGA TTC	Amplification of genomic regions adjacent to *lapA*
P4†	ATT GGA CUC TCC GTGTGACCCGATGG	
P5†	AGT CCA AUG TGA CAG ACC ACC GGG GCC	
P6†	AGG TCG ACU TCG ATT GGT CGA CGG GTA CG	

3.4. Quantification of biofilm growth in 96-well plates

Two-day biofilm formation of *Pseudomonas* strains was determined by crystal violet staining using a 96-well plate lid with pegs extending into each well (Nunc-TSP lid, Invitrogen™ Thermo Fisher Scientific). Briefly, precultures were grown overnight at 30°C to an OD600 nm of 1.0. The cell suspensions were then adjusted to an OD600 nm of 0.1 in M9 medium. A total of 160 µL cell suspension were added to each well. Fresh medium was used as a negative control. The plates were sealed with parafilm and incubated with shaking at 180 rpm at 30°C. The biofilm biomass was quantified with a crystal violet staining assay modified from previously reported CV assays (Ren et al., 2014). CV quantification was performed on the pegs of the Nunc-TSP lid culture system. Briefly, after 48 h of cultivation, the peg lids were taken out and washed three times using PBS. Subsequently, the peg lids were placed in plates with 180 µL of an aqueous 1% (w/v) CV solution. Then, the lids were washed with PBS three times after staining for 20 min. Subsequently, the peg lids with crystal violet stain were placed into a new microtiter plate with 200 µL of 33% (w/v) glacial acetic acid in each well for 15 min. The optical density at 590 nm of each sample was measured by a microplate reader (Tecan SPARK, Männedorf, Switzerland).

3.5. eDNA production in planktonic cultures

The bacterial strains, including *P.putida* KT2440, *P.putida* Δ*lap*A, and *P.putida* DGC, were cultured in modified M9 medium in 500mL Erlenmeyer flasks. These flasks were filled up to one-fifth of their nominal volume and placed on a rotary shaker at 170 r.p.m. at 30°C. The shake flasks were grown in parallel under identical conditions for a period of 30 hours, during which biomass growth and eDNA production were monitored. The cell density was estimated by measuring the OD600 nm (Genesys™ 10 UV-Vis, Thermo Scientific, USA). The eDNA in the supernatant was quantified after precipitation. To achieve this, bacterial cells were removed from 900 µL culture through centrifugation (4 min, 6800 g, Eppendorf™ 5424R). The supernatant (700 µL) was transferred to a sterile Eppendorf tube and mixed with 50 µL protein precipitation solution (Promega, USA) by inverting it ten times before centrifugation (10 min, 12100 g, Eppendorf™ 5424R). Then, 700 µL of the supernatant was mixed with 70 µL 2.5 M NaCl and 1400 µL 96% ethanol (62% final concentration) before being stored at -20 °C for at least 24 hours. The DNA was precipitated by centrifugation (25 min, 4 °C, 23 500 g, Eppendorf™ 5424R), after which it was washed once in 70% ice-cold ethanol and dried for less than 3 minutes at 37°C. The eDNA was quantified using the QuantiFluor dsDNA dye (QuantiFluor dsDNA System, Promega, Madison, WI, USA) according to the manufacturer's protocol. In brief, eDNA in each sample was mixed with 200 µL of freshly prepared QuantiFluor dsDNA dye in TE buffer and incubated for 5 minutes before measuring the fluorescence intensity. The eDNA concentration was measured in 2 µL on a (NanoDrop™ 2000, Thermo Fisher Scientific, UK), using an excitation wavelength of 504 nm and an emission wavelength of 531 nm. For each run, a calibration curve was generated using Lambda DNA from Invitrogen™ Molecular Probes. To ensure the reproducibility of the experiment, the growth and eDNA concentration were determined in three independent samples for each time point. The experiment was also repeated with triplicates for all strains to verify the reproducibility between biological replicates.

3.6. Biomass Quantification

The dry matter of the liquid phase and biofilm phase were determined separately by the Moisture analyzer (HE53 Halogen Moisture Analyzer, Switzerland) according to manufacturer protocol. Briefly, the equipment was first warmed up for 30 minutes, and the standby temperature was set to 60°C. Then, the weighing aluminum pan containing a membrane filter disc (0.2µm, 47mm, Fisherbrand™) was tared

automatically on the balance after being dried at 105°C in the moisture analyzer until reaching a stable weight lasting about 1 minute. The drying temperature was set to 105°C. Next, 10 mL of well-mixed planktonic and biofilm samples (After emptying the flask from planktonic culture, adherent cells were harvested by scraping from the wall of flasks with a cell scraper and resuspended in PBS and well-mixed) were evenly added to the membrane filter and positioned in a vacuum filtration apparatus. The liquid component of the sample was removed substantially by applying a vacuum from a small compressor for 2-5 minutes, leaving the broth solids. The filter and the residual solids were washed with 10 mL of deionized water, and the vacuum was reapplied to remove excess liquid. The filter and solids were replaced on an aluminum pan, and the drying program was set to end when the weight change was less than 0.1 mg min^{-1}. The loss of weight before and after drying is used to calculate biomass as grams of dry weight per liter.

3.7. Flow cytometry analyses (Off-line)

FCM analysis was carried out with an Attune NxT Acoustic Focusing Cytometer (Thermo Fisher Scientific, United States) containing a violet laser 405 nm (50 mW), a blue laser 488 nm (50 mW), and a red laser 638 nm (100 mW). Instrument calibration was performed with Attune performance tracking beads (2.4 and 3.2 μm) (Thermo Fisher, United States). Side scatter (SSC) and Forward scatter (FSC) and BL3 (695/40) for PI (P4170, Sigma-Aldrich) were determined with FC. The software settings were as follows: Fluidics, medium; Threshold, 2000 on SSC-H; Run with limits, 40,000 events at a flow rate of 25 μl/min. Cells were diluted to an appropriate density OD600 (0.001-0.003 ≈700-1500 event/ μl) with filtered 1x PBS. FSC and SSC voltage and threshold were set based on wild-type bacteria. All bacterial samples were stained right before FC analysis by adding 1 μL of the PI stock solution (a stock solution was prepared at 1 mg mL^{-1} in sterile Milli-Q water and used at a final concentration of 1.5 μM in sterilized PBS) to 1 mL of a cell suspension in PBS (($1x10^7$ cells mL^{-1}). The stained samples were incubated for 10 min in the dark at room temperature and analyzed by FC (live-dead gating was done based on heat-killed bacteria at 80°C for 1 h).

3.8. Microscopy images

Samples from *P. putida* KT2440, *P. putida* Δ*lap*A, and *P. putida* DGC culture were taken at 0h,6h, and 24h during the batch phase and subjected to microscopy analysis. Microscopy images were acquired using a Nikon Eclipse Ti2-E inverted automated

epifluorescence microscope (Nikon Eclipse Ti2-E, Nikon France, France) equipped with a DS-Qi2 camera (Nikon camera DSQi2, Nikon France, France), a 100× oil objective (CFI P-Apo DM Lambda 100× Oil (Ph3), Nikon France, France).

3.9. Continuous cultivation with automated flow cytometry

In this study, *P. putida* KT2440 was grown in a stirred bioreactor (Biostat B-Twin, Sartorius) with a total volume of 2 L and a working volume of 1 L. The batch phase was initiated by diluting overnight cultures into a minimal medium to achieve an initial OD600 of 0.3. The culture was maintained at pH 7.2 and 30°C, with stirring set at 800 rpm and an aeration flow rate of 1 L min^{-1} (1 vvm). The depletion of oxygen marked the end of the batch phase and the start of continuous cultivation mode. For chemostat cultivations, the modified M9 medium containing 5 g L^{-1} glucose was continuously fed at a dilution rate of 0.1 h^{-1}. In contrast, for periodic pulsing system cultivations, a modified M9 medium without a carbon source was continuously fed at the same dilution rate, and glucose feed pulses (0.5 g L^{-1} per pulse) were introduced hourly. The Segregostat platform, previously described (Nguyen et al., 2021; Sassi et al., 2019), was used for Segregostat experiments, in which glucose was pulsed based on a predefined set point. A feedback control loop, including a custom MATLAB script based on FC data, activated a pump to pulse an actuator (glucose) accordingly. The regulation was triggered once the fluorescence threshold was exceeded by more than 10% of the PI positive cells (detected based on the FL3-A channel). Throughout the experiments, samples were collected every 12 minutes from the bioreactor and automatically diluted and stained with PI and analyzed in a flow cytometer (BD Accuri C6, BD Biosciences) with an FSC-H analysis threshold of 20,000. Automated FC data were then processed according to custom Python codes **(Figure 4-S4).**

4. Results

4.1. Biofilm switching is initiated early in the planktonic phase by a subpopulation of cells binding to eDNA

We first investigated biofilm switching based on standard cultivations in shake flasks. In order to establish a possible link between early eDNA excretion, PI staining and biofilm formation, we used different strains of *P. putida* exhibiting different biofilm forming capabilities (**Figure 4-1A**). For this purpose, we genetically manipulated the bacteria by either reducing or increasing their biofilm-forming ability. Specifically, we knocked out the *lapA* gene, which encodes the initial

attachment protein, resulting in a strain that is unable to attach to abiotic surfaces. This Δ*lap*A derivative exhibits significantly reduced biofilm formation. To increase biofilm formation, on the other hand, we transformed *P. putida* with plasmid pS638::DGC-244, generating strain called DGC, (di-guanylate cyclase). This strain contains a more active di-guanylate cyclase that elevates the internal concentration of cyclic-di-GMP, a critical regulator of biofilm formation. High levels of c-di-GMP (c-di-GMP), support an adhesive lifestyle, while low levels lead to a planktonic lifestyle(Gjermansen et al., 2006). As expected, the *P. putida* DGC strain, with increased capacity for c-di-GMP production, exhibited the highest biofilm formation capability. On the contrary, the wild-type strain *P. putida* KT2440 exhibited low biofilm forming capability, which was further decreased upon the deletion of *lapA*. These three *P. putida* strains (KT2440 and derivatives) were then cultivated in shaken-flask cultures and monitored for PI staining (based on flow cytometry analyses) and eDNA release (**Figure 4-1B-D**). For all the strains, we observed a progressive accumulation of eDNA in the extracellular medium, correlated with the presence of PI-stained cells in the population. For the *P. putida* DGC strain, this effect was further increased, and cell aggregates were also observed during the cultivation (**Figure 4-1E-G**). The presence of such aggregates is informative about a possible transition to biofilm lifestyle. Taken altogether, these data suggest that it could be possible to use PI as a molecular probe for tracking cells in planktonic phase in an early decision-making process for biofilm formation. The correlation between PI staining and cell eDNA binding was further confirmed based on the use of eDNAse **(Figure 4-S1).**

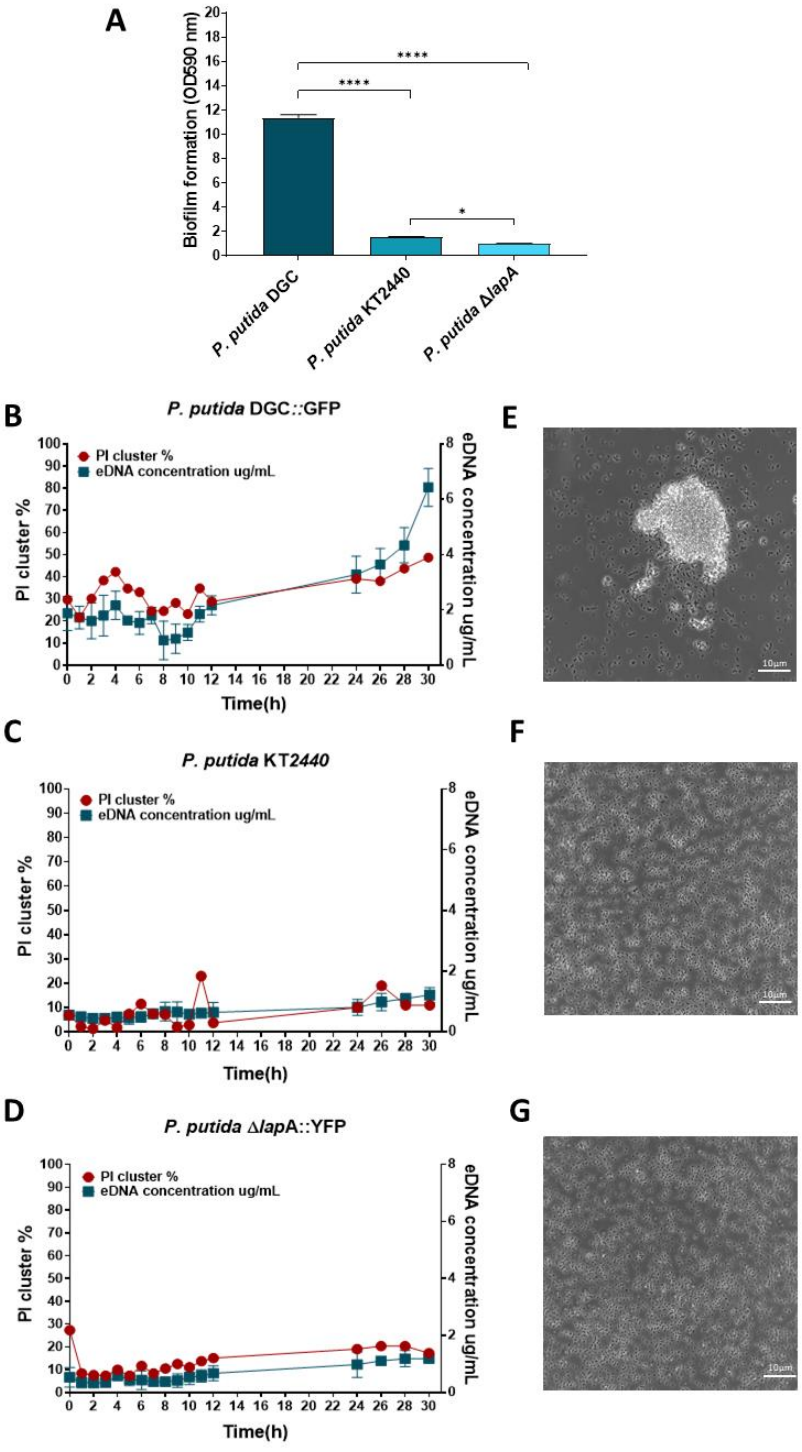
A
Biofilm formation (OD590 nm)
****
****
*
P. putida DGC
P. putida KT2440
P. putida ΔlapA
B
P. putida DGC::GFP
PI cluster %
eDNA concentration ug/mL
Time(h)
C
P. putida KT2440
D
P. putida ΔlapA::YFP
E
F
G
10µm

Figure 4-1. eDNA release increases the fraction of eDNA-associated cells in the planktonic phase. **A** Cristal violet assay for the biofilm forming capability of different derivatives of *P. putida* KT2440. Asterisks over brackets indicate a significant difference between samples (*p*-values: **** $p < 0.0001$, * $p < 0.03$). Results are presented as the mean and standard deviation for three biological replicates. **B-D** Time evolution of eDNA and PI positive cells (determined based on FC) during flask experiments (experiments have been done in triplicates). **E-G** Microscopy images (40x) of cells samples coming from flask experiments for *P. putida* DGC **(E)**, *P. putida* KT2440 WT **(F)** and *P. putida* Δ*lap*A **(G).**

4.2. eDNA binding is correlated with cell auto-aggregation

We used automated flow cytometry (FC) for mapping the population diversification dynamics in continuous culture. For this purpose, we use an in-house developed FC interface for sampling a chemostat at the time interval of 12 minutes (**Figure 4-2A**) (Sassi et al., 2019). In this way, we obtained a high-resolution temporal profile of the evolution of the population based on three parameters i.e., the red fluorescence associated with PI binding (FL3-A channel), as well as the size and morphology of the cells and cell aggregates (FSC-A and SSC-A parameters respectively). Indeed, we observed that the transition to the biofilm lifestyle in *Pseudomonas* was promoted by the formation of cellular aggregates in the planktonic phase (**Figure 4-1E** for *P. putida* KT2440 DGC and **Figure 4-2B&C** for *P. putida* KT2440 WT cultivated in chemostat). We then applied a specific data treatment procedure to the temporal profile obtained based on automated FC. In short, the time scatter plots related to the different signals i.e., PI (**Figure 4-2D**), FSC (**Figure 4-2E**), and SSC (**Figure 4-2F**), are divided into 50 fluorescence bins, each bin containing a specific number of cells. These fluorescence bins are used to compute the fluxes of cells into the phenotypic space by applying a gradient, leading to the quantification of the total fluxes of cells per time interval (F) for all signals (**Figure 4-2G-I**). The observation of the time evolution of the flux of cells through the diversification landscape reveals useful information i.e., that flux of diversification occurs stochastically during chemostat cultivation (**Figure 4-2J**). Interestingly, data analysis pointed out a strong direct relationship between the FC signals (**Figure 4-2K**), suggesting a close interplay between the PI signal and cell auto-aggregation, and subsequent biofilm formation.

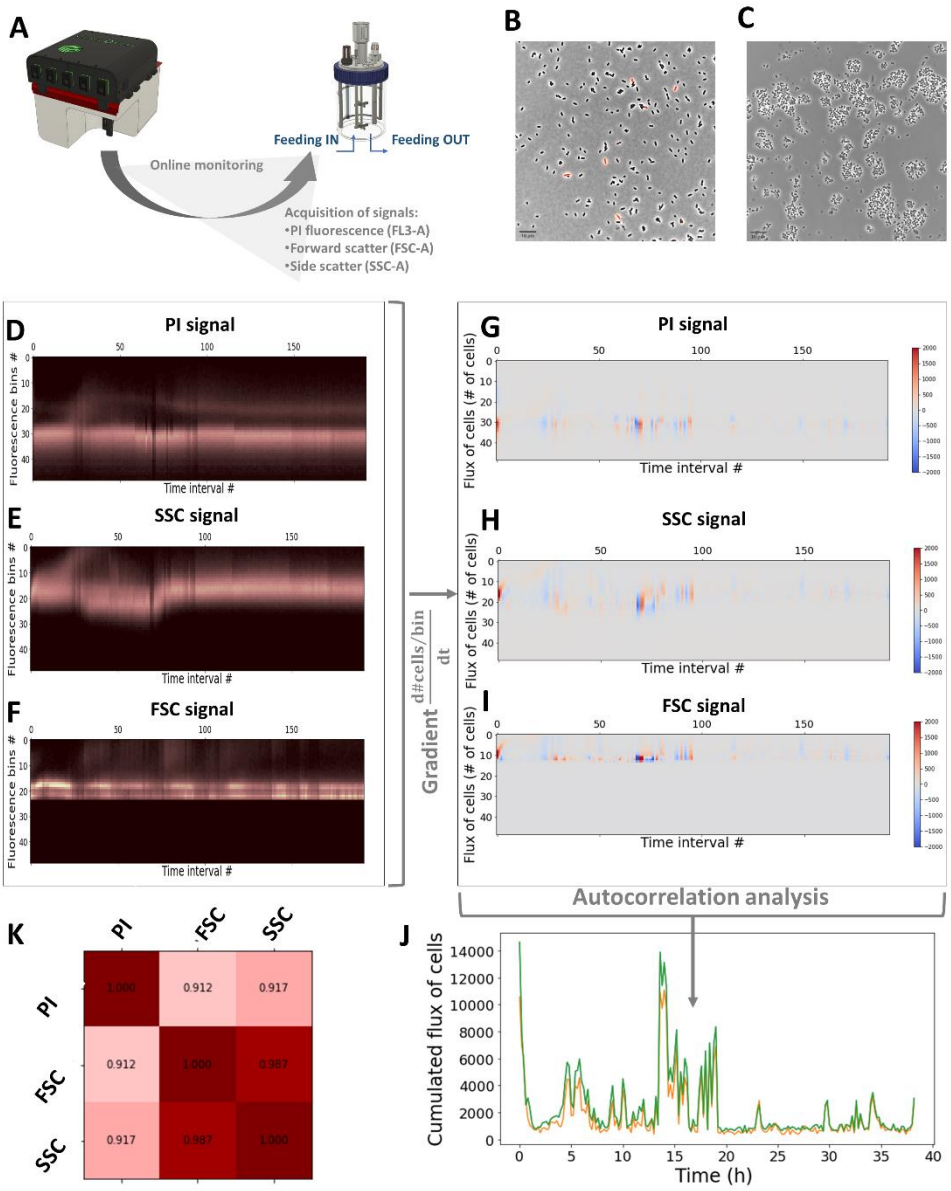

Figure 4-2. Automated FC analyses reveal a strong correlation between eDNA-associated, PI-positive cells and cell auto-aggregation. **A** Scheme of the automated FC set up connected to a continuous cultivation device (Dilution rate D = 0.1 h^{-1}). **B-C** Microscopy images (40X) taken during continuous cultivation after 3h and 23h of cultivation respectively. **D-F** Binning of the time scatter profiles for the PI fluorescence, the FSC and SSC signals respectively. **G-I** computation of the gradient of cells from the binned data for the PI fluorescence, the FSC and SSC signals respectively. **J** Cumulated flux of cells extracted from the gradients of the

three signals. **K** Correlation matrix with the Pearson coefficients indicating a strong direct relationship between the FC signals (p-values < 10^{-78} for all the correlations).

4.3. Fast biofilm switching induces a fitness cost for planktonic growth

As stated in the previous section, fitness cost associated with phenotypic switching (or switching cost) is an essential factor affecting the diversification dynamics of the cell population. In a similar way, it can be expected that cells deciding to adopt a sessile lifestyle exhibit reduced fitness related to growth in the planktonic phase.

When we performed mono-culture with the three strains exhibiting different biofilm forming capabilities, we observed an inverse correlation between the fitness of the strain, as recorded based either on the global growth rate in (**Figure 4-S2**), or based on biomass yield in the planktonic (**Figure 4-3A**) and the biofilm phase (**Figure 4-3B**), and its biofilm forming capability. We further evaluated the switching cost by co-cultivating fast biofilm switcher (e.g., *P. putida* DGC) with strains exhibiting biofilm defect (i.e., *P. putida* Δ*lapA*). For ease of quantification, each strain was tagged with a different fluorescent protein. As expected, *P. putida* DGC::GFP was quickly outcompeted in the liquid phase in these conditions **(Figure 4-3C**) and was mainly found in the biofilm phase at the end of the cultivation (**Figure 4-3D**). The fact that biofilm switching induces a significant reduction in fitness for the planktonic phase will be exploited in the next sections for characterizing the diversification process of *P. putida* and designing biofilm mitigation strategies.

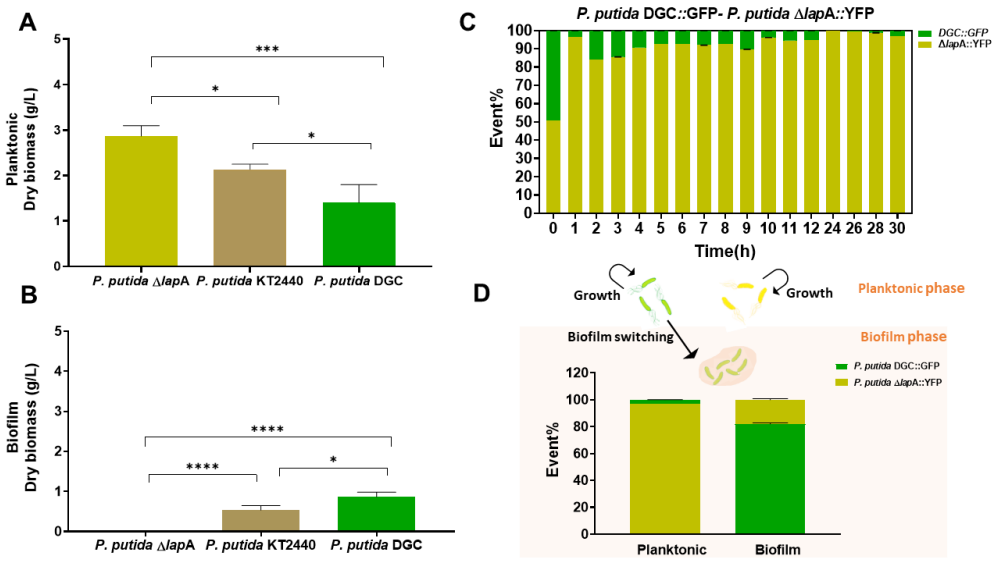

Figure 4-3. A Planktonic dry weight and **B** Biofilm dry weight comparison in mono- and co-cultures after 24h. The significance for the biofilm and planktonic dry weight data was evaluated evaluated (*p*-values: * $p < 0.05$, *** $p < 0.0005$, **** $p < 0.0001$). **C** Dynamics of a co-culture *P. putida* DGC::GFP and *P. putida* Δ*lap*A*::*YFP cultivated in shake flask. Flow cytometry analysis of percentage of each strain in the co-culture ($n \geq 3$). The error bars represent the standard deviation (SD) from three biological replicates. **D** Flow cytometry analysis of percentage of each strain in biofilm sample of co-culture after 24h.

4.4. Biofilm formation is associated with a bursty diversification dynamics

In microbial ecology, phenotypic switching is often associated with a fitness cost. We recently demonstrated that this cost is the main driver for diversification dynamics of the whole population (Henrion et al., 2023). For a very high cost, e.g., in the case of the phenotypic switching associated with sporulation in *Bacillus subtilis*, it is obvious that spore formation leads to a drastic reduction in growth for the cell deciding to switch, a bursty diversification regime is observed. This regime is characterized by the appearance of spontaneous flux of cells (called bursts) phenotypically switching, these cells being progressively washed-out from the continuous cultivation device due to the loss of growth associated with the fitness cost. This specific diversification regime was previously reported during cultivation performed in a device called Segregostat (Henrion et al., 2023). In short, the Segregostat cultivation protocol relies on the use of reactive flow cytometry (**Figure 4-4A**) to detect the bursts of diversification (in a way similar to the determination of the fluxes of cells shown in **Figure 4-2J**). When a burst of diversification is detected, a pulse of glucose is added

in order to interfere with the natural diversification process i.e., by giving a fitness advantage to the cells that are not differentiating. This concept is illustrated in the case of the sporulation in *Bacillus subtilis* (**Figure 4-4B**) (Henrion et al., 2023). In this case, a P_{spoIIE}:GFP transcriptional reporter was used in order to detect the cells deciding to trigger sporulation. The bursts of cells can be visualized from the binned time scatter profile, as well as the concomitant fluxes of cells (**Figure 4-4C**). The observations made in the previous section point out that burstiness could also be associated with biofilm switching for *P. putida*. From a biological perspective, this would make sense since switching to the biofilm state, including cell auto-aggregation, results in a significant cost for the global growth of the population remaining in the liquid phase (**Figure 4-3**). However, a more complex diversification process has to be expected since population dynamics can also be impacted by cell auto-aggregation and cell release from biofilm (**Figure 4-4D**). The diversification profile of *P. putida* associated with biofilm switching was then determined based on Segregostat cultivation and PI staining, according to an automated protocol for PI staining previously established for different Gram-negative bacteria, including *P. putida* (Sassi et al., 2019). As expected, bursts of diversification were also observed in this case (**Figure 4-4E**). While the amplitude of these bursts is reduced compared to the ones observed upon standard chemostat cultivation (**Figure 4-2J**), there are more frequent and follow approximately the same periodicity as for the glucose pulses. In the next section, the detection of these bursts will be considered as an early-warning indicator of biofilm switching for *P. putida* KT2440. The Segregostat system will then be used for interfering with these bursts of diversification and for mitigating biofilm formation.

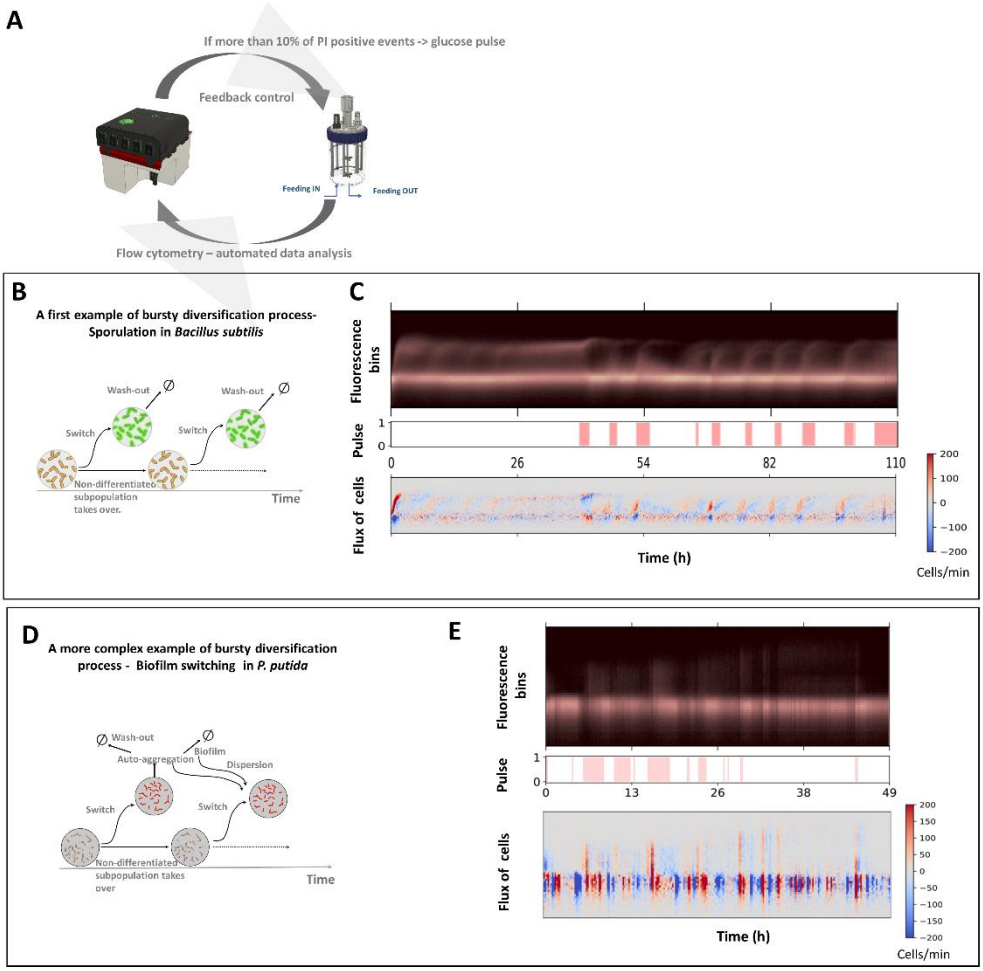

Figure 4-4. **A** Scheme of the Segregostat. Pulses of nutrients are added in the function of the ratio between PI negative and PI positive cells (here set at 10% of PI positive cells), as recorded by automated FC. **B** Example of bursty diversification process involved in the sporulation of *Bacillus subtilis.* **C** By applying environmental forcing based on Segregostat cultivation, the number of bursts is reduced, and the fluxes of cells involved in the process are increased, leading to a substantial but temporary reduction of the entropy for the population (adapted form (Henrion et al., 2023)). **D** A more complex bursty diversification model proposed for *P. putida* KT2440. **E** Time evolution of fluorescence bins associated with PI staining. Flux of cells into the phenotypic space is computed by applying a gradient to the binned data. Time evolution of the total flux of cells into phenotypic space (The fluxes of cells in the phenotypic space F(t) have been computed from the binned fluorescence data).

4.5. Control of bursts leads to reduced population diversification and biofilm formation

In the previous section, we observed that the diversification dynamics associated with biofilm switching were bursty. Our previous experiences with other bursty systems, like the sporulation in *Bacillus subtilis* or the T7-based expression system in *E. coli*, pointed out that these systems can be easily perturbed based on glucose pulsing (Henrion et al., 2023). This approach is expected to control phenotypic switching by conferring additional fitness advantages to non-differentiated cells (i.e., to the PI-negative cells, not associated to eDNA and not committed to biofilm switching) in the liquid phase. This approach seems also to hold in the case of biofilm switching, given the fitness cost observed at this level (**Figure 4-3**). For this purpose, the diversification bursts were detected based on automated FC and glucose pulses were added according to a mode of cultivation called Segregostat. At this stage, two questions arise i.e., i. Does the Segregostat lead to a reduction of the global phenotypic heterogeneity of the population? and ii. Is it necessary to rely on automated FC for triggering glucose pulses, or can periodic pulsing be considered for this purpose?

In an attempt to reply to the first question, we previously used information theory for deriving a proxy that can be used for quantifying the degree of heterogeneity of a cell population i.e., the information entropy (Henrion et al., 2022). The computation of the entropy profile H(t) can be done based on the same binning strategy as the one developed for computing F(t) (**Figure 4-S3**). The second question was challenged by comparing the Segregostat data to the one obtained in the chemostat and continuous culture where glucose pulses were periodically applied (**Figure 4-5A-C)**. Whereas the quantitative measurement of the total amount of biofilm inside the continuous bioreactor is challenging to determine, we can clearly see that, upon Segregostat cultivation, the global entropy profile H(t) is reduced by comparison to standard cultivation or when periodic pulsing is applied **(Figure 4-5D)**. Indeed, the computation of entropy reveals that, in the Segregostat, the microbial population is more homogenous and contains mainly PI negative cells, indicating that biofilm switching is less marked in this case.

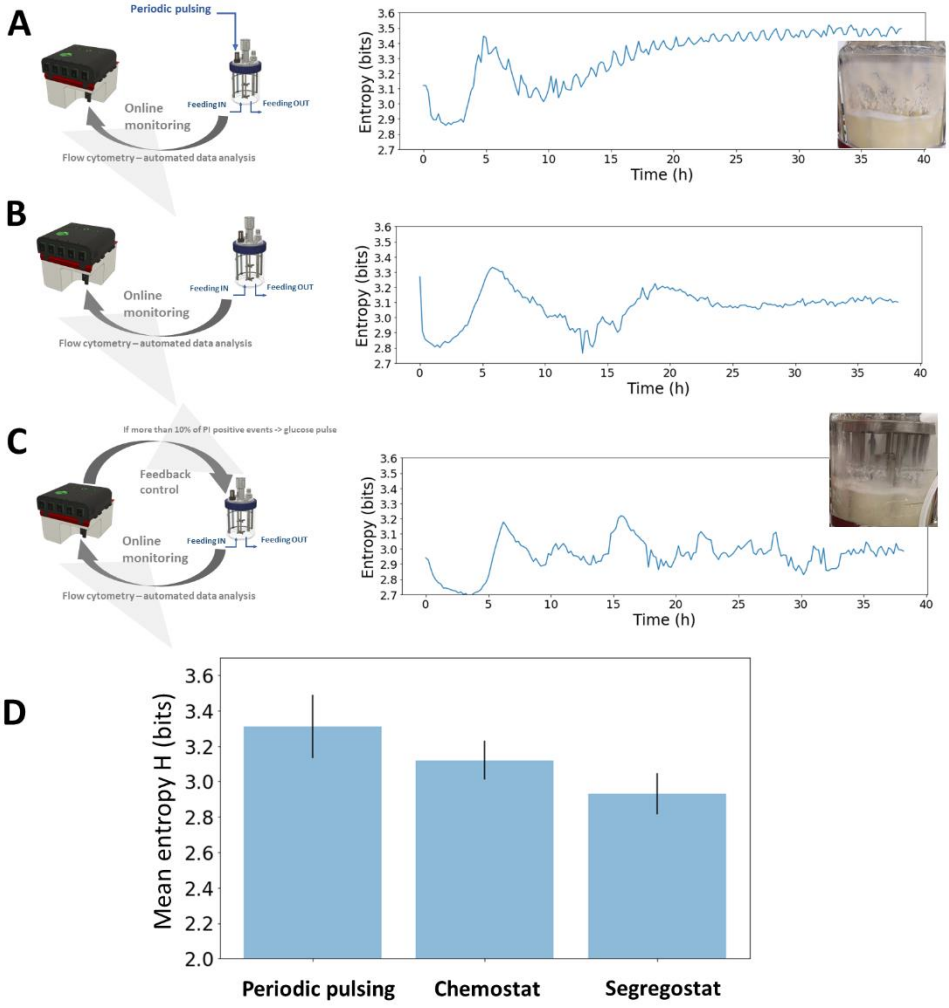

Figure 4-5. Evolution of the entropy H recorded in the function of the fitness cost associated to phenotypic switching in **A** Continuous cultivation at a dilution rate of 0.1 h^{-1} with periodic pulsing of glucose (0.5 g L^{-1} of glucose added each hour). **B** Chemostat cultivation at a dilution rate of 0.1 h^{-1} **C** Segregostat cultivation. Pictures of the biofilm formed on the well of the cultivation vessel are shown for the cultivations performed under periodic pulsing and Segregostat cultivations. **D** Comparative analysis of the mean level of information entropy H for the three modes of cultivation considered.

5. Discussion

Taken altogether, the data displayed in this work suggest that biofilm switching for *Pseudomonas* sp. is a collective decision taken by cells very early during planktonic growth, this decision being influenced by the amount of eDNA released to the extracellular medium. The transition from a planktonic to a biofilm state in bacterial populations is a complex process influenced by various factors and, accordingly, early cell decision-making process related to the switch to biofilm lifestyle has not been thoroughly investigated so far. However, this study suggests that a subpopulation of cells in planktonic cultures plays a pivotal role in initiating biofilm formation by binding to eDNA. Since these cells are associated to eDNA, a simple PI staining can be used for its detection. PI is commonly used in microscopy imaging to visualize extracellular DNA (eDNA) within biofilms or cell aggregates (Deng et al., 2020; Moshynets et al., 2022; Secchi et al., 2022). It has been shown PI as a bacterial viability stain can yield misleading signals of cell death by binding to eDNA (Rosenberg et al., 2019) a characteristic that can be exploited for detecting eDNA in biofilm (Secchi et al., 2022). We observed that the fraction of PI-positive/eDNA-associated cells is correlated with the overall biofilm formation capability of the population. This finding challenges the traditional view of phenotypic switching, where individual cells decide to activate or repress gene circuits based on environmental cues (Kussell & Leibler, 2005)(Thattai & Van Oudenaarden, 2004).Instead, for *Pseudomonas* sp., biofilm switching appears to be determined on a collective basis, driven by the quantity of eDNA molecules released into the supernatant.

In Gram-negative bacteria like *Pseudomonas aeruginosa*, the release of extracellular DNA (eDNA) is mediated through various mechanisms. Quorum sensing, involving N-acyl-L-homoserine lactones (AHL) and the *Pseudomonas* quinolone signal (PQS), triggers eDNA release in planktonic cultures by inducing phage production (Allesen-Holm et al., 2006). Interestingly, recent findings have revealed that eDNA release in *P. aeruginosa* also occurs through oxidative stress caused by the generation of hydrogen peroxide (H2O2) mediated by pyocyanin production (Das & Manefield, 2012). Pyocyanin, a phenazine molecule that is regulated by quorum sensing (Price-Whelan et al., 2006), facilitates the binding of eDNA to *P. aeruginosa* cells. This association between pyocyanin and eDNA can impact the cell surface properties of *P. aeruginosa*, such as size, hydrophobicity, and surface energies, ultimately influencing cell-to-cell interactions and aggregation.

Accordingly, a greater release of eDNA increases the probability of cell binding, which, in turn, promotes cell aggregation and biofilm formation(Secor et al., 2018). Recent reports suggest that the presence of eDNA on bacterial cell surfaces promotes surface hydrophobicity and influences attractive acid-base interactions and therewith promotes initial bacterial adhesion and aggregation (Das et al., 2010, 2011; Liu et al., 2008). The dynamics of the process, as cells within the population switch from planktonic to biofilm state, has been characterized based on automated FC. FC offers a rapid and accurate method for quantifying specific cellular subpopulations within a biofilm(Kerstens et al., 2015). Additionally, it has gained popularity as a means to investigate bacterial auto-aggregation(Espeso et al., 2021; Tomich & Mohr, 2003). PI-positive cells can indeed be easily determined based on FC and can also be used as an early-warning indicator for biofilm formation. Accordingly, we conducted a more precise characterization of biofilm switching based on automated flow cytometry (FC)(Sassi et al., 2019). Automated FC is indeed a valuable tool for monitoring the dynamics of cell population and is used here for tracking changes in the population as it transitions from planktonic to biofilm states(Delvigne & Martinez, 2023). The device can automate environmental transitions based on the phenotypic switching capability of the population(Henrion et al., 2023; Sassi et al., 2019). In this work, we took benefit from Segregostat and the unique characteristics of eDNA to interfere with the biofilm switching mechanisms according to the detection of the burst of PI-positive cells. Furthermore, we demonstrated that using the environmental forcing implemented by Segregostat cultivation led to detection of the bursts of diversification and leads to a reduction in biofilm formation. Based on this experimental set-up, glucose pulses were administered in response to the detection of diversification bursts associated with PI-positive cells, giving a fitness advantage to non-differentiated cells in the liquid phase, thereby controlling phenotypic switching. The results showed that the Segregostat approach reduced the overall heterogeneity of the population, indicating a more homogenous microbial community with predominantly PI-negative cells, suggesting a decrease in biofilm switching. In conclusion, this study provides valuable insights into the early determinants of biofilm switching in *Pseudomonas putida*, shedding light on the relationship between eDNA binding, PI staining, cell auto-aggregation, and biofilm formation. The findings offer new perspectives on microbial population dynamics and strategies for controlling biofilm formation. The application of Segregostat cultivation and the use of automated FC for monitoring and intervening in the diversification process open up possibilities for more targeted

approaches to biofilm mitigation, with potential applications in various fields of microbiology and biotechnology.

6. Supplementary files

Supplementary note 4-S1:

Planktonic cells were double stained with PI and SYTO9, and it was observed that the two stains generally co-localized. Interestingly, within individual sections, green fluorescing cores were observed beneath the red-stained shells, indicating that PI staining was not indicative of membrane integrity, but rather the presence of eDNA outside the intact membrane. The results clearly demonstrated that PI signals were much more intense in the non-treated sample compared to the sample treated with DNase.

DNase enzyme Treatment

Biofilm and planktonic cells were adjusted to (1×10^7 cells mL^{-1}), and samples were resuspended in 500 μL of 1× DNase I buffer (10 mM Tris·HCl, pH = 7.5, 2.5 mM MgCl2, and 0.1 mM CaCl2) with or without DNase I (final concentration 160 U mL^{-1}, Roche, cat.# 04716728001) and were incubated at 37°C 10 for 3 h. After incubation, samples were pelleted by centrifugation at 8500 rpm for 10 min, resuspended in PBS, stained by PI, and analyzed by FCM.

Confocal laser scanning microscopy (CLSM)

All samples were analyzed by confocal laser-scanning microscope (LSM) LSM880 Airyscan super-resolution system (Carl Zeiss, Oberkochen, Germany). The images were taken with the Plan- Apochromat 63×/1.4 Oil objective. We used an excitation wavelength of 488 nm and emission at 500-550 nm for green fluorescence and an excitation wavelength of 561 nm and emission at 580-18 615 nm for red fluorescence. Images were acquired continuously at a pixel resolution of 0.04 μm (regular Airyscan mode) in XY and 1-μm interval in Z step-size using the piezo drive. Before CLSM analysis, staining was performed with one or more fluorescent dyes in the following combinations: PI, SYTO9+PI. An aliquot of 10-15 μL of 1:1 stain mixture solution has been added to a sample of planktonic and biofilm and incubated under the exclusion of light 10 min.

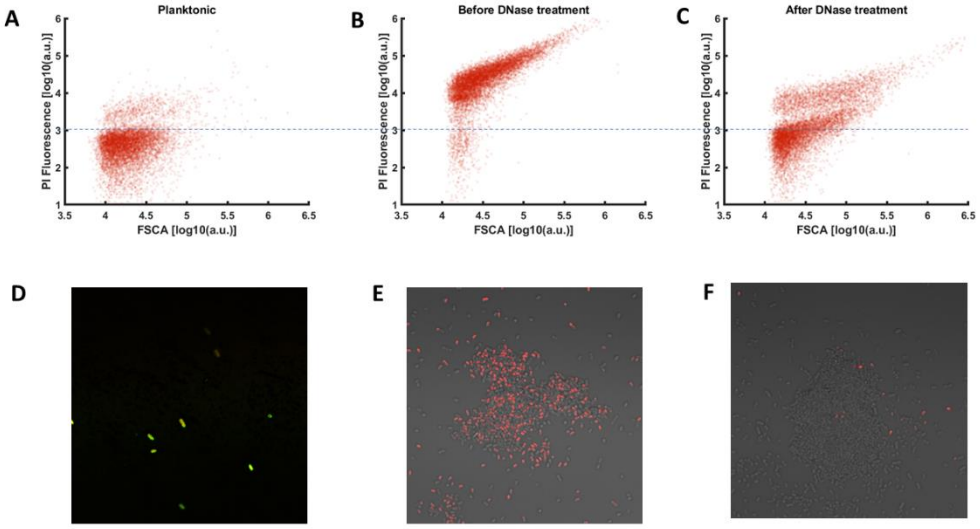

Figure 4-S1. Flow cytometry analysis illustrating the comparison of PI positive percentage among planktonic and biofilm sample and effects of DNase treatment on PI positive fraction of biofilm sample. **A** Planktonic sample co-stained with PI and SYTO 9. **B** Sample showing high PI uptake, before being treated by the DNase enzyme **C** Sample After treatment with DNase enzyme, the PI-positive fraction decreases significantly. Confocal laser scanning microscopy (CSLM) images of *P. Putida* DGC (Planktonic and biofilm) samples **D** Planktonic sample co-stained PI and SYTO 9. **E** Biofilm cells stained with PI before being treated with DNase enzyme. **F** Biofilm cells stained with PI after being treated with DNase enzyme.

Supplementary note 4-S2:

HPLC analysis

Supernatant glucose concentrations were analyzed by high-performance liquid chromatography (Waters Acquity UPLC® H-Class System) using an ion-exchange Aminex HPX-87H column (7.8 × 300 mm, Bio-Rad Laboratories N.V.). The analysis was carried out with an isocratic flow rate of 0.6 mL min−1 for 25 min at 50°C. The mobile phase was composed of an aqueous solution of 5 mM H2SO4. Elution profiles were monitored through a Waters Acquity® Refractive Index Detector (RID) (Waters, Zellik, Belgium). Glucose standard solutions (Sigma-Aldrich, Overijse, Belgium) were used to determine the retention times and construct calibration curves.

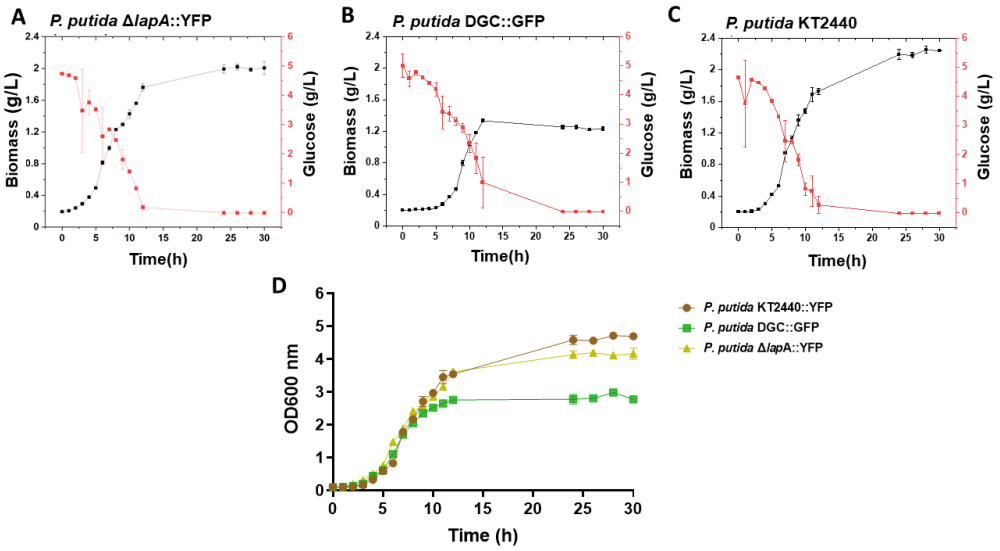

Figure 4-S2. Biomass and glucose consumption (HPLC analysis**)** of **A** *P. putida* Δ*lap*A::YFP , **B** *P. putida* DGC::GFP , **C** *P. putida* KT2440. HPLC assays were carried out offline after the cultivation was ended. **D** Comparison of growth curves of *P. putida* Δ*lap*A::YFP , *P. putida* DGC::GFP , *P. putida* KT2440 during 30h of batch cultivation, n ≥ 3 determined by spectrophotometric measurements (OD600). Each curve resembles a biological replication. The error bars represent the standard deviation (SD) within three technical replicates.

Supplementary note 4-S3:

Microfluidics are typically used for characterizing population dynamics with a single cell resolution (Binder et al., 2017; Dusny & Schmid, 2015). However, microfluidics cultivation experiments, as well as the associated data processing, are quite time consuming. At this level, FC can be considered as an alternative method exhibiting a higher experimental throughput (Delvigne & Martinez, 2023), but at the expense of losing the information about specific trajectories of the individual cells (Ladner et al., 2017).This drawback can be compensated by considering automated FC protocols where more regular snapshots of the population can be acquired. We used automated FC in the context of this work for tracking PI-positive, eDNA-associated, cells. Each 12 minutes, a sample was automatically taken out of the bioreactor, diluted, stained with PI and analyzed by FC. Individual snapshots can then be assembled into a time scatter plot (Supplementary **Figure 3A**).

Additional data treatment steps can also be applied for extracting information about the degree of heterogeneity of the cell population, as well as the fluxes of cells through the phenotypic space. This study employs a proxy derived from information theory i.e., information entropy H, to characterize how cell populations dispersion evolves with time (Henrion et al., 2022) Information theory is being more and more applied to study signal processing by cellular systems (Cheong et al., 2011; Perkins & Swain, 2009; Tan et al., 2007; Tostevin & Ten Wolde, 2009; Zid & O'Shea, 2014). The fundamental basis of information theory relies on the quantification of information entropy (H), serving as a gauge of uncertainty regarding the cell population's response (output) concerning environmental stimuli (input) (Bowsher & Swain, 2014). However, the entropy profile H(t) will be used for characterizing the dynamics of population dispersion over time.

To quantify entropy, we utilize the following equation based onthe PI fluorescence distribution acquired through automated flow cytometry (FC):

$$\textbf{Eqn 1}: H = -\sum_{i=1}^{m} p(x_i).\log_2 p(x_i)$$

Here, m represents the number of observed states (PI classes in our case), and p denotes the probability of observing a cell displaying a specific state i.e., a given PI

fluorescence intensity in our case. The probabilities for various fluorescence classes are easily determined based on automated FC. For this purpose, the PI distribution for a given interval of time is divided into 50 different bins (corresponding to m = 50 in **Equation 4-1**) and the entropy is determined based on the specific number of cells inside each bin by applying **Equation 4-1** (Supplementary **Figure 4-3B**). The number of bins has been previously shown to be optimal for determining the entropy based on FC data (Henrion et al., 2023).

The binned data can also be used for determining the flux of cells (F) through the phenotypic space. For this purpose, a gradient is applied over 2 consecutive binned datasets (Supplementary **Figure 4-3C**). Based on the computation, the F(t) profile can be determined.

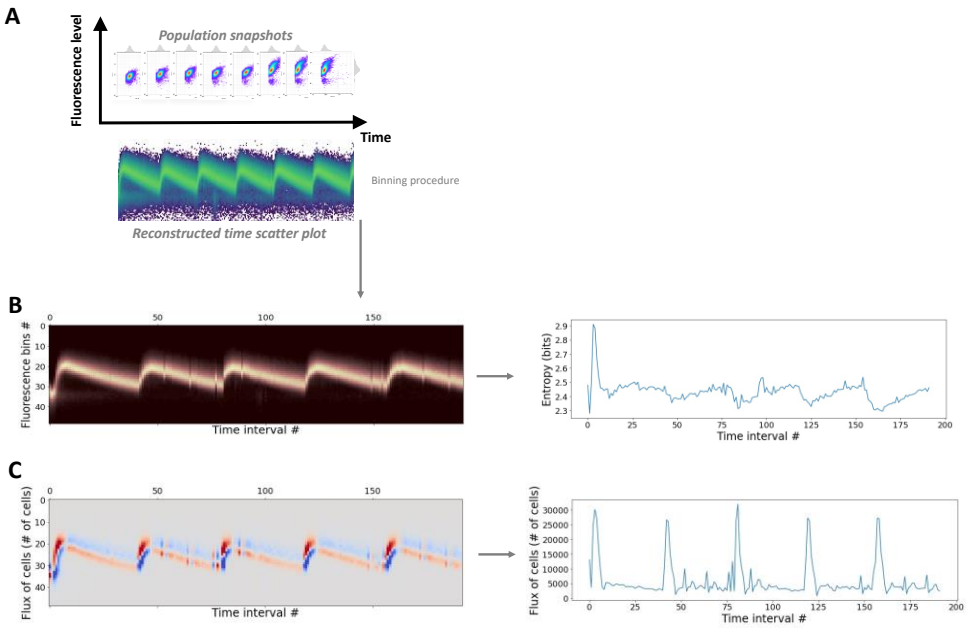

Figure 4-S3. Data processing steps related to automated FC. A Automated FC allows for the acquisition of snapshots of the population at regular time intervals (12 minutes). These snapshots can be assembled into a time scatter profile. B Binning is applied to each snapshot of the time scatter profile for computing the evolution of information entropy H(t). C Binned data can be further processed for determining the flux of cells based on the enrichment or depletion of each bin.

Chapter 5

Biofilm switching influences co-aggregation and the assembly of multi-species biofilm

1. Abstract

Auto-aggregation and co-aggregation interactions are receiving increasing attention across different microbiology research fields. Nevertheless, the role of co-aggregation, as an initial step representing a form of cooperation in mixed biofilms, remains largely unexplored. This study aimed to investigate the potential of co-aggregation, eDNA release in co-culture involving synthetic (*P. putida* DGC::GFP (a biofilm over-producing derivative) and *P. putida* Δ*lap*A::YFP (a biofilm-defective mutant) and *P. putida* KT2440::YFP (WT)) as well as a natural isolates *P. composti* (high aggregation and biofilm producer), *Providencia* sp. (specialize in planktonic growth)) with different aggregation and biofilm formation capabilities. Flow cytometry and propidium iodide (PI) staining were employed as dynamic tracking tools for biofilm switching. Our findings demonstrate that, when cultivating *P. putida* DGC::GFP, a specialist in biofilm formation, with *P. putida* Δ*lap*A::YFP or *Providencia* sp., co-aggregation formation is limited, resulting in a correspondingly low population of PI-positive cells. Under these conditions, *P. putida* DGC::GFP is quickly outcompeted in the liquid phase and primarily resides in the biofilm phase by the end of the cultivation. However, when *P. putida* DGC::GFP is combined with *P. putida* KT2440::YFP, a more cooperative relationship emerges, leading to a higher co-aggregation and, consequently, an increased population of PI-positive cells. This phenomenon is particularly pronounced when combining *P. composti* with *P. putida* Δ*lap*A::YFP, resulting in the formation of macroscopic co-aggregates. Our data highlights a strong correlation between the abilities of biofilm formation, co-aggregation, eDNA release, and the population of PI-positive cells.

Keywords: Auto-aggregation, co-aggregation, fitness, multi-species biofilm, flow cytometry

2. Introduction

Biofilm formation by bacteria encompasses several stages that have been extensively reviewed in several comprehensive reviews (Hall-Stoodley & Stoodley, 2002; Sauer et al., 2022; Simões et al., 2008; Verstraeten et al., 2008). Within bacterial adhesion and formation of micro-colony, microbial auto-aggregation, and co-aggregation may emerge and contribute to biofilm formation and production. Co-aggregation is an extensively observed phenomenon in various bacterial biofilm communities across different environments (Katharios-Lanwermeyer et al., 2014; Stevens et al., 2015) and is commonly considered a key step into the process of biofilm

formation as it drives cell-cell interactions in suspension that will subsequently adhere on a surface. Such interactions mediated by complementary protein adhesins and polysaccharide receptors on the cell surface of co-aggregating cells (Kolenbrander, 2000; Rickard, McBain, et al., 2003). This phenomenon is distinct from auto-aggregation, which is the recognition and adhesion of genetically identical bacteria (Khemaleelakul et al., 2006; Rickard, Gilbert, et al., 2003; Van Houdt & Michiels, 2005). Co-aggregation can promote the development of biofilms, influence their architectural changes, and impact the species composition within biofilms (Hojo et al., 2009; Kolenbrander et al., 2006; Rickard, Gilbert, et al., 2003).

Co-aggregation is considered a significant factor in the formation of biofilms through two pathways (Rickard, Gilbert, et al., 2003). The first pathway involves the specific attachment of individual cells in suspension to genetically distinct cells within the developing biofilm. The second pathway occurs when secondary colonizers co-aggregate in suspension prior to adhering as a co-aggregate to the developing biofilm (Rickard, McBain, et al., 2003). Co-aggregation studies Initially observed in human dental plaque bacteria (Gibbons & Nygaard, 1970), it has expanded to encompass organisms from various environments. This expansion highlights the increasingly recognized role of co-aggregation in developing diverse multi-species biofilms (Kolenbrander, 2000; Rickard et al., 2002). Notably, Min and Rickard (2009) demonstrated that co-aggregation between *Micrococcus* and *Sphingomonas* enhances biofilm formation (Min & Rickard, 2009). Additionally, Simões et al. (2008) discovered that *Acinetobacter calcoaceticus* co-aggregates with several freshwater species, acting as a bridging organism that facilitates the retention of non-co-aggregating strains in freshwater biofilms (Simões et al., 2008).

Extracellular DNA (eDNA) has also been shown to participate in co-aggregation formation and is considered a major structural component of the extracellular polymeric substances (EPS) in biofilms (Böckelmann et al., 2006; Nishimural et al., 2003). In recent years, significant attention has been focused on eDNA as a ubiquitous element in biofilms. In various bacteria, both eDNA alone and in combination with other cellular components have been implicated in aggregate formation (Allesen-Holm et al., 2006; Moscoso et al., 2006; Qin et al., 2007; Whitchurch et al., 2002). Extracellular DNA possesses adhesive properties and can bind to diverse surfaces. For instance, in marine environments, eDNA contributes to the adhesive matrix of free-floating cell aggregates known as "protobiofilms" (Bar-Zeev et al., 2012). Additionally, eDNA is present in aggregates of *P. aeruginosa* cultivated in batch cultures (Alhede et al., 2011). The incorporation of eDNA in aggregates is believed

to serve multiple functions, including acting as a structural component, an energy and nutrient source, or a reservoir for horizontal gene transfer in naturally competent bacteria (Katharios-Lanwermeyer et al., 2014). Consequently, eDNA plays a crucial role in bacterial aggregation and facilitates intercellular adhesion (Lister & Horswill, 2014). These findings align with the discoveries made by Mlynek et al. in *S. aureus*, which suggests a synergistic role of eDNA and PIA (polysaccharide intercellular adhesin) in biofilm formation and bacterial aggregation, regulated by the global regulator CodY (Mlynek et al., 2020). Furthermore, in *P. aeruginosa*, it has been reported that pyocyanin binding to eDNA enhances EPS stability and cellular aggregation (Das et al., 2013).

Quantification of aggregation in bacterial suspensions can be accomplished using various methods. In recent years, flow cytometry (FC) has gained popularity as a means to investigate bacterial auto-aggregation (Beloin, Houry, et al., 2008.; J. S. McLean et al., 2008; Tomich & Mohr, 2003). This indicates that FC could also be applied to co-aggregation studies. For example, Corno et al. (2013) utilized FC to examine the interaction between strains of two aquatic bacterial species *Arthrobacteragilis* and *Brevundimonas* sp. and a protistan predator (Corno et al., 2013). Additionally, propidium iodide (PI) has been extensively utilized by researchers to visualize eDNA in biofilms or cell aggregates using microscopy imaging (Deng et al., 2020; Moshynets et al., 2022; Secchi et al., 2022). Recent studies highlighted that PI, a bacterial viability stain, may produce false signals of cell death by binding to eDNA (Rosenberg et al., 2019).

Taking the above points into consideration, we investigated the potential of co-aggregation and eDNA release in co-cultures involving strains with varying abilities in aggregation and biofilm formation. We utilized both synthetic strains, such as *P. putida* DGC::GFP (a biofilm over-producing derivative), *P. putida* Δ*lap*A::YFP (a biofilm-defective mutant), and *P. putida* KT2440::YFP (WT), as well as semi-synthetic strains including *P. composti* (with high aggregation and biofilm production) and *Providencia* sp. (specializing in planktonic growth). To track the dynamics of the co-cultures, we employed FC and PI staining as monitoring tools. Our results reveal that the co-culture combination of *P. composti* with *P. putida* Δ*lap*A exhibits the highest cooperative relationship, leading to the formation of macroscopic co-aggregates, as indicated by the presence of *P. putida* Δ*lap*A. Furthermore, a similar phenomenon is observed when *P. putida* DGC::GFP is combined with *P. putida* KT2440::YFP, resulting in an increased degree of co-aggregation and consequently a higher population of PI-positive cells. However, when cultivating *P. putida* DGC::GFP, a specialist in biofilm formation, with either *P. putida* Δ*lap*A::YFP or

Providencia sp., co-aggregation formation is limited, leading to a correspondingly low population of PI-positive cells.

3. Material and methods

3.1.1. Bacterial strains and growth conditions

The bacterial strains and plasmids used in this study are listed in **Table 5-1**. All strains were maintained in 25% (v/v) glycerol at –80°C in working seed vials (2 mL). Before conducting the experiments, one colony of each bacterium was used to inoculate 10 mL of lysogeny broth (LB) medium (10 g L^{-1} NaCl, 5 g L^{-1} yeast extract, and 12 g L^{-1} tryptone) The cultures were then grown for 6 hours at 30°C with shaking at 170 rpm.

Both the precultures and main cultures of all bacteria were carried out in modified M9 minimal medium (33.7 mM Na2HPO4, 22.0 mM KH2PO4, 8.55 mM 6 NaCl, 9.35 mM NH4Cl, 1 mM MgSO4, and 0.3 mM CaCl2), supplemented with a trace element solution (13.4 mM EDTA, 3.1 mM FeCl3·6H2O, 0.62 mM ZnCl2, 76 μM CuCl2·2H2O, 42 μM CoCl2·2H2O, 162 μM H3BO3, and 8.1 μM MnCl2·4H2O), 1 μg L^{-1} biotin and 1 μg L^{-1} thiamin). Glucose was provided as the primary carbon source at a concentration of 5 g L^{-1}, and the pH was adjusted to 7.2. For strain, DGC, the medium used in monoculture experiments was supplemented with gentamycin at a final concentration of 10 μg mL^{-1}.

3.1.2. Mono- and dual-species cultivation in shake-flasks

To initiate both single-species and dual-species cultivation, the inoculum was introduced into standard 500 mL non-baffled Erlenmeyer flasks containing 50 ml of the growth medium. In the case of single-species cultivation, the shake flasks were inoculated to achieve a final optical density (OD600) of 0.1. These flasks were then incubated at a temperature of 30°C, with continuous shaking at 170 rpm, for a duration of 30 hours. For dual-species cultivation, the shake flasks were inoculated by combining two strains in a 1:1 ratio (this adjustment was verified using a flow cytometer) based on their respective OD600 values obtained from overnight pre-cultures. The combined OD600 was adjusted to 0.1. The flasks containing the dual culture were subjected to the same incubation conditions as the single-species cultures. Three technical replicates were conducted in the case of both single-species and dual-species.

3.2. Labeling of strains with fluorescent proteins

The following plasmids pSEVA227M and pSEVA227Y (Table 5-1), which have been propagated in *E.coli* and *P.putida* KT2440 (provided kindly from Lorenzo Lab, Spain) respectively have been isolated by plasmid extraction kit (NucleoSpin Plasmid EasyPure, Germany) according to the manufacturer's protocol and stored at -20°C. Electrocompetent cells of *P. putida* Δ*lap*A and *P. putida* KT2440 were prepared according to the slightly modified procedure of (Choi et al., 2006). Briefly, 1 ml of cells in the early stationary phase (OD_{600} = 1–1.5) from cultures grown in LB medium were harvested by centrifugation at 8000×*g* and washed twice with 1 ml of room temperature (RT) 300 mM sucrose. Cells resuspended in 100 µl 300 mM sucrose in order to obtain electrocompetent cells. The *P. putida* DGC was transformed by electroporation, as described by (Taghavi et al., 1994) but with the following modifications: electrocompetent cells were prepared with 10% glycerol. Briefly, 50 ml of cells in the exponential phase (OD600 = 0.8) from cultures grown in LB medium were harvested by centrifugation at 8000×g and washed twice with 50 ice-cold glycerol, centrifuge and resuspend cells in 0.8 ml ice-cold glycerol, keep on ice. Then 50 µl of electrocompetent cells were mixed with 1µl plasmid DNA (50 ng/ µl) in a 1 mm electroporation cuvette. High voltage electroporation was performed using a Gene Pulser Xcell (Bio-Rad Gene Pulser, US) at 25 µF, 200 Ω, and 1600 kV. After applying the pulse, 1 ml of SOC medium was added immediately, and the cells were transferred to a culture tube and incubated at 30 °C for 1 h. Cells were plated on LB agar plates supplemented with 50 µg/mL of kanamycin and incubated at 30 °C for 48–72 h.

Table 5-1. The bacterial strains and plasmids were used in this study.

Strain	Relevant characteristics	Reference or source
***P. putida* KT2440::YFP**	Wild-type strain, derived from *P. putida* mt-2 (Worsey & Williams, 1975) cured of the TOL plasmid pWW0	(Bagdasarian et al., 1981)
***P. putida* Δ*lap*A*::*YFP**	Derivate of *P. putida* KT2440 with a clean deletion of *lapA* (*PP_0168*)	This study
pSEVA227Y	KmR; ori (RK2), pBG 17– YFP	(Silva-Rocha et al., 2013)
***P. putida* DGC::GFP**	Derivate of *P. putida* KT2440 harboring the plasmid pS638::DGC-244	This study
pSEVA227M	Km^R, RK2-based low-copy number vector for construction of transcriptional fusions to msfGFP	(Silva-Rocha et al., 2013)
***Providencia* sp.**	Strains isolated from the cooling tower	(Kang et al., 2022)
P. composti	Strains isolated from the cooling tower	(Kang et al., 2022)

3.3. Crystal violet assay for biofilm quantification

Biofilm formation of the strains after 48h was assessed using a crystal violet staining method in a 96-well plate lid equipped with pegs that extended into each well (Nunc-TSP lid, Invitrogen™ Thermo Fisher Scientific). To begin, overnight precultures were grown at 30°C until reaching an optical density (OD600 nm) of 1.0. The cell suspensions were then adjusted to an OD600 nm of 0.1 in M9 medium. Subsequently, 160 µL of cell suspension was added to each well, while fresh medium served as the negative control. The plates were sealed with parafilm and incubated with shaking at 180 rpm and a temperature of 30°C.

To quantify the biofilm biomass, a modified crystal violet staining assay based on previous studies (Ren et al., 2014) was employed on the pegs of the Nunc-TSP lid culture system. After 48 hours of cultivation, the peg lids were carefully removed and washed three times using phosphate-buffered saline (PBS). Next, the peg lids were placed in plates containing 180 µL of a 1% (w/v) aqueous crystal violet solution and stained for 20 minutes. Following staining, the peg lids were washed three times with PBS. Subsequently, the peg lids, still bearing the crystal violet stain, were transferred to a new microtiter plate containing 200 µL of a 33% (w/v) glacial acetic acid solution

in each well for 15 minutes. The optical density at 590 nm of each sample was then measured using a microplate reader (Tecan SPARK, Männedorf, Switzerland).

3.4. eDNA quantification in the planktonic phase

The bacterial strains, both in mono and dual-species, were cultivated in a modified M9 medium using 500 mL Erlenmeyer flasks. These flasks were filled up to one-fifth of their nominal volume and placed on a rotary shaker at 170 (r.p.m.) at a temperature of 30°C. The shake flasks were grown simultaneously under identical conditions for a duration of 30 hours, during which the growth of biomass and production of extracellular DNA (eDNA) were monitored. Cell density was estimated by measuring the optical density at 600 nm (OD600 nm) by (Genesys™ 10 UV-Vis spectrophotometer, Thermo Scientific, USA). To quantify the eDNA in the supernatant, bacterial cells were separated from a 900 µL culture through centrifugation (4 minutes, 6800 g, Eppendorf™ 5424R). The resulting supernatant (700 µL) was transferred to a sterile Eppendorf tube and mixed with 50 µL of protein precipitation solution (Promega, USA) by gently inverting the tube ten times. This mixture was then centrifuged (10 minutes, 12,100 g, Eppendorf™ 5424R). Next, 700 µL of the supernatant was combined with 70 µL of 2.5 M NaCl and 1400 µL of 96% ethanol (final concentration of 62%) before being stored at -20 °C for a minimum of 24 hours. The eDNA was precipitated by centrifugation (25 minutes, 4 °C, 23,500 g, Eppendorf™ 5424R), followed by a single wash with 70% ice-cold ethanol and drying for less than 3 minutes at 37°C. The eDNA was then quantified using the QuantiFluor dsDNA dye (QuantiFluor dsDNA System, Promega, Madison, WI, USA), according to the manufacturer's instructions. In summary, the eDNA in each sample was mixed with 200 µL of freshly prepared QuantiFluor dsDNA dye in TE buffer and incubated for 5 minutes before measuring the fluorescence intensity. The eDNA concentration was determined by measuring 2 µL of the mixture using a NanoDrop (NanoDrop™ 2000 spectrophotometer from Thermo Fisher Scientific, UK). To ensure reproducibility between biological replicates at each time point, the growth and eDNA concentrations were measured in triplicates for all strains.

3.5. Dry biomass Quantification

The determination of the dry matter in both the liquid phase and biofilm phase was performed separately using a Moisture Analyzer (HE53 Halogen Moisture Analyzer, Switzerland) following the manufacturer's protocol. Initially, the equipment was preheated for 30 minutes, and the standby temperature was set to 60°C. A weighing

aluminum pan containing a membrane filter disc (0.2µm, 47mm, Fisherbrand™) was automatically tared on the balance after being dried at 105°C in the moisture analyzer until a stable weight was achieved, which usually took approximately 1 minute. The drying temperature was maintained at 105°C. Next, 10 mL of thoroughly mixed planktonic and biofilm samples (After emptying the flask from planktonic culture, adherent cells were harvested by scraping from the wall of flasks with a cell scraper and resuspended in PBS and well-mixed) were evenly added to the membrane filter and positioned in a vacuum filtration apparatus. The application of a vacuum from a small compressor for 2-5 minutes effectively removed the liquid component of the sample, leaving behind the solid fraction. To ensure proper washing, the filter and residual solids were rinsed with 10 mL of deionized water, followed by the reapplication of vacuum to remove excess liquid. Subsequently, the filter and solids were transferred back to an aluminum pan, and the drying program was initiated, which terminated when the weight change was less than 0.1 mg min^{-1}. The weight difference before and after drying was used to calculate the biomass as grams of dry weight per liter. This method allowed for the determination of dry matter in both the liquid and biofilm phases, enabling a comprehensive assessment of the overall biomass in the system.

3.6. Microscopy and imaging of co-aggregates formed in liquid culture

Samples from *P. composti* - *P. putida* Δ*lap*A::YFP co-culture were taken at the end of the cultivation period (30h) and subjected to microscopy analysis. Microscopy images were acquired using a Nikon Eclipse Ti2-E inverted automated epifluorescence microscope (Nikon Eclipse Ti2-E, Nikon France, France) equipped with a DS-Qi2 camera (Nikon camera DSQi2, Nikon France,France), a 100× oil objective (CFI P-Apo DM Lambda 100× Oil (Ph3), Nikon France, France). The YFP-2427B cube (excitation filter: 500/24 nm, dichroic mirror: 520 nm, emission filter: 542/27 nm, Nikon France, Nikon) was used to measure YFP. The phase contrast images were recorded with an exposure time of 50ms. The YFP images were recorded with an exposure time of 20 ms and an illuminator's intensity of 4% (SOLA SE II, Lumencor, USA).

3.7. Flow cytometry and PI staining

FC analysis was carried out with an Attune NxT Acoustic Focusing Cytometer (Thermo Fisher Scientific, United States) containing a violet laser 405 nm (50 mW), a blue laser 488 nm (50 mW), and a red laser 638 nm (100 mW). Instrument

calibration was performed with Attune performance tracking beads (2.4 and 3.2 μm) (Thermo Fisher, United States). Side scatter (SSC), Forward scatter (FSC), BL1 (GFP-510/10), BL2 (YFP-540/30) and BL3 (695/40) for PI (P4170, Sigma-Aldrich) were determined with FC. The software settings were as follows: Fluidics, medium; Threshold, 2000 on SSC-H; Run with limits, 20,000 events at a flow rate of 25 μl/min. Cells were diluted to an appropriate density OD600 (0.001-0.003 ≈700-1500 event/ μl) with filtered 1x PBS. FSC and SSC voltage and threshold were set based on wild-type bacteria. All bacterial samples were stained right before FC analysis by adding 1 μL of the PI stock solution (a stock solution was prepared at 1 mg mL^{-1} in sterile Milli-Q water and used at a final concentration of 1.5 μM in sterilized PBS) to 1 mL of a cell suspension in PBS ($1x10^7$ cells mL^{-1}). The stained samples were incubated for 10 min in the dark at room temperature and analyzed by FC (live-dead gating was done based on heat-killed bacteria at 80°C for 1 h).

3.8. Flow cytometry analysis of bacterial auto-aggregation auto and co-aggregation

FC analysis was carried out with an Attune NxT Acoustic Focusing Cytometer (Thermo Fisher Scientific, United States). Before measurements, cell samples were diluted to $1x10^7$ cells mL^{-1}. For each sample, at least 20,000 events were taken and analyzed. FC data sets were first cleaned of electronic instrument noise by eliminating events with negative, infinite, or non-numerical values in the forward and side scattering signals. After that, all doublet events were identified and eliminated by evaluating the standardized residual value (SRV) of the expected linear ratio between the area and the height of the front scattering signal. All data sets presented less than 5% error between the electrical and doublet noise, and after data cleaning, a minimum of 20,000 events were required for further analysis.

For the analysis and quantification of the strains *P. putida* Δ*lap*A::YFP**,** *P. putida* KT2440::YFP and *P. putida* DGC::GFP a linear diagonal gate was implemented separating YFP cells from GFP cells from the Attune FC data. The diagonal linear gate is characterized by the points (2,1.31) and (7,6.3) in the logarithmic space of BL1-A vs BL2-A above this line YFP positive cells can be found, below this line, GFP positive cells can be found. Finally, for the determination and quantification of possible aggregates and analysis similar to the one used in(Velastegui et al., 2023), in this case, a grand mean and standard deviation were calculated to propose a normal probability density function describing the cells that stay in the single non aggregated state (the vast majority) with this we constructed thresholds of increasing probability

for the events to be increasing in size not conforming to a single state population but being part of another population state with different grand mean and standard deviation. Therefore, the events that fall above two standard deviations only have 5/100 probability of being part of a single-cell floating population. Consequently, calculating and comparing the over-representation of this percentile across time gives us a quantitative measurement of cells that are more in not a single-cell floating state. The agglomeration state was then confirmed by observations in a microscope and the final biofilm production.

4. Result

4.1. Using flow cytometry for detecting eDNA release, cellular aggregation, and co-culture composition

Extracellular DNA (eDNA) plays a vital role as a natural adhesive, significantly influencing adhesion and co-aggregation processes(Flemming & Wingender, 2010; Jakubovics et al., 2013). While there are various methods available for quantifying bacterial aggregation in suspensions, flow cytometry has recently gained attention as a powerful single-cell method for characterizing bacterial aggregation. In this study, we utilized flow cytometry in combination with an appropriate single-cell proxy, propidium iodide (PI), as a powerful technical tool to track both co-aggregation and eDNA release in different co-cultures. involving microbial strains exhibiting different biofilm formation abilities. PI was initially used for probing cell viability but has more recently been recognized as also binding to eDNA on the cell surface(Rosenberg et al., 2019). Here, the unique characteristics of eDNA and PI binding were targeted to monitor co-aggregation dynamics at a single-cell level. We have gated aggregation from the planktonic phase based on FSC and SSC signals. Flow cytometry analysis indicated the presence of aggregates of phenotypic particles with a wide forward scatter distribution, indicative of variable particle sizes. These were distinguishable from single cells by their significantly bigger side- and forward-scatter values **(Figure 5-1).**

We utilized our methodology to explore the co-aggregating capabilities of different strains by considering multiple factors, including their biofilm abilities, eDNA-associated cells (as indicated by PI labeling), and the composition of co-cultures (as indicated by fluorescent reporters). Our investigation involved two types of strains: synthetic strains, namely *P. putida* DGC::GFP, *P. putida* Δ*lap*A::YFP, and *P. putida* KT2440::YFP, and natural strains, specifically *P. composti* and *Providencia* sp. These natural strains were previously isolated from industrial cooling tower systems. In

parallel, we employed PI labeling to monitor the release of eDNA and its role in co-aggregation during the planktonic growth of these dual-species. By incorporating this additional aspect, we aimed to gain a comprehensive understanding of the interplay between biofilm formation, eDNA binding, and co-aggregation among the different strains under investigation.

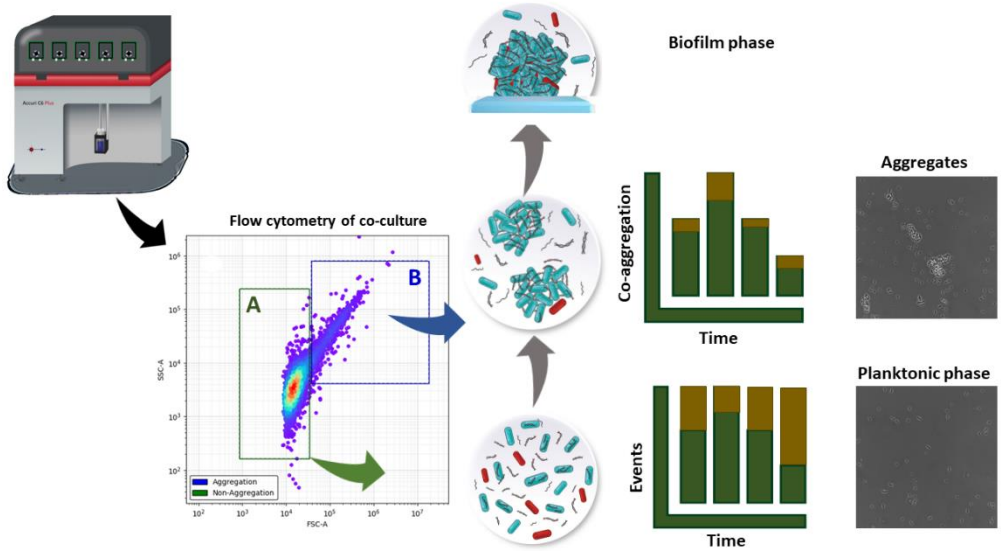

Figure 5-1. Schematic illustration of the methodology used to explore microbial interactions and co-aggregation dynamics resulting from phenotypic switching in synthetic and natural co-cultures using flow cytometry and PI staining. We have implemented a gated aggregation (blue: B panel) technique to separate the planktonic phase (green: A panel) based on forward scatter (FSC) and side scatter (SSC) signals. The resulting aggregates exhibit a wide range of particle sizes, as indicated by their broad forward scatter distribution. Notably, these aggregates can be easily distinguished from individual cells due to their higher side scatter and forward scatter values. PI-staining is used as a single cell proxy to track the DNA-associated cells and the composition of co-cultures assessed by fluorescent reporters i.e., YFP and GFP.

4.2. Cell auto-aggregation is exacerbated at the expense of final biofilm formation for a natural isolate

In order to assess the correlation between biofilm formation abilities and other phenotypic traits associated with biofilm development, such as eDNA release and auto-aggregation, we conducted a comprehensive analysis on synthetic and natural

strains in shake flasks as single species. Additionally, we utilized FC and PI staining to monitor the release of eDNA during planktonic growth.

Consistent with expectations, our evaluation of the biofilm formation ability of the five strains revealed that *P. putida* DGC::GFP exhibited the highest level of biofilm production compared to the other strains **(Figure 5-2A)**. Furthermore, we demonstrated that both *P. putida* DGC::GFP and *P. composti* strains were robust biofilm formers and consequently released larger amounts of eDNA compared to the other tested strains **(Figure 5-2B)**. Notably, *P. composti* exhibited a substantial release of eDNA, which could be attributed to its higher tendency for auto-aggregation.

To further investigate auto-aggregation, we employed flow cytometry to assess the degree of auto-aggregation for *P. putida* DGC::GFP, *P. putida* Δ*lap*A::YFP, *P. putida* KT2440::YFP, and *Providencia* sp. during the batch phase **(Figure 5-2C)**. However, in the case of *P. composti*, the aggregate sizes were too large to be detected by flow cytometry **(Figure 5-2E).** Comparatively, *P. putida* DGC::GFP displayed a significantly higher aggregation percentage than *P. putida* Δ*lap*A::YFP, *P. putida* KT2440::YFP, and *Providencia* sp., which also exhibited lower biofilm production. Nevertheless, due to the significant cell auto-aggregation and the substantial release of eDNA observed in *P. composti*, aggregates formed in the liquid phase are not taken into account in the ultimate formation of the biofilm. Therefore, it appears that in the context of this natural isolate, the floating biofilm is a natural form.

Considering the aforementioned results, we further examined the relationship between biofilm formation, auto-aggregation, eDNA release, and the presence of PI-positive subpopulations by monitoring dynamic changes in the PI-positive subpopulation during the planktonic phase. Interestingly, our findings revealed a significant difference in the PI-positive subpopulation in *P. putida* DGC::GFP and *P. composti* compared to the other strains **(Figure 5-2D).** A comprehensive summary of the characterization of all five strains is presented in **Table 5-S1.** Overall, our results underscore the strong correlation between biofilm formation, the presence of PI-positive subpopulations, eDNA content, and the degree of auto-aggregation within a single species **(Figure 5-2F).**

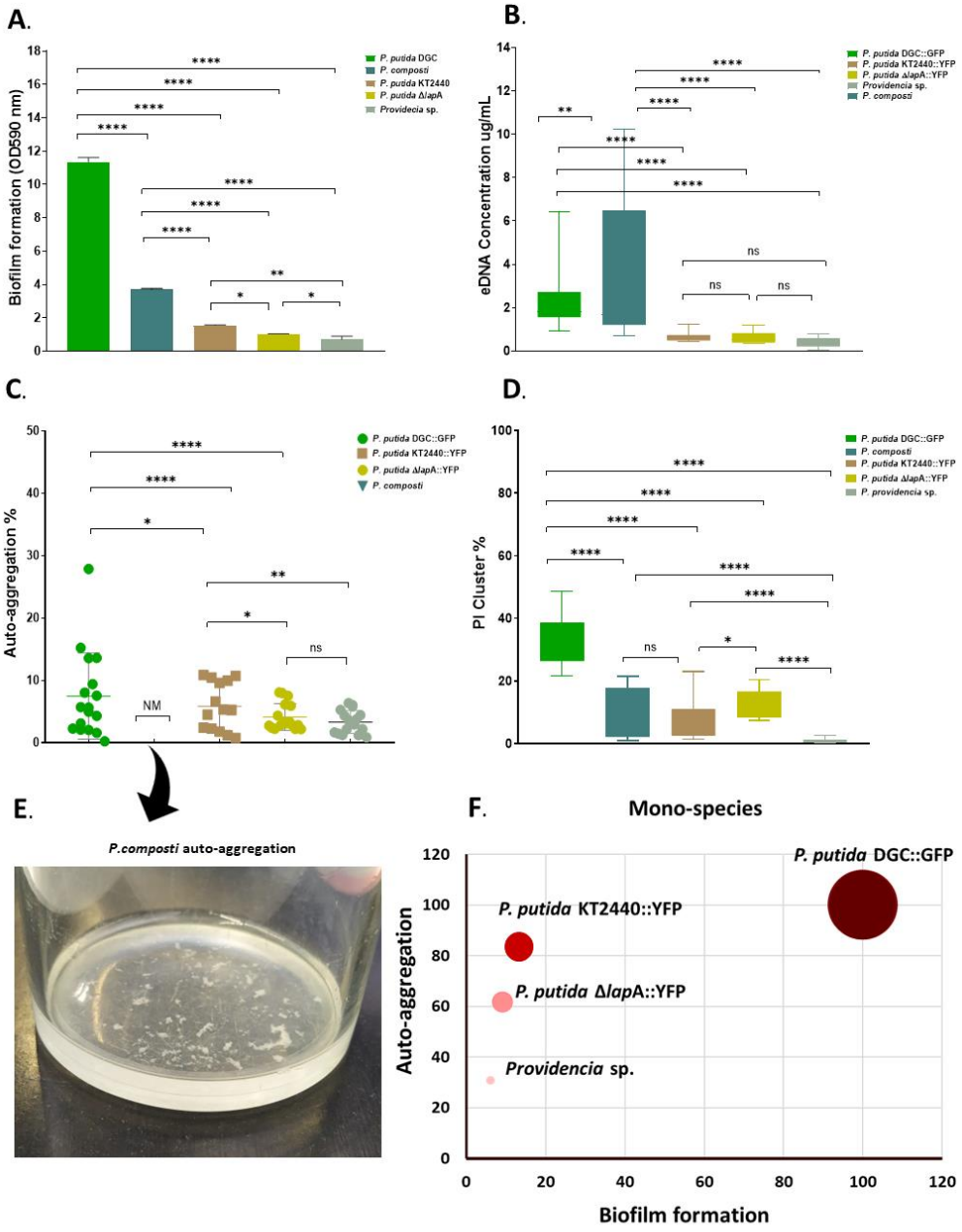

Figure 5-2. Comparing the biofilm formation, eDNA release, PI-positive subpopulation, and auto-aggregation percentage among synthetic and semi-synthetic strains. **A.** Biofilm formation ability of synthetic strains *P. putida* DGC::GFP, *P. putida* Δ*lap*A::YFP, and *P. putida* KT2440::YFP as well as natural strains *P.composti* and *Providencia* sp. after 48h of

batch cultivation, n ≥ 5. **B.** eDNA release, **C.** Auto-aggregation percentage, and **D.** PI-positive subpopulation fraction (%) comparison among synthetic and natural strains during 30h planktonic growth in shake flasks, n ≥ 3. **E.** Macroscopic view of the formation of large aggregates in the case of *P. composti* that were visible to the naked eye at the end of cultivation (30h). **F.** Correlation between biofilm formation, the presence of PI-positive subpopulations, eDNA content, and the degree of auto-aggregation within a single species. A higher intensity of red color represents a higher PI-positive subpopulation. The bigger size of the circle represents a higher amount of eDNA production. Asterisks over brackets indicating a significant difference between samples (*p*-values: **** $p < 0.0001$, ** $p < 0.002$, * $p < 0.03$, ns (not significant), NM (Not measurable)). The error bars represent the standard deviation (SD) within three technical replicates.

4.3. Fast biofilm switcher is able to capture slow biofilm switchers based on co-aggregation, leading to the formation of mixed biofilms

In the previous section, we demonstrated that the *Pseudomonas putida* DGC::GFP strain, when cultivated as a single species, exhibits high levels of biofilm formation and extracellular DNA release. However, it demonstrates lower fitness in the planktonic phase. In order to explore the potential benefits of dual-species cultivation with different biofilm strategies, we conducted experiments using *P. putida* DGC::GFP as a fast biofilm switcher and *P. putida* KT2440::YFP as a slow biofilm switcher.

Our FC data revealed a high synergistic interaction between the two species, mostly during the 8-hour planktonic phase. However, as the cultivation progressed, *P. putida* DGC::GFP was outcompeted in the liquid phase, mainly existing in the biofilm phase **(Figure 5-3A).** On the other hand, *P. putida* KT2440::YFP exhibited greater dominance in the planktonic phase **(Figure 5-3A)**. The results of flow cytometry analysis for the *P. putida* DGC::GFP - *P. putida* KT2440::YFP co-culture revealed higher eDNA content and a subsequent increase in the presence of PI-stained cells within the population. Similar trends were observed for the dynamics of co-aggregation **(Figure 5-S1).** Notably, FC data of the biofilm phase shows a synergistic interaction between the dual-species within the biofilm **(Figure 5-3C)**. Additionally, measurements of dry biomass indicated a significant increase in the dry mass of the planktonic phase for *P. putida* DGC::GFP in co-culture. Conversely, we observed a significant increase in the dry mass of the biofilm phase for *P. putida* KT2440 when the two strains were co-cultured together **(Figure 5-3B)**. These findings confirm the results obtained from FC analysis. Interestingly, when comparing the eDNA content, co-aggregation, and PI-positive subpopulation of the dual-species with that of *P.*

putida KT2440::YFP as a single species, we noticed a significant increase in all cases **(Figure 5-3D)**. These results suggest a possible interaction through co-aggregation and eDNA release in dual-species cultivation. Our findings underscore the remarkable ability of the fast biofilm switcher, *P. putida* DGC ::GFP, to effectively rescue the slower biofilm switchers, *P. putida* KT2440 ::YFP. Furthermore, by applying PI staining, we established a strong correlation between the eDNA content, co-aggregation, and PI-positive subpopulation in this particular case study.

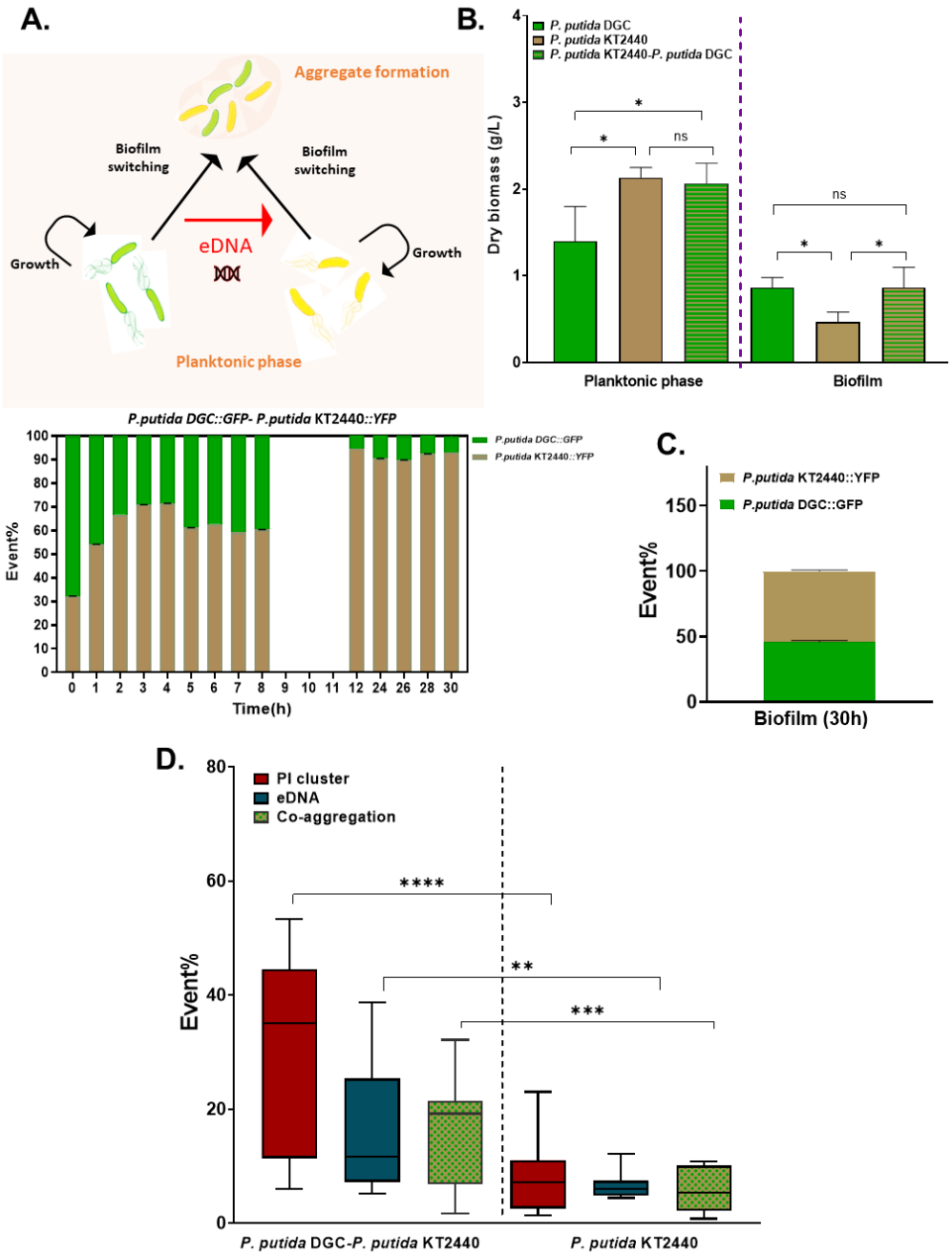

Figure 5-3. A. Dynamics of a co-culture *P. putida* DGC::GFP and *P. putida* KT2440*::*YFP cultivated in a shake flask. Flow cytometry analysis of percentage of each strain in the co-culture ($n \geq 3$). **B.** Planktonic and biofilm dry weight comparison in single species *P. putida*

KT2440*::*YFP and dual-species *P. putida* DGC::GFP-*P. putida* KT2440*::*YFP after 24h, n ≥ 3. The significance of the biofilm and planktonic dry weight data was evaluated (p-values: * $p < 0.03$, ns (not significant)). **C.** Percentage of PI cluster, eDNA release (the data normalized and shows as a percentage), auto-aggregation, and co-aggregation in mono-and dual-species after 30h n ≥ 3. **D.** Flow cytometry analysis of percentage of each strain in biofilm sample of co-culture after 24h, n ≥ 3. Asterisks over brackets indicate a significant difference between samples (*p*-values: **** $p < 0.0001$, *** $p < 0.0004$, ** $p < 0.003$). The error bars represent the standard deviation (SD) from three biological replicates.

4.4. Unveiling co-aggregation capabilities: Enhanced co-aggregation of *P. putida* Δ*lap*A::YFP by natural isolate *P. composti*

Co-aggregation, among other types of interactions, plays a significant role in mixed-species biofilm formation. Based on the findings presented in the previous section, the synergistic interaction between *P. putida* DGC::GFP, and *P. putida* KT2440::YFP, resulted in increased co-aggregation and subsequent eDNA release associated with phenotypic switching, which could be effectively monitored using PI staining. To further investigate this hypothesis, we conducted a study involving three different dual-species co-cultures: *P. putida* DGC::GFP - *P. putida* Δ*lap*A::YFP, *P. putida* DGC::GFP- *Providencia* sp., and *P. composti* - *P. putida* Δ*lap*A::YFP. We systematically analyzed the dynamics of co-aggregation properties and eDNA content in all four dual-species cultures during the planktonic phase, collecting hourly samples over a 30-hour period and subjecting them to flow cytometry analysis. Additionally, growth curves of mono and dual-species were determined by spectrophotometric measurements **(Figure 5-S2).**

The flow cytometry analysis of synthetic dual-species of *P. putida* DGC::GFP - *P. putida* Δ*lap*A::YFP revealed that *P. putida* Δ*lap*A::YFP as slow biofilm switchers were predominantly present in the liquid phase, while *P. putida* DGC::GFP was primarily associated with the biofilm phase towards the end of the cultivation **(Figure 5-4A).** Furthermore, measurements of dry biomass indicated a significant increase in the dry mass of the planktonic phase for *P. putida* DGC::GFP in co-culture, whereas a significant increase in the dry mass of the biofilm phase was observed for *P. putida* Δ*lap*A::YFP when co-cultured with *P. putida* DGC::GFP **(Figure 5-S3)**. Additionally, the flow cytometry analysis of the planktonic phase of this dual-species provided further insights. Notably, during the initial 24 hours of the batch phase, a low percentage of eDNA was observed in the liquid phase, which gradually increased over time **(Figure 5-4D).** Concurrently, the dynamics of co-aggregation steadily increased, potentially due to the dispersion of biofilm cells back into the liquid phase

(Figure 5-4D). These trends were consistent with the dynamics of co-aggregation and the presence of PI-stained cells within the population **(Figure 5-4D)**

In the case of co-culture of synthetic strain *P. putida* DGC::GFP with natural strain *Providencia* sp. FC revealed that *Providencia* sp. as very slow biofilm switchers were predominantly present in the liquid phase, while due to competition interaction in this case, *P. putida* DGC::GFP escaped the liquid phase after 3 hours of cultivation mainly stayed in the biofilm phase **(Figure 5-4B).** Consequently, low eDNA content, as well as limited dynamics of co-aggregation and a low percentage of PI-positive clusters, were observed (**Figure 5-4E**). Moreover, we conducted a comparative analysis of co-aggregation, eDNA content, and the population of PI-positive cells between the dual-species and the corresponding slow biofilm switchers as single species **(Figure 5-S4).** For the *P. putida* DGC::GFP and *P. putida* Δ*lap*A::YFP combination, no significant differences were observed in terms of eDNA release and PI cluster formation between the mono and dual-species conditions. However, a higher percentage of co-aggregation was observed in the dual-species combination, potentially attributed to biofilm dispersion. On the other hand, in the case of *P. putida* DGC::GFP and *Providencia* sp., there were no notable differences in co-aggregation, auto-aggregation, or corresponding PI clusters. Nonetheless, a slight increase in DNA release, particularly at the early stages of the culture, could be attributed to the presence of *P. putida* DGC::GFP at the beginning of the culture period.

Similarly, we conducted the same analysis on the planktonic phase of the *P. composti* and *P. putida* Δ*lap*A::YFP. Interestingly, the FC results demonstrated the presence of both species during the planktonic phase; however, by the end of the cultivation, *P. composti* predominantly transitioned to the biofilm phase **(Figure 5-4C).** Notably, a strong synergistic interaction was observed between *P. composti* and *P. putida* Δ*lap*A::YFP, characterized by the formation of large macroscopic co-aggregates from the beginning of the cultivation (**Figure 5-S6)**. Microscopy imaging of these co-aggregates confirmed the presence and interaction of both species within the aggregates (**Figure 5-S6)**. However, due to the substantial size of the co-aggregates and the technical limitations of FC, it was not possible to determine the degree of co-aggregation in this specific case study. In this case, higher eDNA content was observed during the first 5 hours of the planktonic phase, which subsequently decreased towards the end of the cultivation, possibly due to the formation of these large co-aggregates **(Figure 5-4F).** Flow cytometry analysis, in this case, showed low PI clusters and co-aggregates, which could be attributed to the exclusion of large aggregates during sample preparation to avoid technical issues. In summary, this

observation reinforces our previous findings regarding a strong correlation between aggregate formation, the presence of PI-positive subpopulations, and eDNA content in the case of mono-species and suggests the same correlation holds true even in the case of dual-species **(Figure 5-5).**

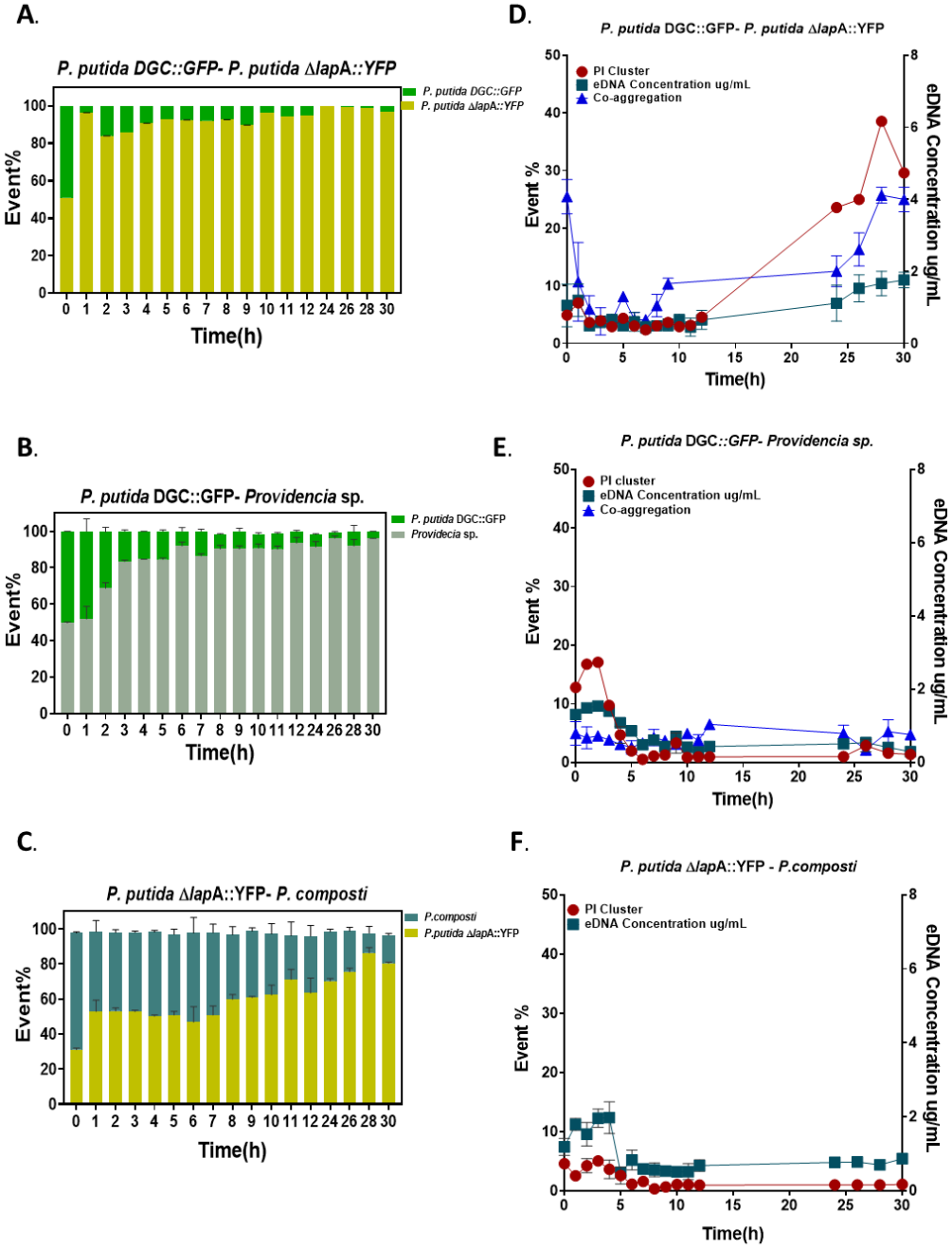

Figure 5-4. Dynamics diversity of composition of synthetic and natural co-cultures cultivated in a shake flask n ≥ 3n. Flow cytometry analysis of the percentage of each strain in

the co-culture of **A.** *P. putida* DGC::GFP - *P. putida* Δ*lap*A::YFP **B.** *P. putida* DGC::GFP-*Providencia* sp. **C.** *P. Composti* - *P. putida* Δ*lap*A::YFP. Comparison of PI-positive cluster (%), co-aggregation (in percentage determined from flow cytometry analyses), and eDNA content. Time evolution of eDNA and PI-positive cells and co-aggregation during the planktonic phase in dual-species during 30h planktonic growth (number of biological replicates n = 3). **D.** *P. putida* DGC::GFP - *P. putida* Δ*lap*A::YFP **E.** *P. putida* DGC::GFP - *Providencia* sp. **F.** *P. composti* - *P. putida* Δ*lap*A::YFP (Co-aggregation dynamic, in this case, has not shown due to limitation of measurement). The error bars represent the standard deviation (SD) for three biological replicates.

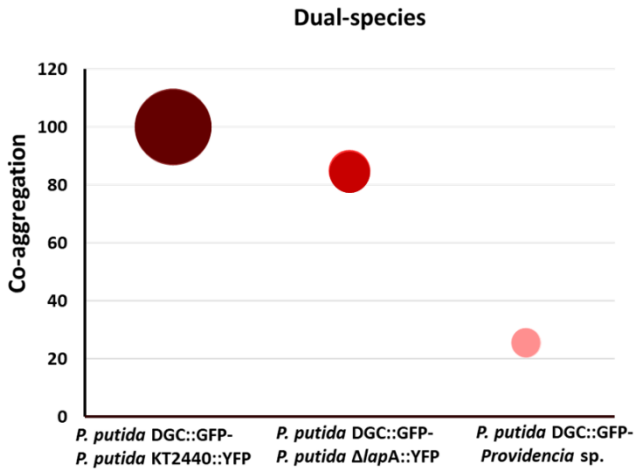

Figure 5-5. Correlation between the presence of PI-positive subpopulations, eDNA content, and the degree of co-aggregation within a dual-species. *P. composti* - *P. putida* Δ*lap*A::YFP co-culture is not present in this figure due to the limitation of measurement of co-aggregation in this case. A higher intensity of red color represents a higher PI-positive subpopulation. The bigger size of the circle represents a higher amount of eDNA production.

5. Discussion

The growing interest in multispecies microbial communities and the development of interdisciplinary research methods have shed new light on the importance of co-aggregation in the formation and dynamics of sessile communities.

Here we used synthetic and natural bacteria with different biofilm formation strategies: biofilm specialist, planktonic specialist, and aggregates forming specialist. As anticipated, the strain *P. putida* DGC::GFP, which possesses a more active di-guanylate that increases the concentration of cyclic-di-GMP internally, displayed a high capacity for biofilm formation compared to other strains. The level of cyclic-di-

GMP serves as a key regulator for biofilm formation, with high concentrations promoting an adhesive lifestyle and low concentrations favoring a planktonic lifestyle (Gjermansen et al., 2006). In contrast, the wild-type strain *P. putida* KT2440::YFP exhibited limited biofilm-forming ability, which further decreased upon the deletion of *lap*A in the *P. putida* Δ*lap*A::YFP strain. LapA plays a crucial role in cell-surface interaction and facilitates the initial, irreversible attachment of bacteria to surfaces (Gjermansen et al., 2010). However, among the natural isolates, *P. composti* demonstrated relatively high biofilm formation ability. It should be noted that this strain produced large aggregates in the liquid phase, which might underestimate the overall biofilm formation. A similar observation has been made in the case of *Pseudomonas aeruginosa*, which forms suspended multicellular aggregates when cultured in a liquid medium (Melaugh et al., 2023). Several studies have reported that natural and infectious biofilms often originate from non-attached biofilm aggregates in the liquid phase (Burmølle et al., 2010; Dogsa et al., 2023; Monier & Lindow, 2003; Schleheck et al., 2009). Another natural isolate, *Providencia* sp. specializes in planktonic growth and lacks the ability to transition into a biofilm state.

Bacteria with aggregation capabilities, such as auto-aggregation and co-aggregation, play a crucial role in enhancing biofilm formation through interbacterial interactions (Rickard et al., 2004). Autoaggregation allows bacteria to benefit from biofilm advantages while maintaining mobility. In marine biofilms, planktonic multicellular aggregates exhibit increased adhesiveness and surface conditioning, accelerating bacterial attachment during early biofilm initiation(Bar-Zeev et al., 2012). Similarly, *P. aeruginosa* demonstrates increased biofilm formation through an affinity for aggregation, potentially providing greater stickiness (Déziel et al., 2001; Häußler et al., 2003). Co-aggregation serves as a key mechanism in biofilm formation, enabling the interaction and integration of different bacterial species within biofilms (Rickard, Gilbert, et al., 2003). Co-aggregation-based interactions significantly influence the formation of multispecies biofilms in aquatic environments. For example, a study by Ana C. Afonso and colleagues reported that the presence of *D. acidovorans* 005P greatly benefited the biofilm formation of *Pseudomonas putida* strains, likely due to the production of extracellular molecules that promote microbial cooperation (Afonso et al., 2021). In our study, we successfully detected early biofilm formation in the planktonic phase by assessing the auto- and co-aggregation abilities of single and dual-species strains using FC. Our results demonstrate a strong correlation between the auto-aggregation ability of the strains and their biofilm formation potential. *P. composti* and *P. putida* DGC::GFP exhibited particularly high

auto-aggregation abilities compared to other strains. However, technical limitations prevented the measurement of auto-aggregation using FC for *P. composti* due to the presence of large floating aggregates in the liquid phase.

Furthermore, we investigated the co-aggregation abilities of dual-species combinations in four case studies, overall, three distinct groups were observed based on coaggregation efficiency: Strong co-aggregators: Case 1 (*P. putida* DGC::GFP - *P. putida* KT2440::YFP) and case 4 (*P. composti* - *P. putida* Δ*lap*A::YFP). Moderate co-aggregators: Case 2 (*P. putida* DGC::GFP - *P. putida* Δ*lap*A::YFP) **(Figure 5-6).** Non-co-aggregators case 3 (*P. putida* DGC::GFP - *Providencia* sp.).To track these bacteria in the planktonic phase, fluorescent reporters were used, enabling their visualization during the experiments conducted using FC.

In our first case study, we observed that the fast biofilm-switching strain *P. putida* DGC::GFP was able to rescue *P. putida* KT2440::YFP. Through FC analysis, we identified synergistic and relatively strong coaggregates interaction during the planktonic phase, which leads to increased biofilm formation. This observation was evidenced by significant increases in the biofilm dry weight of *P. putida* KT2440::YFP in the presence of the dual-species combination **(Figure 5-6)**. It is widely recognized that bacterial cells belonging to the same species or genotype often engage in cooperative behavior to enhance their overall fitness(Griffin et al., 2004). Our observation is consistent with the research conducted by Hansen, which revealed that mixed biofilms exhibit a greater increase in biomass compared to those composed of a single species. Specifically, *P. putida* gains from the coexistence with *Acinetobacter* sp. resulting in increases in biofilm biomass (Hansen et al., 2007). *P. aeruginosa* and *Escherichia coli* can co-colonize and form biofilm structures in capillary flow cells, whereas *E. coli* alone is unable to do so (Klayman et al., 2009). Previous studies have also shown that certain bacteria, such as *Lactobacillus* sp., *Fusobacterium nucleatum*, and *Treponema denticola*, typically do not form mono-specific biofilms but can promote the formation of mixed-species biofilms and enhance biomass production (Filoche et al., 2004; Sharma et al., 2005; Yamada et al., 2005). Furthermore, in our study, we observed an increase in multicellular aggregates and extracellular DNA (eDNA) content in the dual-species combination compared to single species, suggesting a potential role of eDNA in the interaction between these two species.

Initial bacterial adhesion and cellular aggregation are crucial steps in biofilm formation involving eDNA (Mlynek et al., 2020). eDNA, as a significant component of the biofilm matrix, not only facilitates favorable acid-base interactions but also

provides thermodynamic conditions that promote bacterial aggregation and adhesion to surfaces (Flemming & Wingender, 2010; Jakubovics et al., 2013). Moreover, eDNA serves as a site and reservoir for horizontal gene transfer, while also stabilizing the physical structure of biofilms. For example, 3-day-old planktonic cultures of *P. aeruginosa* contain approximately 20-25 μg of eDNA per milliliter of growth medium (Das & Manefield, 2012). In 5-day-old biofilms of *P. aeruginosa* and *P. putida*, the documented amounts of eDNA reach up to 220 and 500 mg of extracellular DNA per gram of biofilm, respectively (Steinberger & Holden, 2005). Addition of exogenous DNA to planktonic cultures has been observed to promote aggregation in DNase I-treated Gram-negative and Gram-positive bacterial cells (Das et al., 2011). Recent findings have shown that the metabolite pyocyanin, produced by *P. aeruginosa*, interacts with eDNA in bacterial extracellular polymeric substances (EPS), facilitating the binding of eDNA to *P. aeruginosa* cells (Das et al., 2013). This interaction enhances the stability of *P. aeruginosa* EPS, influences cell surface properties, and promotes cellular aggregation. By considering the critical role of eDNA in cellular aggregation and biofilm formation, we utilized propidium iodide (PI) bacterial cell viability staining as a proxy to track the early biofilm formation of single and dual species in the planktonic phase. It should be noted that recent studies have highlighted that PI may generate false signals of cell death by binding to eDNA (Rosenberg et al., 2019). PI is a commonly used staining dye for visualizing eDNA in biofilms or cell aggregates using microscopy imaging (Deng et al., 2020; Moshynets et al., 2022; Secchi et al., 2022). Our results demonstrate a strong correlation between eDNA content and PI-staining sub population in both single and dual-species scenarios.

In the synthetic dual-species combinations (Case 2), the FC data indicated a moderate level of co-aggregation between species sharing the same genotype. However, in Case 3, non-coaggregation interactions were observed. Interestingly, the slow biofilm switchers, *P. putida* Δ*lap*A::YFP and *Providencia* sp., were predominantly found in the liquid phase. On the other hand, the FC data from the biofilm sample revealed that *P. putida* DGC::GFP was primarily present in the biofilm phase. These findings suggest a competitive interaction in case 3, where certain species dominate specific phases of bacterial growth. Our results align with previous observations made by J. Zhu in 2018, who reported competitive interactions between *S. Baltica* and *P. fluorescens* in dual-species biofilms. Consequently, we observed lower co-aggregation formation, as well as reduced eDNA content and fewer PI-positive clusters. These findings imply that the competitive nature of the interaction

hinders the co-aggregation process and leads to reduced eDNA production and clustering.

Interestingly, in the dual-species combination (case 4), *P. composti* and *P. putida* Δ*lap*A::YFP exhibited a strong co-aggregation and synergistic interaction in both the planktonic and biofilm phases **(Figure 5-6)**. This interaction was notably enhanced by the formation of noticeable macroscopic co-aggregates in the liquid phase. The microscopy images of these co-aggregates provided visual confirmation of *P. putida* Δ*lap*A::YFP being trapped within the aggregates by *P. composti* **(Figure 5-S6)**. However, during the flow cytometry analysis, a low presence of co-aggregates was observed. This could be attributed to the deliberate exclusion of large aggregates during the sample preparation process to mitigate potential technical complications. It is worth mentioning that initially, there was a higher concentration of eDNA content, which gradually decreased as the cultivation progressed. This decline might be attributed to the formation of these significant co-aggregates **(Figure 5-4F)**, resulting in a lower PI measurement in this specific case. Overall, our findings provide compelling evidence of a strong association among cellular aggregates, biofilm formation capabilities, eDNA content, and the PI-positive subpopulation within the context of these specific case studies involving both single and dual-species interactions.

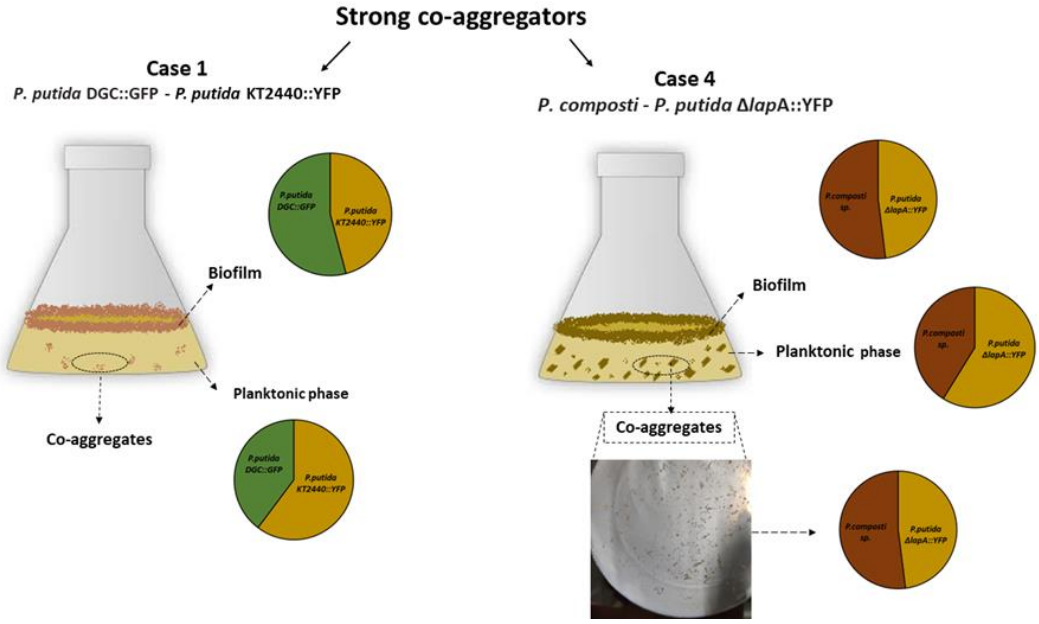

Figure 5-6. Illustration of strong co-aggregators of Case 1 (*P. putida* DGC::GFP - *P. putida* KT2440::YFP) and case 4 (*P. composti* - *P. putida* Δ*lap*A::YFP).

6. Conclusion

The occurrence of coaggregation is highly dependent on the ability of strains to express specific cell surface molecules and is influenced by various physiological and environmental factors. To the best of our knowledge, our study is the first to investigate and analyze auto and co-aggregation in real-time at the single-cell level. By utilizing a unique combination of flow cytometry and appropriate single-cell proxy, we have successfully demonstrated the crucial role of eDNA, particularly in the early stages of biofilm formation in the planktonic phase. Our findings establish strong associations between auto and co-aggregation, eDNA release, and PI-staining subpopulation.

7. Supplementary files

Table 5-S1. Summary of the characterization of synthetic and natural strains.

Strains name	Type of strains	Planktonic	Auto-aggregation	Biofilm	Cell density OD600 (24h)
***P. putida* DGC::GFP**	Synthetic	Moderate	Moderate	High	2.7
P. composti	Natural	low	High	High	1.75
***P. putida* KT2440::YFP**	Synthetic	High	Very low	low	4.6
***P. putida* Δ*lapA*::YFP**	Synthetic	High	Very low	Very low	4.2
***Providencia* sp.**	Natural	Moderate	Very low	Very low	2

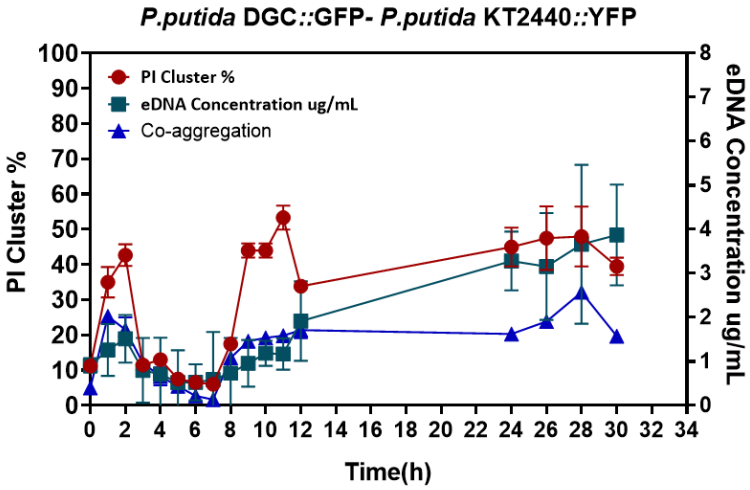

Figure 5-S1. Time evolution of eDNA and PI-positive cells and co-aggregation during the planktonic phase in dual-species *P. putida* DGC::GFP and *P. putida* KT2440::YFP during 30h planktonic growth (number of biological replicates n = 3). The error bars represent the standard deviation (SD) from three biological replicates.

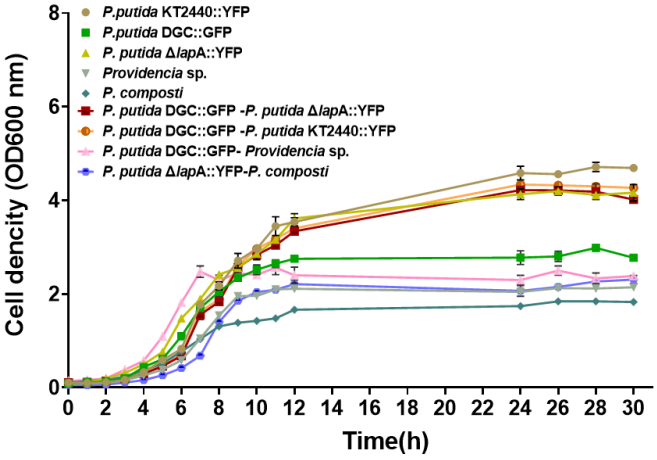

Figure 5-S2. Comparison of growth curves of mono-species and dual-species during 30h of batch cultivation, n ≥ 3 determined by spectrophotometric measurements (OD600). The error bars represent the standard deviation (SD) from three biological replicates.

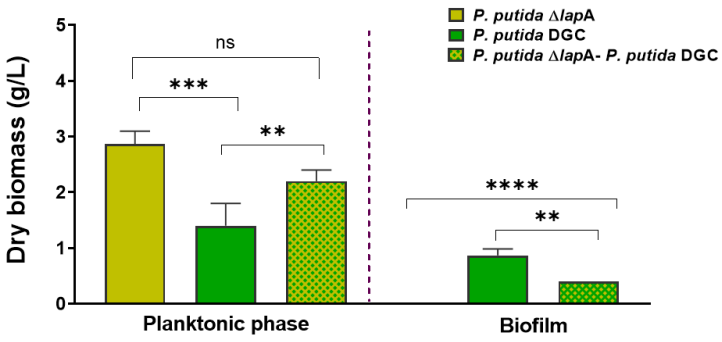

Figure 5-S3: Planktonic and biofilm dry weight comparison in mono and co-culture of *P. putida* DGC::GFP - *P. putida* Δ*lap*A::YFP after 24h, n ≥ 3. The significance of the biofilm and planktonic dry weight data was evaluated (*p*-values: *p*-values: **** $p < 0.00001$, *** $p < 0.0001$, ** $p < 0.01$, ns (not significant)). The error bars represent the standard deviation (SD) from three biological replicates.

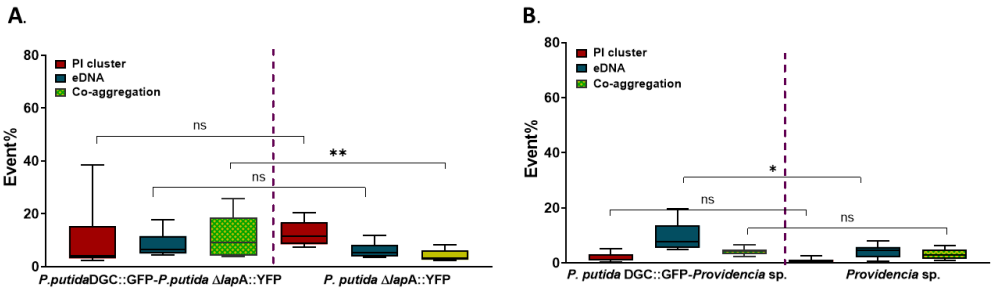

Figure 5-S4. Percentage of PI cluster, eDNA release (the data normalized and shows as a percentage), auto-aggregation, and co-aggregation in mono-and dual-species of A. *P. putida* DGC::GFP - *P. putida* Δ*lap*A::YFP. B. *P. putida* DGC::GFP- *Providencia* sp. after 30h, n ≥ 3. Asterisks over brackets indicate a significant difference between samples (*p*-values: ** $p < 0.001$, *$p < 0.03$, ns (not significant)). The error bars represent the standard deviation (SD) from three biological replicates.

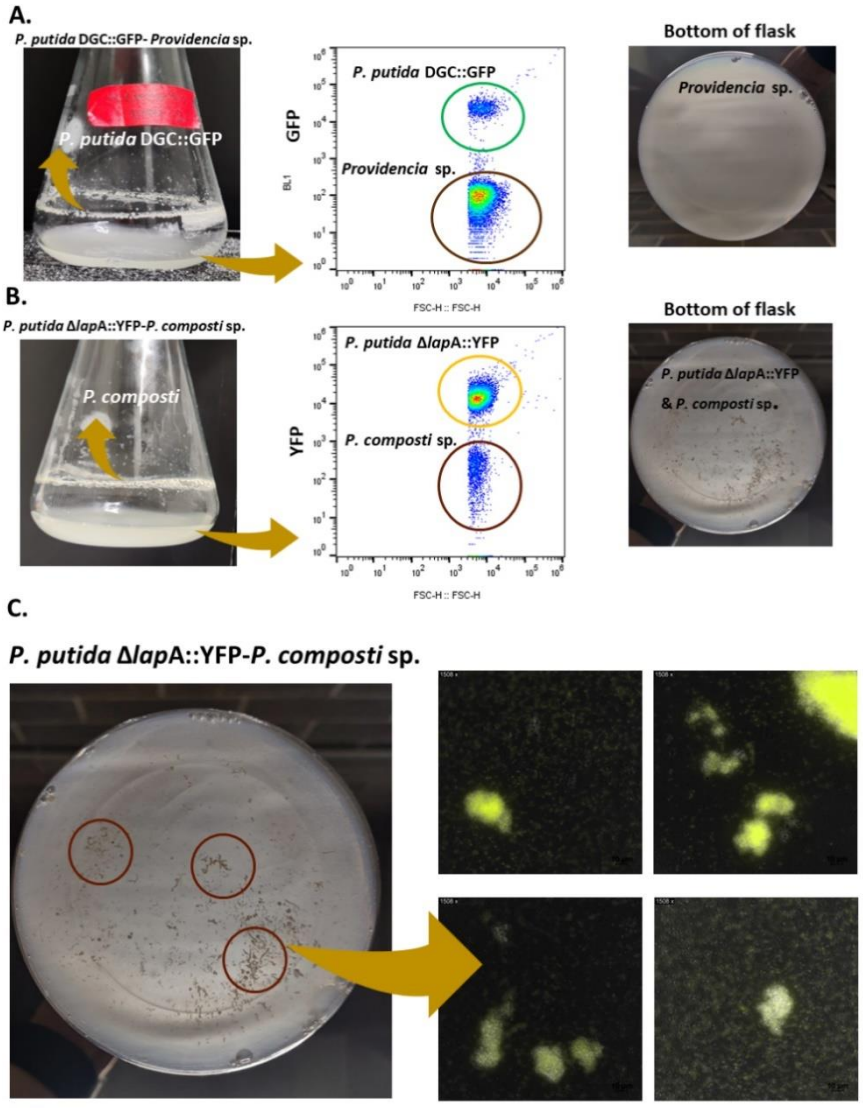

Figure 5-S5: Macroscopic view of shake flasks experiments of semi-synthetic co-culture, n=3. A. *P. putida* DGC::GFP- *Providencia* sp., *P. putida* DGC::GFP is quickly outcompeted in the liquid phase and mainly present in the biofilm phase by the end of the cultivation (30h). In the microscopic picture of the bottom of the flasks, no big size large co-aggregation has been observed. B. *P. composti* - *P. putida* Δ*lap*A::YFP co-culture, at the end of cultivation (30h), mainly *P. composti* switched to biofilm phase. We observed the formation of large co-aggregates at the bottom of a flask that were visible to the naked eye. C. Microscopy imaging of the big aggregates shows the presence of both strains in co-aggregates.

Chapter 6

General conclusion and perspectives

1. Conclusion

Phenotypic switching is an important mechanism that contributes to microbial diversity, playing a fundamental role in bacterial fitness and development. As most environments are dynamic, organisms have evolved the ability to sense and respond to environmental changes by adopting the phenotype that makes them most fit. Through phenotypic switching, bacteria gain the potential to thrive in hostile environments by generating multiple variants capable of withstanding various stresses. Phenotypic switching to biofilm lifestyle is one significant survival strategy employed by bacteria in stress condition, which requires a switch to a biofilm-specific phenotype. These distinct phenotypic states have profound consequences in agriculture, the environment, industry, and medicine. Therefore, accurately predicting the conditions that trigger the transition between these states is of utmost importance. However, studying biofilms is far from simple, as these transitions depend on an intricate interplay of factors determined by both the inherent properties of individual cells and their surrounding environments. While substantial progress has been made in understanding the different phases of biofilm development, quantitatively predicting the conditions that drive planktonic bacteria to transition into the biofilm state remains a formidable challenge. Extensive research consistently demonstrates that bacteria in a sessile growth phase present greater difficulties in terms of control and analysis compared to their free-floating counterparts.

Pseudomonas sp. is known for its remarkable ability to survive in extreme conditions, both in natural environments and within the human body. This exceptional property has been associated with their capacity to form biofilms. While much of the research on biofilms has focused on clinically relevant bacteria, there is a growing interest in studying the role of biofilms in biotechnologically and agriculturally relevant microorganisms, particularly with plant-beneficial strains like *Pseudomonas fluorescens* and *Pseudomonas putida*. These strains utilize biofilm formation as a means of colonizing plants and persisting in the environment (De Weger et al., 1987; Matilla et al., 2011).

Biofilms produced by *Pseudomonas* sp. involve the production of various matrix molecules, including polysaccharides, extracellular DNA (eDNA), and proteins. The process of biofilm development follows a paradigm where individual bacteria initially adhere to a surface, undergo clonal propagation, build a matrix, and eventually mature into a biofilm structure **(Figure 2-1)** (Costerton et al., 1978; Hall-Stoodley et al., 2004; Sauer et al., 2002; Stoodley et al., 2002). This biofilm lifecycle also involves the release or dispersion of small aggregates or individual cells from the biofilm

population, which then seeds uncolonized sites and initiate a new cycle of biofilm formation (Monds & O'Toole, 2009) However, recent evidence suggests that biofilms can form even without surface attachment. Aggregates that form in the liquid phase due to clonal growth, co-aggregation, or the influence of bacterial extracellular polymeric substances (EPS) or host fluids exhibit similar characteristics to surface-associated biofilms. These aggregates, which are not limited to laboratory conditions, have been observed in chronic infection sites within the human microbiota and in the environment (Bay et al., 2018; Bjarnsholt et al., 2013; Qvist et al., 2015). In fact, a revised biofilm cycle model has been proposed to incorporate these free-floating multicellular aggregates (auto-aggregation/co-aggregation) into our understanding of biofilm formation (Sauer et al., 2022). Autoaggregation and microcolony formation are among the initial stages of biofilm formation (Nwoko & Okeke, 2021). Autoaggregation is directly facilitated by specific interactions between proteins or organelles on the cell surfaces and indirectly influenced by the presence of secreted macromolecules like eDNA and exopolysaccharides (Nwoko & Okeke, 2021).

The role of eDNA in *Pseudomonas* sp. encompasses several significant functions, including its contribution to bacterial aggregation, and facilitation of intercellular adhesion (Lister & Horswill, 2014). Extracellular DNA has been identified as a key component in facilitating cell-to-cell connections within *Pseudomonas aeruginosa* biofilms (Nemoto et al., 2003; Whitchurch et al., 2002). It has been observed that the release of extracellular DNA in the planktonic phase of *P. aeruginosa* cultures leads to the formation of clumps(Allesen-Holm et al., 2006). Notably, both proteins and extracellular DNA play interconnected roles in promoting bacterial aggregation and providing stability to biofilms (Dengler et al., 2015; Kavanaugh et al., 2019; Payne & Boles, 2016). In our research, we have observed a strong correlation between the early release of extracellular DNA during the planktonic phase of *Pseudomonas putida* KT2440 and its derivatives, and the subsequent formation of biofilms. The focus of the current thesis primarily revolves around the early biofilm phenotype that emerges in the liquid phase and its regulation through the utilization of Segregostat by using *P. putida* KT2440 and derivatives. After conducting extensive research and analysis, we have successfully tackled three pivotal questions and drawn significant conclusions at every stage. These findings are briefly summarized in **(Table 1-6)** and expanded upon in the subsequent sections for a more comprehensive understanding.

1.1. ***Could we rely on PI-eDNA binding as a single-cell proxy that allows us to decipher the "key" subpopulation of cells involved in early biofilm formation?*** *(Related to chapter 3- "The quest for single-cell proxies related to biofilm switching")*

The early initiation of biofilm formation involves a critical cell-decision making process, wherein individual cells transition from a planktonic state to a sessile one. However, characterizing this process is challenging due to the absence of suitable fluorescent reporters, and the formation of cell aggregates during the transition, interfering with single-cell analyses. Consequently, researchers have explored alternative methods such as c-di-GMP measurement or the development of a fluorescence-based biosensor, with a particular focus on LapA, a key protein involved in initial bacterial attachment to surfaces in *Pseudomonas putida*. However, the intricate gene regulatory network governing biofilm formation in *P. putida* hinders the establishment of a robust single-cell proxy to track the early stages of biofilm development. In our extensive research thesis, we have explored different genetically encoded fluorescent reporters to monitor the dynamics of subpopulations involved in the decision-making process leading to early biofilm formation. Although a fluorescence-based reporter was designed to estimate *lapA* expression or to monitor c-di-GMP levels, its limited sensitivity and detectability constrained its usefulness. These findings prompted us to consider alternative approaches, with a focus on extracellular DNA (eDNA), a vital component of *Pseudomonas* sp. biofilms. eDNA plays a crucial role in several biofilm formation steps, including bacterial attachment, microcolony formation, aggregation, and overall biofilm architecture determination(Das et al., 2010; Qin et al., 2007; Whitchurch et al., 2002). To monitor the early dynamics of biofilm switching at the single-cell level, we targeted the eDNA in planktonic phase. We identified propidium iodide (PI), a bacterial viability stain, as a simple, fast, convenient, and versatile dye that specifically binds to eDNA. During the planktonic state, we observed a subpopulation of cells that associated PI through eDNA outside their intact membranes. The results from flow cytometry (FC) and confocal laser scanning microscopy (CLSM), confirmed the specific binding of PI to eDNA during a specific growth phase. This finding was further confirmed based on DNase treatment or different iron concentrations which modify the quantity of extracellular DNA (iron is known to have a significant impact on eDNA production(Binnenkade et al., 2014; Trappetti et al., 2011; Yang et al., 2007)). These interventions directly affected the PI-stained subpopulation. By employing *P. putida* KT2440 and derivatives exhibiting either enhanced or reduced biofilm formation capabilities, we established strong correlations between biofilm formation, autoaggregation abilities, and the presence of PI-positive subpopulations (PI-eDNA associating cells). Through various strategies, we have validated PI as a reliable single-cell proxy to target the subpopulations of cells involved in early decision-

making processes related to biofilm switching. To enhance our understanding of the initial phases of biofilm formation and the possibility of controlling associated phenotypic switching mechanism, we sought to integrate propidium iodide staining with online flow cytometry.

1.2. ***Can the release of extracellular DNA (eDNA) by Pseudomonas sp. be considered as an early signal for controlling cell population involving biofilm switching?*** *(Related to chapter 4:" Release of extracellular DNA by Pseudomonas species as a major determinant for biofilm switching and an early indicator of cell population control")*

Based on PI staining, we were able to detect a subpopulation of cells associated to eDNA, already visible at the beginning of the cultivation experiments. Interestingly, a correlation was established between the size of the fraction of eDNA-associated/PI-positive cells and the overall biofilm formation capability of *P. putida* KT2440 and its derivatives. This finding emphasizes the pivotal role played by eDNA in early biofilm switching during the planktonic phase.

In order to gain a more comprehensive understanding of the early stages of biofilm formation, we have applied PI staining in continuous cultivation combined with automated flow cytometry, enabling a more detailed investigation of the dynamic of cell population. In this context, the integration of a cell-machine interface presents a remarkable capability to monitor the real-time switching process of individual cells within a population and respond accordingly. This technique revealed that the transition to a biofilm lifestyle was promoted by the formation of cellular aggregates in the planktonic phase. The subsequent data analysis indicated a strong relationship between PI staining and cell auto-aggregation, reinforcing the connection between these factors and biofilm formation.

Moreover, it was observed that fast biofilm switchers *(P. putida* DGC) were outcompeted by the strains with biofilm defects (*P. putida* Δ*lap*A) in the liquid (planktonic) phase and predominantly found in the biofilm phase. In other words, strains that are more proficient at forming biofilms are less successful in the planktonic phase. This trade-off could be attributed to the energy and resources diverted towards biofilm production, which may hinder the strain's ability to thrive as a free-floating organism. Fitness trade-offs underlie how successfully bacteria compete for each lifestyle, such that phenotypes conferring competitive success in

biofilm environments carry selective disadvantages in the planktonic phase, and vice versa (Madsen et al., 2015; Nadell & Bassler, 2011; Oliveira et al., 2015).

Different strategies (i.e., feedback control, control of the composition of microbial communities, genetically encoded control strategies) have been devised to effectively control microbial populations in various fields, spanning from biomedicine to bioprocess engineering (Briat & Khammash, 2018; Din et al., 2020; Perrino et al., 2019). The application of synthetic gene circuits for controlling microbial populations is the most widely employed strategy among these control strategies. Microfluidic devices have emerged as the primary experimental platform for studying gene expression control in cellular systems. These devices offer the advantage of acquiring single-cell data with high spatiotemporal resolution. However, they suffer from low experimental throughput due to the time and computational power required for image analysis (Dusny & Schmid, 2015). Moreover, there is a possibility of technical biases when compared to conventional cultivation devices (Dusny et al., 2015; Westerwalbesloh et al., 2017).

However, a more realistic alternative lies in controlling the cell-switching phenomenon itself, which has become technically achievable through the development of the Segregostat system **(Figure 2-3)** (Delvigne & Noorman, 2017; Nguyen et al., 2021; Sassi et al., 2019). The integration of online measurement not only aligns with the digitalization trend but also brings numerous advantages (Delvigne & Goffin, 2014). It enables the rapid accumulation of data at the population level and facilitates the automated systematic determination of the optimal stimulation frequency for effective synchronization of gene expression across the population (Nguyen et al., 2021). By implementing online measurement through flow cytometry (FC), the limitations of manual sampling intervals are overcome, and a comprehensive understanding of changes in cell population distributions is obtained with exceptional temporal resolution (Arnoldini et al., 2013; Kuystermans et al., 2016)

This approach was used to characterize cell population dynamics and allowed us to set a reactive FC protocol aiming at reducing biofilm formation. In particular, glucose pluses were added automatically in response to the detection of diversification bursts. This approach aimed to provide a competitive advantage to non-differentiated cells in the liquid phase, thus effectively controlling phenotypic switching. By regulating glucose availability in response to diversification bursts, we aimed to favor the growth and survival of non-differentiated cells, preventing them from transitioning into biofilm. The predominance of PI-negative cells (non-eDNA-associated cells),

indicating reduced biofilm switching, further supported the efficacy of the Segregostat approach in reducing biofilm formation.

This significant finding motivates us to explore further the role of eDNA in more intricate cultivation scenarios, such as dual-species cultures involving synthetic and natural isolates.

1.3. What is the role of extracellular DNA (eDNA) in mediating co-aggregation in natural and synthetic co-cultures? (Related to chapter 5: "Biofilm switching influences co-aggregation and the assembly of multi-species biofilm")

Bacteria with aggregation capabilities, such as auto-aggregation and co-aggregation playing a crucial role in enhancing biofilm formation through interbacterial interactions (Rickard et al., 2004).The co-aggregation, as an initial step representing a form of cooperation in the development of mixed biofilms enabling the interaction and integration of different bacterial species (Rickard, Gilbert, et al., 2003). In our research, we performed a thorough analysis to explore the potential of co-aggregation and extracellular DNA release in co-cultures involving both synthetic and natural strains. These strains possess varying capabilities in terms of aggregation and biofilm formation.

We have used flow cytometry and propidium iodide staining as dynamic tracking tools demonstrating initial interaction i.e. co-aggregation during biofilm switching. Our findings demonstrate when cultivating *P. putida* DGC::GFP, with high eDNA release and biofilm formation ability, with *P. putida* KT2440::YFP, a more cooperative relationship emerges, leading to a higher co-aggregation and, consequently, an increased population of eDNA-associated/PI-positive cells.

This phenomenon is particularly pronounced when combining *P. composti* with *P. putida* Δ*lap*A::YFP, the highest cooperative relationship, leading to the formation of macroscopic co-aggregates, as indicated by the presence of *P. putida* Δ*lap*A. Our data highlights a strong correlation between the abilities of biofilm formation, co-aggregation, eDNA release, and the population of PI-positive cells.

Considering that bacteria commonly inhabit environments characterized by varying conditions, such as shear forces, nutrient availability, and physiological conditions, the bacteria within co-aggregated communities will survive and proliferate under conditions that reduce the prevalence of single non-co-aggregated cells(Rickard, Gilbert, et al., 2003). However, the molecular mechanisms underlying co-aggregation in bacteria grown in liquid environments have yet to be thoroughly investigated. The exploration of co-aggregation and the identification of factors influencing the release

of extracellular DNA will provide valuable insights into the understanding of phenotypic switching and the subsequent formation of sessile communities.

Perspectives:

Biofilm formation is a highly intricate complex biological process involving several stages, including initial cell attachment, proliferation, maturation, and eventual detachment **(Figure 2-1).** Various extracellular polymeric substances are used to entrap this multispecies community, forming a biofilm that can either float in liquid environments or adhere to living or non-living surfaces (Sauer et al., 2022). Bacterial biofilms, due to their distinctive characteristics, have been extensively researched across diverse fields, spanning from industrial applications to medical advancements. For instance, biofilms have been used in bioremediation, waste treatment, and the production of valuable chemicals and biofuels (Halan et al., 2012). However, biofilms also pose significant health risks, as they are associated with persistent infections resulting from the contamination of medical devices as well as artificial implants (Kostakioti et al., 2013). Furthermore, biofilms contribute to the pollution of drinking water (Wingender & Flemming, 2011). The global prevalence of microbial biofilm contamination poses significant challenges in natural, industrial, and medical settings, resulting in an estimated annual cost of approximately $4 trillion (Cámara et al., 2022).

Despite extensive efforts to remove biofilms, basal microbial contamination persists, leading to rapid recolonization (Hall-Stoodley et al., 2004; P. S. Stewart et al., 2019). Mature biofilms are known for their strong attachment to substrates and protection provided by the extracellular polymeric substance (EPS), rendering them resilient against chemical and mechanical forces (Lebeaux et al., 2014; Peterson et al., 2015). Conversely, early-stage biofilms are less firmly established, more susceptible to antimicrobials, and easier to manage with chemical treatments (Fu et al., 2021; Høiby et al., 2001). Consequently, the early detection and treatment of biofilms have emerged as a highly effective strategy in combating their formation.

Identifying the initial stages of biofilm formation is an active area of research that requires simple, reliable, and rapid screening methods. Several technologies have been developed for biofilm monitoring, including the biofilm ring test, microtiter plate, and Calgary device. However, the limitations of this model include limited growth space and nutrients, single substrate materials, and not allowing longitudinal study. Moreover, these techniques lack the capability to provide real-time information on biofilm growth (Zhang et al., 2023).

More advanced techniques for monitoring bacterial biofilm growth have been developed, including quartz crystal microbalances (QCM)-based sensors. These sensors are incorporated into a multi-channel instrument designed for online monitoring. The instrument consists of an array of sensors placed inside a multi-well petri plate containing liquid samples. The QCM resonance parameters of each sensor are obtained by measuring their electrical impedance (Salazar et al., 2023). Another method employed is surface plasmon resonance (SPR), which utilizes optical measurements to detect changes in refractive index resulting from the binding of analyte molecules to biorecognize molecules immobilized on the SPR sensor (Funari et al., 2018). Moreover, Electrochemical impedance spectroscopy (EIS) biosensors use a custom flow cell system with integrated sensors to measure real-time impedance changes during biofilm growth under flow conditions (McGlennen et al., 2023). Microfluidic devices are another method used for biofilm studies. These devices feature customized micro-scale channels that allow researchers to manipulate physical and chemical conditions to investigate bacterial response, biofilm formation, and antimicrobial resistance (Bruchmann et al., 2015). While these systems provide real-time biofilm monitoring, they do require additional instrumentation and may have issues such as low sensor stability, cross sensitivity to density and viscoelastic properties in the bulk media, complex fabrication processes, and potential channel blockage in the case of microfluidic devices (Funari et al., 2018; Zhang et al., 2023).

Microscopy techniques, such as atomic force microscopy (AFM), transmission electron microscopy (TEM), and scanning electron microscopy (SEM), are also employed (Azeredo et al., 2017; Fu et al., 2021; Funari & Shen, 2022; Neu & Lawrence, 2015; Pires et al., 2013; Saber et al., 2013; Wilson et al., 2017).

However, many of these methods are endpoint detection techniques that primarily focus on mature biofilms attached to surfaces, lacking the ability to provide online information on early biofilm formation in the liquid phase.

Therefore, it is crucial to establish suitable methodologies for online monitoring of early biofilm formation even before the cell decision-making process related to biofilm switching. Additionally, the absence of a universal target to be used as a proxy for detecting biofilm switching by diverse bacteria poses a fundamental challenge for developing biofilm control strategies that do not rely on biocides or antibiotics (Okshevsky et al., 2015). However, the widespread presence of extracellular DNA (eDNA) within the biofilm matrix makes it an intriguing candidate for biofilm control. Several studies have shown that enzymatic degradation of eDNA using DNase can

impede biofilm formation, and treating an established biofilm with DNase can disperse it effectively (Hymes et al., 2013; Qin et al., 2007; Swartjes et al., 2013).

Our research introduces an innovative methodology that utilizes propidium iodide (PI) as a novel single-cell proxy, targeting eDNA. In this study, we took benefit from PI-eDNA associated cells and implemented online measurements using flow cytometry (FC) in a cutting-edge system called Segrogostat (Henrion et al., 2023; Sassi et al., 2019). This allows us to effectively assess the initial biofilm-phenotype state of bacteria.

By combining control strategies with advancements in computational and control theory, we capitalize on the practical advantages offered by this approach. FC serves as a high-throughput method, enabling rapid measurement of eDNA-associated/PI-positive cells while simultaneously monitoring the formation of multicellular aggregates in the liquid phase. Notably, the Segrogostat device has the capability to trigger automatically environmental transitions by leveraging the phenotypic switching ability of the bacterial population.

Through the accumulation of relevant data with high temprol resolution, and the implementation of control feedback strategies (glucose pulsing), we are able to regulate and manipulate biofilm formation in our study. This integration of online measurement not only aligns with the trend of digitalization but also offers numerous advantages. By employing FC-based online measurement, we achieve continuous monitoring of the process without significant labor and time costs. Our approach effectively closes the gap between manual sampling intervals, allowing us to gain detailed insights into the dynamics of cell population distributions with exceptional temporal resolution. By utilizing this methodology, we can achieve early detection and continuous monitoring of biofilms, presenting a highly promising approach.

However, it is crucial to expand our understanding of single-cell proxies, such as PI-staining, and address the limitations associated with laboratory-based testing. This is necessary to ensure the future technological expansion of this methodology into industrial, medical, and natural environments.

In addition, we suggest exploring c-di-GMP riboswitches as alternative targets for the development of new biosensors. Riboswitches are molecular structures that regulate the expression of essential genes in various bacteria (Reyes-Darias & Krell, 2017). Therefore, they offer alternative molecular targets for the development of new antibiotics and the design of biotechnological tools, such as biosensors, for biofilm control.

To fully capitalize on the capabilities of Segrogostat, further research is required to gain a deeper understanding of the mechanisms underlying eDNA release in *Pseudomonas putida*. While this study focused on the model organism *P. putida*, it is important to recognize that other organisms likely employ different strategies for eDNA release and biofilm formation. Exploring the mechanisms of eDNA release and its impact on early biofilm phenotypes will enable the implementation of more precise control feedback strategies (i.e. iron, ca^{2+}, pyocyanin targeting eDNA modulation) during Segrogostat experiments.

Although we have demonstrated the effect of eDNA release on coaggregation in synthetic and natural strains under specific conditions, it is necessary to investigate the regulatory and control mechanisms governing eDNA release and interactions in diverse biofilm compositions. This includes studying mixed-species and inter-kingdom biofilms. Our preliminary results indicate that different cultivation conditions, such as carbon source and iron concentration, can influence early cell decision-making (eDNA release, aggregation), thereby presenting new avenues for further investigation. Flow cytometry data can be subjected to fingerprinting analysis (Rogers & Holyst, 2009) to discern phenotypic heterogeneity associated with different culture conditions. However, it is important to note that these perspectives primarily apply to biofilms formed through cell aggregation.

To the best of our knowledge, our study represents the first investigation focused on real-time analysis of biofilm switching at the single-cell level. This research provides a solid foundation for controlling phenotypic switching during transitions between planktonic, aggregate, and biofilm states.

Table 6-1. Summary of main conclusion and perspective.

Main scientific questions	Key summary finding	Advantage and Limitations	Perspective
Could we rely on PI-eDNA binding as an FC single-cell proxy to capture the "key" subpopulations involved in early biofilm formation?	PI-staining is associated with extracellular DNA (eDNA) outside of intact membranes. The occurrence of eDNA-binding cell subpopulation is correlated with overall biofilm formation.	**Advantage:** We introduce PI-staining as a simple, reliable, and rapid biomarker for tracking phenotypic switching by binding to eDNA. **Limitation:** **Propidium iodide** is a suspected carcinogen and should be handled with care. It is limited to being used for strains with large aggregation production based on flow cytometry analysis.	We suggest exploring c-di-GMP riboswitches as alternative targets for the development of new biosensors. It is necessary to ensure the future technological expansion of this methodology into industrial, medical, and natural environments.
Can the release of extracellular DNA (eDNA) by *Pseudomonas* sp. be considered a major determinant of biofilm switching and an early indicator of cell population control?	We identify eDNA as a major determinant of phenotypic switching at an early stage of biofilm formation. The Segregostat approach reduced the overall heterogeneity of the population, indicating a more homogenous microbial community with predominantly PI-negative cells, suggesting a decrease in biofilm switching. Our work capitalizes on the practical benefits derived from combining control strategies with the advancements in computational and information theory.	**Advantage: Segregostat** is based on reactive flow cytometry, coupled with a well-designed control strategy and an appropriate single-cell biomarker. It enables rapid measurement of **eDNA-binding cells** while simultaneously monitoring the formation of multicellular aggregates in the liquid phase. The Segrogostat device has the capability to trigger automatically environmental transitions by leveraging the phenotypic switching ability of the bacterial population. This integration of online measurement aligns with the trend of digitalization and also offers continuous monitoring of the process without significant labor and time costs. **Limitation:** Care and additional cleaning steps need to be taken, especially when monitoring biofilm former strains, to avoid technical issues for online FC.	Further research is required to gain a deeper understanding of the mechanisms underlying eDNA release in *Pseudomonas putida*. Exploring the mechanisms of eDNA release and its impact on early biofilm phenotypes will enable the implementation of more precise control feedback strategies (i.e. iron, Ca^{2+}, pyocyanin targeting eDNA modulation) during Segrogostat experiments.
What is the role of extracellular DNA in biofilm switching associated with co-aggregation and assembly of multi-species biofilm?	Assessing the extent of (auto/co) aggregation in planktonic cultures can detect early stages of biofilm development. A strong correlation between the abilities of biofilm formation, co-aggregation, eDNA release, and the population of PI-positive cells was observed.	**Advantage:** We were able to use our methodology based on PI-staining and FC to assess the interaction between co-culture based on **co-aggregation formation** in planktonic cultures. **Limitation:** Assessing macroscopic aggregation formation that floats in the planktonic phase, such as natural isolate *P. composti*, is limited based on PI staining combined with FC.	Investigate the regulatory and control mechanisms governing eDNA release and interactions in diverse biofilm compositions. Our preliminary results indicate that different cultivation conditions, such as carbon source and iron concentration, can influence early cell decision-making (eDNA release, aggregation), thereby presenting new avenues for further investigation.

Chapter 7

References

References

Acar, M., Mettetal, J. T., & Van Oudenaarden, A. (2008). Stochastic switching as a survival strategy in fluctuating environments. *Nature Genetics*, *40*(4), 471–475. https://doi.org/10.1038/ng.110

Achouak, W., Conrod, S., Cohen, V., & Heulin, T. (2004). Phenotypic Variation of Pseudomonas brassicacearum as a Plant Root-Colonization Strategy. In *Molecular Plant-Microbe Interactions MPMI* (Vol. 17, Issue 8).

Afonso, A. C., Gomes, I. B., Saavedra, M. J., Giaouris, E., Simões, L. C., & Simões, M. (2021). Bacterial coaggregation in aquatic systems. In *Water Research* (Vol. 196). Elsevier Ltd. https://doi.org/10.1016/j.watres.2021.117037

Alhede, M., Kragh, K. N., Qvortrup, K., Allesen-Holm, M., van Gennip, M., Christensen, L. D., Jensen, P. Ø., Nielsen, A. K., Parsek, M., Wozniak, D., Molin, S., Tolker-Nielsen, T., Høiby, N., Givskov, M., & Bjarnsholt, T. (2011). Phenotypes of non-attached pseudomonas aeruginosa aggregates resemble surface attached biofilm. *PLoS ONE*, *6*(11). https://doi.org/10.1371/journal.pone.0027943

Allesen-Holm, M., Barken, K. B., Yang, L., Klausen, M., Webb, J. S., Kjelleberg, S., Molin, S., Givskov, M., & Tolker-Nielsen, T. (2006). A characterization of DNA release in Pseudomonas aeruginosa cultures and biofilms. *Molecular Microbiology*, *59*(4), 1114–1128. https://doi.org/10.1111/j.1365-2958.2005.05008.x

Amikam, D., & Galperin, M. Y. (2006). PilZ domain is part of the bacterial c-di-GMP binding protein. *Bioinformatics*, *22*(1), 3–6. https://doi.org/10.1093/bioinformatics/bti739

Anton, V., RougÃ©, P., & DaffÃ©, M. (1996). Identification of the sugars involved in mycobacterial cell aggregation. *FEMS Microbiology Letters*, *144*(2–3), 167–170. https://doi.org/10.1111/j.1574-6968.1996.tb08525.x

Aqeel, H., Weissbrodt, D. G., Cerruti, M., Wolfaardt, G. M., Wilén, B. M., & Liss, S. N. (2019). Drivers of bioaggregation from flocs to biofilms and granular sludge. In *Environmental Science: Water Research and Technology* (Vol. 5, Issue 12). https://doi.org/10.1039/c9ew00450e

Armbruster, C. R., Lee, C. K., Parker-Gilham, J., De Anda, J., Xia, A., Zhao, K., Murakami, K., Tseng, B. S., Hoffman, L. R., Jin, F., Harwood, C. S., Wong, G. C. L., & Parsek, M. R. (2019). Heterogeneity in surface sensing suggests a

division of labor in pseudomonas aeruginosa populations. *ELife*, *8*. https://doi.org/10.7554/eLife.45084

Arnoldini, M., Heck, T., Blanco-Fernańdez, A., & Hammes, F. (2013). Monitoring of dynamic microbiological processes using real-time flow cytometry. *PLoS ONE*, *8*(11). https://doi.org/10.1371/journal.pone.0080117

Azeredo, J., Azevedo, N. F., Briandet, R., Cerca, N., Coenye, T., Costa, A. R., Desvaux, M., Di Bonaventura, G., Hébraud, M., Jaglic, Z., Kačániová, M., Knøchel, S., Lourenço, A., Mergulhão, F., Meyer, R. L., Nychas, G., Simões, M., Tresse, O., & Sternberg, C. (2017). Critical review on biofilm methods. In *Critical Reviews in Microbiology* (Vol. 43, Issue 3, pp. 313–351). Taylor and Francis Ltd. https://doi.org/10.1080/1040841X.2016.1208146

Bagdasarian, M., Lurz, R., Rückert, B., Franklin, F. C. H., Bagdasarian, M. M., Frey, J., & Timmis, K. N. (1981). Specific-purpose plasmid cloning vectors II. Broad host range, high copy number, RSF 1010-derived vectors, and a host-vector system for gene cloning in Pseudomonas. *Gene*, *16*(1–3), 237–247. https://doi.org/10.1016/0378-1119(81)90080-9

Banin, E., Brady, K. M., & Greenberg, E. P. (2006). Chelator-induced dispersal and killing of Pseudomonas aeruginosa cells in a biofilm. *Applied and Environmental Microbiology*, *72*(3), 2064–2069. https://doi.org/10.1128/AEM.72.3.2064-2069.2006

Baraquet, C., Murakami, K., Parsek, M. R., & Harwood, C. S. (2012). The FleQ protein from Pseudomonas aeruginosa functions as both a repressor and an activator to control gene expression from the Pel operon promoter in response to c-di-GMP. *Nucleic Acids Research*, *40*(15), 7207–7218. https://doi.org/10.1093/nar/gks384

Barrientos-Moreno, L., Molina-Henares, M. A., Ramos-González, M. I., & Espinosa-Urgel, M. (2020). Arginine as an environmental and metabolic cue for cyclic diguanylate signalling and biofilm formation in Pseudomonas putida. *Scientific Reports*, *10*(1). https://doi.org/10.1038/s41598-020-70675-x

Bar-Zeev, E., Berman-Frank, I., Girshevitz, O., & Berman, T. (2012). Revised paradigm of aquatic biofilm formation facilitated by microgel transparent exopolymer particles. *Proceedings of the National Academy of Sciences of the United States of America*, *109*(23), 9119–9124. https://doi.org/10.1073/pnas.1203708109

Bay, L., Kragh, K. N., Eickhardt, S. R., Poulsen, S. S., Gjerdrum, L. M. R., Ghathian, K., Calum, H., Ågren, M. S., & Bjarnsholt, T. (2018a). Bacterial Aggregates Establish at the Edges of Acute Epidermal Wounds. *Advances in Wound Care*, *7*(4), 105–113. https://doi.org/10.1089/wound.2017.0770

Bay, L., Kragh, K. N., Eickhardt, S. R., Poulsen, S. S., Gjerdrum, L. M. R., Ghathian, K., Calum, H., Ågren, M. S., & Bjarnsholt, T. (2018b). Bacterial Aggregates Establish at the Edges of Acute Epidermal Wounds. *Advances in Wound Care*, *7*(4), 105–113. https://doi.org/10.1089/wound.2017.0770

Beloin, C., Houry, A., Froment, M., Ghigo, J.-M., & Henry, N. (n.d.). *A Short-Time Scale Colloidal System Reveals Early Bacterial Adhesion Dynamics*. https://doi.org/10.1371/journal.pbio.0060167.g001

Beloin, C., Roux, A., & Ghigo, J. M. (2008). Escherichia coli biofilms. In *Current Topics in Microbiology and Immunology* (Vol. 322). https://doi.org/10.1007/978-3-540-75418-3_12

Beloin, C., Roux, A., & Ghigo, J.-M. (n.d.). *Escherichia coli Biofilms*.

Benedetti, I., de Lorenzo, V., & Nikel, P. I. (2016). Genetic programming of catalytic Pseudomonas putida biofilms for boosting biodegradation of haloalkanes. *Metabolic Engineering*, *33*, 109–118. https://doi.org/10.1016/j.ymben.2015.11.004

Berlanga, M., & Guerrero, R. (2016). Living together in biofilms: The microbial cell factory and its biotechnological implications. *Microbial Cell Factories*, *15*(1), 1–11. https://doi.org/10.1186/s12934-016-0569-5

Bertaux, F., Sosa-Carrillo, S., Gross, V., Fraisse, A., Aditya, C., Furstenheim, M., & Batt, G. (2022). Enhancing bioreactor arrays for automated measurements and reactive control with ReacSight. *Nature Communications*, *13*(1). https://doi.org/10.1038/s41467-022-31033-9

Binder, D., Drepper, T., Jaeger, K. E., Delvigne, F., Wiechert, W., Kohlheyer, D., & Grünberger, A. (2017). Homogenizing bacterial cell factories: Analysis and engineering of phenotypic heterogeneity. In *Metabolic Engineering* (Vol. 42). https://doi.org/10.1016/j.ymben.2017.06.009

Binnenkade, L., Teichmann, L., & Thormanna, K. M. (2014). Iron triggers λSo prophage induction and release of extracellular DNA in shewanella oneidensis MR-1 biofilms. *Applied and Environmental Microbiology*, *80*(17), 5304–5316. https://doi.org/10.1128/AEM.01480-14

Bjarnsholt, T., Alhede, M., Alhede, M., Eickhardt-Sørensen, S. R., Moser, C., Kühl, M., Jensen, P. Ø., & Høiby, N. (2013a). The in vivo biofilm. In *Trends in Microbiology* (Vol. 21, Issue 9, pp. 466–474). https://doi.org/10.1016/j.tim.2013.06.002

Bjarnsholt, T., Alhede, M., Alhede, M., Eickhardt-Sørensen, S. R., Moser, C., Kühl, M., Jensen, P. Ø., & Høiby, N. (2013b). The in vivo biofilm. In *Trends in Microbiology* (Vol. 21, Issue 9, pp. 466–474). https://doi.org/10.1016/j.tim.2013.06.002

Bjarnsholt, T., Jensen, P. Ø., Fiandaca, M. J., Pedersen, J., Hansen, C. R., Andersen, C. B., Pressler, T., Givskov, M., & Høiby, N. (2009). Pseudomonas aeruginosa biofilms in the respiratory tract of cystic fibrosis patients. *Pediatric Pulmonology*, *44*(6), 547–558. https://doi.org/10.1002/ppul.21011

Blakeman, J. T., Morales-García, A. L., Mukherjee, J., Gori, K., Hayward, A. S., Lant, N. J., & Geoghegan, M. (n.d.). *Supplementary Information Extracellular DNA provides structural integrity to a Micrococcus luteus biofilm*.

Böckelmann, U., Janke, A., Kuhn, R., Neu, T. R., Wecke, J., Lawrence, J. R., & Szewzyk, U. (2006). Bacterial extracellular DNA forming a defined network-like structure. *FEMS Microbiology Letters*, *262*(1), 31–38. https://doi.org/10.1111/j.1574-6968.2006.00361.x

Bossier, P., & Verstraete, W. (1996). *MINI-REVIEW Triggers for microbial aggregation in activated sludge?* (Vol. 45, Issue C). Springer-Verlag.

Bowsher, C. G., & Swain, P. S. (2014). Environmental sensing, information transfer, and cellular decision-making. In *Current Opinion in Biotechnology* (Vol. 28). https://doi.org/10.1016/j.copbio.2014.04.010

Boyd, C. D., Jarrod Smith, T., El-Kirat-Chatel, S., Newell, P. D., Dufrêne, Y. F., & O'Toolea, G. A. (2014). Structural features of the Pseudomonas fluorescens biofilm adhesin LapA required for LapG-dependent cleavage, biofilm formation, and cell surface localization. *Journal of Bacteriology*, *196*(15), 2775–2788. https://doi.org/10.1128/JB.01629-14

Briat, C., & Khammash, M. (2018a). Perfect Adaptation and Optimal Equilibrium Productivity in a Simple Microbial Biofuel Metabolic Pathway Using Dynamic Integral Control. *ACS Synthetic Biology*, *7*(2), 419–431. https://doi.org/10.1021/acssynbio.7b00188

Briat, C., & Khammash, M. (2018b). Perfect Adaptation and Optimal Equilibrium Productivity in a Simple Microbial Biofuel Metabolic Pathway Using Dynamic

Integral Control. *ACS Synthetic Biology*, *7*(2), 419–431. https://doi.org/10.1021/acssynbio.7b00188

Brognaux, A., Bugge, J., Schwartz, F. H., Thonart, P., Telek, S., & Delvigne, F. (2013). Real-time monitoring of cell viability and cell density on the basis of a three dimensional optical reflectance method (3D-ORM): Investigation of the effect of sub-lethal and lethal injuries. *Journal of Industrial Microbiology and Biotechnology*, *40*(7), 679–686. https://doi.org/10.1007/s10295-013-1271-9

Brognaux, A., Francis, F., Twizere, J. C., Thonart, P., & Delvigne, F. (2014). Scale-down effect on the extracellular proteome of Escherichia coli: Correlation with membrane permeability and modulation according to substrate heterogeneities. *Bioprocess and Biosystems Engineering*, *37*(8), 1469–1485. https://doi.org/10.1007/s00449-013-1119-8

Bruchmann, J., Sachsenheimer, K., Rapp, B. E., & Schwartz, T. (2015). Multi-channel microfluidic biosensor platform applied for online monitoring and screening of biofilm formation and activity. *PLoS ONE*, *10*(2). https://doi.org/10.1371/journal.pone.0117300

Burmølle, M., Thomsen, T. R., Fazli, M., Dige, I., Christensen, L., Homøe, P., Tvede, M., Nyvad, B., Tolker-Nielsen, T., Givskov, M., Moser, C., Kirketerp-Møller, K., Johansen, H. K., Høiby, N., Jensen, P. Ø., Sørensen, S. J., & Bjarnsholt, T. (2010). Biofilms in chronic infections - A matter of opportunity - Monospecies biofilms in multispecies infections. *FEMS Immunology and Medical Microbiology*, *59*(3), 324–336. https://doi.org/10.1111/j.1574-695X.2010.00714.x

Cai, Y. M. (2020). Non-surface Attached Bacterial Aggregates: A Ubiquitous Third Lifestyle. In *Frontiers in Microbiology* (Vol. 11). https://doi.org/10.3389/fmicb.2020.557035

Cámara, M., Green, W., MacPhee, C. E., Rakowska, P. D., Raval, R., Richardson, M. C., Slater-Jefferies, J., Steventon, K., & Webb, J. S. (2022). Economic significance of biofilms: a multidisciplinary and cross-sectoral challenge. *Npj Biofilms and Microbiomes*, *8*(1). https://doi.org/10.1038/s41522-022-00306-y

Cavaleiro, A. M., Kim, S. H., Seppälä, S., Nielsen, M. T., & Nørholm, M. H. H. (2015). Accurate DNA Assembly and Genome Engineering with Optimized Uracil Excision Cloning. *ACS Synthetic Biology*, *4*(9), 1042–1046. https://doi.org/10.1021/acssynbio.5b00113

Chandler, J. R., Duerkop, B. A., Hinz, A., West, T. E., Herman, J. P., Churchill, M. E. A., Skerrett, S. J., & Greenberg, E. P. (2009). Mutational analysis of Burkholderia thailandensis quorum sensing and self-aggregation. *Journal of Bacteriology*, *191*(19), 5901–5909. https://doi.org/10.1128/JB.00591-09

Cheong, R., Rhee, A., Wang, C. J., Nemenman, I., & Levchenko, A. (2011). Information transduction capacity of noisy biochemical signaling networks. *Science*, *334*(6054), 354–358. https://doi.org/10.1126/science.1204553

Chiang, W. C., Nilsson, M., Jensen, P. Ø., Høiby, N., Nielsen, T. E., Givskov, M., & Tolker-Nielsen, T. (2013). Extracellular DNA shields against aminoglycosides in Pseudomonas aeruginosa biofilms. *Antimicrobial Agents and Chemotherapy*, *57*(5), 2352–2361. https://doi.org/10.1128/AAC.00001-13

Choi, K. H., Kumar, A., & Schweizer, H. P. (2006). A 10-min method for preparation of highly electrocompetent Pseudomonas aeruginosa cells: Application for DNA fragment transfer between chromosomes and plasmid transformation. *Journal of Microbiological Methods*, *64*(3), 391–397. https://doi.org/10.1016/j.mimet.2005.06.001

Christen, B., Christen, M., Paul, R., Schmid, F., Folcher, M., Jenoe, P., Meuwly, M., & Jenal, U. (2006). Allosteric control of cyclic di-GMP signaling. *Journal of Biological Chemistry*, *281*(42), 32015–32024. https://doi.org/10.1074/jbc.M603589200

Christen, M., Kulasekara, H. D., Christen, B., Kulasekara, B. R., Hoffman, L. R., & Miller, S. I. (2010). Asymmetrical distribution of the second messenger c-di-GMP upon bacterial cell division. *Science*, *328*(5983), 1295–1297. https://doi.org/10.1126/science.1188658

Cirz, R. T., O'Neill, B. M., Hammond, J. A., Head, S. R., & Romesberg, F. E. (2006). Defining the Pseudomonas aeruginosa SOS response and its role in the global response to the antibiotic ciprofloxacin. *Journal of Bacteriology*, *188*(20), 7101–7110. https://doi.org/10.1128/JB.00807-06

Claessen, D., Rozen, D. E., Kuipers, O. P., Søgaard-Andersen, L., & Van Wezel, G. P. (2014). Bacterial solutions to multicellularity: A tale of biofilms, filaments and fruiting bodies. In *Nature Reviews Microbiology* (Vol. 12, Issue 2, pp. 115–124). https://doi.org/10.1038/nrmicro3178

Claudine, B., & Harwood, C. S. (2013). Cyclic diguanosine monophosphate represses bacterial flagella synthesis by interacting with the Walker a motif of the enhancer-binding protein FleQ. *Proceedings of the National Academy of*

Sciences of the United States of America, *110*(46), 18478–18483. https://doi.org/10.1073/pnas.1318972110

Corno, G., Jo¨, J., Villiger, J., & Pernthaler, J. (2013). Coaggregation in a microbial predator-prey system affects competition and trophic transfer efficiency. *Ecology*, *94*(4), 870–881. https://doi.org/10.2307/23436300

Costerton, J. W., Geesey, G. G., & Cheng, K. J. (1978a). How bacteria stick. *Scientific American*, *238*(1), 86–95. https://doi.org/10.1038/scientificamerican0178-86

Costerton, J. W., Geesey, G. G., & Cheng, K. J. (1978b). How bacteria stick. *Scientific American*, *238*(1), 86–95. https://doi.org/10.1038/scientificamerican0178-86

D'Alvise, P. W., Sjøholm, O. R., Yankelevich, T., Jin, Y., Wuertz, S., & Smets, B. F. (2010). TOL plasmid carriage enhances biofilm formation and increases extracellular DNA content in Pseudomonas putida KT2440. In *FEMS Microbiology Letters* (Vol. 312, Issue 1, pp. 84–92). https://doi.org/10.1111/j.1574-6968.2010.02105.x

Das, T., Krom, B. P., Van Der Mei, H. C., Busscher, H. J., & Sharma, P. K. (2011). DNA-mediated bacterial aggregation is dictated by acid-base interactions. *Soft Matter*, *7*(6), 2927–2935. https://doi.org/10.1039/c0sm01142h

Das, T., & Manefield, M. (2012). Pyocyanin Promotes Extracellular DNA Release in Pseudomonas aeruginosa. *PLoS ONE*, *7*(10). https://doi.org/10.1371/journal.pone.0046718

Das, T., Sehar, S., Koop, L., Wong, Y. K., Ahmed, S., Siddiqui, K. S., & Manefield, M. (2014). Influence of calcium in extracellular DNA mediated bacterial aggregation and biofilm formation. *PLoS ONE*, *9*(3), 1–11. https://doi.org/10.1371/journal.pone.0091935

Das, T., Sehar, S., & Manefield, M. (2013). The roles of extracellular DNA in the structural integrity of extracellular polymeric substance and bacterial biofilm development. *Environmental Microbiology Reports*, *5*(6), 778–786. https://doi.org/10.1111/1758-2229.12085

Das, T., Sharma, P. K., Busscher, H. J., Van Der Mei, H. C., & Krom, B. P. (2010). Role of extracellular DNA in initial bacterial adhesion and surface aggregation. *Applied and Environmental Microbiology*, *76*(10), 3405–3408. https://doi.org/10.1128/AEM.03119-09

Dastgheyb, S. S., Hammoud, S., Ketonis, C., Liu, A. Y., Fitzgerald, K., Parvizi, J., Purtill, J., Ciccotti, M., Shapiro, I. M., Otto, M., & Hickok, N. J. (2015). Staphylococcal persistence due to biofilm formation in synovial fluid containing

prophylactic cefazolin. *Antimicrobial Agents and Chemotherapy*, *59*(4), 2122–2128. https://doi.org/10.1128/AAC.04579-14

Davey, M. E., & O'toole, G. A. (2000). Microbial Biofilms: from Ecology to Molecular Genetics. In *MICROBIOLOGY AND MOLECULAR BIOLOGY REVIEWS* (Vol. 64, Issue 4). https://journals.asm.org/journal/mmbr

Davidson, E. A., Basu, A. S., & Bayer, T. S. (2013). Programming microbes using pulse width modulation of optical signals. *Journal of Molecular Biology*, *425*(22), 4161–4166. https://doi.org/10.1016/j.jmb.2013.07.036

De Weger, L. A., Van Der Vlugt, C. I. M., Wijfjes, A. H. M., Bakker, P. A. H. M., Schippers, B., & Lugtenberg1, B. (1987). Flagella of a Plant-Growth-Stimulating Pseudomonas fluorescens Strain Are Required for Colonization of Potato Roots. In *JOURNAL OF BACTERIOLOGY* (Vol. 169, Issue 6).

Delvigne, F., Brognaux, A., Francis, F., Twizere, J. C., Gorret, N., Sorensen, S. J., & Thonart, P. (2011). Green fluorescent protein (GFP) leakage from microbial biosensors provides useful information for the evaluation of the scale-down effect. *Biotechnology Journal*, *6*(8), 968–978. https://doi.org/10.1002/biot.201000410

Delvigne, F., & Goffin, P. (2014). Microbial heterogeneity affects bioprocess robustness: Dynamic single-cell analysis contributes to understanding of microbial populations. *Biotechnology Journal*, *9*(1), 61–72. https://doi.org/10.1002/biot.201300119

Delvigne, F., & Martinez, J. A. (2023). Advances in automated and reactive flow cytometry for synthetic biotechnology. In *Current Opinion in Biotechnology* (Vol. 83). Elsevier Ltd. https://doi.org/10.1016/j.copbio.2023.102974

Delvigne, F., & Noorman, H. (2017). *Highlight Scale-up / Scale-down of microbial bioprocesses : a modern light on Highlight Scale-up / Scale-down of microbial bioprocesses : a modern light on an old issue*. *May*. https://doi.org/10.1111/1751-7915.12732

Deng, B., Ghatak, S., Sarkar, S., Singh, K., Das Ghatak, P., Mathew-Steiner, S. S., Roy, S., Khanna, S., Wozniak, D. J., McComb, D. W., & Sen, C. K. (2020). Novel Bacterial Diversity and Fragmented eDNA Identified in Hyperbiofilm-Forming Pseudomonas aeruginosa Rugose Small Colony Variant. *IScience*, *23*(2). https://doi.org/10.1016/j.isci.2020.100827

Dengler, V., Foulston, L., DeFrancesco, A. S., & Losick, R. (2015). An electrostatic net model for the role of extracellular DNA in biofilm formation by

Staphylococcus aureus. *Journal of Bacteriology*, *197*(24), 3779–3787. https://doi.org/10.1128/JB.00726-15

Déziel, E., Comeau, Y., & Villemur, R. (2001). Initiation of biofilm formation by Pseudomonas aeruginosa 57RP correlates with emergence of hyperpiliated and highly adherent phenotypic variants deficient in swimming, swarming, and twitching motilities. *Journal of Bacteriology*, *183*(4), 1195–1204. https://doi.org/10.1128/JB.183.4.1195-1204.2001

Díaz, M., Herrero, M., García, L. A., & Quirós, C. (2010). Application of flow cytometry to industrial microbial bioprocesses. In *Biochemical Engineering Journal* (Vol. 48, Issue 3, pp. 385–407). https://doi.org/10.1016/j.bej.2009.07.013

Dillard, J. P., & Seifert, H. S. (2001). A variable genetic island specific for Neisseria gonorrhoeae is involved in providing DNA for natural transformation and is found more often in disseminated infection isolates. *Molecular Microbiology*, *41*(1), 263–277. https://doi.org/10.1046/j.1365-2958.2001.02520.x

Din, M. O., Martin, A., Razinkov, I., Csicsery, N., & Hasty, J. (2020a). *Interfacing gene circuits with microelectronics through engineered population dynamics*.

Din, M. O., Martin, A., Razinkov, I., Csicsery, N., & Hasty, J. (2020b). *Interfacing gene circuits with microelectronics through engineered population dynamics*.

Dogsa, I., Kostanjšek, R., & Stopar, D. (2023). eDNA Provides a Scaffold for Autoaggregation of B. subtilis in Bacterioplankton Suspension. *Microorganisms*, *11*(2). https://doi.org/10.3390/microorganisms11020332

Doroshenko, N., Tseng, B. S., Howlin, R. P., Deacon, J., Wharton, J. A., Thurner, P. J., Gilmore, B. F., Parsek, M. R., & Stoodley, P. (2014). Extracellular DNA impedes the transport of vancomycin in Staphylococcus epidermidis biofilms preexposed to subinhibitory concentrations of vancomycin. *Antimicrobial Agents and Chemotherapy*, *58*(12), 7273–7282. https://doi.org/10.1128/AAC.03132-14

Drenkard, E. (2003). Antimicrobial resistance of Pseudomonas aeruginosa biofilms. In *Microbes and Infection* (Vol. 5, Issue 13, pp. 1213–1219). Elsevier Masson SAS. https://doi.org/10.1016/j.micinf.2003.08.009

Dusny, C., Grünberger, A., Probst, C., Wiechert, W., Kohlheyer, D., & Schmid, A. (2015). Technical bias of microcultivation environments on single-cell physiology. *Lab on a Chip*, *15*(8). https://doi.org/10.1039/c4lc01270d

Dusny, C., & Schmid, A. (2015). Microfluidic single-cell analysis links boundary environments and individual microbial phenotypes. *Environmental Microbiology*, *17*(6), 1839–1856. https://doi.org/10.1111/1462-2920.12667

Elias, S., & Banin, E. (2012). *Multi-species biofilms : living with friendly neighbors*. https://doi.org/10.1111/j.1574-6976.2012.00325.x

El-Kirat-Chatel, S., Beaussart, A., Boyd, C. D., O'Toole, G. A., & Dufreîne, Y. F. (2014). Single-cell and single-molecule analysis deciphers the localization, adhesion, and mechanics of the biofilm adhesin LapA. *ACS Chemical Biology*, *9*(2), 485–494. https://doi.org/10.1021/cb400794e

Farrell, A., & Quilty, B. (2002). Substrate-dependent autoaggregation of Pseudomonas putida CP1 during the degradation of mono-chlorophenols and phenol. *Journal of Industrial Microbiology & Biotechnology*, *28*(6), 316–324. https://doi.org/10.1038/sj/jim/7000249

Faruque, S. M., Biswas, K., Nashir Udden, S. M., Shafi Ahmad, Q., Sack, D. A., Balakrish Nair, G., & Mekalanos, J. J. (2006). *Transmissibility of cholera: In vivo-formed biofilms and their relationship to infectivity and persistence in the environment*. www.pnas.orgcgidoi10.1073pnas.0601277103

Fazli, M., Almblad, H., Rybtke, M. L., Givskov, M., Eberl, L., & Tolker-Nielsen, T. (2014a). Regulation of biofilm formation in Pseudomonas and Burkholderia species. In *Environmental Microbiology* (Vol. 16, Issue 7, pp. 1961–1981). Blackwell Publishing Ltd. https://doi.org/10.1111/1462-2920.12448

Fazli, M., Almblad, H., Rybtke, M. L., Givskov, M., Eberl, L., & Tolker-Nielsen, T. (2014b). Regulation of biofilm formation in Pseudomonas and Burkholderia species. In *Environmental Microbiology* (Vol. 16, Issue 7, pp. 1961–1981). Blackwell Publishing Ltd. https://doi.org/10.1111/1462-2920.12448

Fazli, M., Almblad, H., Rybtke, M. L., Givskov, M., Eberl, L., & Tolker-Nielsen, T. (2014c). Regulation of biofilm formation in Pseudomonas and Burkholderia species. *Environmental Microbiology*, *16*(7), 1961–1981. https://doi.org/10.1111/1462-2920.12448

Fernández, A. J., & Romero, F. G. (2014). *Regulation of the lifestyle switch in Pseudomonas putida Memoria presentada por*.

Filoche, S. K., Anderson, S. A., & Sissons, C. H. (2004). Biofilm growth of Lactobacillus species is promoted by Actinomyces species and Streptococcus mutans. *Oral Microbiology and Immunology*, *19*(5), 322–326. https://doi.org/10.1111/j.1399-302x.2004.00164.x

Finkel, S. E., & Kolter, R. (2001). DNA as a nutrient: Novel role for bacterial competence gene homologs. *Journal of Bacteriology*, *183*(21), 6288–6293. https://doi.org/10.1128/JB.183.21.6288-6293.2001

Flemming, H. C., & Wingender, J. (2010). The biofilm matrix. In *Nature Reviews Microbiology* (Vol. 8, Issue 9, pp. 623–633). https://doi.org/10.1038/nrmicro2415

Fu, J., Zhang, Y., Lin, S., Zhang, W., Shu, G., Lin, J., Li, H., Xu, F., Tang, H., Peng, G., Zhao, L., Chen, S., & Fu, H. (2021). Strategies for Interfering With Bacterial Early Stage Biofilms. In *Frontiers in Microbiology* (Vol. 12). Frontiers Media S.A. https://doi.org/10.3389/fmicb.2021.675843

Fulaz, S., Vitale, S., Quinn, L., & Casey, E. (2019). Nanoparticle–Biofilm Interactions: The Role of the EPS Matrix. *Trends in Microbiology*, *27*(11), 915–926. https://doi.org/10.1016/j.tim.2019.07.004

Funari, R., Bhalla, N., Chu, K. Y., Söderström, B., & Shen, A. Q. (2018). Nanoplasmonics for Real-Time and Label-Free Monitoring of Microbial Biofilm Formation. *ACS Sensors*, *3*(8), 1499–1509. https://doi.org/10.1021/acssensors.8b00287

Funari, R., & Shen, A. Q. (2022). Detection and Characterization of Bacterial Biofilms and Biofilm-Based Sensors. In *ACS Sensors* (Vol. 7, Issue 2, pp. 347–357). American Chemical Society. https://doi.org/10.1021/acssensors.1c02722

Fuqua, C., Parsek, M. R., & Greenberg, E. P. (2001). *REGULATION OF GENE EXPRESSION BY CELL-TO-CELL COMMUNICATION: Acyl-Homoserine Lactone Quorum Sensing*. www.annualreviews.org

Fuxman Bass, J. I., Russo, D. M., Gabelloni, M. L., Geffner, J. R., Giordano, M., Catalano, M., Zorreguieta, Á., & Trevani, A. S. (2010). Extracellular DNA: A Major Proinflammatory Component of Pseudomonas aeruginosa Biofilms . *The Journal of Immunology*, *184*(11), 6386–6395. https://doi.org/10.4049/jimmunol.0901640

Gallo, P. M., Rapsinski, G. J., Wilson, R. P., Oppong, G. O., Sriram, U., Goulian, M., Buttaro, B., Caricchio, R., Gallucci, S., & Tükel, Ç. (2015). Amyloid-DNA Composites of Bacterial Biofilms Stimulate Autoimmunity. *Immunity*, *42*(6), 1171–1184. https://doi.org/10.1016/j.immuni.2015.06.002

Garcia, J. R., Cha, H. J., Rao, G., Marten, M. R., & Bentley, W. E. (2009). Microbial nar-GFP cell sensors reveal oxygen limitations in highly agitated and aerated

laboratory-scale fermentors. *Microbial Cell Factories*, *8*. https://doi.org/10.1186/1475-2859-8-6

Garcia-Betancur, J. C., Yepes, A., Schneider, J., & Lopez, D. (2012). Single-cell analysis of Bacillus subtilis biofilms using fluorescence microscopy and flow cytometry. *Journal of Visualized Experiments*, *60*. https://doi.org/10.3791/3796

Gião, M. S., & Keevil, C. W. (2014). Listeria monocytogenes can form biofilms in tap water and enter into the viable but non-cultivable state. *Microbial Ecology*, *67*(3), 603–611. https://doi.org/10.1007/s00248-013-0364-3

Gibbons, R., & Nygaard, M. (1970). Interbacterial aggregation of plaque bacteria [Article]. *Archives of Oral Biology.*, *15*(12), 1397-IN39. https://doi.org/10.1016/0003-9969(70)90031-2

Gjermansen, M., Nilsson, M., Yang, L., & Tolker-Nielsen, T. (2010). Characterization of starvation-induced dispersion in Pseudomonas putida biofilms: Genetic elements and molecular mechanisms. *Molecular Microbiology*, *75*(4), 815–826. https://doi.org/10.1111/j.1365-2958.2009.06793.x

Gjermansen, M., Ragas, P., Sternberg, C., Molin, S., & Tolker-Nielsen, T. (2005). Characterization of starvation-induced dispersion in Pseudomonas putida biofilms. *Environmental Microbiology*, *7*(6), 894–904. https://doi.org/10.1111/j.1462-2920.2005.00775.x

Gjermansen, M., Ragas, P., & Tolker-Nielsen, T. (2006). Proteins with GGDEF and EAL domains regulate Pseudomonas putida biofilm formation and dispersal. *FEMS Microbiology Letters*, *265*(2), 215–224. https://doi.org/10.1111/j.1574-6968.2006.00493.x

Gloag, E. S., Turnbull, L., Huang, A., Vallotton, P., Wang, H., Nolan, L. M., Mililli, L., Hunt, C., Lu, J., Osvath, S. R., Monahan, L. G., Cavaliere, R., Charles, I. G., Wand, M. P., Gee, M. L., Prabhakar, R., & Whitchurch, C. B. (2013). Self-organization of bacterial biofilms is facilitated by extracellular DNA. *Proceedings of the National Academy of Sciences of the United States of America*, *110*(28), 11541–11546. https://doi.org/10.1073/pnas.1218898110

Griffin, A. S., West, S. A., & Buckling, A. (2004). Cooperation and competition in pathogenic bacteria. *Nature*, *430*(7003), 1024–1027. https://doi.org/10.1038/nature02744

Haaber, J., Cohn, M. T., Frees, D., Andersen, T. J., & Ingmer, H. (2012). Planktonic aggregates of Staphylococcus aureus protect against common antibiotics. *PLoS ONE*, *7*(7). https://doi.org/10.1371/journal.pone.0041075

Halan, B., Buehler, K., & Schmid, A. (2012). Biofilms as living catalysts in continuous chemical syntheses. In *Trends in Biotechnology* (Vol. 30, Issue 9, pp. 453–465). https://doi.org/10.1016/j.tibtech.2012.05.003

Hall, C. W., & Mah, T. F. (2017). Molecular mechanisms of biofilm-based antibiotic resistance and tolerance in pathogenic bacteria. In *FEMS Microbiology Reviews* (Vol. 41, Issue 3, pp. 276–301). Oxford University Press. https://doi.org/10.1093/femsre/fux010

Hall-Stoodley, L., Costerton, J. W., & Stoodley, P. (2004a). Bacterial biofilms: From the natural environment to infectious diseases. In *Nature Reviews Microbiology* (Vol. 2, Issue 2, pp. 95–108). https://doi.org/10.1038/nrmicro821

Hall-Stoodley, L., Costerton, J. W., & Stoodley, P. (2004b). Bacterial biofilms: From the natural environment to infectious diseases. In *Nature Reviews Microbiology* (Vol. 2, Issue 2, pp. 95–108). https://doi.org/10.1038/nrmicro821

Hall-Stoodley, L., & Stoodley, P. (2002). Developmental regulation of microbial biofilms. In *Current Opinion in Biotechnology* (Vol. 13, Issue 3, pp. 228–233). Elsevier Ltd. https://doi.org/10.1016/S0958-1669(02)00318-X

Halte, M., Wörmann, M. E., Bogisch, M., Erhardt, M., & Tschowri, N. (2022). BldD-based bimolecular fluorescence complementation for in vivo detection of the second messenger cyclic di-GMP. *Molecular Microbiology*, *117*(3), 705–713. https://doi.org/10.1111/mmi.14876

Hamilton, H. L., Domínguez, N. M., Schwartz, K. J., Hackett, K. T., & Dillard, J. P. (2005). Neisseria gonorrhoeae secretes chromosomal DNA via a novel type IV secretion system. *Molecular Microbiology*, *55*(6), 1704–1721. https://doi.org/10.1111/j.1365-2958.2005.04521.x

Hansen, S. K., Rainey, P. B., Haagensen, J. A. J., & Molin, S. (2007a). Evolution of species interactions in a biofilm community. *Nature*, *445*(7127), 533–536. https://doi.org/10.1038/nature05514

Hansen, S. K., Rainey, P. B., Haagensen, J. A. J., & Molin, S. (2007b). Evolution of species interactions in a biofilm community. *Nature*, *445*(7127), 533–536. https://doi.org/10.1038/nature05514

Hare, P. J., Lagree, T. J., Byrd, B. A., Demarco, A. M., & Mok, W. W. K. (2021). Single-cell technologies to study phenotypic heterogeneity and bacterial

persisters. In *Microorganisms* (Vol. 9, Issue 11). MDPI. https://doi.org/10.3390/microorganisms9112277

Häußler, S., Ziegler, I., Löttel, A., Götz, F. V., Rohde, M., Wehmhöhner, D., Saravanamuthu, S., Tümmler, B., & Steinmetz, I. (2003). Highly adherent small-colony variants of Pseudomonas aeruginosa in cystic fibrosis lung infection. *Journal of Medical Microbiology*, *52*(4), 295–301. https://doi.org/10.1099/jmm.0.05069-0

Heijstra, B. D., Pichler, F. B., Liang, Q., Blaza, R. G., & Turner, S. J. (2009). Extracellular DNA and Type IV pili mediate surface attachment by Acidovorax temperans. *Antonie van Leeuwenhoek, International Journal of General and Molecular Microbiology*, *95*(4), 343–349. https://doi.org/10.1007/s10482-009-9320-0

Hengge. (2009). *Nature Reviews | Microbiology*. www.nature.com/reviews/micro

Henrion, L., Delvenne, M., Bajoul Kakahi, F., Moreno-Avitia, F., & Delvigne, F. (2022). Exploiting Information and Control Theory for Directing Gene Expression in Cell Populations. In *Frontiers in Microbiology* (Vol. 13). Frontiers Media S.A. https://doi.org/10.3389/fmicb.2022.869509

Henrion, L., Martinez, J. A., Vandenbroucke, V., Delvenne, M., Telek, S., Zicler, A., Grünberger, A., & Delvigne, F. (2023). Fitness cost associated with cell phenotypic switching drives population diversification dynamics and controllability. *Nature Communications*, *14*(1), 6128. https://doi.org/10.1038/s41467-023-41917-z

Herrera, J. J. R., Cabo, M. L., González, A., Pazos, I., & Pastoriza, L. (2007). Adhesion and detachment kinetics of several strains of Staphylococcus aureus subsp. aureus under three different experimental conditions. *Food Microbiology*, *24*(6), 585–591. https://doi.org/10.1016/j.fm.2007.01.001

Hinsa, S. M., Espinosa-Urgel, M., Ramos, J. L., & O'Toole, G. A. (2003). Transition from reversible to irreversible attachment during biofilm formation by Pseudomonas fluorescens WCS365 requires an ABC transporter and a large secreted protein. *Molecular Microbiology*, *49*(4), 905–918. https://doi.org/10.1046/j.1365-2958.2003.03615.x

Høiby, N., Krogh Johansen, H., Moser, C., Song, Z., Ciofu, O., & Kharazmi, A. (2001). *Pseudomonas aeruginosa and the in vitro and in vivo biofilm mode of growth*.

Hojo, K., Nagaoka, S., Ohshima, T., & Maeda, N. (2009). Critical Review in Oral Biology & Medicine: Bacterial Interactions in Dental Biofilm Development. *Journal of Dental Research*, *88*(11), 982–990. https://doi.org/10.1177/0022034509346811

Hu, Y., Xiao, Y., Liao, K., Leng, Y., & Lu, Q. (2021). Development of microalgal biofilm for wastewater remediation: from mechanism to practical application. *Journal of Chemical Technology and Biotechnology*, *96*(11), 2993–3008. https://doi.org/10.1002/jctb.6850

Hymes, S. R., Randis, T. M., Sun, T. Y., & Ratner, A. J. (2013). DNase inhibits gardnerella vaginalis biofilms in vitro and in vivo. *Journal of Infectious Diseases*, *207*(10), 1491–1497. https://doi.org/10.1093/infdis/jit047

Ibáñez de Aldecoa, A. L., Zafra, O., & González-Pastor, J. E. (2017). Mechanisms and regulation of extracellular DNA release and its biological roles in microbial communities. In *Frontiers in Microbiology* (Vol. 8, Issue JUL). Frontiers Media S.A. https://doi.org/10.3389/fmicb.2017.01390

Irie, Y., Borlee, B. R., O'Connor, J. R., Hill, P. J., Harwood, C. S., Wozniak, D. J., & Parsek, M. R. (2012). Self-produced exopolysaccharide is a signal that stimulates biofilm formation in Pseudomonas aeruginosa. *Proceedings of the National Academy of Sciences of the United States of America*, *109*(50), 20632–20636. https://doi.org/10.1073/pnas.1217993109

Jakubovics, N. S., Shields, R. C., Rajarajan, N., & Burgess, J. G. (2013). Life after death: The critical role of extracellular DNA in microbial biofilms. *Letters in Applied Microbiology*, *57*(6), 467–475. https://doi.org/10.1111/lam.12134

Jennings, L. K., Storek, K. M., Ledvina, H. E., Coulon, C., Marmont, L. S., Sadovskaya, I., Secor, P. R., Tseng, B. S., Scian, M., Filloux, A., Wozniak, D. J., Howell, P. L., & Parsek, M. R. (2015). Pel is a cationic exopolysaccharide that cross-links extracellular DNA in the Pseudomonas aeruginosa biofilm matrix. *Proceedings of the National Academy of Sciences of the United States of America*, *112*(36), 11353–11358. https://doi.org/10.1073/pnas.1503058112

Jiang, Z., Nero, T., Mukherjee, S., Olson, R., & Yan, J. (2021). Searching for the Secret of Stickiness: How Biofilms Adhere to Surfaces. In *Frontiers in Microbiology* (Vol. 12). Frontiers Media S.A. https://doi.org/10.3389/fmicb.2021.686793

Jones, C. J., & Wozniaka, D. J. (2017). Psl Produced by mucoid Pseudomonas aeruginosa contributes to the establishment of biofilms and immune evasion. *MBio*, *8*(3). https://doi.org/10.1128/mBio.00864-17

Jones, H. C., Roth, I. L., & Sanders, W. M. (1969). Electron Microscopic Study of a Slime Layer. In *JOURNAL OF BACTERIOLOGY*.

Joux, F., & Lebaron, P. (2000). *Use of fluorescent probes to assess physiological functions of bacteria at single-cell level*.

Jurcisek, J. A., & Bakaletz, L. O. (2007). Biofilms formed by nontypeable Haemophilus influenzae in vivo contain both double-stranded DNA and type IV pilin protein. *Journal of Bacteriology*, *189*(10), 3868–3875. https://doi.org/10.1128/JB.01935-06

Kampf, J., Gerwig, J., Kruse, K., Cleverley, R., Dormeyer, M., Grünberger, A., Kohlheyer, D., Commichau, F. M., Lewis, R. J., Stülke, J., Kampf, C. J., Nancy Freitag, E. E., & Bioengineering, M. (2018). *Selective Pressure for Biofilm Formation in Bacillus subtilis: Differential Effect of Mutations in the Master Regulator SinR on Bistability*. https://doi.org/10.1128/mBio

Kang, D., Liu, W., Kakahi, F. B., & Delvigne, F. (2022). Combined utilization of metabolic inhibitors to prevent synergistic multi-species biofilm formation. *AMB Express*, *12*(1). https://doi.org/10.1186/s13568-022-01363-4

Karatan, E., & Michael, A. J. (2013). A wider role for polyamines in biofilm formation. In *Biotechnology Letters* (Vol. 35, Issue 11, pp. 1715–1717). https://doi.org/10.1007/s10529-013-1286-3

Karatan, E., & Watnick, P. (2009). Signals, Regulatory Networks, and Materials That Build and Break Bacterial Biofilms. *Microbiology and Molecular Biology Reviews*, *73*(2), 310–347. https://doi.org/10.1128/mmbr.00041-08

Katharios-Lanwermeyer, S., Xi, C., Jakubovics, N. S., & Rickard, A. H. (2014). Mini-review: Microbial coaggregation: ubiquity and implications for biofilm development. *Biofouling*, *30*(10), 1235–1251. https://doi.org/10.1080/08927014.2014.976206

Kavanaugh, J. S., Flack, C. E., Lister, J., Ricker, E. B., Ibberson, C. B., Jenul, C., Moormeier, D. E., Delmain, E. A., Bayles, K. W., & Horswill, A. R. (2019). Identification of extracellular DNA-binding proteins in the biofilm matrix. *MBio*, *10*(3). https://doi.org/10.1128/mBio.01137-19

Kellenberger, C. A., Wilson, S. C., Sales-Lee, J., & Hammond, M. C. (2013). RNA-based fluorescent biosensors for live cell imaging of second messengers cyclic

di-GMP and cyclic AMP-GMP. *Journal of the American Chemical Society*, *135*(13), 4906–4909. https://doi.org/10.1021/ja311960g

Kerstens, M., Boulet, G., Van, M., Clais, S., Lanckacker, E., Delputte, P., Maes, L., & Cos, P. (2015). *A flow cytometric approach to quantify biofilms*. 335–342. https://doi.org/10.1007/s12223-015-0400-4

Khemaleelakul, S., Baumgartner, J. C., & Pruksakom, S. (2006). Autoaggregation and coaggregation of bacteria associated with acute endodontic infections. *Journal of Endodontics*, *32*(4), 312–318. https://doi.org/10.1016/j.joen.2005.10.003

Khomtchouk, K. M., Weglarz, M., Bekale, L. A., Koliesnik, I., Bollyky, P. L., & Santa Maria, P. L. (2019). Quantitative assessment of bacterial growth phase utilizing flow cytometry. *Journal of Microbiological Methods*, *167*. https://doi.org/10.1016/j.mimet.2019.105760

Kiedrowski, M. R., Kavanaugh, J. S., Malone, C. L., Mootz, J. M., Voyich, J. M., Smeltzer, M. S., Bayles, K. W., & Horswill, A. R. (2011). Nuclease modulates biofilm formation in community-associated methicillin-resistant staphylococcus aureus. *PLoS ONE*, *6*(11). https://doi.org/10.1371/journal.pone.0026714

Kim, J., Hahn, J. S., Franklin, M. J., Stewart, P. S., & Yoon, J. (2009). Tolerance of dormant and active cells in Pseudomonas aeruginosa PA01 biofilm to antimicrobial agents. *Journal of Antimicrobial Chemotherapy*, *63*(1), 129–135. https://doi.org/10.1093/jac/dkn462

Klausen, M., Gjermansen, M., Kreft, J. U., & Tolker-Nielsen, T. (2006). Dynamics of development and dispersal in sessile microbial communities: Examples from Pseudomonas aeruginosa and Pseudomonas putida model biofilms. In *FEMS Microbiology Letters* (Vol. 261, Issue 1, pp. 1–11). https://doi.org/10.1111/j.1574-6968.2006.00280.x

Klayman, B. J., Volden, P. A., Stewart, P. S., & Camper, A. K. (2009). Escherichia coli 0157:H7 requires colonizing partner to adhere and persist in a capillary flow cell. *Environmental Science and Technology*, *43*(6), 2105–2111. https://doi.org/10.1021/es802218q

Kolenbrander, P. E. (2000). ORAL MICROBIAL COMMUNITIES: Biofilms, Interactions, and Genetic Systems 1. In *Annu. Rev. Microbiol* (Vol. 54). www.annualreviews.org

Kolenbrander, P. E., Palmer, R. J., Rickard, A. H., Jakubovics, N. S., Chalmers, N. I., & Diaz, P. I. (2006). Bacterial interactions and successions during plaque

development. In *Periodontology 2000* (Vol. 42, Issue 1, pp. 47–79). https://doi.org/10.1111/j.1600-0757.2006.00187.x

Kolter, R., & Greenberg, E. P. (2006). The superficial life of microbes. In *NEWS & VIEWS FEATURE* (Vol. 441, Issue 18).

Konieczny, M., Rhein, P., Czaczyk, K., Białas, W., & Juzwa, W. (2021). Imaging flow cytometry to study biofilm-associated microbial aggregates. *Molecules*, *26*(23). https://doi.org/10.3390/molecules26237096

Kostakioti, M., Hadjifrangiskou, M., & Hultgren, S. J. (2013). Bacterial biofilms: Development, dispersal, and therapeutic strategies in the dawn of the postantibiotic era. *Cold Spring Harbor Perspectives in Medicine*, *3*(4). https://doi.org/10.1101/cshperspect.a010306

Kragh, K. N., Tolker-Nielsen, T., & Lichtenberg, M. (2023). The non-attached biofilm aggregate. In *Communications Biology* (Vol. 6, Issue 1). Nature Research. https://doi.org/10.1038/s42003-023-05281-4

Kulasekara, B. R., Kamischke, C., Kulasekara, H. D., Christen, M., Wiggins, P. A., & Miller, S. I. (2013). c-di-GMP heterogeneity is generated by the chemotaxis machinery to regulate flagellar motility. *ELife*, *2013*(2). https://doi.org/10.7554/eLife.01402

Kussell, E., & Leibler, S. (2005). Ecology: Phenotypic diversity, population growth, and information in fluctuating environments. *Science*, *309*(5743), 2075–2078. https://doi.org/10.1126/science.1114383

Kuystermans, D., Avesh, M., & Al-Rubeai, M. (2016a). Online flow cytometry for monitoring apoptosis in mammalian cell cultures as an application for process analytical technology. *Cytotechnology*, *68*(3), 399–408. https://doi.org/10.1007/s10616-014-9791-3

Kuystermans, D., Avesh, M., & Al-Rubeai, M. (2016b). Online flow cytometry for monitoring apoptosis in mammalian cell cultures as an application for process analytical technology. *Cytotechnology*, *68*(3), 399–408. https://doi.org/10.1007/s10616-014-9791-3

Ladner, T., Grünberger, A., Probst, C., Kohlheyer, D., Büchs, J., & Delvigne, F. (2017). Application of Mini- and Micro-Bioreactors for Microbial Bioprocesses. In *Current Developments in Biotechnology and Bioengineering: Bioprocesses, Bioreactors and Controls*. Elsevier B.V. https://doi.org/10.1016/B978-0-444-63663-8.00015-X

Laganenka, L., Colin, R., & Sourjik, V. (2016). Chemotaxis towards autoinducer 2 mediates autoaggregation in Escherichia coli. *Nature Communications*, *7*. https://doi.org/10.1038/ncomms12984

Lahesaare, A., Ainelo, H., Teppo, A., Kivisaar, M., Heipieper, H. J., & Teras, R. (2016). LapF and its regulation by fis affect the cell surface hydrophobicity of pseudomonas putida. *PLoS ONE*, *11*(11). https://doi.org/10.1371/journal.pone.0166078

Laventie, B. J., Sangermani, M., Estermann, F., Manfredi, P., Planes, R., Hug, I., Jaeger, T., Meunier, E., Broz, P., & Jenal, U. (2019). A Surface-Induced Asymmetric Program Promotes Tissue Colonization by Pseudomonas aeruginosa. *Cell Host and Microbe*, *25*(1), 140-152.e6. https://doi.org/10.1016/j.chom.2018.11.008

Lebeaux, D., Ghigo, J.-M., & Beloin, C. (2014). Biofilm-Related Infections: Bridging the Gap between Clinical Management and Fundamental Aspects of Recalcitrance toward Antibiotics. *Microbiology and Molecular Biology Reviews*, *78*(3), 510–543. https://doi.org/10.1128/mmbr.00013-14

Lee, E. R., Baker, J. L., Weinberg, Z., Sudarsan, N., & Breaker, R. R. (2010). An allosteric self-splicing ribozyme triggered by a bacterial second messenger. *Science*, *329*(5993), 845–848. https://doi.org/10.1126/science.1190713

Lelek, M., Gyparaki, M. T., Beliu, G., Schueder, F., Griffié, J., Manley, S., Jungmann, R., Sauer, M., Lakadamyali, M., & Zimmer, C. (2021). Single-molecule localization microscopy. In *Nature Reviews Methods Primers* (Vol. 1, Issue 1). Springer Nature. https://doi.org/10.1038/s43586-021-00038-x

Lister, J. L., & Horswill, A. R. (2014). Staphylococcus aureus biofilms: Recent developments in biofilm dispersal. *Frontiers in Cellular and Infection Microbiology*, *4*(DEC). https://doi.org/10.3389/fcimb.2014.00178

Liu, H. H., Yang, Y. R., Shen, X. C., Zhang, Z. L., Shen, P., & Xie, Z. X. (2008). Role of DNA in bacterial aggregation. *Current Microbiology*, *57*(2), 139–144. https://doi.org/10.1007/s00284-008-9166-0

Luo, Y., Zhao, K., Baker, A. E., Kuchma, S. L., Coggan, K. A., Wolfgang, M. C., Wong, G. C. L., & O'Toole, G. A. (2015). A hierarchical cascade of second messengers regulates Pseudomonas aeruginosa Surface Behaviors. *MBio*, *6*(1). https://doi.org/10.1128/mBio.02456-14

Madsen, J. S., Lin, Y. C., Squyres, G. R., Price-Whelan, A., Torio, A. de S., Song, A., Cornell, W. C., Sørensen, S. J., Xavier, J. B., & Dietrich, L. E. P. (2015).

Facultative control of matrix production optimizes competitive fitness in Pseudomonas aeruginosa PA14 biofilm models. *Applied and Environmental Microbiology*, *81*(24), 8414–8426. https://doi.org/10.1128/AEM.02628-15

Mah, T. F. C., & O'Toole, G. A. (2001). Mechanisms of biofilm resistance to antimicrobial agents. *Trends in Microbiology*, *9*(1), 34–39. https://doi.org/10.1016/S0966-842X(00)01913-2

Mann, E. E., & Wozniak, D. J. (2012). Pseudomonas biofilm matrix composition and niche biology. In *FEMS Microbiology Reviews* (Vol. 36, Issue 4, pp. 893–916). https://doi.org/10.1111/j.1574-6976.2011.00322.x

Martínez-Garćía, E., Aparicio, T., Goñi-Moreno, A., Fraile, S., & De Lorenzo, V. (2015). SEVA 2.0: An update of the Standard European Vector Architecture for de-/re-construction of bacterial functionalities. *Nucleic Acids Research*, *43*(D1), D1183–D1189. https://doi.org/10.1093/nar/gku1114

Martínez-Gil, M., Ramos-González, M. I., & Espinosa-Urgel, M. (2014). Roles of cyclic Di-GMP and the Gac system in transcriptional control of the genes coding for the Pseudomonas putida adhesins LapA and LapF. *Journal of Bacteriology*, *196*(8), 1484–1495. https://doi.org/10.1128/JB.01287-13

Martínez-Gil, M., Yousef-Coronado, F., & Espinosa-Urgel, M. (2010). LapF, the second largest Pseudomonas putida protein, contributes to plant root colonization and determines biofilm architecture. *Molecular Microbiology*, *77*(3), 549–561. https://doi.org/10.1111/j.1365-2958.2010.07249.x

Martínez-Granero, F., Rivilla, R., & Martín, M. (2006). Rhizosphere selection of highly motile phenotypic variants of Pseudomonas fluorescens with enhanced competitive colonization ability. *Applied and Environmental Microbiology*, *72*(5), 3429–3434. https://doi.org/10.1128/AEM.72.5.3429-3434.2006

Martins Dos Santos, V. A. P., Heim, S., Moore, E. R. B., Strätz, M., & Timmis, K. N. (2004). Insights into the genomic basis of niche specificity of Pseudomonas putida KT2440. *Environmental Microbiology*, *6*(12), 1264–1286. https://doi.org/10.1111/j.1462-2920.2004.00734.x

Matilla, M. A., Travieso, M. L., Ramos, J. L., & Ramos-González, M. I. (2011). Cyclic diguanylate turnover mediated by the sole GGDEF/EAL response regulator in Pseudomonas putida: Its role in the rhizosphere and an analysis of its target processes. *Environmental Microbiology*, *13*(7), 1745–1766. https://doi.org/10.1111/j.1462-2920.2011.02499.x

Mattiazzi Usaj, M., Yeung, C. H. L., Friesen, H., Boone, C., & Andrews, B. J. (2021). Single-cell image analysis to explore cell-to-cell heterogeneity in isogenic populations. In *Cell Systems* (Vol. 12, Issue 6, pp. 608–621). Cell Press. https://doi.org/10.1016/j.cels.2021.05.010

McGlennen, M., Dieser, M., Foreman, C. M., & Warnat, S. (2023). Monitoring biofilm growth and dispersal in real-time with impedance biosensors. *Journal of Industrial Microbiology and Biotechnology*, *50*(1). https://doi.org/10.1093/jimb/kuad022

McLean, J. S., Pinchuk, G. E., Geydebrekht, O. V., Bilskis, C. L., Zakrajsek, B. A., Hill, E. A., Saffarini, D. A., Romine, M. F., Gorby, Y. A., Fredrickson, J. K., & Beliaev, A. S. (2008). Oxygen-dependent autoaggregation in Shewanella oneidensis MR-1. *Environmental Microbiology*, *10*(7). https://doi.org/10.1111/j.1462-2920.2008.01608.x

McLean, R. J. C., Whiteley, M., Stickler, D. J., & Fuqua, W. C. (2006). Evidence of autoinducer activity in naturally occurring biofilms. *FEMS Microbiology Letters*, *154*(2), 259–263. https://doi.org/10.1111/j.1574-6968.1997.tb12653.x

Melaugh, G., Martinez, V. A., Baker, P., Hill, P. J., Howell, P. L., Wozniak, D. J., & Allen, R. J. (2023a). Distinct types of multicellular aggregates in Pseudomonas aeruginosa liquid cultures. *Npj Biofilms and Microbiomes*, *9*(1). https://doi.org/10.1038/s41522-023-00412-5

Melaugh, G., Martinez, V. A., Baker, P., Hill, P. J., Howell, P. L., Wozniak, D. J., & Allen, R. J. (2023b). Distinct types of multicellular aggregates in Pseudomonas aeruginosa liquid cultures. *Npj Biofilms and Microbiomes*, *9*(1). https://doi.org/10.1038/s41522-023-00412-5

Min, K. R., & Rickard, A. H. (2009). Coaggregation by the freshwater bacterium Sphingomonas natatoria alters dual-species biofilm formation. *Applied and Environmental Microbiology*, *75*(12), 3987–3997. https://doi.org/10.1128/AEM.02843-08

Mlynek, K. D., Bulock, L. L., Stone, C. J., Curran, L. J., Sadykov, M. R., Bayles, K. W., & Brinsmade, S. R. (2020). Genetic and biochemical analysis of cody-mediated cell aggregation in staphylococcus aureus reveals an interaction between extracellular DNA and polysaccharide in the extracellular matrix. *Journal of Bacteriology*, *202*(8). https://doi.org/10.1128/JB.00593-19

Molin, S., & Tolker-Nielsen, T. (2003). Gene transfer occurs with enhanced efficiency in biofilms and induces enhanced stabilisation of the biofilm structure. In

Current Opinion in Biotechnology (Vol. 14, Issue 3, pp. 255–261). Elsevier Ltd. https://doi.org/10.1016/S0958-1669(03)00036-3

Monds, R. D., Newell, P. D., Gross, R. H., & O'Toole, G. A. (2007). Phosphate-dependent modulation of c-di-GMP levels regulates Pseudomonas fluorescens Pf0-1 biofilm formation by controlling secretion of the adhesin LapA. *Molecular Microbiology*, *63*(3), 656–679. https://doi.org/10.1111/j.1365-2958.2006.05539.x

Monds, R. D., & O'Toole, G. A. (2009). The developmental model of microbial biofilms: ten years of a paradigm up for review. In *Trends in Microbiology* (Vol. 17, Issue 2, pp. 73–87). https://doi.org/10.1016/j.tim.2008.11.001

Monier, J. M., & Lindow, S. E. (2003). Differential survival of solitary and aggregated bacterial cells promotes aggregate formation on leaf surfaces. *Proceedings of the National Academy of Sciences of the United States of America*, *100*(26), 15977–15982. https://doi.org/10.1073/pnas.2436560100

Moor, H., Teppo, A., Lahesaare, A., Kivisaar, M., & Teras, R. (2014). Fis overexpression enhances Pseudomonas putida biofilm formation by regulating the ratio of LapA and LapF. *Microbiology (United Kingdom)*, *160*, 2681–2693. https://doi.org/10.1099/mic.0.082503-0

Moormeier, D. E., & Bayles, K. W. (2017). Staphylococcus aureus biofilm: a complex developmental organism. In *Molecular Microbiology* (Vol. 104, Issue 3, pp. 365–376). Blackwell Publishing Ltd. https://doi.org/10.1111/mmi.13634

Moscoso, M., García, E., & López, R. (2006). Biofilm formation by Streptococcus pneumoniae: Role of choline, extracellular DNA, and capsular polysaccharide in microbial accretion. *Journal of Bacteriology*, *188*(22), 7785–7795. https://doi.org/10.1128/JB.00673-06

Moshynets, O. V., Pokholenko, I., Iungin, O., Potters, G., & Spiers, A. J. (2022a). eDNA, Amyloid Fibers and Membrane Vesicles Identified in Pseudomonas fluorescens SBW25 Biofilms. *International Journal of Molecular Sciences*, *23*(23). https://doi.org/10.3390/ijms232315096

Moshynets, O. V., Pokholenko, I., Iungin, O., Potters, G., & Spiers, A. J. (2022b). eDNA, Amyloid Fibers and Membrane Vesicles Identified in Pseudomonas fluorescens SBW25 Biofilms. *International Journal of Molecular Sciences*, *23*(23). https://doi.org/10.3390/ijms232315096

Moshynets, O. V., & Spiers, A. J. (2016). Viewing Biofilms within the Larger Context of Bacterial Aggregations. In *Microbial Biofilms - Importance and Applications*. InTech. https://doi.org/10.5772/62912

Mulcahy, H., Charron-Mazenod, L., & Lewenza, S. (2008). Extracellular DNA chelates cations and induces antibiotic resistance in Pseudomonas aeruginosa biofilms. *PLoS Pathogens*, *4*(11). https://doi.org/10.1371/journal.ppat.1000213

Müller, S., & Nebe-Von-Caron, G. (2010). Functional single-cell analyses: Flow cytometry and cell sorting of microbial populations and communities. In *FEMS Microbiology Reviews* (Vol. 34, Issue 4, pp. 554–587). https://doi.org/10.1111/j.1574-6976.2010.00214.x

Musk, D. J., Banko, D. A., & Hergenrother, P. J. (2005). Iron salts perturb biofilm formation and disrupt existing biofilms of Pseudomonas aeruginosa. *Chemistry and Biology*, *12*(7), 789–796. https://doi.org/10.1016/j.chembiol.2005.05.007

Nadell, C. D., & Bassler, B. L. (2011). A fitness trade-off between local competition and dispersal in Vibrio cholerae biofilms. *Proceedings of the National Academy of Sciences of the United States of America*, *108*(34), 14181–14185. https://doi.org/10.1073/pnas.1111147108

Nagler, M., Insam, H., Pietramellara, G., & Ascher-Jenull, J. (2018). Extracellular DNA in natural environments: features, relevance and applications. In *Applied Microbiology and Biotechnology* (Vol. 102, Issue 15, pp. 6343–6356). Springer Verlag. https://doi.org/10.1007/s00253-018-9120-4

Nair, H. A. S., Periasamy, S., Yang, L., Kjelleberg, S., & Rice, S. A. (2017). Real Time, Spatial, and Temporal Mapping of the Distribution of c-di-GMP during Biofilm Development. *Journal of Biological Chemistry*, *292*(2), 477–487. https://doi.org/10.1074/jbc.M116.746743

Nakamura, S., Higashiyama, Y., Izumikawa, K., Seki, M., Kakeya, H., Yamamoto, Y., Yanagihara, K., Miyazaki, Y., Mizuta, Y., & Kohno, S. (2008). The roles of the quorum-sensing system in the release of extracellular DNA, lipopolysaccharide, and membrane vesicles from Pseudomonas aeruginosa. *Japanese Journal of Infectious Diseases*, *61*(5), 375–378. https://doi.org/10.7883/yoken.jjid.2008.375

Nakayama, S., Luo, Y., Zhou, J., Dayie, T. K., & Sintim, H. O. (2012). Nanomolar fluorescent detection of c-di-GMP using a modular aptamer strategy. *Chemical Communications*, *48*(72), 9059–9061. https://doi.org/10.1039/c2cc34379g

Nebe-Von-Caron, G., Stephens, P. J., Hewitt, C. J., Powell, J. R., & Badley, R. A. (2000). Analysis of bacterial function by multi-colour fluorescence flow cytometry and single cell sorting. In *Journal of Methods Microbiological Journal of Microbiological Methods* (Vol. 42). www.elsevier.com/locate/jmicmeth

Nelson, K. E., Weinel, C., Paulsen, I. T., Dodson, R. J., Hilbert, H., Martins dos Santos, V. A. P., Fouts, D. E., Gill, S. R., Pop, M., Holmes, M., Brinkac, L., Beanan, M., DeBoy, R. T., Daugherty, S., Kolonay, J., Madupu, R., Nelson, W., White, O., Peterson, J., … Fraser, C. M. (2002). Complete genome sequence and comparative analysis of the metabolically versatile Pseudomonas putida KT2440. *Environmental Microbiology*, *4*(12), 799–808. https://doi.org/10.1046/j.1462-2920.2002.00366.x

Nemoto, K., Hirota, K., Murakami, K., Taniguti, K., Murata, H., Viducic, D., & Miyake, Y. (2003). Effect of Varidase (streptodornase) on biofilm formed by Pseudomonas aeruginosa. *Chemotherapy*, *49*(3). https://doi.org/10.1159/000070617

Neu, T. R., & Lawrence, J. R. (2015). Innovative techniques, sensors, and approaches for imaging biofilms at different scales. In *Trends in Microbiology* (Vol. 23, Issue 4, pp. 233–242). Elsevier Ltd. https://doi.org/10.1016/j.tim.2014.12.010

Nguyen, T. M., Telek, S., Zicler, A., Andres Martinez, J., Zacchetti, B., Kopp, J., Slouka, C., Herwig, C., Grünberger, A., & Delvigne, F. (2021). Reducing phenotypic and genotypic instabilities of microbial population during continuous cultivation based on stochastic switching dynamics. *BioRxiv*, 2021.01.13.426484. https://doi.org/10.1101/2021.01.13.426484

Nie, H., Xiao, Y., Liu, H., He, J., Chen, W., & Huang, Q. (2017). FleN and FleQ play a synergistic role in regulating lapA and bcs operons in Pseudomonas putida KT2440. *Environmental Microbiology Reports*, *9*(5), 571–580. https://doi.org/10.1111/1758-2229.12547

Nikel, P. I., Martínez-García, E., & De Lorenzo, V. (2014). Biotechnological domestication of pseudomonads using synthetic biology. In *Nature Reviews Microbiology* (Vol. 12, Issue 5, pp. 368–379). Nature Publishing Group. https://doi.org/10.1038/nrmicro3253

Nilsson, M., Chiang, W. C., Fazli, M., Gjermansen, M., Givskov, M., & Tolker-Nielsen, T. (2011). Influence of putative exopolysaccharide genes on

Pseudomonas putida KT2440 biofilm stability. *Environmental Microbiology*, *13*(5), 1357–1369. https://doi.org/10.1111/j.1462-2920.2011.02447.x

Nishimural, S., Tanakal, T., Fujita2, K., Itaya2, M., Hiraishil, A., & Kikuchil, Y. (2003). Extracellular DNA and RNA produced by a marine phot os y n t het i c bacte r i u m Rhodovulum sulfidophilum. In *0.uford University Press Nucleic Acids Research Supplement* (Issue 3). https://academic.oup.com/nass/article/3/1/279/1050603

Nørskov Kragh, K., Alhede, M., Rybtke, M., Stavnsberg, C., Ø Jensen, P., Tolker-Nielsen, T., Whiteley, M., & Bjarnsholt, T. (2018). *The Inoculation Method Could Impact the Outcome of Microbiological Experiments*. https://doi.org/10

Nwoko, E. S. Q. A., & Okeke, I. N. (2021). Bacteria autoaggregation: How and why bacteria stick together. In *Biochemical Society Transactions* (Vol. 49, Issue 3, pp. 1147–1157). Portland Press Ltd. https://doi.org/10.1042/BST20200718

Oh, E., Andrews, K. J., & Jeon, B. (2018). Enhanced biofilm formation by ferrous and ferric iron through oxidative stress in Campylobacter jejuni. *Frontiers in Microbiology*, *9*(JUN), 1–9. https://doi.org/10.3389/fmicb.2018.01204

Okshevsky, M., Regina, V. R., & Meyer, R. L. (2015a). Extracellular DNA as a target for biofilm control. *Current Opinion in Biotechnology*, *33*, 73–80. https://doi.org/10.1016/j.copbio.2014.12.002

Okshevsky, M., Regina, V. R., & Meyer, R. L. (2015b). Extracellular DNA as a target for biofilm control. In *Current Opinion in Biotechnology* (Vol. 33, pp. 73–80). Elsevier Ltd. https://doi.org/10.1016/j.copbio.2014.12.002

Oliveira, N. M., Martinez-Garcia, E., Xavier, J., Durham, W. M., Kolter, R., Kim, W., & Foster, K. R. (2015). Biofilm formation as a response to ecological competition. *PLoS Biology*, *13*(7). https://doi.org/10.1371/journal.pbio.1002191

O'Toole, G. A., Pratt, L. A., Watnick, P. I., Newman, D. K., Weaver, V. B., & Kolter, R. (1999). [6] Genetic approaches to study of biofilms [Bookitem]. In *Biofilms /* (Vol. 310). Academic Press,. https://doi.org/10.1016/S0076-6879(99)10008-9

O'toole, G., Kaplan, H. B., & Kolter, R. (2000). *BIOFILM FORMATION AS MICROBIAL DEVELOPMENT*. www.annualreviews.org

Pakkulnan, R., Anutrakunchai, C., Kanthawong, S., Taweechaisupapong, S., Chareonsudjai, P., & Chareonsudjai, S. (2019). Extracellular DNA facilitates bacterial adhesion during Burkholderia pseudomallei biofilm formation. *PLoS ONE*, *14*(3). https://doi.org/10.1371/journal.pone.0213288

Pamp, S. J., Sternberg, C., & Tolker-Nielsen, T. (2009). Insight into the microbial multicellular lifestyle via flow-cell technology and confocal microscopy. *Cytometry Part A*, *75*(2), 90–103. https://doi.org/10.1002/cyto.a.20685

Parsek, M. R., & Greenberg, E. P. (2005). Sociomicrobiology: The connections between quorum sensing and biofilms. In *Trends in Microbiology* (Vol. 13, Issue 1, pp. 27–33). https://doi.org/10.1016/j.tim.2004.11.007

Paul, K., Nieto, V., Carlquist, W. C., Blair, D. F., & Harshey, R. M. (2010). The c-di-GMP Binding Protein YcgR Controls Flagellar Motor Direction and Speed to Affect Chemotaxis by a "Backstop Brake" Mechanism. *Molecular Cell*, *38*(1), 128–139. https://doi.org/10.1016/j.molcel.2010.03.001

Paul, R., Weiser, S., Amiot, N. C., Chan, C., Schirmer, T., Giese, B., & Jenal, U. (2004). Cell cycle-dependent dynamic localization of a bacterial response regulator with a novel di-guanylate cyclase output domain. *Genes and Development*, *18*(6), 715–727. https://doi.org/10.1101/gad.289504

Payne, D. E., & Boles, B. R. (2016). Emerging interactions between matrix components during biofilm development. In *Current Genetics* (Vol. 62, Issue 1, pp. 137–141). Springer Verlag. https://doi.org/10.1007/s00294-015-0527-5

Penesyan, A., Paulsen, I. T., Kjelleberg, S., & Gillings, M. R. (2021). Three faces of biofilms: a microbial lifestyle, a nascent multicellular organism, and an incubator for diversity. In *npj Biofilms and Microbiomes* (Vol. 7, Issue 1). https://doi.org/10.1038/s41522-021-00251-2

Peng, N., Cai, P., Mortimer, M., Wu, Y., Gao, C., & Huang, Q. (2020). The exopolysaccharide-eDNA interaction modulates 3D architecture of Bacillus subtilis biofilm. *BMC Microbiology*, *20*(1). https://doi.org/10.1186/s12866-020-01789-5

Perez-Soto, N., Creese, O., Fernandez-Trillo, F., & Krachler, A. M. (2018). Aggregation of Vibrio cholerae by Cationic Polymers Enhances Quorum Sensing but Overrides Biofilm Dissipation in Response to Autoinduction. *ACS Chemical Biology*, *13*(10), 3021–3029. https://doi.org/10.1021/acschembio.8b00815

Perkins, T. J., & Swain, P. S. (2009). Strategies for cellular decision-making. In *Molecular Systems Biology* (Vol. 5). https://doi.org/10.1038/msb.2009.83

Perrino, G., Napolitano, S., Galdi, F., La Regina, A., Fiore, D., Giuliano, T., di Bernardo, M., & di Bernardo, D. (2021). Automatic synchronisation of the cell

cycle in budding yeast through closed-loop feedback control. *Nature Communications*, *12*(1). https://doi.org/10.1038/s41467-021-22689-w

Perrino, G., Wilson, C., Santorelli, M., & di Bernardo, D. (2019). Quantitative Characterization of α-Synuclein Aggregation in Living Cells through Automated Microfluidics Feedback Control. *Cell Reports*, *27*(3), 916-927.e5. https://doi.org/10.1016/j.celrep.2019.03.081

Petchiappan, A., Sujay, &, Naik, Y., & Chatterji, D. (n.d.). *Tracking the homeostasis of second messenger cyclic-di-GMP in bacteria*. https://doi.org/10.1007/s12551-020-00636-1/Published

Petersen, E., Mills, E., & Miller, S. I. (2019). Cyclic-di-GMP regulation promotes survival of a slow-replicating subpopulation of intracellular Salmonella Typhimurium. *Proceedings of the National Academy of Sciences of the United States of America*, *116*(13), 6335–6340. https://doi.org/10.1073/pnas.1901051116

Peterson, B. W., He, Y., Ren, Y., Zerdoum, A., Libera, M. R., Sharma, P. K., van Winkelhoff, A. J., Neut, D., Stoodley, P., van der Mei, H. C., & Busscher, H. J. (2015). Viscoelasticity of biofilms and their recalcitrance to mechanical and chemical challenges. In *FEMS Microbiology Reviews* (Vol. 39, Issue 2, pp. 234–245). Oxford University Press. https://doi.org/10.1093/femsre/fuu008

Philipp, L. A., Bühler, K., Ulber, R., & Gescher, J. (2023). Beneficial applications of biofilms. In *Nature Reviews Microbiology*. Nature Research. https://doi.org/10.1038/s41579-023-00985-0

Pires, L., Sachsenheimer, K., Kleintschek, T., Waldbaur, A., Schwartz, T., & Rapp, B. E. (2013). Online monitoring of biofilm growth and activity using a combined multi-channel impedimetric and amperometric sensor. *Biosensors and Bioelectronics*, *47*, 157–163. https://doi.org/10.1016/j.bios.2013.03.015

Platt, R., Drescher, C., Park, S. K., & Phillips, G. J. (2000). Genetic system for reversible integration of DNA constructs and lacZ gene fusions into the Escherichia coli chromosome. *Plasmid*, *43*(1), 12–23. https://doi.org/10.1006/plas.1999.1433

Price-Whelan, A., Dietrich, L. E. P., & Newman, D. K. (2006). Rethinking "secondary" metabolism: Physiological roles for phenazine antibiotics. In *Nature Chemical Biology* (Vol. 2, Issue 2, pp. 71–78). Nature Publishing Group. https://doi.org/10.1038/nchembio764

Qin, Z., Ou, Y., Yang, L., Zhu, Y., Tolker-Nielsen, T., Molin, S., & Qu, D. (2007). Role of autolysin-mediated DNA release in biofilm formation of Staphylococcus epidermidis. *Microbiology*, *153*(7), 2083–2092. https://doi.org/10.1099/mic.0.2007/006031-0

Qvist, T., Eickhardt, S., Kragh, K. N., Andersen, C. B., Iversen, M., Høiby, N., & Bjarnsholt, T. (2015). Chronic pulmonary disease with Mycobacterium abscessus complex is a biofilm infection. In *European Respiratory Journal* (Vol. 46, Issue 6). https://doi.org/10.1183/13993003.01102-2015

Ramos-González, M. I., Travieso, M. L., Soriano, M. I., Matilla, M. A., Huertas-Rosales, Ó., Barrientos-Moreno, L., Tagua, V. G., & Espinosa-Urgel, M. (2016a). Genetic dissection of the regulatory network associated with high c-di-GMP levels in Pseudomonas putida KT2440. *Frontiers in Microbiology*, *7*(JUL). https://doi.org/10.3389/fmicb.2016.01093

Ramos-González, M. I., Travieso, M. L., Soriano, M. I., Matilla, M. A., Huertas-Rosales, Ó., Barrientos-Moreno, L., Tagua, V. G., & Espinosa-Urgel, M. (2016b). Genetic dissection of the regulatory network associated with high c-di-GMP levels in Pseudomonas putida KT2440. *Frontiers in Microbiology*, *7*(JUL). https://doi.org/10.3389/fmicb.2016.01093

Ren, D., Madsen, J. S., de la Cruz-Perera, C. I., Bergmark, L., Sørensen, S. J., & Burmølle, M. (2014). High-Throughput Screening of Multispecies Biofilm Formation and Quantitative PCR-Based Assessment of Individual Species Proportions, Useful for Exploring Interspecific Bacterial Interactions. *Microbial Ecology*, *68*(1), 146–154. https://doi.org/10.1007/s00248-013-0315-z

Reyes-Darias, J. A., & Krell, T. (2017). Riboswitches as Potential Targets for the Development of Anti-Biofilm Drugs. *Current Topics in Medicinal Chemistry*, *17*(17), 1945–1953. https://doi.org/10.2174/1568026617666170407163517

Rickard, A. H., Gilbert, P., High, N. J., Kolenbrander, P. E., & Handley, P. S. (2003). Bacterial coaggregation: An integral process in the development of multi-species biofilms. In *Trends in Microbiology* (Vol. 11, Issue 2, pp. 94–100). Elsevier Ltd. https://doi.org/10.1016/S0966-842X(02)00034-3

Rickard, A. H., Leach, S. A., Hall, L. S., Buswell, C. M., High, N. J., & Handley, P. S. (2002). Phylogenetic relationships and coaggregation ability of freshwater biofilm bacteria. *Applied and Environmental Microbiology*, *68*(7), 3644–3650. https://doi.org/10.1128/AEM.68.7.3644-3650.2002

Rickard, A. H., McBain, A. J., Ledder, R. G., Handley, P. S., & Gilbert, P. (2003). Coaggregation between freshwater bacteria within biofilm and planktonic communities. *FEMS Microbiology Letters*, *220*(1), 133–140. https://doi.org/10.1016/S0378-1097(03)00094-6

Rickard, A. H., McBain, A. J., Stead, A. T., & Gilbert, P. (2004). Shear rate moderates community diversity in freshwater biofilms. *Applied and Environmental Microbiology*, *70*(12), 7426–7435. https://doi.org/10.1128/AEM.70.12.7426-7435.2004

Rodesney, C. A., Roman, B., Dhamani, N., Cooley, B. J., Katira, P., Touhami, A., & Gordon, V. D. (2017). Mechanosensing of shear by Pseudomonas aeruginosa leads to increased levels of the cyclic-di-GMP signal initiating biofilm development. *Proceedings of the National Academy of Sciences of the United States of America*, *114*(23), 5906–5911. https://doi.org/10.1073/pnas.1703255114

Rogers, W. T., & Holyst, H. A. (2009). FlowFP: A Bioconductor Package for Fingerprinting Flow Cytometric Data. *Advances in Bioinformatics*, *2009*, 1–11. https://doi.org/10.1155/2009/193947

Römling, U., Galperin, M. Y., & Gomelsky, M. (2013). Cyclic di-GMP: the First 25 Years of a Universal Bacterial Second Messenger. *Microbiology and Molecular Biology Reviews*, *77*(1), 1–52. https://doi.org/10.1128/mmbr.00043-12

Römling, U., Gomelsky, M., & Galperin, M. Y. (2005). C-di-GMP: The dawning of a novel bacterial signalling system. In *Molecular Microbiology* (Vol. 57, Issue 3, pp. 629–639). https://doi.org/10.1111/j.1365-2958.2005.04697.x

Rosenberg, M., Azevedo, N. F., & Ivask, A. (2019a). Propidium iodide staining underestimates viability of adherent bacterial cells. *Scientific Reports*, *9*(1). https://doi.org/10.1038/s41598-019-42906-3

Rosenberg, M., Azevedo, N. F., & Ivask, A. (2019b). Propidium iodide staining underestimates viability of adherent bacterial cells. *Scientific Reports*, *9*(1), 1–14. https://doi.org/10.1038/s41598-019-42906-3

Rumbaugh, K. P., & Sauer, K. (2020). Biofilm dispersion. In *Nature Reviews Microbiology* (Vol. 18, Issue 10, pp. 571–586). Nature Research. https://doi.org/10.1038/s41579-020-0385-0

Rybtke, M. T., Borlee, B. R., Murakami, K., Irie, Y., Hentzer, M., Nielsen, T. E., Givskov, M., Parsek, M. R., & Tolker-Nielsen, T. (2012). Fluorescence-based reporter for gauging cyclic Di-GMP levels in Pseudomonas aeruginosa. *Applied*

and Environmental Microbiology, *78*(15), 5060–5069. https://doi.org/10.1128/AEM.00414-12

Saber, N., Ju, Y., Hsu, H. Y., & Lee, S. H. (2013). A feasibility study on the application of microwaves for online biofilm monitoring in the pipelines. *International Journal of Pressure Vessels and Piping*, *111–112*, 99–105. https://doi.org/10.1016/j.ijpvp.2013.05.005

Sarkar, S. (n.d.). *MINI-REVIEW Release mechanisms and molecular interactions of Pseudomonas aeruginosa extracellular DNA*. https://doi.org/10.1007/s00253-020-10687-9/Published

Sassi, H., Nguyen, T. M., Telek, S., Gosset, G., Grünberger, A., & Delvigne, F. (2019a). Segregostat: a novel concept to control phenotypic diversification dynamics on the example of Gram-negative bacteria. *Microbial Biotechnology*, *12*(5), 1064–1075. https://doi.org/10.1111/1751-7915.13442

Sassi, H., Nguyen, T. M., Telek, S., Gosset, G., Grünberger, A., & Delvigne, F. (2019b). Segregostat: a novel concept to control phenotypic diversification dynamics on the example of Gram-negative bacteria. *Microbial Biotechnology*, *12*(5), 1064–1075. https://doi.org/10.1111/1751-7915.13442

Sauer, K., Camper, A. K., Ehrlich, G. D., Costerton, J. W., & Davies, D. G. (2002). Pseudomonas aeruginosa displays multiple phenotypes during development as a biofilm. *Journal of Bacteriology*, *184*(4), 1140–1154. https://doi.org/10.1128/jb.184.4.1140-1154.2002

Sauer, K., Stoodley, P., Goeres, D. M., Hall-Stoodley, L., Burmølle, M., Stewart, P. S., & Bjarnsholt, T. (2022). The biofilm life cycle: expanding the conceptual model of biofilm formation. In *Nature Reviews Microbiology* (Vol. 20, Issue 10, pp. 608–620). Nature Research. https://doi.org/10.1038/s41579-022-00767-0

Saunders, S. H., Tse, E. C. M., Yates, M. D., Otero, F. J., Trammell, S. A., Stemp, E. D. A., Barton, J. K., Tender, L. M., & Newman, D. K. (2020). Extracellular DNA Promotes Efficient Extracellular Electron Transfer by Pyocyanin in Pseudomonas aeruginosa Biofilms. *Cell*, *182*(4), 919-932.e19. https://doi.org/10.1016/j.cell.2020.07.006

Schleheck, D., Barraud, N., Klebensberger, J., Webb, J. S., McDougald, D., Rice, S. A., & Kjelleberg, S. (2009). Pseudomonas aeruginosa PAO1 Preferentially Grows as Aggregates in Liquid Batch Cultures and Disperses upon Starvation. *PLoS ONE*, *4*(5), e5513. https://doi.org/10.1371/journal.pone.0005513

Schreiber, F., & Ackermann, M. (2020). Environmental drivers of metabolic heterogeneity in clonal microbial populations. In *Current Opinion in Biotechnology* (Vol. 62, pp. 202–211). Elsevier Ltd. https://doi.org/10.1016/j.copbio.2019.11.018

Secchi, E., Savorana, G., Vitale, A., Eberl, L., Stocker, R., & Rusconi, R. (2022). *The structural role of bacterial eDNA in the formation of biofilm streamers*. https://doi.org/10.1073/pnas

Secor, P. R., Michaels, L. A., Ratjen, A., Jennings, L. K., & Singh, P. K. (2018). Entropically driven aggregation of bacteria by host polymers promotes antibiotic tolerance in Pseudomonas aeruginosa. *Proceedings of the National Academy of Sciences of the United States of America*, *115*(42), 10780–10785. https://doi.org/10.1073/pnas.1806005115

Serra, D. O., & Hengge, R. (2019). A c-di-GMP-Based Switch Controls Local Heterogeneity of Extracellular Matrix Synthesis which Is Crucial for Integrity and Morphogenesis of Escherichia coli Macrocolony Biofilms. *Journal of Molecular Biology*, *431*(23), 4775–4793. https://doi.org/10.1016/j.jmb.2019.04.001

Sharma, A., Inagaki, S., Sigurdson, W., & Kuramitsu, H. K. (2005). Synergy between Tannerella forsythia and Fusobacterium nucleatum in biofilm formation. *Oral Microbiology and Immunology*, *20*(1), 39–42. https://doi.org/10.1111/j.1399-302X.2004.00175.x

Silva-Rocha, R., Martínez-García, E., Calles, B., Chavarría, M., Arce-Rodríguez, A., De Las Heras, A., Páez-Espino, A. D., Durante-Rodríguez, G., Kim, J., Nikel, P. I., Platero, R., & De Lorenzo, V. (2013a). The Standard European Vector Architecture (SEVA): A coherent platform for the analysis and deployment of complex prokaryotic phenotypes. *Nucleic Acids Research*, *41*(D1). https://doi.org/10.1093/nar/gks1119

Silva-Rocha, R., Martínez-García, E., Calles, B., Chavarría, M., Arce-Rodríguez, A., De Las Heras, A., Páez-Espino, A. D., Durante-Rodríguez, G., Kim, J., Nikel, P. I., Platero, R., & De Lorenzo, V. (2013b). The Standard European Vector Architecture (SEVA): A coherent platform for the analysis and deployment of complex prokaryotic phenotypes. *Nucleic Acids Research*, *41*(D1). https://doi.org/10.1093/nar/gks1119

Simm, R., Morr, M., Kader, A., Nimtz, M., & Römling, U. (2004). GGDEF and EAL domains inversely regulate cyclic di-GMP levels and transition from sessibility

to motility. *Molecular Microbiology*, *53*(4), 1123–1134. https://doi.org/10.1111/j.1365-2958.2004.04206.x

Simões, L. C., Simões, M., & Vieira, M. J. (2008). Intergeneric coaggregation among drinking water bacteria: Evidence of a role for Acinetobacter calcoaceticus as a bridging bacterium. *Applied and Environmental Microbiology*, *74*(4), 1259–1263. https://doi.org/10.1128/AEM.01747-07

Sriramulu, D. D., Lünsdorf, H., Lam, J. S., & Römling, U. (2005). Microcolony formation: A novel biofilm model of Pseudomonas aeruginosa for the cystic fibrosis lung. *Journal of Medical Microbiology*, *54*(7), 667–676. https://doi.org/10.1099/jmm.0.45969-0

Steinberger, R. E., & Holden, P. A. (2005). Extracellular DNA in single- and multiple-species unsaturated biofilms. *Applied and Environmental Microbiology*, *71*(9), 5404–5410. https://doi.org/10.1128/AEM.71.9.5404-5410.2005

Stevens, M. R. E., Luo, T. L., Vornhagen, J., Jakubovics, N. S., Gilsdorf, J. R., Marrs, C. F., Møretrø, T., & Rickard, A. H. (2015). Coaggregation occurs between microorganisms isolated from different environments. *FEMS Microbiology Ecology*, *91*(11). https://doi.org/10.1093/femsec/fiv123

Stewart, G. J., Carlson, C. A., & Ingraham, J. L. (1983). Evidence for an Active Role of Donor Cells in Natural Transformation of Pseudomonas stutzeri. In *JOURNAL OF BACTERIOLOGY* (Vol. 156, Issue 1).

Stewart, P. S., White, B., Boegli, L., Hamerly, T., Williamson, K. S., Franklin, M. J., Bothner, B., James, G. A., Fisher, S., Vital-Lopez, F. G., & Wallqvist, A. (2019). Conceptual model of biofilm antibiotic tolerance that integrates phenomena of diffusion, metabolism, gene expression, and physiology. *Journal of Bacteriology*, *201*(22). https://doi.org/10.1128/JB.00307-19

Stoodley, P., Sauer, K., Davies, D. G., & Costerton, J. W. (2002). Biofilms as complex differentiated communities. *Annual Review of Microbiology*, *56*, 187–209. https://doi.org/10.1146/annurev.micro.56.012302.160705

Sudarsan, N., Lee, E. R., Weinberg, Z., Moy, R. H., Kim, J. N., Link, K. H., & Breaker, R. R. (2008). Riboswitches in eubacteria sense the second messenger cyclic Di-GMP. *Science*, *321*(5887), 411–413. https://doi.org/10.1126/science.1159519

Swartjes, J. J. T. M., Das, T., Sharifi, S., Subbiahdoss, G., Sharma, P. K., Krom, B. P., Busscher, H. J., & Van Der Mei, H. C. (2013). A functional DNase i coating to prevent adhesion of bacteria and the formation of biofilm. *Advanced*

Functional Materials, *23*(22), 2843–2849. https://doi.org/10.1002/adfm.201202927

Taghavi, S., Van Der Lelie, D., & Mergeay, M. (1994). Electroporation of Alcaligenes eutrophus with (Mega) Plasmids and Genomic DNA Fragments. In *APPLIED AND ENVIRONMENTAL MICROBIOLOGY*.

Tahrioui, A., Duchesne, R., Bouffartigues, E., Rodrigues, S., Maillot, O., Tortuel, D., Hardouin, J., Taupin, L., Groleau, M. C., Dufour, A., Déziel, E., Brenner-Weiss, G., Feuilloley, M., Orange, N., Lesouhaitier, O., Cornelis, P., & Chevalier, S. (2019). Extracellular DNA release, quorum sensing, and PrrF1/F2 small RNAs are key players in Pseudomonas aeruginosa tobramycin-enhanced biofilm formation. *Npj Biofilms and Microbiomes*, *5*(1). https://doi.org/10.1038/s41522-019-0088-3

Tan, C., Reza, F., & You, L. (2007). Noise-limited frequency signal transmission in gene circuits. *Biophysical Journal*, *93*(11). https://doi.org/10.1529/biophysj.107.110403

Thattai, M., & Van Oudenaarden, A. (n.d.-a). *Stochastic Gene Expression in Fluctuating Environments*.

Thattai, M., & Van Oudenaarden, A. (n.d.-b). *Stochastic Gene Expression in Fluctuating Environments*.

Thattai, M., & Van Oudenaarden, A. (n.d.-c). *Stochastic Gene Expression in Fluctuating Environments*.

Timmis, K. N. (2002). Pseudomonas putida: A cosmopolitan opportunist par excellence. In *Environmental Microbiology* (Vol. 4, Issue 12, pp. 779–781). https://doi.org/10.1046/j.1462-2920.2002.00365.x

Tischler, A. D., & Camilli, A. (2004). Cyclic diguanylate (c-di-GMP) regulates Vibrio cholerae biofilm formation. *Molecular Microbiology*, *53*(3), 857–869. https://doi.org/10.1111/j.1365-2958.2004.04155.x

Tomich, M., & Mohr, C. D. (2003). Adherence and autoaggregation phenotypes of a Burkholderia cenocepacia cable pilus mutant. *FEMS Microbiology Letters*, *228*(2), 287–297. https://doi.org/10.1016/S0378-1097(03)00785-7

Tostevin, F., & Ten Wolde, P. R. (2009). Mutual information between input and output trajectories of biochemical networks. *Physical Review Letters*, *102*(21). https://doi.org/10.1103/PhysRevLett.102.218101

Trappetti, C., Gualdi, L., Di Meola, L., Jain, P., Korir, C. C., Edmonds, P., Iannelli, F., Ricci, S., Pozzi, G., & Oggioni, M. R. (2011). The impact of the competence

quorum sensing system on Streptococcus pneumoniae biofilms varies depending on the experimental model. *BMC Microbiology*, *11*(1), 75. https://doi.org/10.1186/1471-2180-11-75

Turnbull, L., Toyofuku, M., Hynen, A. L., Kurosawa, M., Pessi, G., Petty, N. K., Osvath, S. R., Cárcamo-Oyarce, G., Gloag, E. S., Shimoni, R., Omasits, U., Ito, S., Yap, X., Monahan, L. G., Cavaliere, R., Ahrens, C. H., Charles, I. G., Nomura, N., Eberl, L., & Whitchurch, C. B. (2016). Explosive cell lysis as a mechanism for the biogenesis of bacterial membrane vesicles and biofilms. *Nature Communications*, *7*. https://doi.org/10.1038/ncomms11220

Van Den Broek, D., Chin-A-Woeng, T. F. C., Eijkemans, K., Mulders, I. H. M., Bloemberg, G. V, & Lugtenberg, B. J. J. (2003). *Biocontrol Traits of Pseudomonas spp. Are Regulated by Phase Variation* (Vol. 16, Issue 11).

Van Houdt, R., & Michiels, C. W. (2005). Role of bacterial cell surface structures in Escherichia coli biofilm formation. In *Research in Microbiology* (Vol. 156, Issues 5–6, pp. 626–633). https://doi.org/10.1016/j.resmic.2005.02.005

Vandana, & Das, S. (2022a). Genetic regulation, biosynthesis and applications of extracellular polysaccharides of the biofilm matrix of bacteria. In *Carbohydrate Polymers* (Vol. 291). Elsevier Ltd. https://doi.org/10.1016/j.carbpol.2022.119536

Vandana, & Das, S. (2022b). Genetic regulation, biosynthesis and applications of extracellular polysaccharides of the biofilm matrix of bacteria. In *Carbohydrate Polymers* (Vol. 291). Elsevier Ltd. https://doi.org/10.1016/j.carbpol.2022.119536

Vatansever, C., & Turetgen, I. (2021). Investigation of the effects of various stress factors on biofilms and planktonic bacteria in cooling tower model system. *Archives of Microbiology*, *203*(4), 1411–1425. https://doi.org/10.1007/s00203-020-02116-2

Velastegui, E., Quezada, J., Guerrero, K., Altamirano, C., Martinez, J. A., Berrios, J., & Fickers, P. (2023). Is heterogeneity in large-scale bioreactors a real problem in recombinant protein synthesis by Pichia pastoris? *Applied Microbiology and Biotechnology*, *107*(7–8), 2223–2233. https://doi.org/10.1007/s00253-023-12434-2

Verstraeten, N., Braeken, K., Debkumari, B., Fauvart, M., Fransaer, J., Vermant, J., & Michiels, J. (2008). Living on a surface: swarming and biofilm formation. In

Trends in Microbiology (Vol. 16, Issue 10, pp. 496–506). https://doi.org/10.1016/j.tim.2008.07.004

Vestby, L. K., Grønseth, T., Simm, R., & Nesse, L. L. (2020). Bacterial biofilm and its role in the pathogenesis of disease. In *Antibiotics* (Vol. 9, Issue 2). MDPI AG. https://doi.org/10.3390/antibiotics9020059

Vilain, S., Pretorius, J. M., Theron, J., & Brözel, V. S. (2009). DNA as an adhesin: Bacillus cereus requires extracellular DNA to form biofilms. *Applied and Environmental Microbiology*, *75*(9), 2861–2868. https://doi.org/10.1128/AEM.01317-08

Vlamakis, H., Aguilar, C., Losick, R., & Kolter, R. (2008). Control of cell fate by the formation of an architecturally complex bacterial community. *Genes and Development*, *22*(7), 945–953. https://doi.org/10.1101/gad.1645008

Vlamakis, H., Chai, Y., Beauregard, P., Losick, R., & Kolter, R. (2013). Sticking together: Building a biofilm the Bacillus subtilis way. In *Nature Reviews Microbiology* (Vol. 11, Issue 3, pp. 157–168). https://doi.org/10.1038/nrmicro2960

Volke, D. C., Friis, L., Wirth, N. T., Turlin, J., & Nikel, P. I. (2020). Synthetic control of plasmid replication enables target- and self-curing of vectors and expedites genome engineering of Pseudomonas putida. *Metabolic Engineering Communications*, *10*. https://doi.org/10.1016/j.mec.2020.e00126

Volke, D. C., & Nikel, P. I. (2018a). Getting Bacteria in Shape: Synthetic Morphology Approaches for the Design of Efficient Microbial Cell Factories. *Advanced Biosystems*, *2*(11), 1800111. https://doi.org/https://doi.org/10.1002/adbi.201800111

Volke, D. C., & Nikel, P. I. (2018b). Getting Bacteria in Shape: Synthetic Morphology Approaches for the Design of Efficient Microbial Cell Factories. In *Advanced Biosystems* (Vol. 2, Issue 11). Wiley-VCH Verlag. https://doi.org/10.1002/adbi.201800111

W Catlin, B. B., & Cunningham, L. S. (1958). Studies of Extracellular and Intracellular Bacterial Deoxyribonucleic Acids. In *J. gen. Microbiol* (Vol. 19).

Wang, D., Yu, J. M., Dorosky, R. J., Pierson, L. S., & Pierson, E. A. (2016). The phenazine 2-hydroxy-phenazine-1- carboxylic acid promotes extracellular DNA release and has broad transcriptomic consequences in pseudomonas chlororaphis 30-84. *PLoS ONE*, *11*(1). https://doi.org/10.1371/journal.pone.0148003

Wang, S., Liu, X., Liu, H., Zhang, L., Guo, Y., Yu, S., Wozniak, D. J., & Ma, L. Z. (2015). The exopolysaccharide Psl-eDNA interaction enables the formation of a biofilm skeleton in Pseudomonas aeruginosa. *Environmental Microbiology Reports*, *7*(2), 330–340. https://doi.org/10.1111/1758-2229.12252

Webb, J. S., Thompson, L. S., James, S., Charlton, T., Tolker-Nielsen, T., Koch, B., Givskov, M., & Kjelleberg, S. (2003). Cell death in Pseudomonas aeruginosa biofilm development. *Journal of Bacteriology*, *185*(15), 4585–4592. https://doi.org/10.1128/JB.185.15.4585-4592.2003

Weimer, A., Kohlstedt, M., Volke, D. C., Nikel, P. I., & Wittmann, C. (2020). Industrial biotechnology of Pseudomonas putida: advances and prospects. In *Applied Microbiology and Biotechnology* (Vol. 104, Issue 18, pp. 7745–7766). Springer. https://doi.org/10.1007/s00253-020-10811-9

Westerwalbesloh, C., Grünberger, A., Wiechert, W., Kohlheyer, D., & von Lieres, E. (2017). Coarse-graining bacteria colonies for modelling critical solute distributions in picolitre bioreactors for bacterial studies on single-cell level. *Microbial Biotechnology*, *10*(4). https://doi.org/10.1111/1751-7915.12708

Whitchurch, C. B., Tolker-Nielsen, T., Ragas, P. C., & Mattick, J. S. (2002). Extracellular DNA required for bacterial biofilm formation. *Science*, *295*(5559), 1487. https://doi.org/10.1126/science.295.5559.1487

William Costeton, J., Lewandowski, Z., Caldwell, D. E., Korber, D. R., & Appin-Scott, H. M. (n.d.). *MICROBIAL BIOFILMS*.

Wilson, C., Lukowicz, R., Merchant, S., Valquier-Flynn, H., Caballero, J., Sandoval, J., Okuom, M., Huber, C., Durham Brooks, T., Wilson, E., Clement, B., Wentworth, C. D., & Holmes, A. E. (2017). Quantitative and Qualitative Assessment Methods for Biofilm Growth: A Mini-review HHS Public Access. In *Res Rev J Eng Technol* (Vol. 6, Issue 4).

Wilton, M., Charron-Mazenod, L., Moore, R., & Lewenza, S. (2016). Extracellular DNA acidifies biofilms and induces aminoglycoside resistance in Pseudomonas aeruginosa. *Antimicrobial Agents and Chemotherapy*, *60*(1), 544–553. https://doi.org/10.1128/AAC.01650-15

Wingender, J., & Flemming, H. C. (2011). Biofilms in drinking water and their role as reservoir for pathogens. *International Journal of Hygiene and Environmental Health*, *214*(6), 417–423. https://doi.org/10.1016/j.ijheh.2011.05.009

Wirth, N. T., Kozaeva, E., & Nikel, P. I. (2020a). Accelerated genome engineering of Pseudomonas putida by I-SceI—mediated recombination and CRISPR-Cas9

counterselection. *Microbial Biotechnology*, *13*(1), 233–249. https://doi.org/10.1111/1751-7915.13396

Wirth, N. T., Kozaeva, E., & Nikel, P. I. (2020b). Accelerated genome engineering of Pseudomonas putida by I-SceI—mediated recombination and CRISPR-Cas9 counterselection. *Microbial Biotechnology*, *13*(1), 233–249. https://doi.org/10.1111/1751-7915.13396

Wojciech, J., Kamila, M., & Wojciech, B. (2018). Investigation of the population dynamics within a Pseudomonas aeruginosa biofilm using a flow based biofilm model system and flow cytometric evaluation of cellular physiology. *Biofouling*, *34*(8), 835–850. https://doi.org/10.1080/08927014.2018.1508569

Wolfe, A. J., & Berg, H. C. (1989). Migration of bacteria in semisolid agar (Escherichia coli/motility/chemotais/swarm plates). In *Proc. NatI. Acad. Sci. USA* (Vol. 86).

Worlitzsch, D., Tarran, R., Ulrich, M., Schwab, U., Cekici, A., Meyer, K. C., Birrer, P., Bellon, G., Berger, J., Weiss, T., Botzenhart, K., Yankaskas, J. R., Randell, S., Boucher, R. C., & Döring, G. (2002). Effects of reduced mucus oxygen concentration in airway Pseudomonas infections of cystic fibrosis patients. *Journal of Clinical Investigation*, *109*(3), 317–325. https://doi.org/10.1172/jci200213870

Worsey, M. J., & Williams, A. P. (1975). Metablism of toluene and xylenes by Pseudomonas putida (arvilla) mt 2: evidence for a new function of the TOL plasmid. *Journal of Bacteriology*, *124*(1), 7–13. https://doi.org/10.1128/jb.124.1.7-13.1975

Yamada, M., Ikegami, A., & Kuramitsu, H. K. (2005). Synergistic biofilm formation by Treponema denticola and Porphyromonas gingivalis. *FEMS Microbiology Letters*, *250*(2), 271–277. https://doi.org/10.1016/j.femsle.2005.07.019

Yang, L., Barken, K. B., Skindersoe, M. E., Christensen, A. B., Givskov, M., & Tolker-Nielsen, T. (2007). Effects of iron on DNA release and biofilm development by Pseudomonas aeruginosa. *Microbiology*, *153*(5), 1318–1328. https://doi.org/10.1099/mic.0.2006/004911-0

Yin, W., Wang, Y., Liu, L., & He, J. (2019). Biofilms: The microbial “protective clothing” in extreme environments. *International Journal of Molecular Sciences*, *20*(14). https://doi.org/10.3390/ijms20143423

Zhang, Y., Young, P., Traini, D., Li, M., Ong, H. X., & Cheng, S. (2023). Challenges and current advances in in vitro biofilm characterization. In *Biotechnology*

Journal (Vol. 18, Issue 11). John Wiley and Sons Inc. https://doi.org/10.1002/biot.202300074

Zid, B. M., & O'Shea, E. K. (2014). Promoter sequences direct cytoplasmic localization and translation of mRNAs during starvation in yeast. *Nature*, *514*(7520). https://doi.org/10.1038/nature13578

Zweig, M., Schork, S., Koerdt, A., Siewering, K., Sternberg, C., Thormann, K., Albers, S. V., Molin, S., & Van der Does, C. (2014). Secreted single-stranded DNA is involved in the initial phase of biofilm formation by Neisseria gonorrhoeae. *Environmental Microbiology*, *16*(4), 1040–1052. https://doi.org/10.1111/1462-2920.12291